The degradation of organic solar cells

Doumon, Nutifafa Yao

DOI:
10.33612/diss.98539626

The Degradation of Organic Solar Cells

From Chemistry to Device Physics through Materials

To Essie Awunyo and Frederick Doumon

Nutifafa Yao Doumon

The Degradation of Organic Solar Cells

From Chemistry to Device Physics through Materials

Nutifafa Yao Doumon
PhD thesis
University of Groningen, The Netherlands

Zernike Institute PhD thesis series 2019-27
ISSN: 1570-1530
ISBN: 978-94-034-2021-9 (printed version)
978-94-034-2020-2 (electronic version)

The research described in this thesis was conducted in the Photophysics & Optoelectronic research group of the Zernike Institute for Advanced Materials at the University of Groningen, The Netherlands. This work is funded by the Zernike Bonus Incentive Scheme (Zernike Dieptestrategie). This is a publication by the Foundation for Fundamental Research of Matter (FOM) Focus Group *Next Generation Organic Photovoltaics*, participating in the Dutch Institute for Fundamental Energy Research (DIFFER).

university of groningen / faculty of science and engineering / zernike institute for advanced materials

Cover design: In collaboration with *Saurabh Soni*. The fabrics are of a traditional Ghanaian design originally known as “Kente”. Though both show some orderings, they illustrate the complexity in the donor:acceptor blend morphology and their chemical structure (background molecules on the cover) interactions, partly addressed in the thesis. Pictures of fabrics by *Elena Leonova* from VectorStock.com

Printed by Ipskamp Drukkers, Enschede, The Netherlands.

university of groningen

The Degradation of Organic Solar Cells

From Chemistry to Device Physics through Materials

PhD thesis

to obtain the degree of PhD at the
University of Groningen
on the authority of the
Rector Magnificus Prof. C. Wijmenga
and in accordance with
the decision by the College of Deans.

This thesis will be defended in public on

Friday 25 October 2019 at 16.15 hours

by

Nutifafa Yao Doumon

born on 3 July 1980
in Aflao, Ghana

Supervisors

Prof. L. J. A. Koster
Prof. R. C. Chiechi

Assessment Committee

Prof. R. A. J. Janssen
Prof. T. Kirchartz
Prof. M. S. Pchenitchnikov

Contents

1

General Introduction

"It is those ugly caterpillars that turn into beautiful butterflies after season." – African Proverb

1

1.1. Introduction

Energy is essential to almost every activity of humanity.[1] It has implications for our home, environment, transportation, information technology, and economy. In brief, energy affects everyday life. Global development is entrenched in a constant and sufficient supply of energy. There is a direct link between energy, well-being, and prosperity across the globe. The divide in this regard is enormous between countries that keep up with the demand and those that cannot. This is very evident when one looks at the NASA night light earth map.[2–4] The global energy demand is constantly on the rise.[5] The year 2050 may be important in human history. It is the projected year for the net-zero carbon dioxide (CO_2) emission to save our planet according to recent experts' report on climate change.[6] As of 2016, about 80% of global energy consumption is reliant on non-renewable fossil fuels such as oil, natural gas, and coal.[7] Meanwhile, the recent 2018 United Nations report on climate change[6], published by the intergovernmental panel on climate change on the 8th October 2018, sounds an alarm around the risks involved if we do not change course from our current energy way of life. The report also has it that the need for limiting global warming is also to give people and ecosystems more room to adapt and remain below relevant risk thresholds.[6]

Given the situation, the rapidly increasing energy demand, and the quest for creating a balance between demand and supply; other sources of safe, sustainable, and cheaper energy must be explored. Photovoltaics (PVs) is

emerging as one way to a sustainable, greener, and possibly cheaper source of energy, among others. PVs emerged on the energy scene with silicon (Si) solar cells in the 1950s[8] and was then mainly used as an off-grid power supply for satellite application. The drive for greener energy sources has seen the advent of other optoelectronic devices. This is made possible with the discovery of organic/polymer semiconductors.[9] Organic semiconductors[1,10–26] have attracted great interest these last few decades due to their good electrical conductivity properties. This explains their applications in many fields of organic electronics[10,27–32] and/or molecular electronics[22].

1.2. Basic Concept on Organic Semiconductors

The word ***"organic"*** is initially used to denote a class of chemical compounds comprising only of those existing in or derived from living organisms such as plants or animals.[33] Nowadays, it includes all other compounds of carbon.[33] An organic material as used here is artificially synthesised in the laboratory and is defined by its carbon-based compounds, hydrocarbons, or their derivatives.

For this thesis, organic materials are limited to conjugated molecular structures based on carbon-carbon bonds, i.e., chain of ***C=C*** bonds as a backbone; that which exhibit optical and electrical properties. Thus, the whole thesis is based on organic optoelectronic materials. They are defined as loosely bound molecular solids held together by weak van der Waals

interactions[24] with a profound effect on their electrical and physical properties. According to quantum chemistry, the energy state of a single atom is depicted by discrete energy levels populated by electrons.[34] Following the Aufbau principle, a carbon atom exhibits an electron configuration $1s^2 2s^1 2p^3$ in its excited state. This configuration allows different hybridisations between 2*s* and 2*p* atomic orbitals leading to distinct electron "localisations" and bonding possibilities. For example, in ethylene (See **Figure 1.1**), C_2H_4, sp^2 hybridisation leads to σ-bonds between the carbon and the hydrogen atoms. The remaining p_z orbitals overlap above and below the sp^2 plane, forming a weaker π-bond related to a π-molecular orbital.

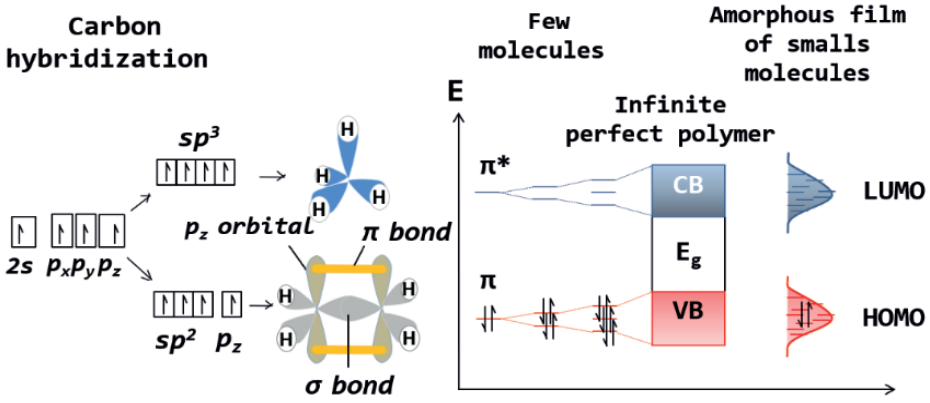

Figure 1.1: Energy level construction: Methane (CH_4) and Ethylene (C_2H_4). Image by F. V. Houard.

The electrons are delocalised along the conjugated backbone, alternating σ- and π-bonds, and responsible for charge carrier transport in organic compounds. Electrons in organic semiconductors can only move along a well-

defined "path" by thermal activated "hopping" due to a globally disordered structure[35], while electrons in inorganic semiconductors can move around in the whole bulk of the material via band transport in a long-range ordered crystal.

1.2.1. Organic Materials over the Years

Contrary to their inorganic counterparts that are already in use for many applications including the first PV cell based on Si in 1954[8], organic materials only came into use in the 1970s with the discovery of the electrical conductivity of polymers[9,36]. Even though they have been known for years, this discovery has diverted more attention to the field of organic electronics – the discovery by Heeger et *al.*[37,38] is so important that it won them the Nobel Prize in Chemistry in 2000.[39] The appeal towards organic materials initially stems from their potential applications as a low-cost replacement for conventional semiconductor and lighting technologies. These materials are divided into three categories based on their structure and presented here in increasing order of complexity: small molecules, polymers, and biological molecules.

1.2.2. Commonly Used Organic Materials

Even though conductivity of organic compounds can be traced back to 1906[40] in photoconductivity of solid anthracene, it was only after the discovery

of the conductivity of polyacetylene[9,36] that extensive synthesis work was carried out on organic materials for application in organic electronics. Small molecule and polymer semiconductors are the most widely explored.

The commonly used organic small molecules over the years include the acene compounds and their derivatives, fullerene (C_{60}) and its derivatives, etc. of which some are promising semiconductor for OFETs[41–47] and OPVs. However, their low solubility in organic solvents and their instability in air led researchers to look for other options. Since the advent of polyacetylene, semiconductor polymers are extensively used in organic electronics. Poly[2-methoxy-5-(2-ethylhexyloxy)-1,4-phenylenevinylene], MEH-PPV,[48–51] poly(2,3-dihydrothieno-1,4-dioxin)-poly(styrenesulfonate), PEDOT:PSS,[29,52–59] and poly(3-hexylthiophene-2,5-diyl), P3HT,[28,54,55,60–73] served as the workhorse materials. P3HT has been the most representative conjugated polymer donor material for polymer solar cells (PSCs)[27,28,49,54,55,60,61,63–66,68–70,72–103], however, due to the low efficiency of the P3HT-based PSCs, new polymers have seen the day. Recent advances in semiconductor polymer materials are briefly discussed in the following section.

1.2.3. Novel Design

There are limitations in the use of the workhorse organic materials and other polymers used over the years. These are due to high-cost synthesis techniques, lack of mechanical flexibility, less stability and short lifetime, and most importantly, low efficiency (partly due to high energy

band gap). These limitations are addressed by the introduction of many ideas spanning doping, interface engineering, and an increase in either material dielectric constant or materials solubility, etc. These varied methods to resolve the impasse fall under novel design. As our discussion is eventually narrowing down to PSCs, permit me to use this type of device as a basis for discussion on novel design.

In 2005, the power conversion efficiency (PCE) of P3HT and [6,6]-phenyl-C61-butyric acid methyl ester, $PC_{61}BM$ (PCBM)-based solar cell was only 4.4%.[104] Though P3HT has a simple molecular structure[66] (as shown in **Figure 1.2a)** with high hole mobility, it has a high highest occupied molecular orbital (HOMO) about -5.0 eV and a high bandgap as well (~2 eV) as depicted in **Figure 1.2b**. These combined characteristics resulted in poor light-harvesting when used with PCBM in PSCs. It became necessary to introduce concepts for the achievement of higher mobility, lower HOMO level, a broad absorption band, and solution processability. Incorporation of functional groups in organic/polymer semiconductors to improve their solubility in organic solvents and facilitate the formation of semiconductor thin films by cost-effective solution deposition techniques became the cornerstones of new engineered/designed materials.

Main-chain engineering involves the copolymerisation of different electron-donating and electron-accepting units.[18] Moreover, the planar main chain is also crucial for enhancing the interchain interaction, and high hole mobility of the conjugated polymers.[18] Side-chain engineering mostly helps in improving the solubility, and aggregation properties of the polymers.[18]

Typical examples are the flexible side-chains on polythiophene derivatives, electron-withdrawing side-chains, and conjugated side-chains (see **Figure 1.2c**). A lot has been achieved in making successfully efficient fullerene acceptor-based PSCs with either small molecules[105–107] or polymers[108–114]; and also recently, with non-fullerene small molecule and polymer acceptor-based solar cells[115–145]. These accomplishments came through different processing techniques, morphological changes, device structures, and engineered materials. However, one area in the field that needs more attention is stability and degradation.

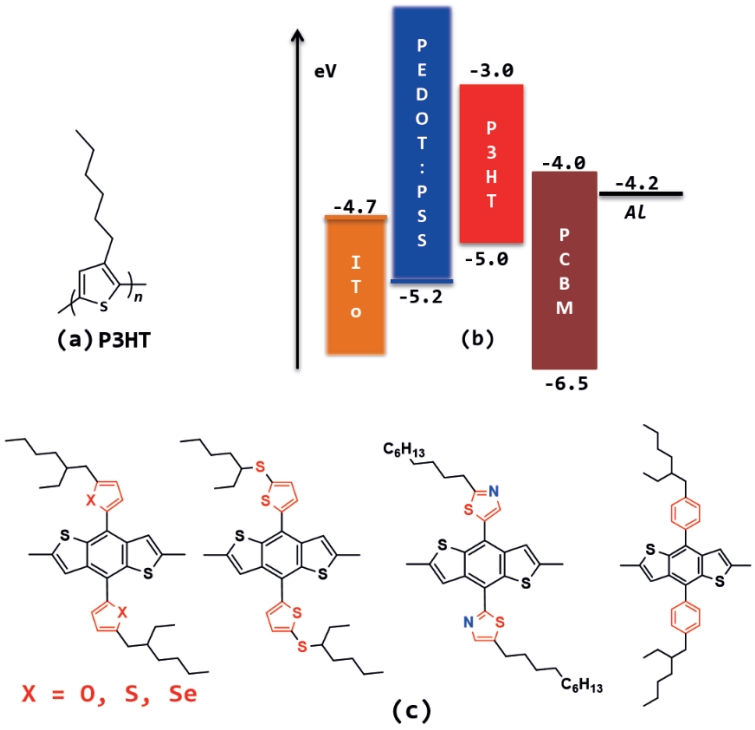

Figure 1.2: Molecular structure of P3HT **(a)**; energy level diagram of P3HT in a conventional solar cell **(b)**; and benzodithiophene (BDT)-unit with different side-chains **(c)**. Images adapted from Ref. [18,66].

1.3. Organic Photovoltaics

Organic photovoltaics[14,57,146–151] (OPVs) is a third-generation PV technology based on π-conjugated organic electronic materials, including both organic small molecules and polymers. They have potential advantages over their inorganic counterparts. They are lightweight, mechanically flexible, compatible with large areas, high throughput, and are low-cost processing.[1,30,86,152–158] Polymer solar cells, a subcategory of organic solar cells (OSCs) are at the forefront of the OPV technology. They have broad applications, ranging from flexible solar modules to building applications as semitransparent solar cells in windows.[30]

1.4. Brief History of OPV

It is widely known that the first efficient OPV device, a two-layer OPV, was demonstrated by Tang.[159] However, the first organic solar cell was made by Gosch and Feng.[160] The technology has evolved over the years to what is currently accepted as the most efficient active layer configuration: the bulk heterojunction (BHJ). The monolayer or homojunction depicts devices with only one organic material in the active layer. The heterojunction era, which saw the advent of devices with two organic materials in the active layer, evolved since 1986 from planar heterojunction (known as bilayer) to the BHJ devices in 1995.[48] This historical evolution nurtured parallel advancement in materials usage, processing techniques, device physics, and performance improvement.

1.5. Materials and Processing Techniques

1.5.1. Materials

The heterojunction with its first configuration as bilayer reported by Tang with 1% PCE[159] in 1986 was a stacked double layer consisting of two organic materials, a donor (D) and an acceptor (A). For this kind of cells, the two materials are consecutively deposited forming two distinct layers with a D/A interface. The widely used organic donor materials are PPV and MDMO-PPV with organic acceptor materials being C_{60} and PCBM. The first appreciable performance of bilayer device was observed for the polymer donor MEH-PPV and a thermally evaporated C_{60} acceptor.[161]

The BHJ is achieved by co-deposition, leading to D-A blend film with a much higher internal interface. The first donor materials used in these devices included PPVs, especially MEH-PPV and MDMO-PPV.[154,162] The most widely used donor polymer in bulk heterojunction has been P3HT. The acceptor was eventually C_{60} and its derivative $PC_{61}BM$. Since the incorporation of PCBM, it remained the standard acceptor. Nowadays, high-efficiency devices use a functionalized derivative of C_{70}, $PC_{71}BM$.[163] The technology partly moved on from using small organic molecules to functionalized conjugated polymers.

Current research work is done using push-pull[164] or donor-acceptor-type copolymers as donors and $PC_{71}BM$ and non-fullerene organic molecules as acceptors. These new polymers are initially developed to address limitations encountered in the use of workhorse polymers such as MEH-PPV and P3HT. Thus, the push-pull conjugated polymers, according to Pirotte et

al.[164], are readily tuned by choice of appropriate constituent building blocks and solubilising side-chains patterns to meet the specific requirements of each application. Most of these polymers are carefully designed to highly prevent exciton recombination, reduce recombination generally before the electrons and the holes reach the electrodes, and also improve transport within layers, through careful selection and mixing of the composite materials.

1.5.2. Processing Techniques

The processing methods are highly dependent on the type of materials. Based on the type of organic semiconductor materials, whether small molecules or conjugated polymers, we can identify two classes of techniques. The most spread and preferred method for small molecules is the vacuum thermal evaporation and other direct competitors.[165–168] The other class of techniques fits only semiconductor polymers. It includes printing techniques[169] such as screen printing, inkjet printing, spray printing, roll-to-roll (R2R) printing, micro-contacting printing, and coating techniques like spray coating, and spin coating, which is a laboratory scale technique, is used in this thesis.

1.6. Important Parameters in Organic/Polymer Solar Cells

Figure 1.3 shows a typical *J-V* curve of a solar cell when illuminated.

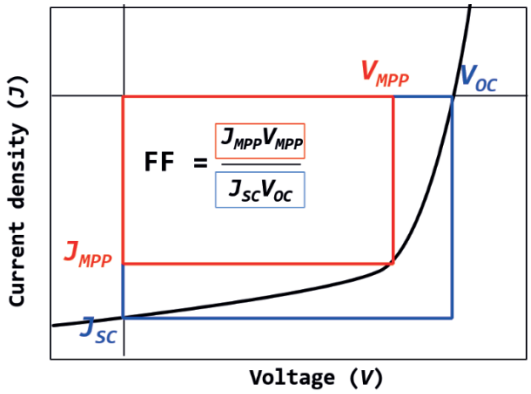

Figure 1.3: Typical *J-V* curve of a solar cell showing the essential parameters in their electrical characterisation. Adapted from Bartesaghi et *al.*[170]

The *J-V* curve is voltage-dependent, and the maximum power as indicated in red is the maximum product of *J* and *V*. The more the *J-V* curve takes the shape of the blue rectangle with area $J_{SC}\times V_{OC}$ (product of the short-circuit current and the open-circuit voltage), the larger the maximum power. This gives a notion of the quality of the curve. The measure of the quality of the shape of the *J-V* characteristics is known as the fill factor (FF) and is given by[171]:

$$\mathbf{FF} = \frac{(JV)_{\mathbf{max}}}{J_{SC}V_{OC}} = \frac{\mathbf{P_{max}}}{J_{SC}V_{OC}} \qquad \textbf{(1.1)}$$

Thus, the maximum power, P_{max}, is given by:

$$\mathbf{P_{max}} = \mathbf{FF}(J_{SC}V_{OC}) \qquad \textbf{(1.2)}$$

Another important parameter is the power conversion efficiency (PCE). The PCE of a solar cell relates the maximum output power P_{max} to the power of the incident light (also known as input power), P_{in}:

$$PCE = \frac{P_{max}}{P_{in}} = FF\frac{J_{sc}V_{oc}}{P_{in}} \quad (1.3)$$

Other characteristic parameters in OSC are the internal and external quantum efficiencies. The internal quantum efficiency (IQE) is the measure of the number of electrons collected to the number of photons absorbed in the device[1,156]. While the external quantum efficiency (EQE) is the measure of the number of photogenerated electrons to the number of photons incident onto the device.[1,156] To reliably compare solar cells efficiencies, solar radiation standards have been set. The most common standard is the AM 1.5G spectrum, which can be achieved with commercial solar simulators.

1.7. Exciton and Charge Transfer/Transport

PSCs are excitonic solar cells mostly made of polymer blends or small molecule acceptor and polymer donor blends. Charge transport within a polymer is a combination of two processes: intramolecular carrier movement and intermolecular charge transfer. Intermolecular transport typically occurs through a hopping process[172,173] as a charge carrier overcomes an energy barrier to move from one molecule to the next[24].

In PSC, excitons are products of photon absorption. Electrons excited to the LUMO of the molecule/polymer are “coulombically” bound to the holes left behind in the HOMO. These excitons must then get broken into free charge carriers to be collected at the electrodes to extract power from

the device. As shown in **Figure 1.4**, there are five steps involved in the creation of excitons and migration of charges in OSC:

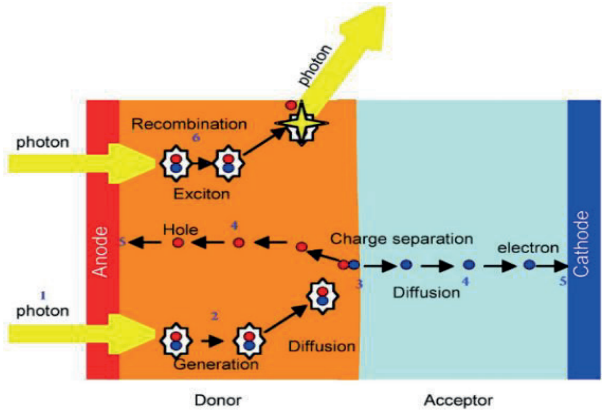

Figure 1.4: Steps in solar cell operation process. The involved mechanisms (1-6), are explained below. Image taken from [174].

- **Photon Absorption (1):** We mostly use Glass/ITO/PEDOT:PSS, which allows light to pass through them and to be absorbed by the active layer.
- **Exciton Generation/Formation (2):** The incident light creates excitons which begin to migrate in the system. Whether the excitons in the donor reach the interface with the acceptor depends on the exciton diffusion length, L_D, where D is the diffusion coefficient and τ the exciton lifetime.

$$L_D = \sqrt{D\tau} \qquad (1.4)$$

- **Exciton Dissociation / Charge Separation (3):** Once the excitons reach the interface, they are separated into charges (electrons and holes).

- **Charge Migration (4):** The built-in potential due to the difference in work functions of the electrodes causes drift/diffusion of charges with the electrons to the cathode and the holes to the anode.
- **Charge Collection/Extraction (5):** At the electrodes, the charges are efficiently collected and extracted to power an external circuit.

A sixth mechanism, recombination, can also occur in different forms, but not positively counted into the operation mechanisms of PSC as it is a source of loss mechanism.

1.8. Recombination

Recombination between electrons and holes, a loss process limiting the efficiency of PSC, occurs in two phases: geminate or non-geminate recombination phases[181]. The latter includes bimolecular, surface, and trap-assisted recombination.

1.9. Progress in OPV: Efficiency - Processing - Stability

According to Kalowekamo and Baker[175], OPVs have a chance to compete on the market if only the 15% efficiency and the 15 years lifetime requirements are met. Since then, more work has been done on OPV to achieve higher efficiency.[138,176–180] Since its inclusion in the solar cell efficiency chart

by the National Renewable Energy Laboratory (NREL)[181] with ~3% efficiency, OSCs have greatly evolved over the years[182] as depicted in **Figure 1.5.** Today, the efficiency of a single junction OSC is over 16%[183,184] and is fast approaching the predicted 20%.[25] Lots of concepts have helped the field to reach this far. This involves different approaches and advances. There were notable advances in processing techniques, device physics and structure, morphology and contact/interface engineering, materials synthesis and novel design.[59,69,107,158,185–187] Finally, the advent of non-fullerene acceptors has opened the door for better device performance in terms of efficiency. Still, the device stability is lagging behind.

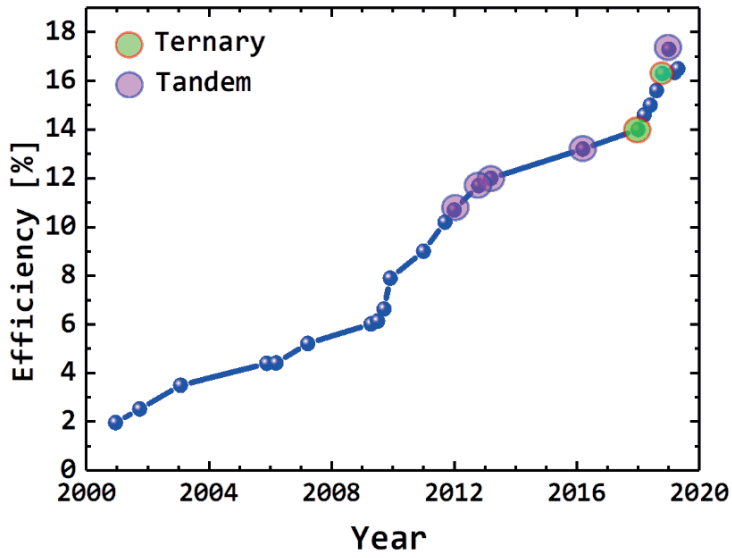

Figure 1.5: Time evolution of the efficiency of organic solar cells technology. The plot depicts updated record efficiencies (initial data points collected and provided by L.J.A. Koster) over the years of different structures and systems of the technology: single junction (binary and ternary systems) and multijunction (or tandem).

1.10. OPV Bottleneck: Lifetime and Degradation

OPV may have a future on the market. It boasts of advantages as disposable and niche products emphasising lightweight, portability, reduced cost over performance, large-scale production viability, high throughput, R2R manufacturing, etc.[24].

The only thing that requires more attention and investigation is stability in OPV. Stability is one of the major hurdles that must be tackled before PSC can enter the market[30]. Stability is the study of degradation and the mechanisms that are behind this phenomenon. Degradation is the observed detrimental effects on efficiency and lifetime. Degradation is generally classified into two sources, namely, intrinsic and extrinsic. The intrinsic instability is related to the interface and interior of the working device, while extrinsic is caused by external factors such as corrosion and/or cracks formation.[188] In this thesis, we pay particular attention to the degradation of the active layer materials in a way that it becomes the predominant factor that governs our studies. Thus, we mainly focus on explaining the mechanisms that govern the photodegradation in bulk – active layer – of the solar cells. The intrinsic degradation of the bulk is caused by several factors, resulting in photooxidation, morphological changes, and interface degradation. The factors that we consider the most influential in the degradation pathways[151,189–193] are:

- oxygen and moisture causing oxidative degradation and delamination;
- temperature variation or heat causing thermal degradation;

- and most importantly, UV light and visible NIR light causing photodegradation, which is the topic of the thesis.

The last factor is light-induced; thus, the term photo-induced degradation. It occurs in the presence of continuous exposure to light. While one can go around the first two if necessary, this factor cannot be avoided as solar cells must be exposed to light to generate electricity. Under real conditions, these factors do not operate in isolation. In the worst-case scenario and usually, all three processes co-occur, making the study of degradation more complicated than anticipated.

Research is advancing slowly in degradation and stability of PSC. This has been the focus and rightly so, currently in our research group with notable works on BDT-TT polymers and other works reported in this thesis and beyond. To simplify our task and to arrive at solid conclusions based on the accurate phenomenon, we decide to exclude other possible factors that can make our task complex and only critically look at photo-induced degradation of the studied polymer solar cells. Thus, i) thermal degradation was avoided by operating the cell at a constant temperature (room temperature), usually below or around the solar cell processing temperature, although this is difficult to achieve under real-life conditions; and ii) oxidative degradation was prevented by fabricating and working with the devices under an inert atmosphere.

1.11. Outline of the Thesis

In the past few months, interesting developments occurred in the PSC technology with record efficiencies of above 16% for single junction[183,184] and 17.3% for multijunction[180] devices. This is enabled by the advent of newly synthesised materials. The focus of this thesis is on the investigation of the degradation behaviour of the current workhorse materials used in the fabrication of PSCs. ***Chapter 1*** gives, in a nutshell, a review of the field, touching upon the device physics and operation. ***Chapter 2*** gives an account of the materials used and briefly touches on some theories and related characterisation techniques explored in the quest of our investigations:

Chapter 3: Relating polymer donor chemical structure to the photostability of their solar cells

- The role of the side chains on the BDT-unit of the PBDT-TT polymers in the photodegradation of their solar cells
- The role of the chemical structure changes of the TT-unit of the PBDT-TT polymers in the photodegradation of their solar cells

Chapter 4: Relating the acceptor chemical structure to the photostability of their solar cells

- Photostability of fullerene and non-fullerene polymer solar cells
- Chemical structure changes in ITIC: Effect on the photostability of their solar cells

Chapter 5: The role of additives in the photostability of organic solar cells - 1,8-diiodooctane as a photoacid

Chapter 6: Making solar cells more stable? - Improved photostability of organic solar cells using ternary blends

Finally, ***Chapter 7*** looks at the implication of this study to the field and the society at large.

Bibliography

[1] J. Xue, *Polym. Rev.* **2010**, *50*, 411.
[2] M. O. Román, Z. Wang, Q. Sun, V. Kalb, S. D. Miller, A. Molthan, L. Schultz, J. Bell, E. C. Stokes, B. Pandey, K. C. Seto, D. Hall, T. Oda, R. E. Wolfe, G. Lin, N. Golpayegani, S. Devadiga, C. Davidson, S. Sarkar, C. Praderas, J. Schmaltz, R. Boller, J. Stevens, O. M. Ramos González, E. Padilla, J. Alonso, Y. Detrés, R. Armstrong, I. Miranda, Y. Conte, N. Marrero, K. MacManus, T. Esch, E. J. Masuoka, *Remote Sens. Environ.* **2018**, *210*, 113.
[3] "earth_lights.gif (4320×2160)," https://eoimages.gsfc.nasa.gov/images/imagerecords/55000/55167/earth_lights.gif, **(accessed on Nov. 10, 2018).**
[4] "blackmarble2016-1500px_0.jpg (1500×750)," https://www.nasa.gov/sites/default/files/thumbnails/image/blackmarble2016-1500px_0.jpg, **(accessed on Nov. 10, 2018).**
[5] Shell International, *London Shell Int. Ltd.* **2001**, pp. 60.
[6] IPCC, 2018/24/PR IPCC PRESS RELEASE **2018**, 13.
[7] Shell International, *Shell Int. BV* **2017**, 17.
[8] D. M. Chapin, C. S. Fuller, G. L. Pearson, *J. Appl. Phys.* **1954**, *25*, 676.
[9] C. K. Chiang, C. R. Fincher, Y. W. Park, A. J. Heeger, H. Shirakawa, E. J. Louis, S. C. Gau, A. G. MacDiarmid, *Phys. Rev. Lett.* **1977**, *39*, 1098.
[10] E. Voroshazi, B. Verreet, A. Buri, R. Müller, D. Di Nuzzo, P. Heremans, *Org. Electron. physics, Mater. Appl.* **2011**, *12*, 736.
[11] M. Y. Jo, Y. E. Ha, Y. S. Won, S. Il Yoo, J. H. Kim, *Org. Electron.* **2015**, *25*, 85.
[12] K. Feron, W. J. Belcher, C. J. Fell, P. C. Dastoor, *Int. J. Mol. Sci.* **2012**, *13*, 17019.
[13] A. Facchetti, *Chem. Mater.* **2011**, *23*, 733.
[14] K. M. Coakley, K. M. Coakley, M. D. Mcgehee, M. D. Mcgehee, *Chem. Mater.* **2004**, 4533.
[15] N. Cho, C. W. Schlenker, K. M. Knesting, P. Koelsch, H. L. Yip, D. S. Ginger, A. K. Y. Jen, *Adv. Energy Mater.* **2014**, *4*, DOI 10.1002/aenm.201301857.
[16] E. R. Bittner, J. G. S. Ramon, S. Karabunarliev, *J. Chem. Phys.* **2005**, *122*, DOI 10.1063/1.1924540.
[17] J. Adams, G. D. Spyropoulos, M. Salvador, N. Li, S. Strohm, L. Lucera, S. Langner, F. Machui, H. Zhang, T. Ameri, M. M. Voigt, F. C. Krebs, C. J. Brabec, *Energy Environ. Sci.* **2014**, *00*, 1.
[18] Z.-G. Zhang, Y. Li, *Sci. China Chem.* **2014**, *58*, 192.
[19] D. Veldman, S. C. J. Meskers, R. A. J. Janssen, *Adv. Funct. Mater.* **2009**, *19*, 1939.
[20] V. A. Trukhanov, V. V. Bruevich, D. Y. Paraschuk, *Sci. Rep.* **2015**, *5*, 11478.
[21] R. A. Street, S. Cowan, A. J. Heeger, *Phys. Rev. B - Condens. Matter Mater. Phys.* **2010**, *82*, 11.
[22] H. Spanggaard, F. C. Krebs, *Sol. Energy Mater. Sol. Cells* **2004**, *83*, 125.
[23] J. D. Servaites, M. A. Ratner, T. J. Marks, *Energy Environ. Sci.* **2011**, *4*, 4410.
[24] J. D. Myers, J. Xue, *Polym. Rev.* **2012**, *52*, 1.
[25] L. J. A. Koster, S. E. Shaheen, J. C. Hummelen, *Adv. Energy Mater.* **2012**, *2*, 1246.
[26] A. Köhler, H. Bässler, *J. Mater. Chem.* **2011**, *21*, 4003.
[27] M. O. Reese, A. J. Morfa, M. S. White, N. Kopidakis, S. E. Shaheen, G. Rumbles, D. S. Ginley, *Sol. Energy Mater. Sol. Cells* **2008**, *92*, 746.

[28] M. H. Park, J. H. Li, A. Kumar, G. Li, Y. Yang, *Adv. Funct. Mater.* **2009**, *19*, 1241.
[29] J. Ouyang, C. Chu, F. Chen, Q. Xu, Y. Yang, *J. Macromol. Sci. Part A* **2004**, *41*, 1497.
[30] G. Li, R. Zhu, Y. Yang, *Nat. Photonics* **2012**, *6*, 153.
[31] M. Jørgensen, K. Norrman, F. C. Krebs, *Sol. Energy Mater. Sol. Cells* **2008**, *92*, 686.
[32] Y. Wakayama, R. Hayakawa, H.-S. Seo, *Sci. Technol. Adv. Mater.* **2014**, *15*, 024202.
[33] "Organic | Define Organic at Dictionary.com," https://www.dictionary.com/browse/organic, **(accessed on Nov. 11, 2018).**
[34] W. Tress, in *Reinhold Pub. Corp*, **2014**, pp. 15–65.
[35] V. Coropceanu, J. Cornil, D. A. da S. Filho, Y. Olivier, A. Robert Silbey, J.-L. Brédas, *Chem. Rev.* **2007**, *107*, 926.
[36] H. Shirakawa, J. Louis, A. G. Macdiarmid, *J. C. S. Chem. Comm* **1977**, 578.
[37] A. J. Heeger, *Rev. Mod. Phys.* **2001**, *73*, 681.
[38] H. Shirakawa, *Rev. Mod. Phys.* **2001**, *73*, 713.
[39] N. P. Organisation, "The Nobel Prize in Chemistry 2000," https://www.nobelprize.org/prizes/chemistry/2000/summary/, **2000 (accessed on Nov. 12, 2018).**
[40] Y. Okamota, W. Brenner, *Reinhold Pub. Corp* **1964**, 184.
[41] H. Klauk, D. J. Gundlach, M. Bonse, C. C. Kuo, T. N. Jackson, *Appl Phys Lett* **2000**, *76*, 1692.
[42] G. Horowitz, *Adv. Mater.* **1998**, *10*, 365.
[43] C. D. Dimitrakopoulos, *Science* **1999**, *283*, 822.
[44] C. D. Dimitrakopoulos, P. R. L. Malenfant, *Adv. Mater. (Weinheim, Ger.)* **2002**, *14*, 99.
[45] C. A. Di, G. Yu, Y. Liu, X. Xu, D. Wei, Y. Song, Y. Sun, Y. Wang, D. Zhu, *Adv. Funct. Mater.* **2007**, *17*, 1567.
[46] S. Kim, T. Lim, K. Sim, H. Kim, Y. Choi, K. Park, S. Pyo, *ACS Appl. Mater. Interfaces* **2011**, *3*, 1451.
[47] C. Liu, T. Minari, Y. Li, A. Kumatani, M. V. Lee, S. H. Athena Pan, K. Takimiya, K. Tsukagoshi, *J. Mater. Chem.* **2012**, *22*, 8462.
[48] G. Yu, J. Gao, J. C. Hummelen, F. Wudl, A. J. Heeger, *Science* **1995**, *270*, 1789.
[49] T. Tromholt, M. Manceau, M. Helgesen, J. E. Carlé, F. C. Krebs, *Sol. Energy Mater. Sol. Cells* **2011**, *95*, 1308.
[50] D. Abbaszadeh, N. Y. Doumon, G.-J. A. H. Wetzelaer, L. J. A. Koster, P. W. M. Blom, *Synth. Met.* **2016**, *215*, 64.
[51] D. Abbaszadeh, G.-J. A. H. Wetzelaer, N. Y. Doumon, P. W. M. Blom, *J. Appl. Phys.* **2016**, *119*, 1.
[52] M. T. Lloyd, C. H. Peters, A. Garcia, I. V. Kauvar, J. J. Berry, M. O. Reese, M. D. McGehee, D. S. Ginley, D. C. Olson, *Sol. Energy Mater. Sol. Cells* **2011**, *95*, 1382.
[53] R. Steim, F. R. Kogler, C. J. Brabec, *J. Mater. Chem.* **2010**, *20*, 2499.
[54] A. L. Ayzner, D. D. Wanger, C. J. Tassone, S. H. Tolbert, B. J. Schwartz, *J. Phys. Chem. C* **2008**, *112*, 18711.
[55] S. A. Gevorgyan, M. Jørgensen, F. C. Krebs, *Sol. Energy Mater. Sol. Cells* **2008**, *92*, 736.
[56] K. Kawano, R. Pacios, D. Poplavskyy, J. Nelson, D. D. C. Bradley, J. R. Durrant, *Sol. Energy Mater. Sol. Cells* **2006**, *90*, 3520.
[57] K. Norrman, N. B. Larsen, F. C. Krebs, *Sol. Energy Mater. Sol. Cells* **2006**, *90*, 2793.

[58] K. X. Steirer, J. P. Chesin, N. E. Widjonarko, J. J. Berry, A. Miedaner, D. S. Ginley, D. C. Olson, *Org. Electron. physics, Mater. Appl.* **2010**, *11*, 1414.
[59] M. Manceau, D. Angmo, M. Jørgensen, F. C. Krebs, *Org. Electron. physics, Mater. Appl.* **2011**, *12*, 566.
[60] W. Ma, J. Y. Kim, K. Lee, A. J. Heeger, *Macromol. Rapid Commun.* **2007**, *28*, 1776.
[61] S. Han, W. S. Shin, M. Seo, D. Gupta, S. J. Moon, S. Yoo, *Org. Electron. physics, Mater. Appl.* **2009**, *10*, 791.
[62] G. Lu, H. Usta, C. Risko, L. Wang, A. Facchetti, M. A. Ratner, T. J. Marks, *J. Am. Chem. Soc.* **2008**, *130*, 7670.
[63] M. Zhang, X. Guo, Y. Yang, J. Zhang, Z.-G. Zhang, Y. Li, *Polym. Chem.* **2011**, *2*, 2900.
[64] R. Bechara, N. Leclerc, P. Lévêque, F. Richard, T. Heiser, G. Hadziioannou, *Appl. Phys. Lett.* **2008**, *93*, 013306.
[65] M. Campoy-Quiles, Y. Kanai, A. El-Basaty, H. Sakai, H. Murata, *Org. Electron.* **2009**, *10*, 1120.
[66] M. D. Irwin, D. B. Buchholz, A. W. Hains, R. P. H. Chang, T. J. Marks, *PNAS* **2008**, *105*, 2783.
[67] R. P. Singh, O. S. Kushwaha, *Macromol. Symp.* **2013**, *327*, 128.
[68] T. Stubhan, J. Krantz, N. Li, F. Guo, I. Litzov, M. Steidl, M. Richter, G. J. Matt, C. J. Brabec, *Sol. Energy Mater. Sol. Cells* **2012**, *107*, 248.
[69] T. Stubhan, H. Oh, L. Pinna, J. Krantz, I. Litzov, C. J. Brabec, *Org. Electron.* **2011**, *12*, 1539.
[70] A. Distler, P. Kutka, T. Sauermann, H. J. Egelhaaf, D. M. Guldi, D. Di Nuzzo, S. C. J. Meskers, R. A. J. Janssen, *Chem. Mater.* **2012**, *24*, 4397.
[71] C. H. Peters, I. T. Sachs-Quintana, J. P. Kastrop, S. Beaupré, M. Leclerc, M. D. McGehee, *Adv. Energy Mater.* **2011**, *1*, 491.
[72] P. Schilinsky, U. Asawapirom, U. Scherf, M. Biele, C. J. Brabec, *Chem. Mater.* **2005**, *17*, 2175.
[73] S. R. Cowan, N. Banerji, W. L. Leong, A. J. Heeger, *Adv. Funct. Mater.* **2012**, *22*, 1116.
[74] B. Zimmermann, U. Würfel, M. Niggemann, *Sol. Energy Mater. Sol. Cells* **2009**, *93*, 491.
[75] E. Voroshazi, B. Verreet, T. Aernouts, P. Heremans, *Sol. Energy Mater. Sol. Cells* **2011**, *95*, 1303.
[76] L. Tzabari, N. Tessler, *J. Appl. Phys.* **2011**, *109*, 064501.
[77] G. Shi, J. Yuan, X. Huang, Y. Lu, Z. Liu, J. Peng, G. Ding, S. Shi, J. Sun, K. Lu, H. Q. Wang, W. Ma, *J. Phys. Chem. C* **2015**, *119*, 25298.
[78] A. Rivaton, S. Chambon, M. Manceau, J. L. Gardette, N. Lemaître, S. Guillerez, *Polym. Degrad. Stab.* **2010**, *95*, 278.
[79] M. O. Reese, A. M. Nardes, B. L. Rupert, R. E. Larsen, D. C. Olson, M. T. Lloyd, S. E. Shaheen, D. S. Ginley, G. Rumbles, N. Kopidakis, *Adv. Funct. Mater.* **2010**, *20*, 3476.
[80] Y. Ohori, S. Fujii, H. Kataura, Y. Nishioka, *Jpn. J. Appl. Phys.* **2015**, *09*, 1.
[81] K. S. Nalwa, H. K. Kodali, B. Ganapathysubramanian, S. Chaudhary, *Appl. Phys. Lett.* **2011**, *99*, 4.
[82] M. Manceau, A. Rivaton, J. L. Gardette, S. Guillerez, N. Lemaître, *Polym. Degrad. Stab.* **2009**, *94*, 898.
[83] M. Manceau, A. Rivaton, J. L. Gardette, S. Guillerez, N. Lemaître, *Sol. Energy Mater. Sol. Cells* **2011**, *95*, 1315.
[84] T. Liu, A. Troisi, *J. Phys. Chem. C* **2011**, *115*, 2406.
[85] F. J. Lim, A. Krishnamoorthy, G. W. Ho, *ACS Appl. Mater. Interfaces* **2015**, *7*, 12119.

[86] S. J. Lee, H. P. Kim, A. R. B. M. Yusoff, J. Jang, *Org. Electron.* **2015**, *25*, 50.
[87] M. Koppe, C. J. Brabec, S. Heiml, A. Schausberger, W. Duffy, M. Heeney, I. McCulloch, *Macromolecules* **2009**, *42*, 4661.
[88] J. Kniepert, M. Schubert, J. Blakesley, D. Neher, *J. Phys. Chem. Lett.* **2011**, *700*.
[89] P. P. Khlyabich, B. Burkhart, B. C. Thompson, *J. Am. Chem. Soc.* **2012**, *134*, 9074.
[90] P. P. Khlyabich, B. Burkhart, B. C. Thompson, *J. Am. Chem. Soc.* **2011**, *133*, 14534.
[91] W. Keawsongsaeng, J. Gasiorowski, P. Denk, K. Oppelt, D. H. Apaydin, R. Rojanathanes, K. Hingerl, M. Scharber, N. S. Sariciftci, P. Thamyongkit, *Adv. Energy Mater.* **2016**, *6*, 1.
[92] J. J. Jasieniak, J. Seifter, J. Jo, T. Mates, A. J. Heeger, *Adv. Funct. Mater.* **2012**, *22*, 2594.
[93] G. Itskos, A. Othonos, T. Rauch, S. F. Tedde, O. Hayden, M. V. Kovalenko, W. Heiss, S. A. Choulis, *Adv. Energy Mater.* **2011**, *1*, 802.
[94] J. H. Huang, Y. S. Hsiao, E. Richard, C. C. Chen, P. Chen, G. Li, C. W. Chu, Y. Yang, *Appl. Phys. Lett.* **2013**, *103*, 1.
[95] S. Holliday, R. S. Ashraf, A. Wadsworth, D. Baran, S. A. Yousaf, C. B. Nielsen, C.-H. Tan, S. D. Dimitrov, Z. Shang, N. Gasparini, M. Alamoudi, F. Laquai, C. J. Brabec, A. Salleo, J. R. Durrant, I. McCulloch, *Nat. Commun.* **2016**, *7*, 11585.
[96] H. Hintz, H. J. Egelhaaf, H. Peisert, T. Chassé, *Polym. Degrad. Stab.* **2010**, *95*, 818.
[97] F. Hermerschmidt, A. Savva, E. Georgiou, S. M. Tuladhar, J. R. Durrant, I. McCulloch, D. D. C. Bradley, C. J. Brabec, J. Nelson, S. A. Choulis, *ACS Appl. Mater. Interfaces* **2017**, *9*, 14136.
[98] S. A. Hawks, J. C. Aguirre, L. T. Schelhas, R. J. Thompson, R. C. Huber, A. S. Ferreira, G. Zhang, A. A. Herzing, S. H. Tolbert, B. J. Schwartz, *J. Phys. Chem. C* **2014**, *118*, 17413.
[99] X. Guo, C. Cui, M. Zhang, L. Huo, Y. Huang, J. Hou, Y. Li, *Energy Environ. Sci.* **2012**, *5*, 7943.
[100] A. Guerrero, B. Dörling, T. Ripolles-Sanchis, M. Aghamohammadi, E. Barrena, M. Campoy-Quiles, G. Garcia-Belmonte, *ACS Nano* **2013**, *7*, 4637.
[101] I. F. Domínguez, P. D. Topham, P. O. Bussière, D. Bégué, A. Rivaton, *J. Phys. Chem. C* **2015**, *119*, 2166.
[102] T. Ameri, J. Min, N. Li, F. Machui, D. Baran, M. Forster, K. J. Schottler, D. Dolfen, U. Scherf, C. J. Brabec, *Adv. Energy Mater.* **2012**, *2*, 1198.
[103] J. C. Aguirre, S. A. Hawks, A. S. Ferreira, P. Yee, S. Subramaniyan, S. A. Jenekhe, S. H. Tolbert, B. J. Schwartz, *Adv. Energy Mater.* **2015**, *5*, 1.
[104] G. Li, V. Shrotriya, J. Huang, Y. Yao, T. Moriarty, K. Emery, Y. Yang, *Nat. Mater.* **2005**, *4*, 864.
[105] Q. Zhang, B. Kan, F. Liu, G. Long, X. Wan, X. Chen, Y. Zuo, W. Ni, H. Zhang, M. Li, Z. Hu, F. Huang, Y. Cao, Z. Liang, M. Zhang, T. P. Russell, Y. Chen, *Nat. Photonics* **2014**, *9*, 35.
[106] A. Garcia, G. C. Welch, E. L. Ratcliff, D. S. Ginley, G. C. Bazan, D. C. Olson, *Adv. Mater.* **2012**, *24*, 5368.
[107] L. A. Perez, J. T. Rogers, M. A. Brady, Y. Sun, G. C. Welch, K. Schmidt, M. F. Toney, H. Jinnai, A. J. Heeger, M. L. Chabinyc, G. C. Bazan, E. J. Kramer, *Chem. Mater.* **2014**, *26*, 6531.
[108] H.-Y. Chen, J. Hou, S. Zhang, Y. Liang, G. Yang, Y. Yang, L. Yu, Y. Wu, G. Li, *Nat. Photonics* **2009**, *3*, 649.
[109] L. Dou, J. You, J. Yang, C.-C. Chen, Y. He, S. Murase, T. Moriarty, K. Emery, G. Li, Y. Yang, *Nat. Photonics* **2012**, *6*, 180.

[110] Z. He, C. Zhong, S. Su, M. Xu, H. Wu, Y. Cao, *Nat. Photonics* **2012**, *6*, 593.
[111] S. H. Liao, H. J. Jhuo, Y. S. Cheng, S. A. Chen, *Adv. Mater.* **2013**, *25*, 4766.
[112] S. H. Liao, H. J. Jhuo, P. N. Yeh, Y. S. Cheng, Y. L. Li, Y. H. Lee, S. Sharma, S. A. Chen, *Sci. Rep.* **2014**, *4*, 6813.
[113] C. Yi, X. Hu, H. C. Liu, R. Hu, C.-H. Hsu, J. Zheng, X. Gong, *J. Mater. Chem. C* **2015**, *3*, 26.
[114] J. You, L. Dou, K. Yoshimura, T. Kato, K. Ohya, T. Moriarty, K. Emery, C.-C. Chen, J. Gao, G. Li, Y. Yang, *Nat. Commun.* **2013**, *4*, 1446.
[115] X. Du, T. Heumueller, W. Gruber, A. Classen, T. Unruh, N. Li, C. J. Brabec, *Joule* **2018**, 1.
[116] H. Li, T. Earmme, S. Subramaniyan, S. A. Jenekhe, *Adv. Energy Mater.* **2015**, 1402041.
[117] L. Ye, W. Zhao, S. Li, S. Mukherjee, J. H. Carpenter, O. Awartani, X. Jiao, J. Hou, H. Ade, *Adv. Energy Mater.* **2017**, *7*, 1.
[118] L. Ye, W. Jiang, W. Zhao, S. Zhang, Y. Cui, Z. Wang, J. Hou, *Org. Electron.* **2015**, *17*, 295.
[119] V. A. Trukhanov, D. Y. Paraschuk, *Polym. Sci. Ser. C* **2014**, *56*, 72.
[120] H. Sun, X. Song, J. Xie, P. Sun, P. Gu, C. Liu, F. Chen, Q. Zhang, Z.-K. Chen, W. Huang, *ACS Appl. Mater. Interfaces* **2017**, *9*, 29924.
[121] F. Shen, J. Xu, X. Li, C. Zhan, *J. Mater. Chem. A* **2018**, *6*, 15433.
[122] X. Liu, L. Ye, W. Zhao, S. Zhang, S. Li, G. M. Su, C. Wang, H. Ade, J. Hou, *Mater. Chem. Front.* **2017**, DOI 10.1039/C7QM00182G.
[123] Y. Lin, Y. Jin, S. Dong, W. Zheng, J. Yang, A. Liu, F. Liu, Y. Jiang, T. P. Russell, F. Zhang, F. Huang, L. Hou, *Adv. Energy Mater.* **2018**, *8*, 1.
[124] X. Li, X. Liu, W. Zhang, H. Q. Wang, J. Fang, *Chem. Mater.* **2017**, *29*, 4176.
[125] S. Li, L. Ye, W. Zhao, S. Zhang, S. Mukherjee, H. Ade, J. Hou, *Adv. Mater.* **2016**, *28*, 9423.
[126] S. Li, L. Ye, W. Zhao, S. Zhang, H. Ade, J. Hou, *Adv. Energy Mater.* **2017**, *7*, DOI 10.1002/aenm.201700183.
[127] W. Zhao, L. Ye, S. Li, X. Liu, S. Zhang, Y. Zhang, M. Ghasemi, C. He, H. Ade, J. Hou, *Sci. China Mater.* **2017**, *1109*, DOI 10.1007/s40843-017-9080-x.
[128] Y.-J. Hwang, B. a. E. Courtright, A. S. Ferreira, S. H. Tolbert, S. A. Jenekhe, *Adv. Mater.* **2015**, 27 (31), 4578-4584.
[129] N. Gasparini, A. Wadsworth, M. Moser, D. Baran, I. Mcculloch, C. J. Brabec, *Adv. Energy Mater.* **2018**, *1703298*, 1.
[130] N. Gasparini, M. Salvador, S. Strohm, T. Heumueller, I. Levchuk, A. Wadsworth, J. H. Bannock, J. C. de Mello, H. J. Egelhaaf, D. Baran, I. Mcculloch, C. J. Brabec, *Adv. Energy Mater.* **2017**, *1700770*, 1.
[131] N. Gasparini, M. Salvador, T. Heumueller, M. Richter, A. Classen, S. Shrestha, G. J. Matt, S. Holliday, S. Strohm, H. J. Egelhaaf, A. Wadsworth, D. Baran, I. Mcculloch, C. J. Brabec, *Adv. Energy Mater.* **2017**, *1701561*, 1.
[132] Y. Firdaus, L. P. Maffei, F. Cruciani, M. A. Müller, S. Liu, S. Lopatin, N. Wehbe, G. O. N. Ndjawa, A. Amassian, F. Laquai, P. M. Beaujuge, *Adv. Energy Mater.* **2017**, *1700834*, 1.
[133] B. Fan, L. Ying, P. Zhu, F. Pan, F. Liu, J. Chen, F. Huang, Y. Cao, *Adv. Mater.* **2017**, *1703906*, 1.
[134] A. F. Eftaiha, J.-P. Sun, I. G. Hill, G. C. Welch, *J. Mater. Chem. A* **2014**, *2*, 1201.
[135] Y. Cui, G. Jia, J. Zhu, Q. Kang, H. Yao, L. Lu, B. Xu, J. Hou, *Chem. Mater.* **2018**, *30*, 1078.
[136] H. Cha, J. Wu, A. Wadsworth, J. Nagitta, S. Limbu, S. Pont, Z. Li, J. Searle, M. F. Wyatt, D. Baran, J. S. Kim, I. McCulloch, J. R. Durrant, *Adv. Mater.* **2017**, *29*, 1.

[137] D. Baran, N. Gasparini, A. Wadsworth, C. H. Tan, N. Wehbe, X. Song, Z. Hamid, W. Zhang, M. Neophytou, T. Kirchartz, C. J. Brabec, J. R. Durrant, I. Mcculloch, *Nat. Commun.* **2018**, *9*, 2059.
[138] W. Zhao, D. Qian, S. Zhang, S. Li, O. Inganäs, F. Gao, J. Hou, *Adv. Mater.* **2016**, 4734.
[139] M. An, F. Xie, X. Geng, J. Zhang, J. Jiang, Z. Lei, D. He, Z. Xiao, L. Ding, *Adv. Energy Mater.* **2017**, *7*, 2.
[140] W. Zhao, S. Li, H. Yao, S. Zhang, Y. Zhang, B. Yang, J. Hou, *J. Am. Chem. Soc.* **2017**, *139*, 7148.
[141] J. Zhao, Y. Li, H. Lin, Y. Liu, K. Jiang, C. Mu, T. Ma, J. Y. Lin Lai, H. Hu, D. Yu, H. Yan, *Energy Environ. Sci.* **2015**, *8*, 520.
[142] Y. Zhang, Y. Xu, M. J. Ford, F. Li, J. Sun, X. Ling, Y. Wang, J. Gu, J. Yuan, W. Ma, *Adv. Energy Mater.* **2018**, *8*, 1.
[143] X. Zhang, C. Zhan, J. Yao, *ACS Chem. Mater.* **2015**, *27*, 166.
[144] S. Zhang, Y. Qin, J. Zhu, J. Hou, *Adv. Mater.* **2018**, *1800868*, 1.
[145] T. Yu, X. Xu, G. Zhang, J. Wan, Y. Li, Q. Peng, *Adv. Funct. Mater.* **2017**, *27*, 1.
[146] P. Kumaresan, S. Vegiraju, Y. Ezhumalai, S. Yau, C. Kim, W.-H. Lee, M.-C. Chen, *Polymers (Basel).* **2014**, *6*, 2645.
[147] N. Grossiord, J. M. Kroon, R. Andriessen, P. W. M. Blom, *Org. Electron.* **2012**, *13*, 432.
[148] M. C. Scharber, D. Mühlbacher, M. Koppe, P. Denk, C. Waldauf, A. J. Heeger, C. J. Brabec, *Adv. Mater.* **2006**, *18*, 789.
[149] B. C. Thompson, J. M. J. Fréchet, *Angew. Chemie - Int. Ed.* **2008**, *47*, 58.
[150] J. Xue, S. Uchida, B. P. Rand, S. R. Forrest, *Appl. Phys. Lett.* **2004**, *84*, 3013.
[151] H. C. Weerasinghe, S. E. Watkins, N. Duffy, D. J. Jones, A. D. Scully, *Sol. Energy Mater. SolarCells* **2014**, *132*, 485.
[152] S. R. Forrest, *Nature* **2004**, *428*, 911.
[153] W. Ma, C. Yang, X. Gong, K. Lee, A. J. Heeger, *Adv. Funct. Mater.* **2005**, *15*, 1617.
[154] S. E. Shaheen, C. J. Brabec, N. S. Sariciftci, F. Padinger, T. Fromherz, J. C. Hummelen, *Appl. Phys. Lett.* **2001**, *78*, 841.
[155] P. Wang, A. Abrusci, H. M. P. Wong, M. Svensson, M. R. Andersson, N. C. Greenham, *Nano Lett.* **2006**, *6*, 1789.
[156] P. Peumans, A. Yakimov, S. R. Forrest, *J. Appl. Phys.* **2003**, *93*, 3693.
[157] J. Peet, J. Y. Kim, N. E. Coates, W. L. Ma, D. Moses, A. J. Heeger, G. C. Bazan, *Nat. Mater.* **2007**, *6*, 497.
[158] I. Gur, N. A. Fromer, C. P. Chen, A. G. Kanaras, A. P. Alivisatos, *Nano Lett.* **2007**, *7*, 409.
[159] C. W. Tang, *Appl. Phys. Lett.* **1986**, *48*, 183.
[160] A. K. Ghosh, T. Feng, *J. Appl. Phys.* **1978**, *49*, 5982.
[161] N. S. Sariciftci, D. Braun, C. Zhang, V. I. Srdanov, A. J. Heeger, G. Stucky, F. Wudl, *Appl. Phys. Lett.* **1993**, *62*, 585.
[162] M. M. Wienk, J. M. Kroon, W. J. H. Verhees, J. Knol, J. C. Hummelen, P. A. van Hal, R. A. J. Janssen, *Angew. Chemie* **2003**, *115*, 3493.
[163] J. C. Hummelen, B. W. Knight, F. LePeq, F. Wudl, J. Yao, C. L. Wilkins, *J. Org. Chem.* **1995**, *60*, 532.
[164] G. Pirotte, P. Verstappen, D. Vanderzande, W. Maes, *Adv. Electron. Mater.* **2018**, *4*, 1700481.
[165] M. Baldo, M. Deutsch, P. Burrows, H. Gossenberger, M. Gerstenberg, V. Ban, S. Forrest, *Adv. Mater.* **1998**, *10*, 1505.
[166] M. Shtein, P. Peumans, J. B. Benziger, S. R. Forrest, *J. Appl. Phys.* **2003**, *93*, 4005.

[167] M. Shtein, P. Peumans, J. B. Benziger, S. R. Forrest, *J. Appl. Phys.* **2004**, *96*, 4500.
[168] Y. Sun, M. Shtein, S. R. Forrest, *Appl. Phys. Lett.* **2005**, *86*, 113504.
[169] F. C. Krebs, *Sol. Energy Mater. Sol. Cells* **2009**, *93*, 394.
[170] D. Bartesaghi, I. D. C. Pérez, J. Kniepert, S. Roland, M. Turbiez, D. Neher, L. J. A. Koster, *Nat. Commun.* **2015**, *6*, 7083.
[171] H. Hoppe, N. S. Sariciftci, *J. Mater. Res.* **2004**, *19*, 1924.
[172] N. F. Mott, *Can. J. Phys.* **1956**, *34*, 1356.
[173] R. Hoffmann, C. Janiak, C. Kollmar, *Macromolecules* **1991**, *24*, 3725.
[174] B. L. Olivia-Chatelain & A. R. Barron, **2011**, 14.
[175] J. Kalowekamo, E. Baker, *Sol. Energy* **2009**, *83*, 1224.
[176] S.-H. Liao, H.-J. Jhuo, P.-N. Yeh, Y.-S. Cheng, Y.-L. Li, Y.-H. Lee, S. Sharma, S.-A. Chen, *Sci. Rep.* **2014**, 4, 6813.
[177] J. Yuan, Y. Zhang, L. Zhou, G. Zhang, H.-L. Yip, T.-K. Lau, X. Lu, C. Zhu, H. Peng, P. A. Johnson, M. Leclerc, Y. Cao, J. Ulanski, Y. Li, Y. Zou, *Joule* **2019**, DOI 10.1016/J.JOULE.2019.01.004.
[178] S. Li, L. Ye, W. Zhao, H. Yan, B. Yang, D. Liu, W. Li, H. Ade, J. Hou, *J. Am. Chem. Soc.* **2018**, jacs. 8b02695.
[179] T. Kumari, S. M. Lee, S. H. Kang, S. Chen, C. Yang, *Energy Environ. Sci.* **2017**, *10*, 258.
[180] L. Meng, Y. Zhang, X. Wan, C. Li, X. Zhang, Y. Wang, X. Ke, Z. Xiao, L. Ding, R. Xia, H.-L. Yip, Y. Cao, Y. Chen, *Science* **2018**, *361*, 1094.
[181] NREL, "Best Research-Cell Efficiency Chart | Photovoltaic Research | NREL," https://www.nrel.gov/pv/cell-efficiency.html, **2019 (accessed on Mar. 6, 2019)** .
[182] M. A. Green, K. Emery, D. L. King, S. Igari, W. Warta, *Prog. Photovoltaics Res. Appl.* **2004**, *12*, 55.
[183] X. Xu, K. Feng, Z. Bi, W. Ma, G. Zhang, Q. Peng, *Adv. Mater.* **2019**, 1901872.
[184] Y. Cui, H. Yao, J. Zhang, T. Zhang, Y. Wang, L. Hong, K. Xian, B. Xu, S. Zhang, J. Peng, Z. Wei, F. Gao, J. Hou, *Nat. Commun.* **2019**, *10*, 2515.
[185] P. Cheng, L. Ye, X. Zhao, J. Hou, Y. Li, X. Zhan, *Energy Environ. Sci.* **2014**, *7*, 1351.
[186] L. A. Perez, K. W. Chou, J. A. Love, T. S. Van Der Poll, D. M. Smilgies, T. Q. Nguyen, E. J. Kramer, A. Amassian, G. C. Bazan, *Adv. Mater.* **2013**, *25*, 6380.
[187] A. Zusan, B. Gieseking, M. Zerson, V. Dyakonov, R. Magerle, C. Deibel, *Sci. Rep.* **2015**, *5*, 1.
[188] F. C. Krebs, *Stability and Degradation of Organic and Polymer Solar Cells*, **2012**, pp. 341.
[189] M. O. Reese, A. M. Nardes, B. L. Rupert, R. E. Larsen, D. C. Olson, M. T. Lloyd, S. E. Shaheen, D. S. Ginley, G. Rumbles, N. Kopidakis, *Adv. Funct. Mater.* **2010**, *20*, 3476.
[190] W. R. Mateker, T. Heumueller, R. Cheacharoen, I. T. Sachs-Quintana, M. D. McGehee, J. Warnan, P. M. Beaujuge, X. Liu, G. C. Bazan, *Chem. Mater.* **2015**, *27*, 6345.
[191] M. Manceau, S. Chambon, A. Es Rivaton, J.-L. Gardette, S. Guillerez, N. L. Lemaˆıtre, **2010**, DOI 10.1016/j.solmat.2010.03.012.
[192] M. Jørgensen, K. Norrman, S. A. Gevorgyan, T. Tromholt, B. Andreasen, F. C. Krebs, *Adv. Mater.* **2012**, *24*, 580.
[193] S. A. Gevorgyan, M. V. Madsen, B. Roth, M. Corazza, M. Hösel, R. R. Søndergaard, M. Jørgensen, F. C. Krebs, *Adv. Energy Mater.* **2016**, *6*, 1501208.

2

Materials, Devices, and Tools to Probe Degradation Mechanisms

"There are more colourful flowers on the path of life, but the prettiest have the sharpest thorns." – African Proverb

Partly based on the Publications in the next four chapters

2.1. Introduction

This chapter gives an account of the general setting of the thesis regarding experiments and theories. First, the various materials considered under the studies are presented spanning polymer donor materials, to fullerene derivatives, and small molecule acceptor materials through solvents and solvent additives. Next, it briefly touches on the type of devices considered in the entire thesis. Finally, we look at the tools and related characterisation techniques for probing the performance of the devices (both efficiency and stability) and some of the few theories behind the methods explored in the quest of our investigations to explain the findings of the thesis as expounded in each of the imminent chapters.

2.2. Materials

The bulk heterojunction (BHJ) active layer configuration[1] is explored throughout the whole thesis for blend devices. The active layer mostly consists of a donor (D) material and an acceptor (A) material in a binary system.[2–10] In a ternary system, it either consists of donor materials 1 and 2 (D_1, D_2) and an acceptor material (A) in a D_1:D_2:A configuration or of a donor material (D) and acceptor materials 1 and 2 (A_1, A_2) in a D:A_1:A_2 configuration.[2–6,9–40] In our case, the ternary system consists of two acceptor materials in a D:A_1:A_2 configuration.

2.2.1. Donor materials

In the following chapters, semiconducting polymers are used as donor materials. Our focus is on the state-of-the-art high-performing polymers regarding efficiency in the polymer solar cell technology. We probe both fullerene and non-fullerene polymer solar cells (PSCs). In both types of cells we target the push-pull[2,23,34,41–74] or donor(D)-acceptor(A) type of polymers, especially in our case, the benzodithiophene (BDT)-units based polymers[44,72,73,75–88]. This alternation of electron-rich (donor/push) and electron-deficient (acceptor/pull) moieties leads to a substantial decrease of the bandgap. We study a wide range of benzodithiophene-co-thieno[3,4-b]thiophene (BDT-TT) unit polymers,[14,27,40,50,78,81,82,86,89–126] with their structures shown in **Figure 2.1.**

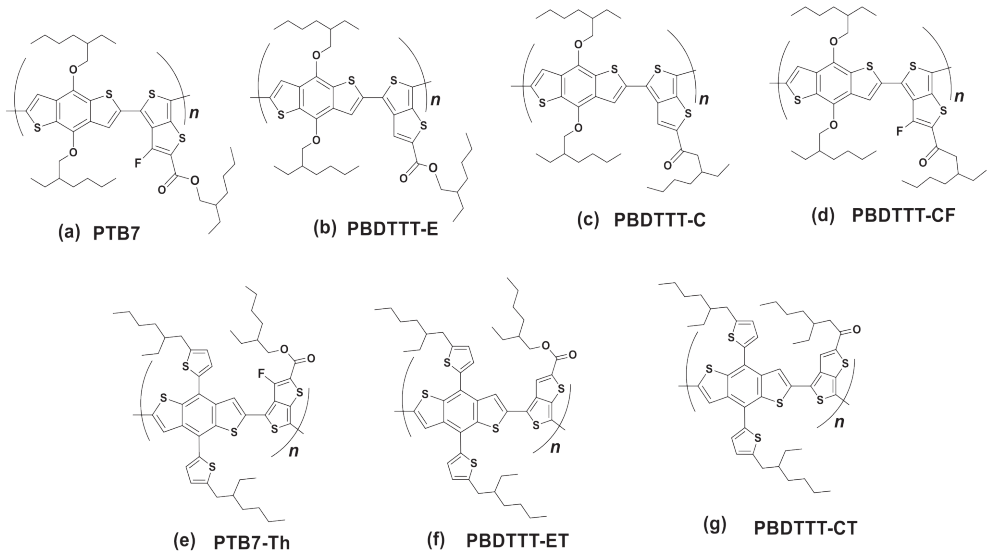

Figure 2.1: Chemical structures of used BDT-TT polymer donor materials. This class of polymers yielded above 10% efficiency in fullerene-based solar cells.

The structure of the other studied polymer, PBDB-T, is shown in **Figure 2.2.** All polymers are either purchased from Solarmer Energy Inc. and Brilliant Matters (only in the case of PBDB-T) or obtained from the Hou group (Chinese Academy of Sciences). In chapters 3 and 7, BDT-monomers are used to elucidate the role played by the BDT-side chains in the photostability of the solar cells. The BDT-monomers are synthesised by the Chiechi group (University of Groningen).

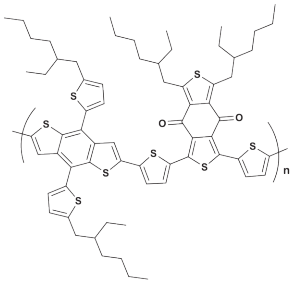

Figure 2.2: Chemical structure of PBDB-T. This polymer heralded the breakthrough in recent times in non-fullerene solar cells with more than 11% initial efficiency.

2.2.2. Acceptor Materials

The commonly used acceptor materials are fullerene derivatives[127] and small molecules[74,128–131]. In this thesis, we mainly consider [70]PCBM as the fullerene derivative acceptor material and ITIC with its derivatives, IT-M[128] and IT-F[129,132], as the small molecule acceptor materials. **Figure 2.3** displays the structures of all acceptors employed in the thesis. The fullerene derivative acceptors are purchased from Solenne BV, while the ITIC derivatives are either bought from Brilliant Matters or Solarmer Energy Inc. or obtained from the Hou group.

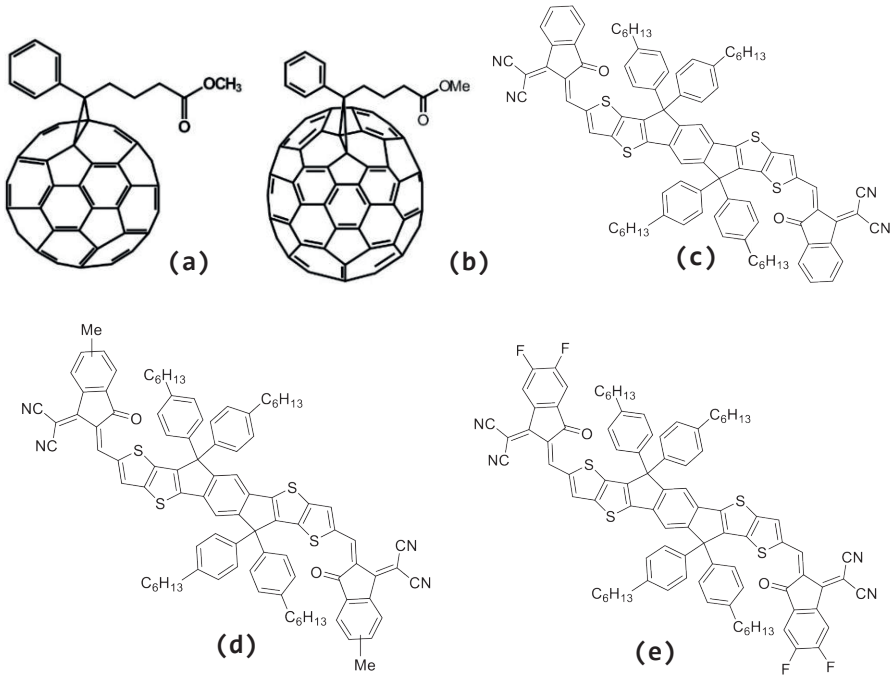

Figure 2.3: Chemical structure of fullerene derivatives from Ref. [133,134]: [60]PCBM **(a)** and [70]PCBM **(b)**; and ITIC derivatives: ITIC **(c)**, IT-M **(d)**, and IT-F **(e)**.

2.2.3. Solvents and Solvent Additives

The used donor and acceptor materials are soluble in halogenated organic solvents, mostly chlorinated, such as chlorobenzene (CB), 1,2-dichlorobenzene (oDCB), and chloroform (CF). In some rare cases, solvent additives such as 1,8-diiodooctane (DIO), 1-chloronaphthalene (CN), and 1,8-octanedithiol (ODT) are used for intended improvement in the active layer morphology, resulting in a probable increase in the efficiency. All used solvents are anhydrous, acquired from Sigma-Aldrich Co., and used as received without further purification.

2.3. Solution Processing of the Donor and Acceptor Materials

For solar cells, two active layer systems are studied, namely, the D:A binary system and the D:A_1:A_2 ternary system. In the binary system, for the polymer:ITIC and polymer:[70]PCBM solutions, blends in a ratio of 1:1 and 1:1.5 are respectively dissolved in anhydrous CB or oDCB with or without solvent additive at a concentration of 20 (or 25) mg.mL^{-1} and stirred at 40 (or 60)°C overnight in a glovebox. In the ternary system, the same concentrations are used, except only the acceptor ratio (A_1:A_2) is varied from 0 to 1. This ratio changes from 0 to 1.5 when PTB7-Th is used. When the solar cells are processed with a solvent additive, DIO is mostly used unless otherwise specified. It is 3v% of the total volume of the solvent when used in a polymer:[70]PCBM active layer solution, while, amounting only to 0.5v% of the solution in polymer:ITIC active layer solution.

For single carrier devices, either [70]PCBM (60 mg.mL^{-1}), or ITIC derivatives (15 mg.mL^{-1}), or pristine polymers (20 mg.mL^{-1}), or blends as described above are similarly dissolved, mostly in either anhydrous CF, or CB, or oDCB with or without DIO.

2.4. Devices

Spin coating is used as the technique for processing the active layer for the solar cells, single carrier devices, and films on glass for thin film characterisation unless otherwise stated. Before the spin coating process,

glass or pre-patterned ITO glass substrates are cleaned respectively in soap, deionised water, then in acetone and isopropanol with ultrasonic bath for at least 10 minutes each and spin dried. Next, the substrates are annealed in an oven at 140°C for 10 minutes and then treated in UV-ozone for 20 minutes. The dissolved materials are used to either fabricate conventional solar cells, inverted solar cells, single carrier devices, or films on glass.

For solar cells, the blend solutions are spin coated at 800 rpm for 5 seconds and spin dried for 120 seconds for the BDT-TT polymer-based devices and 1500 rpm for 5 seconds and spin dried for 60 seconds for PBDB-T-based devices. The films are left in vacuum overnight, and the devices are finished by thermal evaporation at < 10^{-8} Torr. For single carrier devices, the solutions are spin coated at 600 rpm for 5 seconds and spin dried for 120 seconds for the BDT-TT polymer-based devices and 1200 rpm for 5 seconds and spin dried for 60 seconds for PBDB-T-based devices atop their respective substrates. The thickness of the active layers of the devices varies depending on the materials used and the spin coating parameters.

Finally, films of pristine polymers, of [70]PCBM, and of blends are made either by spin coating on glass substrates for two-dimensional grazing incidence wide-angle X-ray scattering (2D GIWAXS), atomic force microscopy (AFM), and UV-Vis absorption measurements or by drop casting on potassium bromide (KBr) crystals for Fourier transform infra-red (FTIR) spectroscopy measurements.

2.4.1. Solar cells

The thorough photo-induced degradation investigation in this work makes a unique effort to combine studies at the frontiers of chemistry, device physics, and new technological tools to probe the different mechanisms. Thus, the reader will frequently come across studies conducted on the aforementioned materials, on the one hand, in the liquid state involving absorption and ^{1}H-NMR measurements; and on the other hand, in the solid state, notably, in thin films and in full devices, comprising among others of absorption, electrical characteristics, AFM, etc. The devices include solar cells and single carrier devices.

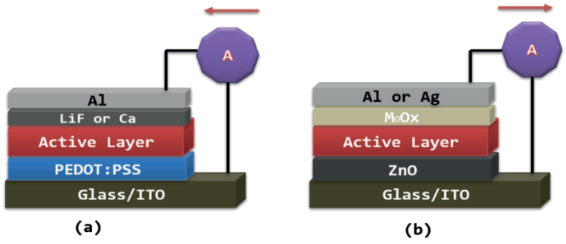

Figure 2.4: Bulk heterojunction Solar cell device structures employed in the thesis: Conventional **(a)** and inverted **(b)** solar cells with the current at V < V_{oc}.

2.4.2. Conventional Solar Cells

To obtain conventional solar cells, PEDOT:PSS (VP AI4083, H.C. Starck) solution is spin coated in ambient conditions atop the pre-patterned ITO glass substrates to form a 45-55 nm layer which is subsequently dried in an oven at 140°C for 10 minutes. The PEDOT:PSS layer serves as the hole transporting layer (HTL) on top of the ITO. Then, the active layer solution

is spin coated to achieve an almost homogeneous thin film, and the devices are finished with lithium fluoride (LiF, 1 nm) or calcium (Ca, 20 nm) and aluminium (Al, 100 nm) with the following structure ITO/PEDOT:PSS/Blend with or without DIO/LiF (Ca)/Al. When ITIC is employed in the active layer, the thin films are annealed at 100°C for 10 minutes before the deposition of the top electrodes. The structural illustration of a conventional device is shown in **Figure 2.4a**.

2.4.3. Inverted Solar Cells

In the inverted structure, PEDOT:PSS is replaced by zinc oxide (ZnO, ~30 nm) while, LIF/Al or Ca/Al is replaced by molybdenum oxide (MoO_x, 5-10 nm) with either Al or silver (Ag). The final device structure, as shown in **Figure 2.4b,** is ITO/ZnO/blend with or without DIO/MoO_x/Al (Ag). When ITIC is used in the active layer, the thin films are annealed at 160°C for 10 minutes before the evaporation of the top electrodes. The ZnO solution is prepared by dissolving zinc acetate (109.67 mg) in 2-methoxyethanol (1 mL) and ethanolamine (30.2 µL). The solution is then stirred at room temperature for a few hours.

2.4.4. Single Carrier Devices

Single carrier devices are designed in such a way that only one carrier type, either electrons or holes, is injected into the devices. Or in other

words, these devices are predominantly either electron-driven or hole-driven, that is the injection of either carrier type is enhanced or suppressed. Thus, they are referred to as electron-only (EO) or hole-only (HO) devices. Their active layer can either be made of only pristine materials: i) acceptors for EO devices and ii) donors for HO devices, or blends of D:A materials for both EO and HO devices.

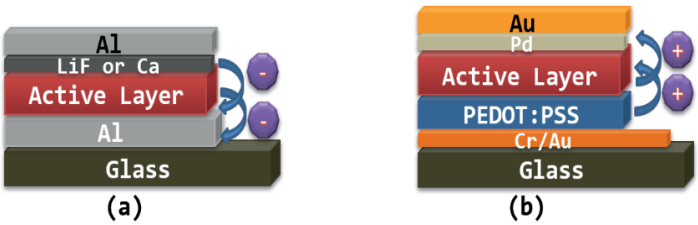

Figure 2.5: Single carrier device structures: electron-only **(a)** and hole-only **(b)** devices.

To fabricate the single carrier devices, the solutions are spin coated atop their respective substrates, composed of glass and previously evaporated bottom contacts: Al (20 nm) for EO devices or chromium (Cr, 1 nm) and gold (Au, 20 nm) for HO devices. Atop the active layers, the top electrodes are evaporated under the same condition as previously described. The EO devices have the following structure: Al (20 nm)/[70]PCBM (blend)/LiF (1 nm)/Al (100 nm) and the HO devices have the following structure: Cr (1 nm)/Au (20 nm)/PEDOT:PSS/pristine polymer (or blend)/Pd (15 nm)/Au (80 nm), where Pd is palladium. Other commonly used geometrical structures for EO and HO devices are respectively ITO/ZnO/active layer/(Ca)/Al (or Ag) and ITO/PEDOT:PSS/active layer/Au.[135] **Figure 2.5** presents the architecture of the single carrier devices mostly studied in the thesis.

2.5. Tools to Probe Degradation Mechanisms

We exclusively focus on photodegradation, the effect of continuous exposure of the solar cells to sunlight. To achieve this goal, we solely fabricated and studied our devices under glovebox conditions, an inert atmosphere (with H_2O and O_2 <0.1 ppm). We also kept the cells at constant room temperature ~295 K by active cooling with the aid of a controlled nitrogen gas flow using a liquid nitrogen bath. A simulated AM 1.5G white light with an irradiance of 1000 $W.m^{-2}$, a Steuernaugel SolarConstant 1200 metal halide lamp is used.

2.5.1. Current-Voltage Characterization

The current density-voltage (*J-V*) characteristics is a simple but powerful tool to i) measure with a high degree of certainty the performance of the solar cells both regarding efficiency and stability, ii) monitor the recombination dynamics in the solar cells, and iii) study the charge transport mechanisms in single carrier devices.

2.5.2. Solar cells: Efficiency

The *J-V* characteristics help to determine the solar cell parameters discussed in chapter 1, section 1.6. In all our experiments, the *J-V* parameters are measured, and the curves are obtained for unencapsulated

PSCs in the dark and under illumination in the glovebox, using a computer-controlled Keithley 2400 source meter. The intensity of the light is calibrated using a mono-silicon reference cell for one sunlight intensity of 1000 $W.m^{-2}$ and corrected for the spectral mismatch.[136]

2.5.3. Solar cells: Stability/Photodegradation

The behaviour of the *J-V* parameters of a solar cell over time, in the presence of degradation agents, is used to assess the stability performance of a solar cell. The trend in the time-evolution behaviour of, for example, J_{sc}, V_{oc}, and FF may give a preliminary indication/idea about the possible source of degradation. Further investigations are, however, needed to pinpoint the source/cause of the observed degradation. The procedure for studying stability in organic solar cells is so complex and diverse that protocols have been put in place and must be followed for public and scientific community trust. The details of these protocols can be found under "characterisation and reporting of OPV device lifetime".[137] The reported solar cells in this thesis are operated under open circuit conditions, in a controlled environment using the light-soaking test (ISOS-L). It simply aims at degrading the devices under indoor conditions using solar simulator light sources such as the one described above. Reporting the lifetime of a solar cell is not so trivial. This is due to the different decay curves that have been recorded over the years, making it hard to single out a quantity that would correctly describe and report the lifetime.

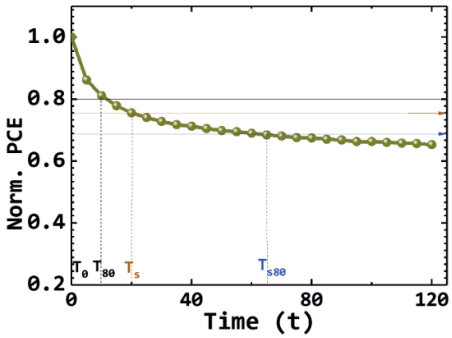

Figure 2.6: Solar cell lifetime estimation. T_o time at initial efficiency and T_s time close to before the start of the linear slow degradation regime. T_{80} is the lifetime of a solar cell according to a typical degradation curve and T_{s80} is the lifetime of the solar cell considering the stretched exponential regime of the decay curve.

In our study, a typical decay curve would have two regimes. Namely, a rapid non-linear decay regime, also referred to as burn-in,[43,104,108,138–141] followed by a slow stretched exponential degradation regime. The lifetime of such solar cell behaviour can be reported using the well-accepted lifetime parameter, T_{80}.[103,137,141–145] T_{80} is the time it takes a solar cell to retain 80% of its initial efficiency. In other words, it is the time at which the solar cell achieves a 20% decay or loses 20% of its initial efficiency. In some cases where T_{80} underestimates the lifetime of the solar cell depending on the nature of the curve or how pronounced the burn-in phase is, then T_{s80}[120,137,141] is used. T_{s80} is the time it takes the solar cell to retain 80% of its efficiency after the T_{80} or considering the stretched exponential regime of the decay curve.

For the photodegradation stability measurement, the cells are continuously exposed to simulated light, in an inert atmosphere (with <0.1 ppm H_2O and

<0.1 ppm O_2) for two hours while being kept at ~295 K by actively cooling. The time evolution of the *J-V* parameters is monitored. Measurements are taken at intervals of 5 minutes for 1 hour, 2 hours, 4 hours, and 8 hours. The preliminary measurements revealed that the 2 hour-measurement is representative of the time-evolution behaviour of the cells. Due to the load, the intensive nature of the work presented in this thesis, and to be able to measure devices within a day or two, we opt for the 2 hour-measurements as the benchmark, and thus, all results presented in the thesis are solely for this timeframe unless otherwise stated.

2.5.4. Recombination: Bimolecular and Trap-assisted

Light intensity dependence measurements on OPVs may reveal relevant information on the recombination dynamics present in the solar cells, either bimolecular or trap-assisted recombination or both. The ideality factor (n) as determined from the dependence of V_{oc} on the light intensity, can be used to assess the recombination losses in solar cells.[146] nKT/q, the slope of the V_{oc} against varying light intensity, is a signature of the recombination mechanisms present in a solar cell. A stronger dependence of V_{oc} on light intensity reveals that there are more traps in the system.[147] If $1<n<2$ then trap-assisted recombination is dominant,[147] however, $n\sim1$ means bimolecular recombination is dominant. The α (as in $J\sim I^{\alpha}$) value as determined from the dependence of J_{sc} on light intensity is seldom used to also assess the recombination in solar cells.

For light intensity dependence measurement, the solar cells, kept at ~295 K, are continuously exposed to light calibrated with a long-pass filter to one sun for a duration of two to three (2-3) hours and the *J-V* sweeps are recorded at 1-hour interval with varying light intensity using a set of neutral density filters coupled with the long-pass filter.

2.5.5. Charge Transport in Single Carrier Devices

In single carrier devices, the current flow is limited by a build-up of space charges and referred to as space charge limited current (SCLC). The SCLC method is a simple but reliable tool to determine the mobility in an experimental setting.[148] The obtained data from the charge transport measurements are fitted to the modified Mott–Gurney (Murgatroyd) equation:[149]

$$J = \frac{9}{8}\,\varepsilon_o\varepsilon_r\mu_{on}\exp(0.891\gamma_n\sqrt{\frac{V_{int}}{L}})\,\frac{V_{int}^2}{L^3} \qquad (2.1)$$

where J is SCLC density, ε_o and ε_r are the electric permittivity of free space and the relative dielectric constant of the active layer respectively, μ_{on} is the charge carrier mobility, L is the thickness of the device and γ_n is the electric field-activation factor, with the voltage on the active layer given by: $V_{int} = V - V_{bi} - V_{rs}$ (2.2)

where V is the applied voltage, V_{bi} the built-in voltage and V_{rs} is the voltage drop due to the series resistance of the contacts.

The ratio of the maximum mobility to the minimum mobility (μ_{max}/μ_{min}) gives an idea of how balanced the charge carriers are in the active layer system. When (μ_{max}/μ_{min})=1, then charge carriers are balanced in the system; however, a ratio >1 indicates the opposite.

For the single carrier devices, the active layer films are first exposed to light for an hour at ~295 K before the evaporation of the top contact electrodes. The *J-V* sweeps are obtained under dark only for fresh and exposed devices. The data are all fitted to equation (2.1), and the mobilities are extracted. The electron and/or hole mobilities can be indirectly estimated by cautiously selecting the electrodes to either suppress or enhance the injection of one type of charge carriers.

2.5.6. Absorption

The UV-VIS-NIR spectroscopy is a tool used to measure the absorption spectrum of (OPV) materials. It can also be used to monitor the relative stability of the materials by detecting a loss rate in absorption caused by degradation agents throughout ageing.

For the UV-VIS-NIR absorption measurement, pristine acceptor, pristine donor polymer, and blend (polymer:acceptor) solutions are spin coated into films on glass and measured before and after 2 hours of light exposure.[80] The spectra of the films are obtained against the spectrum of a glass reference using a UV-VIS-NIR spectrometer (UV-3600) with tungsten-iodide (WI) monochromatic light source scanning within a 300–900 nm range.[80]

2.5.7. Atomic Force Microscopy

The use of atomic force microscopy (AFM) as a tool[150] to study degradation is merely restricted to a support role to other established and insightful methods. AFM images reveal the nanoscale morphology of the films; mainly, it is used to monitor the changes in the active layer.

The AFM images are obtained in collaboration with the Chiechi group. As-cast and exposed pristine films of donor polymers or acceptors and blend films of donor:acceptor (D:A) on glass are investigated for morphological differences in ScanAsyst mode on a Bruker Multimode 8 microscope (Model number: MMAFM-2) with ScanAsyst-Air probes (spring constant: 0.4 $N.m^{-1}$, resonant frequency: 70 kHz, nominal tip radius: 2 nm). All samples are scanned at 5 µm, 1 µm, and 500 nm at a scan rate of 0.8 Hz and a resolution of 640 samples per line. Both height and peak force errors are collected.

2.5.8. ^{1}H-Nuclear Magnetic Resonance

The most versatile yet simple analytical technique to determine the spatial structure of a compound is the nuclear magnetic resonance (NMR). In the context of degradation, any change in local structure can be observed when comparing the initial spectrum to the spectrum of the degraded material in the same solvent. It is understood degradation by-products result in either chemical peak shifting or disappearance and/or appearance of new peaks.

The ^{1}H NMR measurements are conducted by our collaborators from the Chiechi group. BDT-unit monomer solutions are prepared in an inert atmosphere and put into air-tight NMR glass tubes. The fresh solutions are transferred from the glovebox into the NMR set-up, a computer-controlled Varian AMX 600 (600 MHz), where ^{1}H-NMR spectra are obtained and recorded. Next, the solutions are exposed to UV light (IntelliRay, Uvitron 600 W, shuttered UV floodlight, at 50% power) in steps of 10 minutes for 100 minutes. ^{1}H-NMR spectra are measured after each 10-minute exposure to UV. Chemical shift values are reported in ppm with the solvent resonance as the internal standard.

2.5.9. Fourier Transform Infrared Spectroscopy

The chemical changes that occur as a consequence of degradation result in the formation of decomposition products in the active films, involving functional groups specific to a particular type of polymer or material and at a rate that strongly depend on the polymer chemical structure.[80,137,151,152] The Fourier transform infrared spectroscopy (FTIR) has become the modern technique in this direction for precise documentation of these products and perhaps vital to understand the degradation mechanisms. The chemical changes and by-products lead to substantial changes in the IR spectrum which can be obtained either in transmission mode or absorption mode. The comparison of the initial spectrum to the one obtained after degradation or subtraction of the initial spectrum from the one obtained after

degradation gives a fair idea of the rate of the degradation, the products formed, and the possible mechanisms involved.

The measurements are performed on both the as-cast and exposed films against KBr crystal as a reference with a Shimadzu IR-Tracer-100 FTIR spectrometer in transmittance mode from 400 to 4000 cm^{-1}. The spectra are then converted to absorbance for comparison.

2.5.10. 2D Grazing-Incidence Wide-Angle X-ray Scattering

Grazing-Incidence Wide-Angle X-ray Scattering (GIWAXS) is used to monitor structural details or changes wherein wide-angle scattering is collected.[153]

The GIWAXS measurements are conducted by our collaborators from the Portale group (University of Groningen). GIWAXS measurements are performed using the MINA instrument, an X-ray scattering instrument built on a Cu rotating anode source (l=1.5413 Å). 2D patterns are collected using a Vantec500 detector (1024x1024 pixel array with a pixel size 136 x 136 microns) located 122 mm away from the sample. The thin films are placed in reflection geometry at certain incident angles a_i to the direct beam using a Huber goniometer. GIWAXS patterns were acquired using incident angles of 0.2° (close to the incident angle of the materials). An exposure time of 1 h per pattern is used. The direct beam centre position on the detector and the sample-to-detector distance were calibrated using the diffraction rings

from standard silver behenate and Al_2O_3 powders. The 2D GIWAXS patterns are presented as a function of the in-plane modulus of the scattering vector q_y and that of the near out-of-plane scattering vector q_z, defined as:

$$q_y = \frac{2\pi}{\lambda}\left[sin(2\theta_f)cos(\alpha_f)\right] \quad \textbf{(2.3)}$$

and $$q_z = \frac{2\pi}{\lambda}\left[sin(\alpha_f) + sin(\alpha_i)\right] \quad \textbf{(2.4)}$$

In the following chapters, a combination of theories and experiments involving device physics, chemistry, and the above-discussed characterisation tools are employed to elucidate the role of the difference in chemical structures of either the donor materials or the acceptor materials in the photostability of both conventional and inverted solar cells. Our work systematically investigates comparatively the different materials, namely donors and acceptors.

Bibliography

[1] G. Yu, J. Gao, J. C. Hummelen, F. Wudl, A. J. Heeger, *Science* **1995**, *270*, 1789.
[2] L. Lu, M. A. Kelly, W. You, L. Yu, *Nat. Photonics* **2015**, *9*, 491.
[3] H. Lu, J. Zhang, J. Chen, Q. Liu, X. Gong, S. Feng, X. Xu, W. Ma, Z. Bo, *Adv. Mater.* **2016**, *28*, 9559.
[4] W. Zhong, J. Cui, B. Fan, L. Ying, Y. Wang, X. Wang, G. Zhang, X. F. Jiang, F. Huang, Y. Cao, *Chem. Mater.* **2017**, *29*, 8177.
[5] P. P. Khlyabich, B. Burkhart, B. C. Thompson, *J. Am. Chem. Soc.* **2011**, *133*, 14534.
[6] R. Yu, H. Yao, J. Hou, *Adv. Energy Mater.* **2018**, *1702814*, 1.
[7] S. Westenhoff, I. A. Howard, J. M. Hodgkiss, K. R. Kirov, H. A. Bronstein, C. K. Williams, N. C. Greenham, R. H. Friend, *J. Am. Chem. Soc.* **2008**, *130*, 13653.
[8] J. De Chen, Y. Q. Li, J. Zhu, Q. Zhang, R. P. Xu, C. Li, Y. X. Zhang, J. S. Huang, X. Zhan, W. You, J. X. Tang, *Adv. Mater.* **2018**, *1706083*, 1.
[9] G. Itskos, A. Othonos, T. Rauch, S. F. Tedde, O. Hayden, M. V. Kovalenko, W. Heiss, S. A. Choulis, *Adv. Energy Mater.* **2011**, *1*, 802.
[10] C. Kästner, S. Rathgeber, D. A. M. Egbe, H. Hoppe, *J. Mater. Chem. A* **2013**, *1*, 3961.
[11] R. Betancur, A. Martínez-Otero, X. Elias, P. Romero-Gómez, S. Colodrero, H. Miguez, J. Martorell, *Sol. Energy Mater. Sol. Cells* **2012**, *104*, 87.
[12] M. Campoy-Quiles, Y. Kanai, A. El-Basaty, H. Sakai, H. Murata, *Org. Electron.* **2009**, *10*, 1120.
[13] P. Cheng, J. Wang, Q. Zhang, W. Huang, J. Zhu, R. Wang, S. Y. Chang, P. Sun, L. Meng, H. Zhao, H. W. Cheng, T. Huang, Y. Liu, C. Wang, C. Zhu, W. You, X. Zhan, Y. Yang, *Adv. Mater.* **2018**, *30*, 1.
[14] A. D. de Zerio, C. Müller, *Adv. Energy Mater.* **2018**, *1702741*, 1.
[15] B. Gao, H. Yao, J. Hou, R. Yu, L. Hong, Y. Xu, J. Hou, *J. Mater. Chem. A* **2018**, DOI 10.1039/C8TA09830A.
[16] N. Gasparini, L. Lucera, M. Salvador, M. Prosa, G. D. Spyropoulos, P. Kubis, H. J. Egelhaaf, C. J. Brabec, T. Ameri, *Energy Environ. Sci.* **2017**, *10*, 885.
[17] Y. J. Hwang, H. Li, B. A. E. Courtright, S. Subramaniyan, S. A. Jenekhe, *Adv. Mater.* **2016**, *28*, 124.
[18] L. Ke, J. Min, M. Adam, N. Gasparini, Y. Hou, J. D. Perea, W. Chen, H. Zhang, S. Fladischer, A. C. Sale, E. Spiecker, R. R. Tykwinski, C. J. Brabec, T. Ameri, *Adv. Energy Mater.* **2016**, *6*, 1.
[19] W. Keawsongsaeng, J. Gasiorowski, P. Denk, K. Oppelt, D. H. Apaydin, R. Rojanathanes, K. Hingerl, M. Scharber, N. S. Sariciftci, P. Thamyongkit, *Adv. Energy Mater.* **2016**, *6*, 1.
[20] P. P. Khlyabich, B. Burkhart, B. C. Thompson, *J. Am. Chem. Soc.* **2012**, *134*, 9074.
[21] K. Kranthiraja, U. K. Aryal, V. G. Sree, K. Gunasekar, C. Lee, M. Kim, B. J. Kim, M. Song, S. H. Jin, *ACS Appl. Mater. Interfaces* **2018**, *10*, 13748.
[22] T. Kumari, S. M. Lee, S. H. Kang, S. Chen, C. Yang, *Energy Environ. Sci.* **2017**, *10*, 258.
[23] J. W. Lee, Y. S. Choi, H. Ahn, W. H. Jo, *ACS Appl. Mater. Interfaces* **2016**, *8*, 10961.
[24] T. Liu, Y. Guo, Y. Yi, L. Huo, X. Xue, X. Sun, H. Fu, W. Xiong, D. Meng, Z. Wang, F. Liu, T. P. Russell, Y. Sun, *Adv. Mater.* **2016**, *28*, 10008.
[25] L. Lu, T. Xu, W. Chen, E. S. Landry, L. Yu, *Nat. Photonics* **2014**, *8*, 716.
[26] L. Meng, Y. Zhang, X. Wan, C. Li, X. Zhang, Y. Wang, X. Ke, Z. Xiao, L. Ding, R. Xia, H. Yip, Y. Cao, Y. Chen, *Science* **2018**, *2612*, 1.

[27] D. Qian, Z. Zheng, H. Yao, W. Tress, T. R. Hopper, S. Chen, S. Li, J. Liu, S. Chen, J. Zhang, X. K. Liu, B. Gao, L. Ouyang, Y. Jin, G. Pozina, I. A. Buyanova, W. M. Chen, O. Inganäs, V. Coropceanu, J. L. Bredas, H. Yan, J. Hou, F. Zhang, A. a. Bakulin, F. Gao, *Nat. Mater.* **2018**, *17*, 703.
[28] V. Sharapov, Q. Wu, A. Neshchadin, D. Zhao, Z. Cai, W. Chen, L. Yu, *J. Phys. Chem. C* **2018**, *122*, 11305.
[29] R. A. Street, D. Davies, P. P. Khlyabich, B. Burkhart, B. C. Thompson, *J. Am. Chem. Soc.* **2013**, *135*, 986.
[30] Y. Wang, M. J. Jafari, N. Wang, D. Qian, F. Zhang, T. Ederth, E. Moons, J. Wang, O. Inganäs, W. Huang, F. Gao, *J. Mater. Chem. A* **2018**, *6*, 11884.
[31] Z. Xiao, X. Jia, L. Ding, *Sci. Bull.* **2017**, *62*, 1562.
[32] Y. Xie, F. Yang, Y. Li, M. A. Uddin, P. Bi, B. Fan, Y. Cai, X. Hao, H. Y. Woo, W. Li, F. Liu, Y. Sun, *Adv. Mater.* **2018**, *1803045*, 1803045.
[33] Y. (Michael) Yang, W. Chen, L. Dou, W.-H. Chang, H.-S. Duan, B. Bob, G. Li, Y. Yang, *Nat. Photonics* **2015**, *9*, 190.
[34] J. You, L. Dou, Z. Hong, G. Li, Y. Yang, *Prog. Polym. Sci.* **2013**, *38*, 1909.
[35] R. Yu, S. Zhang, H. Yao, B. Guo, S. Li, H. Zhang, M. Zhang, J. Hou, *Adv. Mater.* **2017**, *29*, 1.
[36] J. Zhang, Y. Zhang, J. Fang, K. Lu, Z. Wang, W. Ma, Z. Wei, *J. Am. Chem. Soc.* **2015**, *137*, 8176.
[37] L. Zhong, L. Gao, H. Bin, Q. Hu, Z. G. Zhang, F. Liu, T. P. Russell, Z. Zhang, Y. Li, *Adv. Energy Mater.* **2017**, *7*, 1.
[38] T. Ameri, J. Min, N. Li, F. Machui, D. Baran, M. Forster, K. J. Schottler, D. Dolfen, U. Scherf, C. J. Brabec, *Adv. Energy Mater.* **2012**, *2*, 1198.
[39] D. Baran, R. S. Ashraf, D. A. Hanifi, M. Abdelsamie, N. Gasparini, J. A. Röhr, S. Holliday, A. Wadsworth, S. Lockett, M. Neophytou, C. J. M. Emmott, J. Nelson, C. J. Brabec, A. Amassian, A. Salleo, T. Kirchartz, J. R. Durrant, I. McCulloch, *Nat. Mater.* **2017**, *16*, 363.
[40] R. Bechara, N. Leclerc, P. Lévêque, F. Richard, T. Heiser, G. Hadziioannou, *Appl. Phys. Lett.* **2008**, *93*, 013306.
[41] T. Wang, A. J. Pearson, D. G. Lidzey, *J. Mater. Chem. C* **2013**, *1*, 7266.
[42] B. J. Tremolet De Villers, K. A. O'Hara, D. P. Ostrowski, P. H. Biddle, S. E. Shaheen, M. L. Chabinyc, D. C. Olson, N. Kopidakis, *Chem. Mater.* **2016**, *28*, 876.
[43] A. Tournebize, A. Rivaton, J. L. Gardette, C. Lombard, B. Pépin-Donat, S. Beaupré, M. Leclerc, *Adv. Energy Mater.* **2014**, *4*, 1.
[44] A. Tournebize, J.-L. Gardette, C. Taviot-Guého, D. Bégué, M. A. Arnaud, C. Dagron-Lartigau, H. Medlej, R. C. Hiorns, S. Beaupré, M. Leclerc, A. Rivaton, *Polym. Degrad. Stab.* **2015**, *112*, 175.
[45] Y. Sun, G. C. Welch, W. L. Leong, C. J. Takacs, G. C. Bazan, A. J. Heeger, *Nat. Mater.* **2011**, *11*, 44.
[46] G. D. Sharma, P. A. Angaridis, S. Pipou, G. E. Zervaki, V. Nikolaou, R. Misra, A. G. Coutsolelos, *Org. Electron.* **2015**, *25*, 295.
[47] J. Niklas, K. L. Mardis, B. P. Banks, G. M. Grooms, A. Sperlich, S. Beaupr, **2013**, *15*, 9562.
[48] J. Nelson, *Mater. Today* **2011**, *14*, 462.
[49] L. Marin, L. Lutsen, D. Vanderzande, W. Maes, *Org. Biomol. Chem.* **2013**, *11*, 5866.
[50] L. Lu, T. Zheng, T. Xu, D. Zhao, L. Yu, *Chem. Mater.* **2015**, *27*, 537.
[51] F. J. Lim, A. Krishnamoorthy, G. W. Ho, *ACS Appl. Mater. Interfaces* **2015**, *7*, 12119.
[52] H. C. Liao, C. C. Ho, C. Y. Chang, M. H. Jao, S. B. Darling, W. F. Su, *Mater. Today* **2013**, *16*, 326.
[53] W. Li, W. S. C. Roelofs, M. Turbiez, M. M. Wienk, R. A. J. Janssen, *Adv. Mater.* **2014**, *26*, 3304.

[54] G. Li, R. Zhu, Y. Yang, *Nat. Photonics* **2012**, *6*, 153.
[55] P. Kumaresan, S. Vegiraju, Y. Ezhumalai, S. Yau, C. Kim, W.-H. Lee, M.-C. Chen, *Polymers (Basel)*. **2014**, *6*, 2645.
[56] T. Kirchartz, T. Agostinelli, M. Campoy-Quiles, W. Gong, J. Nelson, *J. Phys. Lett.* **2012**, *3*, 3470.
[57] B. Kippelen, J.-L. Bredas, *Organic Photovoltaics*, *Energy Environ. Sci.* **2009**, 2, 3, 251-256.
[58] J. Kesters, P. Verstappen, J. Raymakers, W. Vanormelingen, J. Drijkoningen, J. D'Haen, J. Manca, L. Lutsen, D. Vanderzande, W. Maes, *Chem. Mater.* **2015**, *27*, 1332.
[59] J. Huang, *Organic and Hybrid Solar Cells*, **2014**, pp. 337.
[60] S. Holliday, R. S. Ashraf, A. Wadsworth, D. Baran, S. A. Yousaf, C. B. Nielsen, C.-H. Tan, S. D. Dimitrov, Z. Shang, N. Gasparini, M. Alamoudi, F. Laquai, C. J. Brabec, A. Salleo, J. R. Durrant, I. McCulloch, *Nat. Commun.* **2016**, *7*, 11585.
[61] D. Baran, N. Gasparini, A. Wadsworth, C. H. Tan, N. Wehbe, X. Song, Z. Hamid, W. Zhang, M. Neophytou, T. Kirchartz, C. J. Brabec, J. R. Durrant, I. McCulloch, *Nat. Commun.* **2018**, *9*, 2059.
[62] A. S. Ferreira, J. C. Aguirre, S. Subramaniyan, S. A. Jenekhe, S. H. Tolbert, B. J. Schwartz, *J. Phys. Chem. C* **2016**, *120*, 22115.
[63] L. Dou, Y. Liu, Z. Hong, G. Li, Y. Yang, *Chem. Rev.* **2015**, *115*, 12633.
[64] I. F. Domínguez, P. D. Topham, P. O. Bussière, D. Bégué, A. Rivaton, *J. Phys. Chem. C* **2015**, *119*, 2166.
[65] C. J. Brabec, S. Gowrisanker, J. J. M. Halls, D. Laird, S. Jia, S. P. Williams, *Adv. Mater.* **2010**, *22*, 3839.
[66] M. An, F. Xie, X. Geng, J. Zhang, J. Jiang, Z. Lei, D. He, Z. Xiao, L. Ding, *Adv. Energy Mater.* **2017**, *7*, 2.
[67] J. C. Aguirre, S. A. Hawks, A. S. Ferreira, P. Yee, S. Subramaniyan, S. A. Jenekhe, S. H. Tolbert, B. J. Schwartz, *Adv. Energy Mater.* **2015**, *5*, 1.
[68] O. Adebanjo, P. Maharjan, P. Adhikary, M. Wang, S. Yang, Q. Qiao, *Energy Environ. Sci.* **2013**, *6*, 3150.
[69] Aldrich, *Organic and Molecular Electronics*, **2009**, 4, 3, 32.
[70] Z.-G. Zhang, Y. Li, *Sci. China Chem.* **2014**, *58*, 192.
[71] G. Zhang, J. Zhao, P. C. Y. Chow, K. Jiang, J. Zhang, Z. Zhu, J. Zhang, F. Huang, H. Yan, *Chem. Rev.* **2018**, acs. chemrev.7b00535.
[72] T. Yu, X. Xu, G. Zhang, J. Wan, Y. Li, Q. Peng, *Adv. Funct. Mater.* **2017**, *27*, 1.
[73] L. Ye, S. Q. Zhang, L. J. Huo, M. J. Zhang, J. H. Hou, *Acc. Chem. Res.* **2014**, *47*, 1595.
[74] H. Yao, Y. Chen, Y. Qin, R. Yu, Y. Cui, B. Yang, S. Li, K. Zhang, J. Hou, *Adv. Mater.* **2016**, 8283.
[75] J. M. Jiang, H. K. Lin, Y. C. Lin, H. C. Chen, S. C. Lan, C. K. Chang, K. H. Wei, *Macromolecules* **2014**, *47*, 70.
[76] L. Huo, J. Hou, *Polym. Chem.* **2011**, *2*, 2453.
[77] J. Hou, M. Park, S. Zhang, Y. Yao, L.-M. Chen, J.-H. Li, Y. Yang, *Macromolecules* **2008**, *41*, 6012.
[78] J. Hou, M. Park, S. Zhang, Y. Yao, L. Chen, J. Li, Y. Yang, *Society* **2008**, 6012.
[79] A. Giovannitti, K. J. Thorley, C. B. Nielsen, J. Li, M. J. Donahue, G. G. Malliaras, J. Rivnay, I. McCulloch, *Adv. Funct. Mater.* **2018**, *1706325*, 1.
[80] N. Y. Doumon, G. Wang, R. C. Chiechi, L. J. A. Koster, *J. Mater. Chem. C* **2017**, *5*, 6611.
[81] S. Alem, S. Wakim, J. Lu, G. Robertson, J. Ding, Y. Tao, *ACS Appl. Mater. Interfaces* **2012**, *4*, 2993.
[82] X. Zhou, X. Li, Y. Liu, R. Li, K. Jiang, J. Xia, *Org. Electron.* **2015**, *25*,

245.
[83] H. Zhou, L. Yang, S. Xiao, S. Liu, W. You, *Macromolecules* **2010**, *43*, 811.
[84] S. Zhang, L. Ye, W. Zhao, D. Liu, H. Yao, J. Hou, *Macromolecules* **2014**, *47*, 4653.
[85] J. Yuan, W. Ma, *J. Mater. Chem. A* **2015**, *3*, 7077.
[86] J. Razzell-Hollis, J. Wade, W. C. Tsoi, Y. Soon, J. Durrant, J.-S. Kim, *J. Mater. Chem. A* **2014**, *2*, 20189.
[87] Z. Liu, D. Liu, W. Chen, J. Wang, F. Li, D. Wang, Y. Li, M. Sun, R. Yang, *J. Mater. Chem. C* **2017**, *5*, 6798.
[88] B. Kan, Q. Zhang, M. Li, X. Wan, W. Ni, G. Long, Y. Wang, X. Yang, H. Feng, Y. Chen, *J. Am. Chem. Soc.* **2014**, *136*, 15529.
[89] H. Zhang, L. Ye, J. Hou, *Polym. Int.* **2015**, *64*, 957.
[90] C. Zhang, S. Langner, A. V. Mumyatov, D. a. Anokhin, J. Min, J. D. Perea, K. L. Gerasimov, A. Osvet, D. Ivanov, P. Troshin, N. Li, C. J. Brabec, *J. Mater. Chem. A* **2017**, 17570.
[91] L. Ye, Y. Jing, X. Guo, H. Sun, S. Zhang, M. Zhang, L. Huo, J. Hou, *J. Phys. Chem. C* **2013**, *117*, 14920.
[92] D. Yang, F. C. Löhrer, V. Körstgens, A. Schreiber, S. Bernstorff, J. M. Buriak, P. Müller-Buschbaum, *ACS Energy Lett.* **2019**, *4*, 464.
[93] Y. Xie, X. Hu, J. Yin, L. Zhang, X. Meng, G. Xu, Q. Ai, W. Zhou, Y. Chen, **2017**, DOI 10.1021/acsami.6b16538.
[94] G. Wang, T. Jiu, G. Tang, J. Li, P. Li, X. Song, F. Lu, J. Fang, *ACS Sustain. Chem. Eng.* **2014**, *2*, 1331.
[95] D. H. Wang, P. Morin, C. Lee, K. Ko, *J. Mater. Chem. A* **2014**, *2*, 1.
[96] B. Wang, Y. Fu, C. Yan, R. Zhang, Q. Yang, Y. Han, Z. Xie, *Front. Chem.* **2018**, *6*, 1.
[97] C. H. To, A. Ng, Q. Dong, A. B. Djurišić, J. A. Zapien, W. K. Chan, C. Surya, *ACS Appl. Mater. Interfaces* **2015**, *7*, 13198.
[98] R. Tipnis, D. Laird, M. Mathai, *Mater. Matters* **2008**, *3*, 92.
[99] Y. Sun, C. J. Takacs, S. R. Cowan, J. H. Seo, X. Gong, A. Roy, A. J. Heeger, *Adv. Mater.* **2011**, *23*, 2226.
[100] A. C. Stuart, J. R. Tumbleston, H. Zhou, W. Li, S. Liu, H. Ade, W. You, *J. Am. Chem. Soc.* **2013**, *135*, 1806.
[101] G. Shi, J. Yuan, X. Huang, Y. Lu, Z. Liu, J. Peng, G. Ding, S. Shi, J. Sun, K. Lu, H. Q. Wang, W. Ma, *J. Phys. Chem. C* **2015**, *119*, 25298.
[102] S. Qu, H. Wang, D. Mo, P. Chao, Z. Yang, L. Li, L. Tian, W. Chen, F. He, *Macromolecules* **2017**, *50*, 4962.
[103] C. H. Peters, I. T. Sachs-Quintana, J. P. Kastrop, S. Beaupré, M. Leclerc, M. D. McGehee, *Adv. Energy Mater.* **2011**, *1*, 491.
[104] A. J. Pearson, P. E. Hopkinson, E. Couderc, K. Domanski, M. Abdi-Jalebi, N. C. Greenham, *Org. Electron. physics, Mater. Appl.* **2016**, *30*, 225.
[105] Y. Ohori, S. Fujii, H. Kataura, Y. Nishioka, *Jpn. J. Appl. Phys.* **2015**, *09*, 1.
[106] P. Morvillo, R. Diana, R. Ricciardi, E. Bobeico, C. Minarini, **n.d.**, 4.
[107] D. Mo, H. Wang, H. Chen, S. Qu, P. Chao, Z. Yang, L. Tian, Y.-A. Su, Y. Gao, B. Yang, W. Chen, F. He, *Chem. Mater.* **2017**, *29*, 2819.
[108] W. R. Mateker, M. D. McGehee, *Adv. Mater.* **2017**, *29*, DOI 10.1002/adma.201603940.
[109] S. H. Liao, H. J. Jhuo, Y. S. Cheng, S. A. Chen, *Adv. Mater.* **2013**, *25*, 4766.
[110] Y. Liang, Z. Xu, J. Xia, S.-T. Tsai, Y. Wu, G. Li, C. Ray, L. Yu, *Adv. Mater.* **2010**, *22*, E135.
[111] V. M. Le Corre, A. R. Chatri, N. Y. Doumon, L. J. A. Koster, *Adv. Energy Mater.* **2018**, *7*, 1803125.
[112] W. Kim, J. K. Kim, E. Kim, T. K. Ahn, D. H. Wang, J. H. Park, *J. Phys. Chem. C* **2015**, *119*, 5954.

[113] L. N. Inasaridze, A. I. Shames, I. V. Martynov, B. Li, A. V. Mumyatov, D. K. Susarova, E. A. Katz, P. A. Troshin, *J. Mater. Chem. A* **2017**, 8044.
[114] L. Huo, S. Zhang, X. Guo, F. Xu, Y. Li, J. Hou, *Angew. Chemie - Int. Ed.* **2011**, *50*, 9697.
[115] D. Huang, Y. Li, Z. Xu, S. Zhao, L. Zhao, J. Zhao, *Phys. Chem. Chem. Phys.* **2015**, *17*, 8053.
[116] S. Holliday, C. K. Luscombe, *Adv. Electron. Mater.* **2017**, *1700416*, 1700416.
[117] X. Guo, M. Zhang, W. Ma, L. Ye, S. Zhang, S. Liu, H. Ade, F. Huang, J. Hou, *Adv. Mater.* **2014**, *26*, 4043.
[118] A. Giovannitti, K. J. Thorley, C. B. Nielsen, J. Li, M. J. Donahue, G. G. Malliaras, J. Rivnay, I. McCulloch, *Adv. Funct. Mater.* **n.d.**, DOI 10.1002/ADFM.201706325.
[119] S. Foster, F. Deledalle, A. Mitani, T. Kimura, K.-B. Kim, T. Okachi, T. Kirchartz, J. Oguma, K. Miyake, J. R. Durrant, S. Doi, J. Nelson, *Adv. Energy Mater.* **2014**, *4*, 1400311.
[120] L. Fernandes, H. Gaspar, J. P. C. Tomé, F. Figueira, G. Bernardo, *Polym. Bull.* **2018**, *75*, 515.
[121] I. Etxebarria, A. Guerrero, J. Albero, G. Garcia-Belmonte, E. Palomares, R. Pacios, *Org. Electron.* **2014**, *15*, 2756.
[122] S. Das, J. K. Keum, J. F. Browning, G. Gu, B. Yang, O. Dyck, C. Do, W. Chen, J. Chen, I. N. Ivanov, K. Hong, A. J. Rondinone, P. C. Joshi, D. B. Geohegan, G. Duscher, K. Xiao, *Nanoscale* **2015**, *7*, 15576.
[123] C. Cui, W.-Y. Wong, Y. Li, *Energy Environ. Sci.* **2014**, *7*, 2276.
[124] D. Bartesaghi, G. Ye, R. C. Chiechi, L. J. A. Koster, *Adv. Energy Mater.* **2016**, *6*, DOI 10.1002/aenm.201502338.
[125] S. Zhang, L. Ye, W. Zhao, D. Liu, H. Yao, J. Hou, *Macromolecules* **2014**, *47*, 4653.
[126] S. Zhang, L. Ye, J. Hou, *Adv. Energy Mater.* **2016**, *6*, DOI 10.1002/aenm.201502529.
[127] B. W. Knight, F. Wudl, *J. Org. Chem* **1995**, *60*, 532.
[128] S. Li, L. Ye, W. Zhao, S. Zhang, S. Mukherjee, H. Ade, J. Hou, *Adv. Mater.* **2016**, *28*, 9423.
[129] W. Zhao, S. Li, H. Yao, S. Zhang, Y. Zhang, B. Yang, J. Hou, *J. Am. Chem. Soc.* **2017**, *139*, 7148.
[130] W. Zhao, D. Qian, S. Zhang, S. Li, O. Inganäs, F. Gao, J. Hou, *Adv. Mater.* **2016**, 4734.
[131] W. Chen, X. Yang, G. Long, X. Wan, Y. Chen, Q. Zhang, *J. Mater. Chem. C* **2015**, *4698*, 4698.
[132] Y. Cui, G. Jia, J. Zhu, Q. Kang, H. Yao, L. Lu, B. Xu, J. Hou, *Chem. Mater.* **2018**, *30*, 1078.
[133] "High purity [70]PCBM for high performance polymer-fullerene OPV," https://solennebv.com/product/70pcbm/, **(Accessed on Jan. 25, 2019).**
[134] "High quality PCBM for organic photovoltaics and organic electronics," https://solennebv.com/product/60pcbm/, **(Accessed on Jan. 25, 2019).**
[135] W. Zhao, D. Qian, S. Zhang, S. Li, O. Inganäs, F. Gao, J. Hou, *Adv. Mater.* **2016**, *28*, 4734.
[136] J. M. Kroon, M. M. Wienk, W. J. H. Verhees, J. C. Hummelen, *Thin Solid Films* **2002**, *403–404*, 223.
[137] F. C. Krebs, *Stability and Degradation of Organic and Polymer Solar Cells*, **2012**, pp. 341.
[138] N. Li, J. D. Perea, T. Kassar, M. Richter, T. Heumueller, G. J. Matt, Y. Hou, N. S. Güldal, H. Chen, S. Chen, S. Langner, M. Berlinghof, T. Unruh, C. J. Brabec, *Nat. Commun.* **2017**, *8*, 14541.
[139] N. Gasparini, M. Salvador, S. Strohm, T. Heumueller, I. Levchuk, A. Wadsworth, J. H. Bannock, J. C. de Mello, H. J. Egelhaaf, D. Baran, I. Mcculloch, C. J.

Brabec, *Adv. Energy Mater.* **2017**, *1700770*, 1.
[140] J. Kong, S. Song, M. Yoo, G. Y. Lee, O. Kwon, J. K. Park, H. Back, G. Kim, S. H. Lee, H. Suh, K. Lee, *Nat. Commun.* **2014**, *5*, 5688.
[141] R. Cheacharoen, W. R. Mateker, Q. Zhang, B. Kan, D. Sarkisian, X. Liu, J. A. Love, X. Wan, Y. Chen, T. Q. Nguyen, G. C. Bazan, M. D. McGehee, *Sol. Energy Mater. Sol. Cells* **2017**, *161*, 368.
[142] E. Voroshazi, B. Verreet, A. Buri, R. Müller, D. Di Nuzzo, P. Heremans, *Org. Electron. physics, Mater. Appl.* **2011**, *12*, 736.
[143] A. Savva, E. Georgiou, G. Papazoglou, A. Z. Chrusou, K. Kapnisis, S. A. Choulis, *Sol. Energy Mater. Sol. Cells* **2015**, *132*, 507.
[144] M. Jørgensen, K. Norrman, S. A. Gevorgyan, T. Tromholt, B. Andreasen, F. C. Krebs, *Adv. Mater.* **2012**, *24*, 580.
[145] Y. Zhang, J. Lee, S. R. Forrest, *Nat. Commun.* **2014**, *5*, 1.
[146] L. J. A. Koster, V. D. Mihailetchi, R. Ramaker, P. W. M. Blom, *Appl. Phys. Lett.* **2005**, *86*, 1.
[147] M. M. Mandoc, F. B. Kooistra, J. C. Hummelen, B. De Boer, P. W. M. Blom, *Appl. Phys. Lett.* **2007**, *91*, 2007.
[148] L. J. A. Koster, *Device Physics of Donor / Acceptor-Blend Solar Cells*, **2007**, ISBN-13: 9789036729413.
[149] J. C. Blakesley, F. A. Castro, W. Kylberg, G. F. A. Dibb, C. Arantes, R. Valaski, M. Cremona, J. S. Kim, J.-S. Kim, *Org. Electron.* **2014**, *15*, 1263.
[150] A. Stylianou, M. Lekka, T. Stylianopoulos, *Nanoscale* **2018**, *10*, 20930.
[151] N. Y. Doumon, G. Wang, X. Qiu, A. J. Minnaard, R. C. Chiechi, L. J. A. Koster, *Sci. Rep.* **2019**, *9*, 4350.
[152] N. Y. Doumon, L. J. A. Koster, *Sol. RRL* **2019**, *3*, 1800301.
[153] Wikkipedia, "GIWAXS - GISAXS," http://gisaxs.com/index.php/GIWAXS, **2015 (Accessed on Jan. 11, 2019).**

3

Relating Polymer Chemical Structure to the Photostability of Polymer:Fullerene Solar Cells

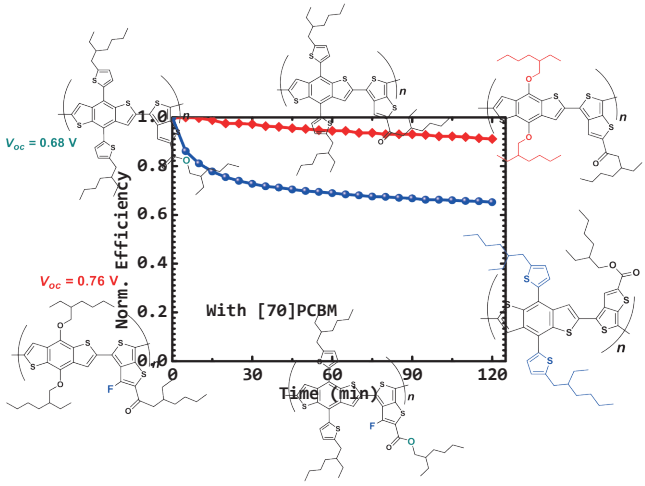

Chapter based on publications number 6 and 8

3

SUMMARY

Polymer solar cells are capable of transforming our daily usage of energy in small appliances and mobile devices. The advent of new semiconducting polymers shifted more attention to bulk heterojunction solar cells in the past years. An example is the synthesis, through chemical structure engineering, of the one and two-dimensional benzodithiophene-co-thieno[3,4-b]thiophene polymer families. They help achieve for the first-time efficiency close to 10% in fullerene-based solar cells. However, their performance is limited by some factors amongst which their low open circuit voltage (V_{oc}) and stability. Much effort is directed into improving the V_{oc}, and thus, the efficiency. Typical examples are addition (chlorination or fluorination) and/or reduction (from alkyl-ester to alkyl-ketone substituents) mechanisms. In this chapter, we study the effect of these structural changes on the performance of the polybenzodithiophene-thienothiophene polymers in polymer:fullerene solar cells. Specifically, it looks at seven polymers of the polybenzodithiophene-thienothiophene family, identifying the structural changes in the side chains of the benzodithiophene and the thienothiophene units or their moieties as a function of efficiency in relation to their photostability.

On the one hand, under continuous illumination, solar cells of polymers with alkoxy-side-chains are more photostable than those with alkylthienyl-side-chains. On the other hand, fluorination of the TT-units or having alkyl-ester groups as substituents on the TT-units is bad for photostability, however, when these alkyl-ester groups are reduced into alkyl-ketone substituents, the photostability behaviour improves. These results pave the way for novel materials for efficient as well as stable organic solar cells.

3.1. Introduction

The last decade or so has seen tremendous advances in polymer:fullerene blend solar cells (PSC). Their performance in terms of efficiency has advanced with the development of novel organic materials. Typical examples are the benzodithiophene (BDT) polymers.[1–3] As BDT polymers turned out to be a step in the good direction, the chemistry community, through materials chemical structure engineering, went a step further, fusing in thienothiophene (TT) units, thus, creating the benzodithiophene-thienothiophene (BDT-TT) polymers.[4] In retrospect, the 1D BDT-alkoxy-substituted polybenzodithiophene-thienothiophene (PBDT-TT) polymers were first synthesised and soon followed by the design of their 2D counterparts, the BDT-alkylthienyl-substituted PBDT-TT polymers.[4,5] This change in substitution of the BDT-side-chains generally enhanced the performance of the optimised devices roughly by some percentages in efficiency.[6–12] An example is the replacement of the alkoxy-side-chains on the BDT-unit of PTB7 by alkylthienyl-side-chains to form PTB7-Th.[13,14]

Additionally, within the structure of the PBDT-TT polymers, the TT-units are either fluorinated or chlorinated and/or mostly substituted with either an alkyl-ester or an alkyl-ketone or a sulfonyl group as side chains.[1,9,15–22] These changes in structure consist, on the one hand, of *addition* reactions such as the fluorination,[15,17,18,20,21,23] chlorination,[24,25] or sulfonylation[19] of the TT-unit. On the other hand, it involves *reduction* reaction on the TT-substituents, that is the removal of one oxygen atom and thus, moving from alkyl-ester-[26,27] to alkyl-ketone-substituent group

on the TT-unit. These changes focus on the improvement in device performance, specifically, the open circuit voltage (V_{oc}); thus, the power conversion efficiency (PCE).[14,17–23,27,28] Soon after, single junction bulk heterojunction polymer:fullerene solar cells (PSCs) reach PCE beyond 10%.[7,29–32] Indeed, the predicted potentials are partly achieved with even a new quest to push the efficiency further by the advent of the non-fullerene acceptors with the current PCE beyond 17%.[33]

Meanwhile, while the focal point in the performance of the devices is on PCE, the stability of these polymers lacks attention, and thus, creating a gap in the foreseen potentials of the PSC technology. Stability and longevity are fundamental to the performance of the solar cells and the advancement of the field. Photostability of these polymers is one key concern which is not yet sufficiently investigated. Previous studies showed that the introduction of the 2D polymers slightly improves thermal stability.[34] The changes in the BDT- or TT-units admittedly improved the performance of the device regarding efficiency, but the literature remains silent on their effects on photostability.

This chapter investigates the photostability performance of the PBDT-TT polymers. In particular, the specific objective of this work is to assess the effect of the substituents of the BDT-units and TT-moieties on the photodegradation of their solar cells. To arrive at this end, conventional solar cells, single-carrier devices, and films on glass are fabricated based on these polymers and exposed continuously at open circuit condition to a simulator lamp of the AM1.5G spectrum at room temperature in an inert

atmosphere. They are subsequently characterised to determine their photodegradation in PCE, charge transport, and absorbance. To undertake this study comprehensively, seven polymers of the PBDT-TT family are selected: 1D polymers (alkoxy-substituted-BDT-unit polymers) and 2D polymers (alkylthienyl-substituted-BDT-unit polymers).

The first part of the chapter explores the PBDT-TT polymers as shown in **Figure 3.1**, to elucidate the effects of substituting the alkoxy groups on the BDT-units of these polymers (PTB7, PBDTTT-E, and PBDTTT-C) with the alkylthienyl groups (PTB7-Th, PBDTTT-ET, and PBDTTT-CT) on PCE and device stability under illumination. The focus is to learn about the effect of the polymer chemical structure on the photostability of the devices. The results disclosed that even though alkylthienyl-side-chains improve PCE as compared to the alkoxy-side-chains, they are inferior performers with regards to photodegradation and stability. We demonstrated that alkylthienyl groups accelerate photodegradation in the PSC throughout the exposure.

The second part of the chapter explores the same polymers; however, in their respective groups (1D or 2D). In each group, polymer 1 (PBDTTT-E and PBDTTT-ET) differs from polymer 2 (PBDTTT-C and PBDTTT-CT) by the *reduction* of the alkyl-ester-substituent on the TT-unit to an alkyl-ketone-substituent, that is the removal of an oxygen atom. Polymer 1 differs from polymer 3 (PTB7 and PTB7-Th) by an *addition* reaction, the fluorination of the TT-unit. To underline the effect of fluorination on the photostability, a seventh polymer, PBDTTT-CF, a 1D polymer is introduced into the study.

This polymer differs from polymer 2 only in the fluorination of the TT-unit. The transition from polymer 1 to polymer 2 or polymer 3 increases V_{oc}. The transition from polymer 1 to polymer 4 means more increase in V_{oc}. The goal is to find how these subtle changes in the chemical structure of the TT-unit of the polymers affect the photodegradation in their PSCs. We discover that the alkyl-ketone-TT-unit PSCs are the most photostable, followed by the alkyl-ester-TT-unit polymer ones, and then by the fluorinated-TT-unit PSCs.

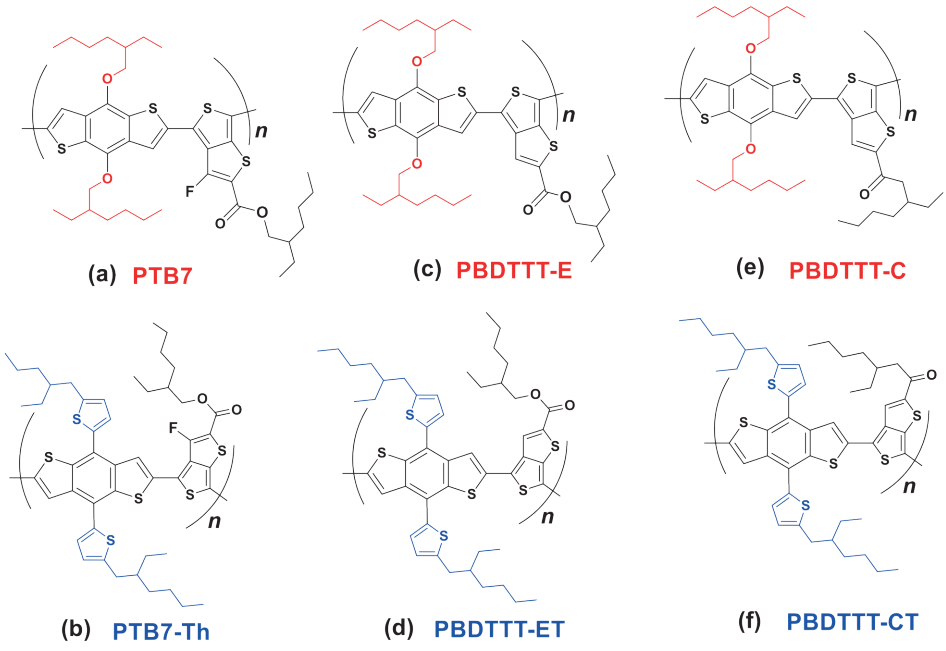

Figure 3.1: Chemical structures of polymers with alkoxy-side-chains (A-p) **(a,c,e)** and alkylthienyl-side-chains (AT-p) **(b,d,f):** PTB7 **(a)** vs PTB7-Th **(b)**; PBDTTT-E **(c)** vs PBDTTT-ET **(d)**; and PBDTTT-C **(e)** vs PBDTTT-CT **(f)**.

3.2. Results and Discussions

3.2.1. Performance Of BDT-based Polymer Solar Cells

The first part of the chapter investigates the effects of replacing the alkoxy-side-chains on the BDT-unit of the PBDT-TT polymers with alkylthienyl-side-chains on the performances of their solar cells in terms of efficiency and photostability. We explore in total six polymers, two by two, under the same experimental conditions as described in chapter 2, in film, solution, solar cell or single carrier device configuration. **Figure 3.1** shows the chemical structures of the studied polymers with the alkoxy-side-chains (A-p) in red and the alkylthienyl-side-chains (AT-p) in blue.

3.2.1.1. Changes in BDT-Side Chains: Efficiency

Table 3.1: Photovoltaic performance of conventional PSCs without DIO under same conditions. Average values are for at least 20 selected devices. *L* (Thickness)

Devices	*L* (nm)	J_{sc} (mA.cm^{-2})	V_{oc} (V)	FF (%)	PCE (%)	Average PCE (%)
PTB7	100	10.10	0.798	56.4	4.5	4.2±0.5
PTB7-Th	110	15.60	0.804	68.7	8.6	8.7±0.4
PBDTTT-E	100	10.23	0.686	55.4	3.9	3.6±0.2
PBDTTT-ET	100	12.73	0.727	55.3	5.1	4.3±0.4
PBDTTT-C	130	12.33	0.743	45.5	4.2	3.8±0.2
PBDTTT-CT	110	12.60	0.839	54.9	5.8	5.3±0.3

Conventional PSCs are made from the six polymers. The reproducibility of the efficiency of the PSCs is checked for all polymers each time devices are fabricated, to ascertain the reliability of the work discussed in this

thesis. The experiments are performed on fabricated conventional devices without additives under the same conditions to ensure there are no differences in processing and environmental conditions. The active layers are spin coated from dissolved blends of [70] PCBM with each polymer of the two classes of the PBDT-TT polymers in 1,2-dichlorobenzene (oDCB). As indicated earlier, the alkylthienyl-side-chains PSCs outperform the alkoxy-side-chains ones in terms of efficiency. **Table 3.1** clearly shows the differences in the current density-voltage (*J-V*) parameters. The better photovoltaic performance of the AT-p devices is possibly credited to their slightly broadened absorption band in **Figure 3.2a**, with slightly red-shifted onset in **Figure 3.2b**, reverberated in the increase of the short circuit current (J_{SC}) (**Figure 3.2d**); the slightly lower HOMO (see **Figure 3.2c**) in the case of PTB7-Th (AT-p_1); and their enhanced charge carrier mobility, explained by seemingly better surface morphology of the blend. **Figure 3.2e** depicts the spread in PCE for some PSCs as examples.

3.2.1.2. Changes in BDT-Side Chains: Device Stability

The stability tests are performed in a glovebox on each device kept at room temperature, 295 K, by active cooling in an inert environment (with <0.1 ppm H_2O and <0.1 ppm O_2), under continuous illumination for 2 hours. All devices are fabricated under the same conditions to prevent the influence of processing on the differences in the photodegradation pathway.

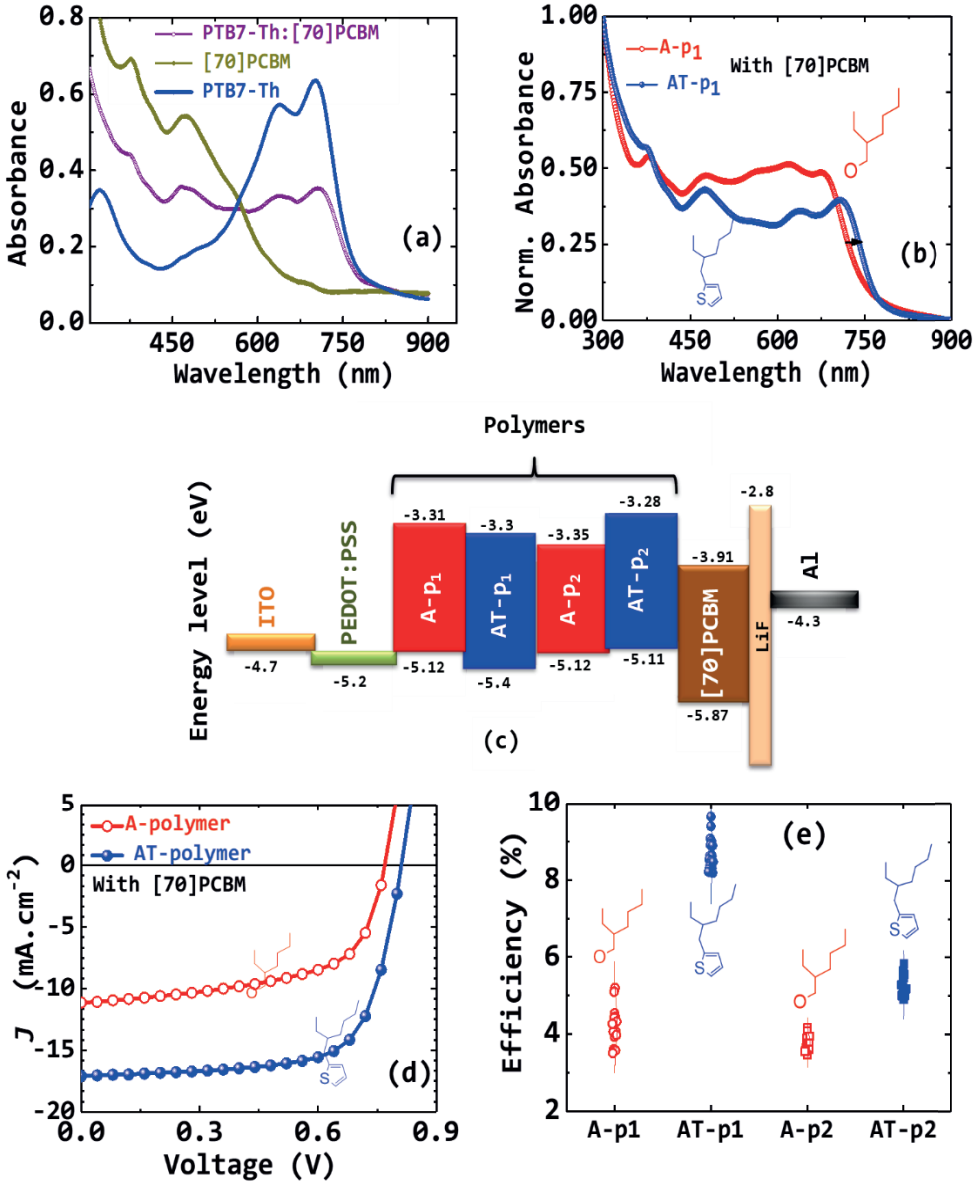

Figure 3.2: Absorption spectra of typical pristine and blend materials used for the solar cells **(a)**; Normalised spectra for typical alkoxy-polymer:[70]PCBM and alkylthienyl-polymer:[70]PCBM **(b)**; energy level of some polymer studied materials with respect to electrodes and interlayers **(c)**; *J-V* curves of typical alkoxy-polymer:[70]PCBM and alkylthienyl-polymer:[70]PCBM solar cells **(d)**; and efficiency distribution of four studied polymer:[70]PCBM solar cells **(e)**.

Figure 3.3(a,b,c) displays the PCE photodegradation pathway of the A-p-based solar cells compared to AT-p-based ones. The average PCE-decay is within the limit of ~10% of the original PCEs for the A-p-based devices under continuous illumination, while the AT-p-based devices show over the same period an average PCE-decay of ~25%. The observation looks rather surprising as alkoxy-side-chains are known to impact polymer stability negatively.[36] That is not the case for the observed photodegradation behaviours of their solar cells. Even under thermal stability, it is not entirely clear if this is the case per our observation (figures not shown). Details of the decay rate of the other *J-V* parameters are revealed in **Figure 3.3(d,e,f).**

In **Figure 3.3d**, the J_{SC} remained almost constant with similar decay behaviour for all six polymer:fullerene solar cells two by two. In **Figure 3.3e**, the V_{OC} apparently decreased for the AT-p-based devices. In **Figure 3.3f**, the FF decreased for AT-p-based devices but remained largely constant for A-p-based devices upon illumination. T_{80}, the lifetime of both type of devices, is determined to further examine the extent of their photodegradation. T_{80} is the time at which a device retains 80% of its initial PCE irrespective of the testing conditions.[37] The average lifetime of the AT-p-based devices is found to be between 35-60 min. For the A-p-based devices, since the devices do not decay to 80% of their initial PCE during the measurements, we could only assume a minimum lifetime of 2 hours.

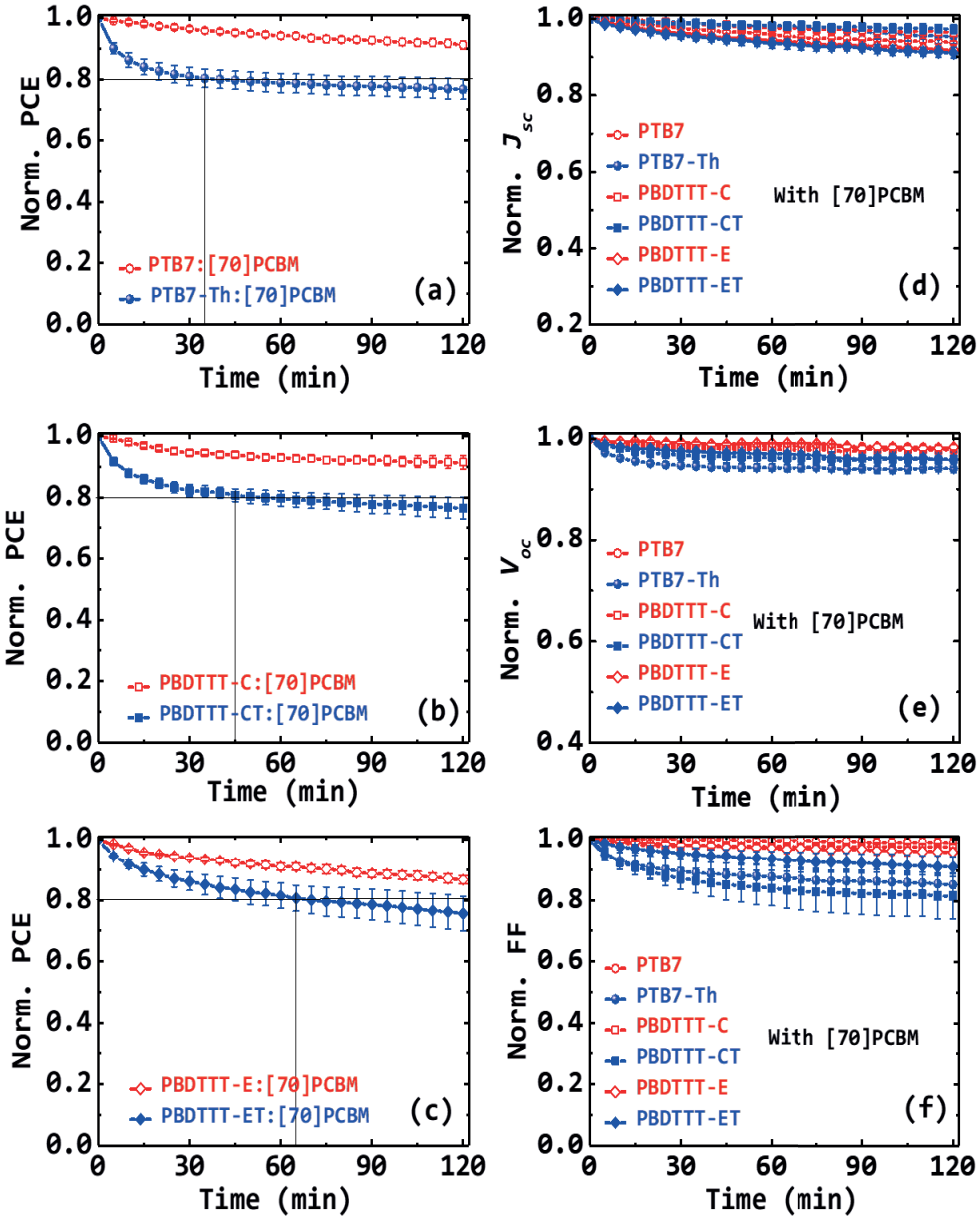

Figure 3.3: Time evolution of normalized *J-V* parameters decay under 1-sun continuous illumination. PCE decay of PTB7:[70]PCBM vs PTB7-Th:[70]PCBM **(a)**, PBDTTT-C:[70]PCBM vs PBDTTT-CT:[70]PCBM **(b)**, and PBDTTT-E:[70]PCBM vs PBDTTT-ET:[70]PCBM **(c)**. J_{sc} **(d)**, V_{oc} **(e)**, and FF **(f)** decay of all considered solar cells. Clearly, A-p-based solar cells are more photostable than AT-p-based ones.

PEDOT:PSS is a good hole transporting layer (HTL). However, it is found to be bad for device stability. Thus, researchers replace it with metal oxides in both conventional or inverted solar cells for better stability.[38–42] It is held that since PEDOT:PSS is acidic, it could react more with the AT-polymers and may explain the observed accelerated photodegradation in this type of devices. The hypothesis is tested with fabricated conventional devices with a pH-neutral PEDOT:PSS layer and without the PEDOT:PSS layer. Furthermore, there are also concerns about LiF being a major factor in the observed degradation as it can diffuse into the active layer of the device. Hence, to crosscheck, we replaced LiF by Ca in the fabricated devices, ITO/PEDOT:PSS/Blend/Ca/Al. All the above-described devices are illuminated under the same conditions as the original ones. As expected, the cells show a decrease in PCE, however, surprisingly, as shown in **Figure 3.4(a,b,c)**, these three cases show similar decay trends as earlier observed: the AT-p-based devices decayed faster than the A-p-based ones.

As seen in **Figure 3.2(a,b)** on page 64, both the polymers and [70]PCBM absorb differently in the UV-Vis range. Thus, any observed substantial variation in any of the devices compared to the others can be due to that particular polymer. Photobleaching could be the cause of the observed decay. To check if the photodegradation is due to photobleaching, absorption spectra of the blend films are taken before and after 2 hours of continuous exposure to simulated sunlight. **Figure 3.5(a,b)** reveals no apparent change in spectra before and after the exposure. Hence, the observed photodegradation cannot be due to photobleaching, at least over the period of our study.

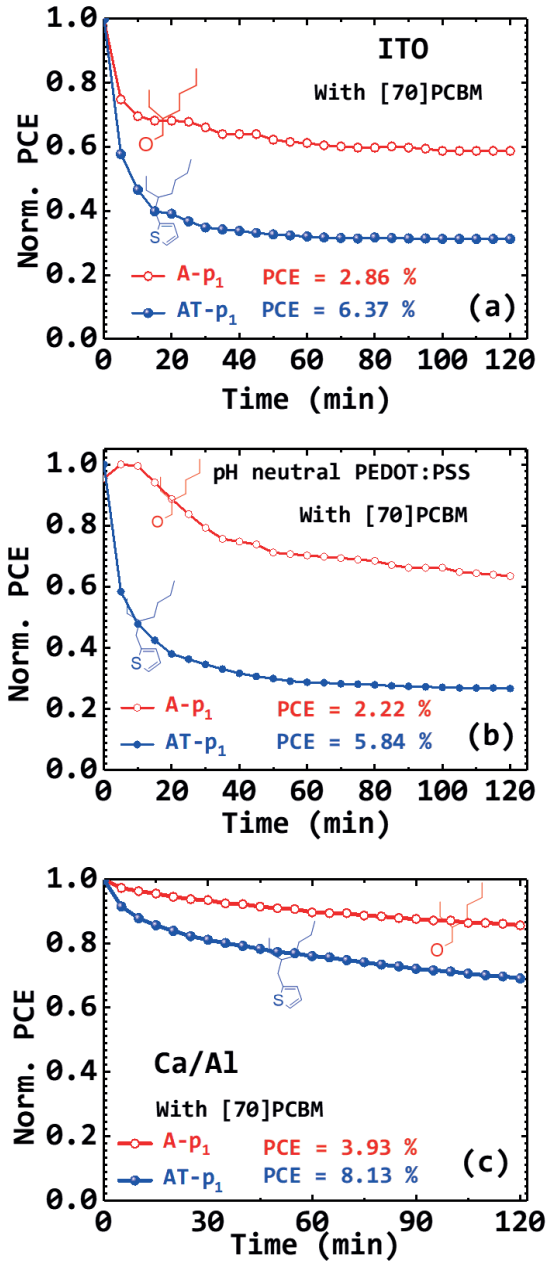

Figure 3.4: Time evolution of normalized PCE decay under 1-sun continuous illumination of devices without PEDOT:PSS **(a)**, with pH-neutral PEDOT:PSS **(b)**, and with Ca **(c)**.

Also, AFM images of fresh and exposed blend films show no notable differences in features. Thus, the observed degradation trend cannot be due to pronounced phase separation upon illumination, though morphology change cannot be totally discounted.

We, therefore, ascribed the fast photodegradation in the AT-p-based devices to the alkylthienyl-side-chain byproducts or free radical species that could result from the pronounced photochemical reactions of the alkylthienyl-side-chains initiated by the exposure to UV-light. These species can act as deep traps that hinder the stability of the AT-p-based devices more than the alkoxy-side-chain free radical species do to the A-p-based devices.

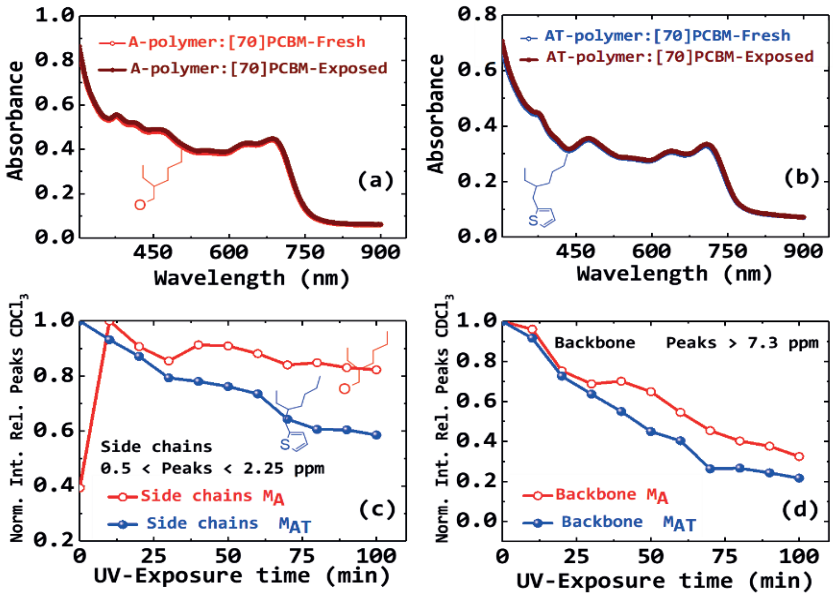

Figure 3.5: Absorption spectra of fresh and exposed (2 hours, brown) blend films of A-p polymer:[70]PCBM **(a)**, AT-p polymer:[70]PCBM **(b)**. Normalized integrated relative peaks to $CDCl_3$ solvent of ^{1}H-NMR of alkoxy (red) and alkylthienyl (blue)-monomers: Side-chains peaks **(c)** and backbone peaks **(d)**.

The assertion that the observed photodegradation behaviour is due to UV-radiation is checked by continuously exposing the solar cells to a UV-filtered light. The spectrum of the lamp and the results are displayed in Appendix **Figure A3.1.** The solar cells exposed to the UV-filtered light show different behaviour; they remained stable throughout the experiment.

To investigate the formation of the byproducts that we hypothesised to be responsible for the observed photodegradation, ^{1}H-NMR spectra are recorded for dissolved BDT-monomers, M_A, and M_{AT}, with their structures shown in Appendix **Figure A3.2.** The ^{1}H-NMR measurement is carried out in an inert atmosphere using sealed NMR tubes with the solutions prepared in a glovebox. The outcomes, shown in **Figure 3.5(c,d)** and **3.6**, support our hypothesis.

Figure 3.5(c,d) shows a decline in the corresponding monomers integrated side-chain and backbone peaks relative to the solvent ($CDCl_3$) peak. The decline of the peaks of the M_{AT} solution is faster than that of the M_A solution (see **Figure 3.5(c,d)**). While both monomer solutions spectra degrade upon UV-exposure, the rate of degradation of M_{AT} is faster than that of M_A, especially as shown in **Figure 3.5c**. For example, the M_{AT} proton peak at 1.5 ppm disappeared just after 10 min exposure, see **Figure 3.6b.** The ^{1}H-NMR spectrum of the M_A solution reveals the appearance of new peaks (in purple circles, see **Figure 3.6a**) and the decline in the initial peaks (in red circles). The new peaks show the same multiplicity as the monomer but are shifted down-field, signifying the likely formation of a quinone moiety upon cleavage of the alkoxy-side-chains, present in the solution. In the M_{AT} spectrum, however, there are almost no new peaks. This does not

mean there are no byproducts. A careful study of the spectrum of the exposed M_{AT} spectrum reveals that there is likely cleavage of the alkyl or the alkylthienyl-side-chains (with possible ring opening) which rather generate insoluble byproducts, and therefore, not detected by ^{1}H-NMR.

The photodegradation of PSCs was recently attributed to either effect activated by charge collection layers and interfaces[43] or hot carriers breaking C-H bonds at the donor/acceptor interface.[44] The latter claim requires energies above 4 eV. However, our results reveal that the monomers themselves are unstable to UV-radiation, which undoubtedly does not involve homolytic cleavage of C-H bonds. If hot carriers were breaking apart C-H bonds, then almost no polymer would be stable, but that is not the case. The observed trend in the complete devices, however, echoes the role played by the active layer composition.

The byproducts could impede charge transport. The observed degradation trends suggest a reduction in the hole current of the illuminated devices. We study the charge transport of the systems to determine if it could be linked to device degradation. Single carrier devices of pristine polymers and blend materials are fabricated and treated under conditions previously described in Chapter 2. **Figure 3.7** presents the analysis of the empirical data recorded from the charge transport measurements for PTB7 and PTB7-Th based devices as representative examples of the A-p and AT-p devices. In all-polymer pristine single carrier devices, the hole currents are reduced upon irradiation (**Figure 3.7(a,b)**). However, the electron current of [70]PCBM remained almost constant (Appendix **Figure A3.3.**). This appears to

suggest that the polymers degrade in the presence of UV, while [70]PCBM does not.

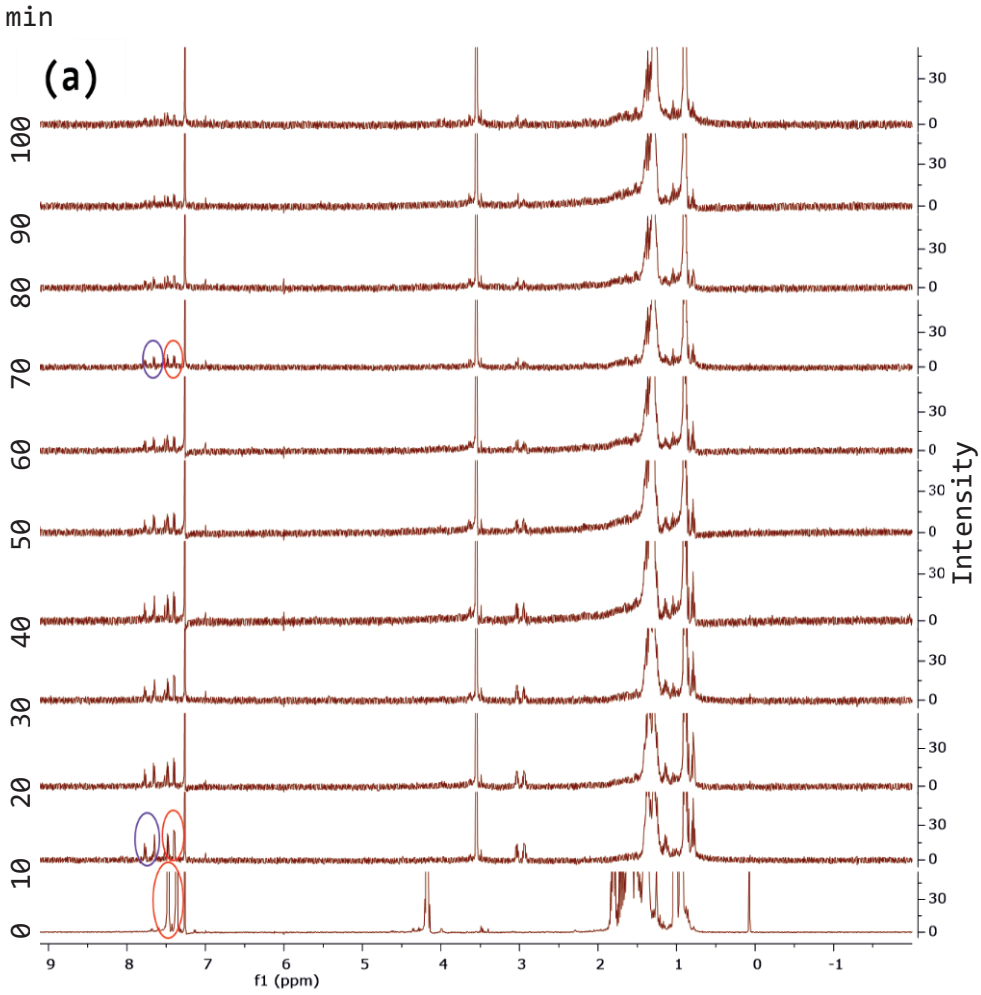

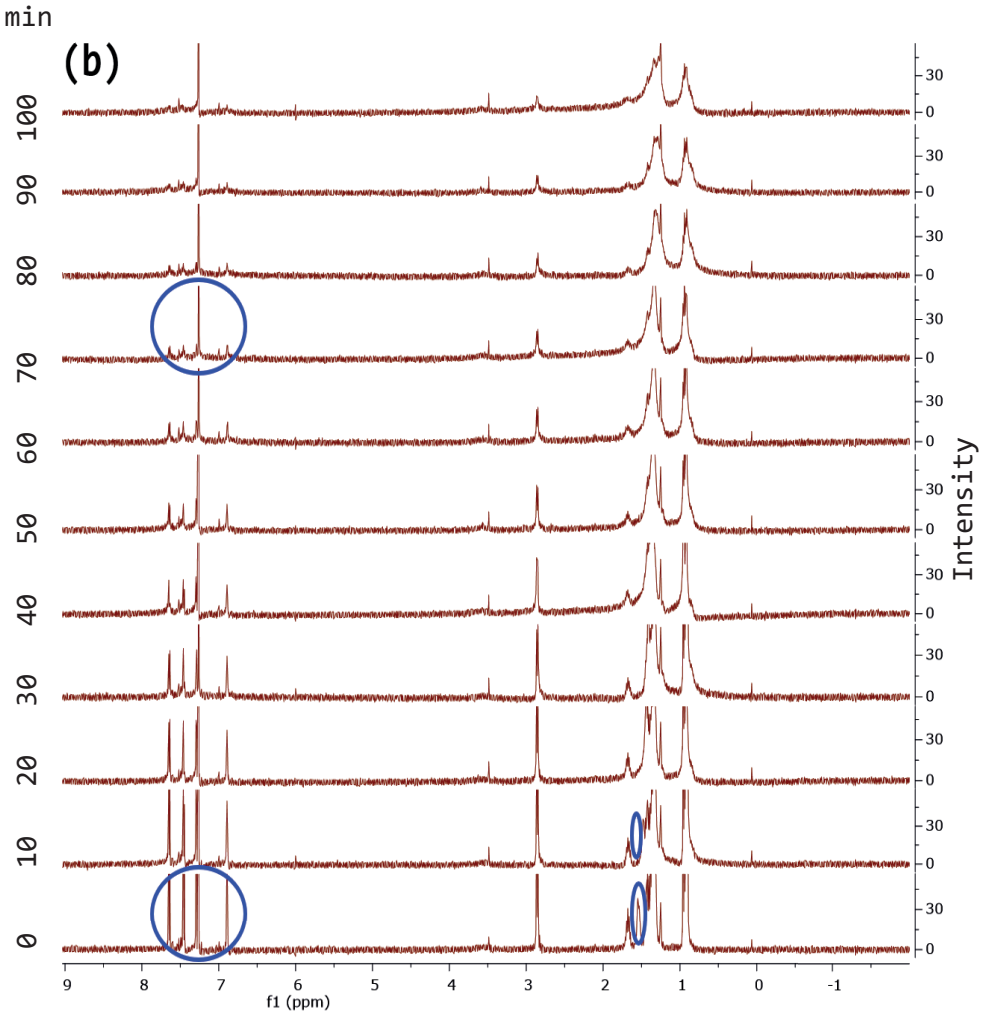

Figure 3.6: ^{1}H-NMR spectra of the monomer solutions of M_A **(a)** and M_{AT} **(b)**showing the peaks (initial and after exposure to a shuttered UV floodlight, 315-400, nm at intervals of 10 minutes for 100 mins with the initial spectrum labelled as 0).

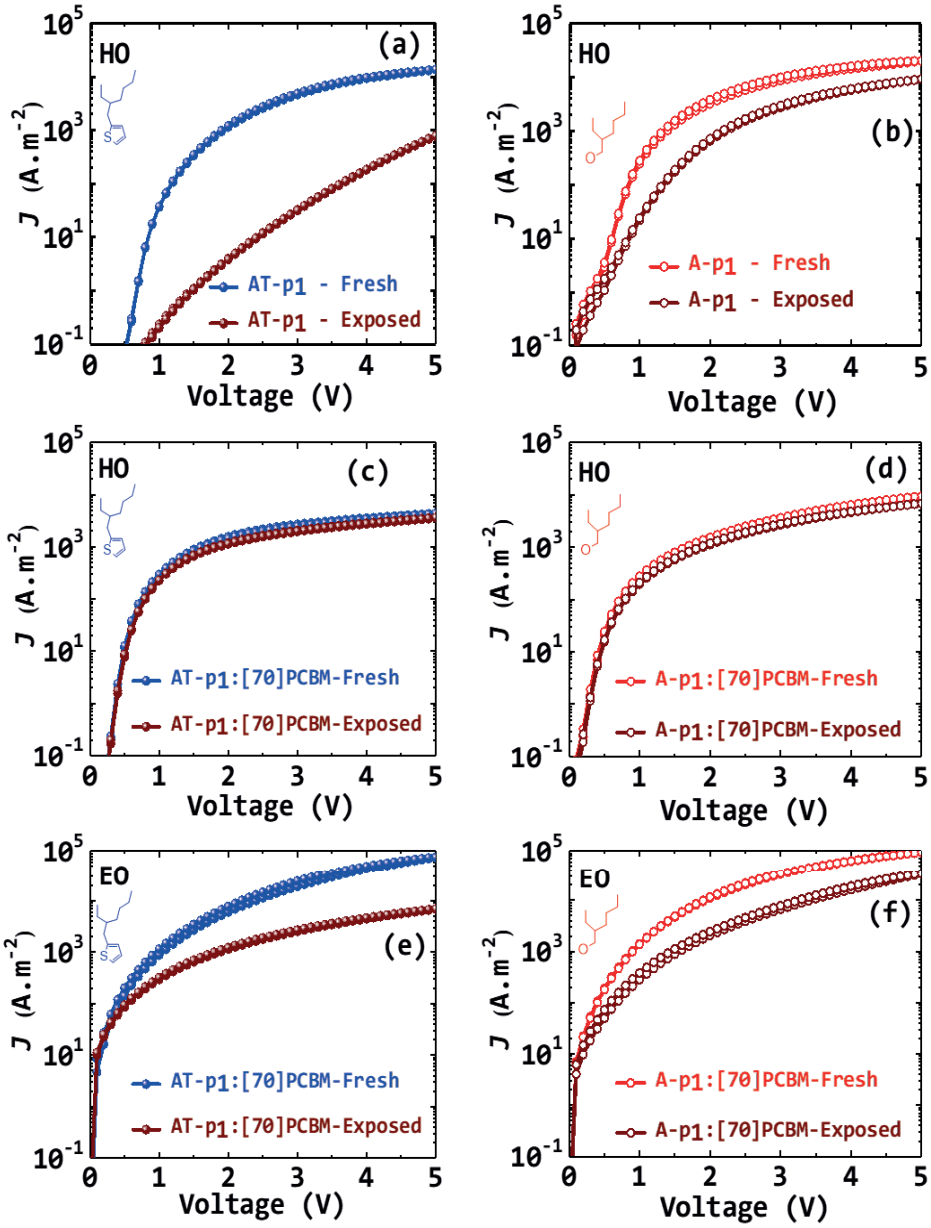

Figure 3.7: *J-V* Characteristics of fresh (AT-p, Blue; A-p, Red) and exposed (1-hour, Brown). Pristine polymer hole-only devices of AT-p_1 **(a)** and A-p_1 **(b)**; Blend hole-only devices of AT-p_1 **(c)** and A-p_1 **(d)**; Blend electron-only devices of AT-p_1 **(e)** and A-p_1 **(f)**. Device Thickness: Pristine (130-160 nm) and blend (100–130 nm).

This reduction in hole current is more significant for the AT-p devices than the A-p ones. Contrary to what is expected, upon UV-exposure, the hole currents of the blend devices, as shown in **Figure 3.7(c,d)**, remained rather almost constant (comparable to the current of the degraded pristine hole single carrier devices), while, the electron currents in **Figure 3.7(e,f)** are reduced. One would expect the opposite scenario where the hole current of the blends rather reduces upon illumination. The observed photodegradation behaviour in the monomer solutions and polymer devices suggests that the cleaved side-chains form byproducts that act as traps for electrons, resulting in the reduction of the electron current of the blends upon illumination (ageing). The photodegradation of all polymers may be initiated by their excited states. [70]PCBM quenches these states in the process and thereby fairly slows down the photooxidation,[45–47] especially, in the case of A-p devices. The alkoxy-side-chain cleavage leads to the oxidation of the quinone core. From the ^{1}H-NMR, it is evident that photodegradation leads to the formation of the oxidised form of the quinone moiety, which is quite stable.

On the other hand, there is a precipitated reduction of electron transport as observed in all cases. This deterioration is more pronounced in the AT-p devices than in the A-p devices. Thus, indicative of more negative effects of the AT-p decomposition products, acting as traps in the AT-p devices due to the broken molecules in the film. The pronounced destabilisation in AT-p devices coupled with the currents limiting effect is a possible explanation to why A-p devices are more photostable than the AT-p devices. To validate the argument of traps, light intensity dependence measurements

are performed on all polymer:fullerene solar cells. As explained in chapter 2, the ideality factor (n) as determined from the slope of V_{oc} against light intensity is used to evaluate the recombination losses in solar cells.[48] As a reminder, a stronger dependence of V_{OC} on light intensity reveals an increase of traps in the system[49], i.e., $1<n<2$. However, $n=1$ means bimolecular recombination is dominant, presupposing no traps.

Table 3.2: Ideality factor (n) of A-p solar cells vs. AT-p ones under continuous illumination (Fresh and exposed – 1 hr, 2 hrs, and 3 hrs).

Polymer	*n* Fresh	*n* 1hr	*n* 2hrs	*n* 3hrs
PTB7	1.50	1.70	1.77	1.80
PTB7-Th	1.09	1.30	1.34	1.35
PBDTTT-C	1.07	1.21	1.28	1.33
PBDTTT-CT	1.00	1.20	1.26	1.28
PBDTTT-E	1.66	1.66	1.66	1.66
PBDTTT-ET	1.43	1.58	1.58	1.54

In their fresh states, the fabricated AT-p devices have little or no trap-assisted recombination compared to their A-p counterparts, explaining their slightly better performance in PCE. For the fresh devices, the ideality factors are 1.50, 1.07, and 1.66 for A-p devices while AT-p devices recorded 1.09, 1, and 1,43. An increase in n is observed after continuous light exposure for almost all devices, confirming an increase in traps under illumination. **Table 3.2** displays the results; however, **Figure 3.8** puts them better in perspective. These relative percentage increases do not readily translate into known percentages of increases in traps. However, as shown in **Figure 3.8**, it points slightly to more increase in traps in the AT-p devices than the A-p ones upon UV-exposure. This may also

account for their faster decay. Thus, the photodegradation of these polymer:fullerene solar cells is dependent on the chemical structure of the polymers.

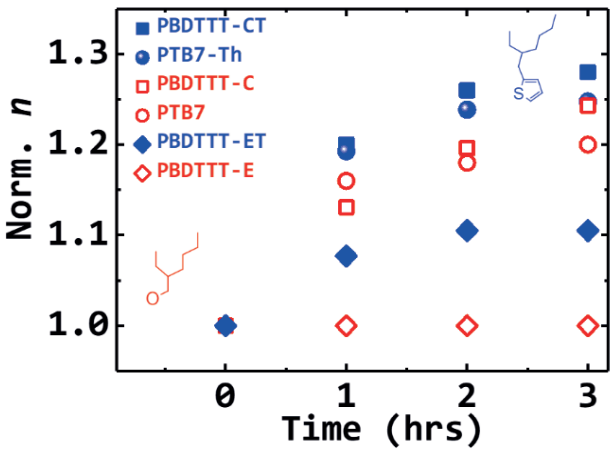

Figure 3.8: Time-dependent ideality factor (n) of the solar cells normalized to n_{Fresh}.

3.2.2. Performance: Reduced/Fluorinated TT-unit Polymer Solar Cells

Here, we aim to identify the effects of the structural changes in the thienothiophene (TT)-units or their moieties on the V_{oc} behaviour in relation to their photostability. These changes involve fluorination (addition reaction) of the TT-moiety and/or reduction of the alkyl-ester (AE) group on the TT-unit into an alkyl-ketone (AK) group. These subtle changes aim to improve device performance, clearly, the V_{oc}; thus, the PCE.[14,17–23,27,28]

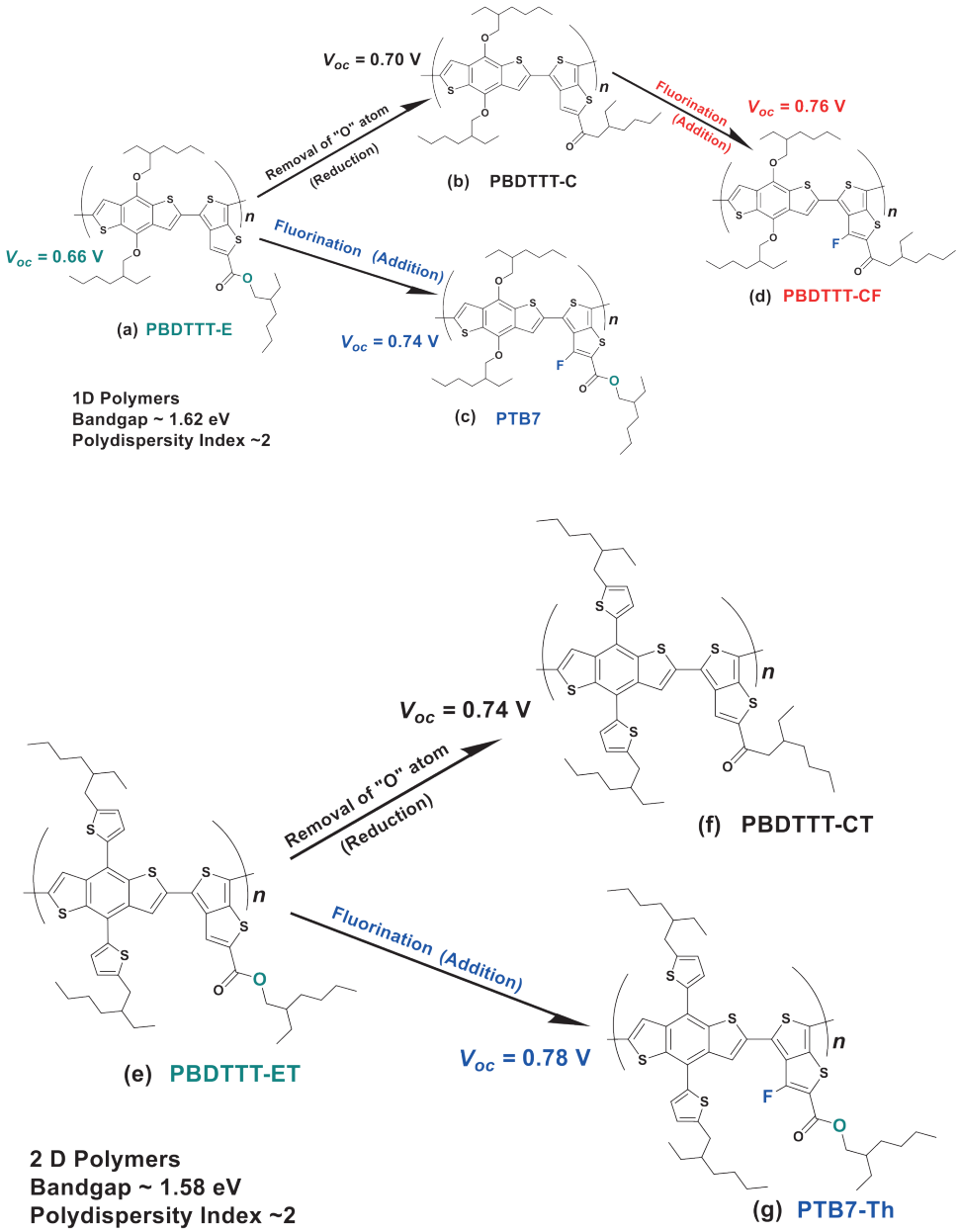

Figure 3.9: Chemical structures of the BDT-TT polymers. 1D: PBDTTT-E **(a)**, PBDTTT-C **(b)**, PTB7 **(c)**, and PBDTTT-CF **(d)**; and 2D: PBDTTT-ET **(e)**, PBDTTT-CT **(f)**, PTB7-Th **(g)**.

We are interested in the effects of these changes on photostability which until now are unknown. We selected seven BDT-TT polymers for a comprehensive study. They are classified into 1D and 2D polymers. Conventional solar cells are fabricated from the blend of the polymers (with a similar bandgap, molecular weight, and a polydispersity index of 2, see **Figure 3.9**) with [70]PCBM. The current-voltage characteristics are measured under continuous AM1.5G simulated light source illumination at open circuit, in an inert environment with H_2O and O_2 levels below 0.1 ppm.

Table 3.3: Photovoltaic parameters of blends of PBDT-TT:[70]PCBM solar cells under study. Thickness L ~100 nm, avg.: average

Polymers	TT-unit structural Changes	J_{sc} (mA.cm^{-2})	V_{oc} (V)	FF (%)	PCE (PCE$_{avg}$) (%)
PBDTTT-E[a]	Alkyl-ester (AE)	09.97	*0.689*	55.1	3.8 (3.5±0.3)
PBDTTT-C[b]	Alkyl-Ketone (AK)	13.00	*0.731*	52.7	5.0 (4.2±0.5)
PTB7[c]	AE-Fluorinated	11.52	*0.773*	58.4	5.2 (4.2±0.4)
PBDTTT-CF[d]	K-Fluorinated	12.30	*0.782*	56.0	5.6 (4.4±1.0)
PBDTTT-ET[e]	**Alkyl-ester (AE)**	**11.65**	***0.721***	**57.3**	**4.8 (4.4±0.4)**
PBDTTT-CT[f]	**Alkyl-Ketone (AK)**	**12.60**	***0.839***	**54.9**	**5.8 (5.5±0.3)**
PTB7-Th[g]	**AE-Fluorinated**	**17.28**	***0.806***	**67.4**	**9.4 (8.7±0.6)**

[A]22 devices, [B]32 devices, [C]37 devices, [d]17 devices, [e]27 devices, [f]25 devices, [g]32 devices)

3.2.2.1. Changes in TT-unit: Power Conversion Efficiency

Table 3.3 shows the current-voltage characteristics of the best performing (amidst roughly 190 solar cells altogether) devices of each of the seven types of cells together with their average efficiencies. The current-

voltage parameters in **Table 3.3**, as well as the current-voltage curves in **Figure 3.10(a,b)** show notable increasing trends in V_{oc}:

- from the alkyl-ester-TT-substituents to alkyl-ketone-TT-substituents and
- with the fluorination of the TT-units, whether from alkyl-ester-TT to fluorinated alkyl-ester-TT or alkyl-ketone-TT to fluorinated alkyl-ketone-TT.

This observation confirms the idea behind these changes and other results from the literature[14,17–23,27,28], however, with a good number of polymers. Also, the increasing trend is fairly observed in the J_{sc}. These effects explain the differences observed in the PCEs of the devices. For example, in the 1D polymers the reduction of the alkyl-ester-TT-polymer (PBDTTT-E) to the alkyl-ketone-TT-polymer (PBDTTT-C) improves the V_{oc} from 0.69 V to 0.73 V. The fluorination of the TT-unit of PBDTTT-E into PTB7 profits from an improvement in V_{oc} from 0.69 V to 0.77 V. Likewise, the fluorination of the TT-unit of PBDTTT-C into PBDTTT-CF improves the V_{oc} from 0.73 V to 0.78 V. These increase in V_{oc} effects coupled with those of J_{sc} lead respectively to increment in PCE, from 3.8% to 5.0%, then to 5.2%, and from 5.0% to 5.6%.

Similarly, for the 2D polymers, the *reduction* leads to an increase in V_{oc} from 0.72 V to 0.84 V and the fluorination yields an increase in V_{oc} from 0.72 V to 0.81 V, translating partly into an increase in PCEs respectively from 4.8% to 5.8%, and then to 9.4%. Details of device counts with the efficiency spread of the 1D and 2D PSCs are displayed in **Figure 3.10 (c,d)**.

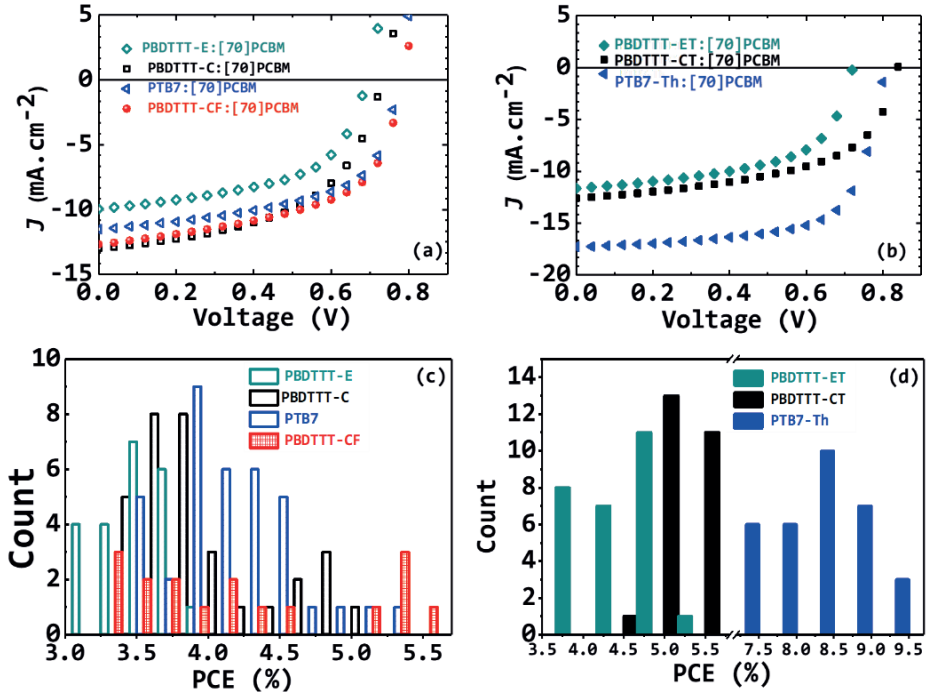

Figure 3.10: Efficiency performance of the TT-moieties-polymer solar cells. *J-V* characteristic curves: 1D polymers **(a)** and 2D polymers **(b)**; device count vs efficiency: 1D polymers **(c)** and 2D polymers **(d)**. We can see enhancement in the performance (V_{oc}) of the solar cells due to the changes on the TT-units.

3.2.2.2. Relating Subtle Changes in TT-unit to Device Stability

It is fascinating how these subtle changes in polymer chemical structure could lead to tremendous improvements in the efficiency of their solar cells. However, the question is, "how do these changes affect the performance of the devices regarding stability?". To answer this question, the relationship between these changes in structure and the photostability of the solar cells is studied in an inert atmosphere at room temperature by active cooling. The findings lead to the general observation that,

reduction of the alkyl-ester-substituents on the TT-unit into an alkyl-ketone-substituents improves the photostability of the solar cell while the fluorination of the TT-units leads to a rapid decline in photostability as depicted in **Figures 3.11** and **3.12**.

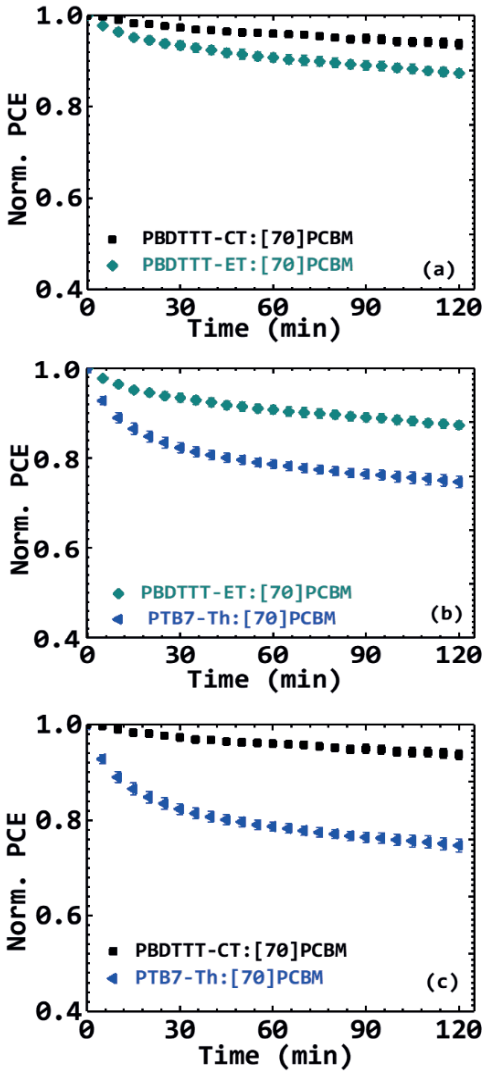

Figure 3.11: Time evolution of average PCE of 2D polymer:fullerene solar cells. PBDTTT-ET vs: PBDTTT-CT **(a)** and PTB7-Th **(b)**; PBDTTT-CT vs PTB7-Th **(c)**.

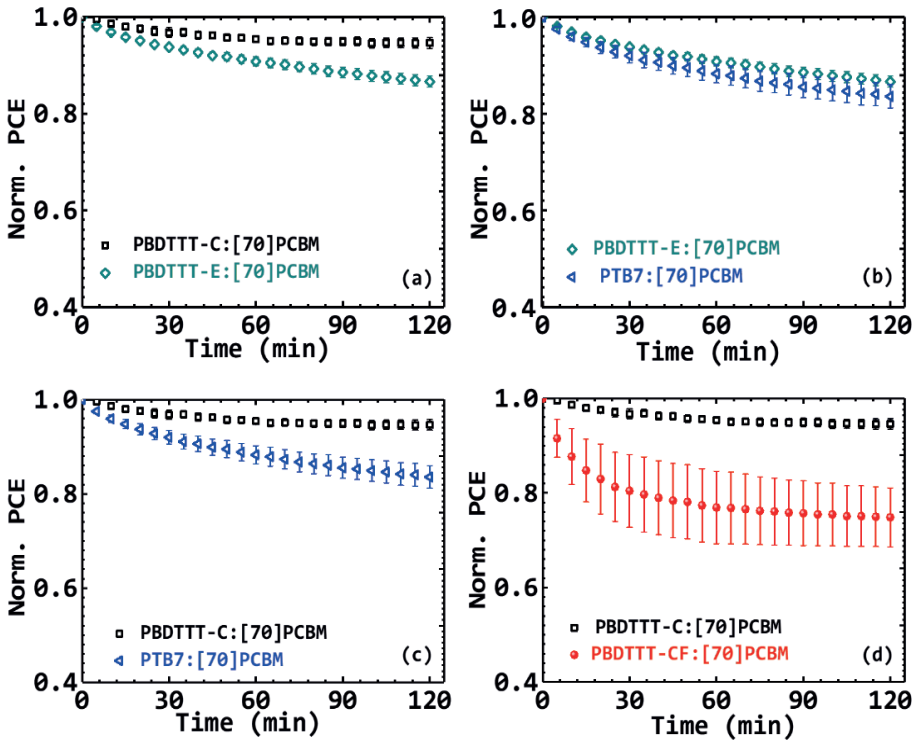

Figure 3.12: Time evolution of average PCE of 1D polymer:fullerene solar cells. PBDTTT-E vs: PBDTTT-C **(a)** and PTB7 **(b)**; PBDTTT-C vs: PTB7 **(c)** and PBDTTT-CF **(d)**.

The figures display comparative average PCE decays for all seven types of PSCs. The trends are similar in both 1D and 2D PSCs. However, it is more distinct in the 2D PSCs, certainly due to the effect of the alkylthienyl substituent on the BDT, which are previously discussed [35,51] in section 3.2.1.2.

For example, in **Figure 3.11a** and **3.12a**, when one moves from an alkyl-ester-substituted-TT-unit PSC to an alkyl-ketone-substituted-TT-unit PSC, improvements in the photostability are recorded. On the average, from 13.4%

PCE decay to 5.4% decay for 1D PSCs and from 12.6% PCE decay to 6.3% decay for 2D PSCs. In **Figure 3.11b** and **3.12(b,c)**, the fluorination of the alkyl-ester- or alkyl-ketone-substituted-TT-units shows deteriorations in the photostability of the cells.

On average, there is an acceleration in PCE decay for 1D PSCs from 13.4% to 16.5% and from 5.4% to 25.1%. A similar increase in PCE decay is observed for 2D PSCs from 12.6% to 25.3%. This decay in the photostability becomes wider when one moves from alkyl-ketone-substituted-TT-unit PSCs to alkyl-ester-fluorinated-TT-unit PSCs. **Figure 3.11c** and **3.12d** depict the changes with an increase in the average PCE degradation from 5.4% to 16.5% for 1D PSCs and from 6.3% to 25.3% for the 2D PSCs.

A quick look at the decay of the other *J-V* parameters in **Figure 3.13** reveals that the loss in J_{sc} is chiefly the main contributing factor to the PCE decay in all considered polymers, except for the fluorinated-TT-units polymer PBDTTT-CF (1D) and PTB7-Th (2D) cells which also record considerable losses in FF.

To further grasp the reason behind these observations, charge transport and V_{oc} light intensity dependence studies are performed. In general, for charge transport, there are decreases in the hole currents of the pristine polymer devices and electron currents of the blend film devices upon UV-exposure, with observed exacerbation when fluorinated. While the hole currents of the blend hole-only devices remain unchanged. In brief, these findings point to the fact that, in our case, *reduction* improves photostability while fluorination deteriorates photostability.

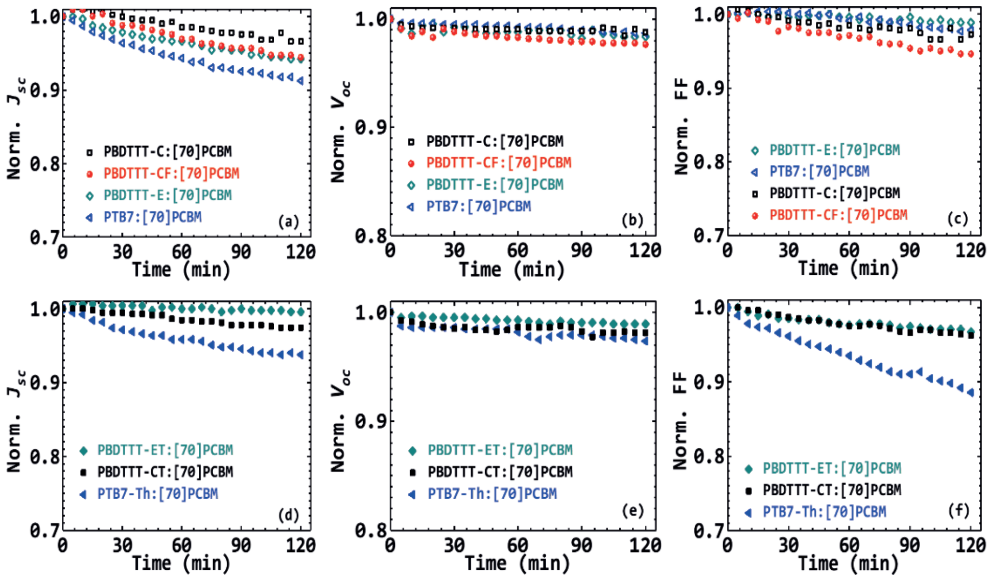

Figure 3.13: Time evolution of other *J-V* parameters (J_{sc}, V_{oc}, FF) for 1D polymers **(a,b,c)** and 2D polymers **(d,e.f)**.

Table 3.4: Ideality factor (*n*), at different illumination time, of the 1D or 2D polymer:[70]PCBM solar cells processed from oDCB.

Class of PBDT-TT polymer	Polymer	TT-unit structural Changes	*n* Fresh	*n* 1hr	*n* 2hrs
1D polymer	PBDTTT-E	Alkyl-ester (AE)	1.66	1.66	1.66
	PBDTTT-C	Alkyl-ketone (AK)	1.00	1.04	1.04
	PTB7	AE-Fluorinated	1.39	1.48	1.52
	PBDTTT-CF	AK-Fluorinated	1.04	1.00	1.00
2D polymer	PBDTTT-ET	Alkyl-ester	1.43	1.54	1.58
	PBDTTT-CT	Alkyl-ketone	1.12	1.12	1.04
	PTB7-Th	AE-Fluorinated	1.20	1.31	1.33

Finally, V_{oc} light intensity dependence measurements reveal in **Table 3.4** that both *reduction* and fluorination decrease the ideality factor (n). Thus, the number of initial traps present in their corresponding PSCs. The slope of the V_{oc} against light intensity, $n\frac{KT}{q}$, tells about the type of recombination mechanisms present in a solar cell. Fewer traps will also lead to higher V_{oc} as it reduces trap-assisted recombination. This confirms why the rest of the PSCs perform better in efficiency compared to the alkyl-ester-TT based solar cells. For example, *reduction* decreases n from 1.66 to 1.00, in the case of 1D polymers, while it decreases it from 1.43 to 1.12 in the case of 2D ones. Fluorination reduces n from 1.66 to 1.39 when one transits from PBDTTT-E to PTB7, and from 1.43 to 1.2 while going from PBDTTT-ET to PTB7-Th.

Upon continuous exposure to light for 1 hour and 2 hours, n increases for the alkyl-ester-TT and the fluorinated-TT polymers, especially for PBDTTT-ET from 1.43 to 1.54, and then to 1.58; for PTB7 from 1.39 to 1.48, and then to 1.52; and for PTB7-Th from 1.20 to 1.31, and then to 1.33. However, n remains fairly constant for the alkyl-ketone-TT polymers, that is for PBDTTT-C from 1.00 to 1.04 and for PBDTTT-CT from 1.12 to 1.12, and then to 1.04. This implies that the presence of the fluorine atom and that of the alkyl-ester groups on the TT-units (upon cleavage under the effect of illumination) are possible sources of extra traps in the solar cells. Thus, leading to their faster photodegradation compared to the other solar cells of the same family. This supports the notion that the increase in trap density is the reason behind the observed trends in photodegradation.

3.3. Conclusions

The experiments on the BDT-unit polymers confirm that the observed photodegradation in the solar cells is neither due to photobleaching nor is the accelerated degradation of the AT-p devices compared to the A-p ones due to the acidity of the PEDOT:PSS layer or the doping effect of LiF. This leads us to attribute the enhanced photodegradation of the AT-p-based solar cells to their chemical structures, especially to the alkylthienyl-side-chains. Moreover, ^{1}H-NMR studies revealed a faster photodegradation mechanism for the AT-p polymer solar cells based on the monomer solution study. Furthermore, V_{OC} light intensity dependence study also suggests a higher increase in traps, and thus, alludes to a faster photodegradation mechanism in AT-p based solar cells.

These findings boost our understanding of the critical role played by the chemical structure of polymers in the stability of PSCs. The data suggest that stable organic solar cells can be achieved if more studies are done in this direction. At this stage, it is evident that alkoxy-side-chains polymers are better performers in general, in terms of photostability than the alkylthienyl-side-chains ones of the same backbone. Finally, the study leads us to the following observations: i) BDT-unit polymers degrade. When used for solar cells there is a need for long pass filters and ii) the polymer degradation in the devices under illumination which is also observed in the reduction of the pristine hole currents does not always translate into a loss in the hole current of the blends.

For the TT-unit polymers, the *reduction* of the alkyl-ester-groups on the TT-unit into alkyl-ketone-substituents significantly improves the photostability of the solar cells. In contrast, the *addition* reaction, in this case, the fluorination of the TT-units results in the opposite effect. It greatly worsens the photostability of the solar cells in all three considered cases. In general, regarding photostability of the solar cells, alkyl-ketone-TT unit polymers are the best performers (PBDTTT-C and PBDTTT-CT), followed by the alkyl-ester-TT unit polymers (PBDTTT-E and PBDTTT-ET) and the least photostable are the fluorinated-TT unit polymers (PTB7, PBDTTT-CF, and PTB7-Th). These findings, first of the kind, add to the limited understanding in the literature on the effect that the structural changes in polymers for V_{oc} enhancement have on the stability of their solar cells. Though the results are important additions to the knowledge of the scientific community, they are only limited to PBDT-TT polymers and may not be generalised to all polymers. It would be interesting to see if this is the case for all fluorinated, chlorinated, sulfonated or alkyl-ester polymers. The results would pave the way for new materials that yield efficient as well as stable organic solar cells.

Bibliography

[1] L. Ye, S. Q. Zhang, L. J. Huo, M. J. Zhang, J. H. Hou, *Acc. Chem. Res.* **2014**, *47*, 1595.

[2] J. Hou, M. Park, S. Zhang, Y. Yao, L.-M. Chen, J.-H. Li, Y. Yang, *Macromolecules* **2008**, *41*, 6012.

[3] H. Zhang, L. Ye, J. Hou, *Polym. Int.* **2015**, *64*, 957.

[4] Y. Liang, Y. Wu, D. Feng, S.-T. Tsai, H.-J. Son, G. Li, L. Yu, *J. Am. Chem. Soc.* **2008**, *131*, 56.

[5] Y. Huang, X. Guo, F. Liu, L. Huo, Y. Chen, T. P. Russell, C. C. Han, Y. Li, J. Hou, *Adv. Mater.* **2012**, *24*, 3383.

[6] L. Dou, Y. Liu, Z. Hong, G. Li, Y. Yang, *Chem. Rev.* **2015**, *115*, 12633.

[7] J. Huang, C. Z. Li, C. C. Chueh, S. Q. Liu, J. S. Yu, A. K. Y. Jen, *Adv. Energy Mater.* **2015**, *5*, 4.

[8] C. Liu, K. Wang, X. Hu, Y. Yang, C.-H. Hsu, W. Zhang, S. Xiao, X. Gong, Y. Cao, *ACS Appl. Mater. Interfaces* **2013**, *5*, 12163.

[9] L. Ye, S. Zhang, W. Zhao, H. Yao, J. Hou, *Chem. Mater.* **2014**, *26*, 3603.

[10] S. Zhang, L. Ye, J. Hou, *Adv. Energy Mater.* **2016**, *6*, DOI 10.1002/aenm.201502529.

[11] W. Zhao, L. Ye, S. Zhang, M. Sun, J. Hou, *J. Mater. Chem. A* **2015**, *3*, 12723.

[12] H. Zhou, Y. Zhang, C. K. Mai, S. D. Collins, G. C. Bazan, T. Q. Nguyen, A. J. Heeger, *Adv. Mater.* **2015**, *27*, 1767.

[13] L. Huo, S. Zhang, X. Guo, F. Xu, Y. Li, J. Hou, *Angew. Chemie - Int. Ed.* **2011**, *50*, 9697.

[14] J. Yuan, Z. Zhai, H. Dong, J. Li, Z. Jiang, Y. Li, W. Ma, *Adv. Funct. Mater.* **2013**, *23*, 885.

[15] Y. Liang, Z. Xu, J. Xia, S. T. Tsai, Y. Wu, G. Li, C. Ray, L. Yu, *Adv. Mater.* **2010**, *22*, 135.

[16] S. H. Liao, H. J. Jhuo, Y. S. Cheng, S. A. Chen, *Adv. Mater.* **2013**, *25*, 4766.

[17] P. Liu, K. Zhang, F. Liu, Y. Jin, S. Liu, T. P. Russell, H. L. Yip, F. Huang, Y. Cao, *Chem. Mater.* **2014**, *26*, 3009.

[18] S. C. Price, A. C. Stuart, L. Yang, H. Zhou, W. You, *J. Am. Chem. Soc.* **2011**, *133*, 4625.

[19] Y. Huang, L. Huo, S. Zhang, X. Guo, C. C. Han, Y. Li, J. Hou, *Chem. Commun. (Camb).* **2011**, *47*, 8904.

[20] A. C. Stuart, J. R. Tumbleston, H. Zhou, W. Li, S. Liu, H. Ade, W. You, *J. Am. Chem. Soc.* **2013**, *135*, 1806.

[21] H. Bronstein, J. M. Frost, A. Hadipour, Y. Kim, C. B. Nielsen, R. S. Ashraf, B. P. Rand, S. Watkins, I. McCulloch, *Chem. Mater.* **2013**, *25*, 277.

[22] C. Cui, W.-Y. Wong, Y. Li, *Energy Environ. Sci.* **2014**, *7*, 2276.

[23] C. Wang, C. J. Mueller, E. Gann, A. C. Y. Liu, M. Thelakkat, C. R. McNeill, *J. Polym. Sci. Part B Polym. Phys.* **2017**, 55(1), 49-59.

[24] S. Qu, H. Wang, D. Mo, P. Chao, Z. Yang, L. Li, L. Tian, W. Chen, F. He, *Macromolecules* **2017**, *50*, 4962.

[25] D. Mo, H. Wang, H. Chen, S. Qu, P. Chao, Z. Yang, L. Tian, Y.-A. Su, Y. Gao, B. Yang, W. Chen, F. He, *Chem. Mater.* **2017**, *29*, 2819.

[26] J. Hou, H.-Y. Chen, S. Zhang, R. I. Chen, Y. Yang, Y. Wu, G. Li, *J. Am. Chem. Soc.* **2009**, *131*, 15586.

[27] M. Zhang, X. Guo, Y. Yang, J. Zhang, Z.-G. Zhang, Y. Li, *Polym. Chem.* **2011**, *2*, 2900.

[28] Q. Peng, X. Liu, D. Su, G. Fu, J. Xu, L. Dai, *Adv. Mater.* **2011**, *23*, 4554.

[29] Y. Liu, J. Zhao, Z. Li, C. Mu, W. Ma, H. Hu, K. Jiang, H. Lin, H. Ade, H. Yan, *Nat. Commun.* **2014**, *5*, 5293.

[30] J.-D. Chen, C. Cui, Y.-Q. Li, L. Zhou, Q.-D. Ou, C. Li, Y. Li, J.-X. Tang,

Adv. Mater. **2015**, *27*, 1035.
[31] S. H. Liao, H. J. Jhuo, P. N. Yeh, Y. S. Cheng, Y. L. Li, Y. H. Lee, S. Sharma, S. A. Chen, *Sci. Rep.* **2014**, *4*, 6813.
[32] C. Liu, C. Yi, K. Wang, Y. Yang, R. S. Bhatta, M. Tsige, S. Xiao, X. Gong, *ACS Appl. Mater. Interfaces* **2015**, *7*, 4928.
[33] L. Meng, Y. Zhang, X. Wan, C. Li, X. Zhang, Y. Wang, X. Ke, Z. Xiao, L. Ding, R. Xia, H. Yip, Y. Cao, Y. Chen, *Science* **2018**, *2612*, 1.
[34] L. Fernandes, H. Gaspar, J. P. C. Tomé, F. Figueira, G. Bernardo, *Polym. Bull.* **2018**, 75(2), 515-532.
[35] N. Y. Doumon, G. Wang, R. C. Chiechi, L. J. A. Koster, *J. Mater. Chem. C* **2017**, *5*, 6611.
[36] M. Manceau, E. Bundgaard, J. E. Carlé, O. Hagemann, M. Helgesen, R. Søndergaard, M. Jørgensen, F. C. Krebs, *J. Mater. Chem.* **2011**, *21*, 4132.
[37] S. A. Gevorgyan, M. V. Madsen, B. Roth, M. Corazza, M. Hösel, R. R. Søndergaard, M. Jørgensen, F. C. Krebs, *Adv. Energy Mater.* **2016**, *6*, 1.
[38] Y. Sun, C. J. Takacs, S. R. Cowan, J. H. Seo, X. Gong, A. Roy, A. J. Heeger, *Adv. Mater.* **2011**, *23*, 2226.
[39] W. J. E. Beek, M. M. Wienk, M. Kemerink, X. Yang, R. a J. Janssen, *J. Phys. Chem. B* **2005**, *109*, 9505.
[40] G. Wang, T. Jiu, G. Tang, J. Li, P. Li, X. Song, F. Lu, J. Fang, *ACS Sustain. Chem. Eng.* **2014**, *2*, 1331.
[41] R. Steim, F. R. Kogler, C. J. Brabec, *J. Mater. Chem.* **2010**, *20*, 2499.
[42] A. Garcia, G. C. Welch, E. L. Ratcliff, D. S. Ginley, G. C. Bazan, D. C. Olson, *Adv. Mater.* **2012**, *24*, 5368.
[43] M. O. Reese, A. J. Morfa, M. S. White, N. Kopidakis, S. E. Shaheen, G. Rumbles, D. S. Ginley, *Sol. Energy Mater. Sol. Cells* **2008**, *92*, 746.
[44] F. Fungura, W. R. Lindemann, J. Shinar, R. Shinar, *Adv. Energy Mater.* **2016**, 1601420.
[45] C. J. Brabec, G. Zerza, G. Cerullo, S. De Silvestri, S. Luzzati, J. C. Hummelen, S. Sariciftci, *Chem. Phys. Lett.* **2001**, *340*, 232.
[46] M. Manceau, A. Rivaton, J. L. Gardette, S. Guillerez, N. Lemaître, *Polym. Degrad. Stab.* **2009**, *94*, 898.
[47] M. O. Reese, A. M. Nardes, B. L. Rupert, R. E. Larsen, D. C. Olson, M. T. Lloyd, S. E. Shaheen, D. S. Ginley, G. Rumbles, N. Kopidakis, *Adv. Funct. Mater.* **2010**, *20*, 3476.
[48] L. J. A. Koster, V. D. Mihailetchi, R. Ramaker, P. W. M. Blom, *Appl. Phys. Lett.* **2005**, *86*, 1.
[49] M. M. Mandoc, F. B. Kooistra, J. C. Hummelen, B. De Boer, P. W. M. Blom, *Appl. Phys. Lett.* **2007**, *91*, 2007.
[50] N. Y. Doumon, L. J. A. Koster, *Sol. RRL* **2019**, *3*, 1800301.
[51] N. Y. Doumon, G. Wang, X. Qiu, A. J. Minnaard, R. C. Chiechi, L. J. A. Koster, *Sci. Rep.* **2019**, *9*, 4350.
[52] D. Bartesaghi, G. Ye, R. C. Chiechi, L. J. A. Koster, *Adv. Energy Mater.* **2016**, *6*, 1.

Appendix 3 (A3)

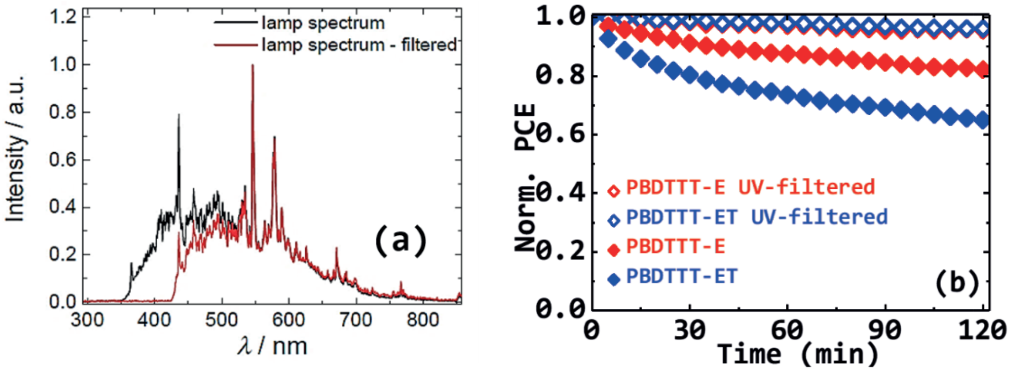

Figure A3.1: Spectrum of unfiltered (black line) and UV-filtered (red line) lamp used during the (degradation) experiment[52] **(a)** and PCE normalized decay of PBDTTT-E:[70]PCBM and PBDTTT-ET:[70]PCBM solar cells exposed to unfiltered and UV-filtered lamp **(b)**.[51] The cells remain stable when exposed to a UV-filtered lamp.

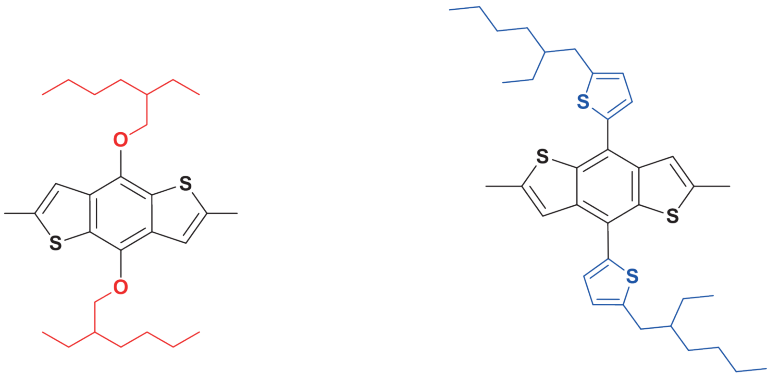

(a) Alkoxy BDT-monomer (M_A) (b) Alkylthienyl BDT-monomer (M_{AT})

Figure A3.2: Chemical Structures of the BDT-monomers. Alkoxy-polymer-based monomer, M_A **(a)** and Alkylthienyl-polymer-based monomer, M_{AT} **(b)**.

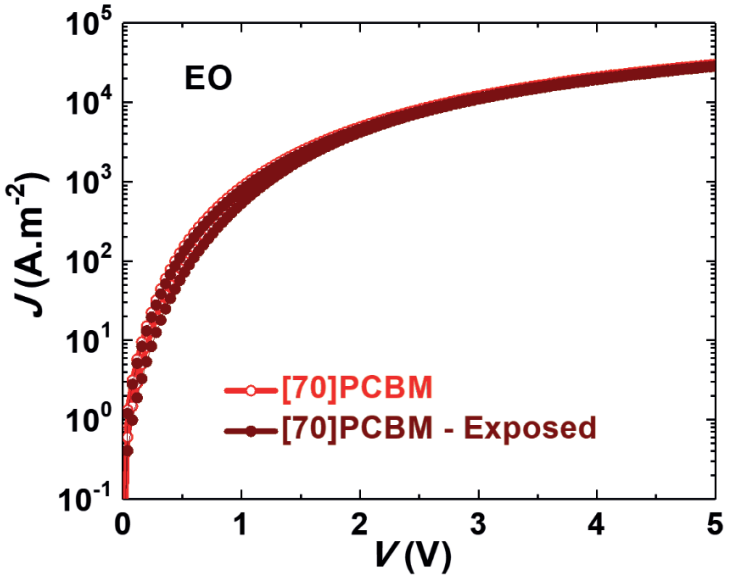

Figure A3.3: *J-V* curves of fresh (red) and exposed (brown, 1 hr) [70]PCBM Electron-only device.

4

Photostability of Fullerene and Non-Fullerene Polymer Solar Cells: The Role of the Acceptor

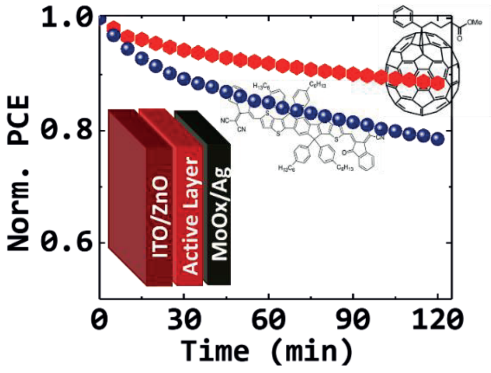

Chapter based on publications number 2 and 5

4

SUMMARY

Recently, the advent of non-fullerene acceptors (NFAs) made it possible for organic solar cells (OSCs) to break the 10% efficiency barrier hardly attained by fullerene acceptors (FAs). In the past five years alone, more than hundreds of NFAs with applications in organic photovoltaics (OPVs) have been synthesized, enabling a notable current record efficiency of above 16%. Hence, there is a shift in interest towards the use of NFAs in OPVs. However, there has been little work on the stability of these new materials in devices. More importantly, there is very little comparative work on the photo-stability of FAs vs. NFAs solar cells, to ascertain the pros and cons of the two systems. Here, we show the photo-stability of solar cells based on two workhorse acceptors, in both conventional and inverted structures, namely ITIC (as NFA) and [70]PCBM (as FA) blended with either PBDB-T or PTB7-Th polymer. We found that irrespective of the polymer, the cell structure, or the initial efficiency, the [70]PCBM devices are more photo-stable than the ITIC ones. This observation, however, opposes the assumption that NFA solar cells are more photo-chemically stable. These findings suggest that complementary absorption should not take precedence in the design rules for the synthesis of new molecules, and there is still work left to be done to achieve stable as well as efficient OSCs.

4.1. Introduction

Many industrious works[1–15] aid in improving the efficiency of organic solar cells (OSCs), by tuning the donor material's compatibility with the fullerene acceptors (FAs), mostly [70]PCBM with an efficiency rarely surpassing 10%.[12,13,16–18] Fullerene derivatives are limited by their poor absorption of the solar spectrum and energy level tunability. Thus, improvement in the performance of OSCs became a hurdle. All-polymer solar cells[19–22] or non-fullerene solar cells[4,23–29] have become the norm. The workhorse of these non-fullerene acceptors (NFAs) is ITIC, a small organic molecule. These novel acceptors boosted the power conversion efficiency (PCE) above 16% in single junction[30–32] and 17.3% for multijunction[33] OSCs. With the advent of the NFAs, currently outperforming the FAs, the focus has been on the device efficiency and little is done to understand their stability[29,34–36]. One such study, among others, shows IDTBR NFAs to be more stable.[25,37,38] However, the solar cells are considered under their presumed optimal conditions, i.e., the FA-based cells are processed with additives, namely 1,8-diiodooctane, DIO.[37,38] DIO is known to affect photostability negatively.[39–41]

This chapter is dedicated to exploring the role of the acceptors in the photodegradation of their respective solar cells without DIO. An extensive comparative study between the fullerene derivative acceptor, [70]PCBM, and the widely used non-fullerene small molecule acceptor, ITIC, is reported mainly on blends with PBDB-T polymer in section 4.2 (also with PTB7-Th, a second polymer, to corroborate the findings). **Figure 4.1** displays the

chemical structures of the molecules. Section 4.3 briefly discusses the effect of the chemical structure changes in ITIC[26,35,42,43] for improved efficiency[29,35,44] on photostability. The study of the photodegradation behavior of the devices is done with a combination of measurement techniques such as i) changes in current-voltage parameters for monitoring charge transport and recombination processes; ii) UV-Vis-NIR absorption for tracking changes in absorption; iii) atomic force microscopy (AFM) for detecting changes in morphology; and iv) transient photovoltage (TPV) together with extraction measurement for monitoring changes in rates of recombination and extraction. The differences in performance in both PCE and photostability of [70]PCBM and ITIC with its derivatives are elucidated.

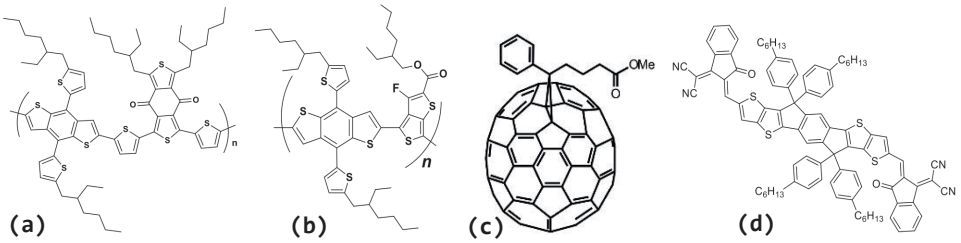

Figure 4.1: Chemical structure: PBDB-T **(a)**, PTB7-Th **(b)**, [70]PCBM **(c)**, and ITIC **(d)**.

4.2. FA vs. NFAs - Results and Discussions

4.2.1. Performance: Power Conversion Efficiency

Conventional and inverted solar cells, with active layers processed from chlorobenzene (CB), are fabricated as described in chapter 2. Their

current-voltage (*J-V*) characteristics are monitored under continuous illumination. The measurements are conducted at room temperature by active cooling, in an inert atmosphere, in a glovebox with both O_2 and H_2O levels kept below 0.1 ppm. The performance in terms of efficiency and photostability of the cells are evaluated. The best performing solar cells yield 7.1% for PBDB-T:[70]PCBM while PBDB-T:ITIC solar cells recorded 8.1%. The same trend is observed for inverted solar cells, with 5.7% for [70]PCBM-based solar cells and 8.6% for ITIC-based ones. The best *J-V* parameters and average values of the PCEs are displayed in **Table 4.1**.

Table 4.1: Device parameters of cells under study with mean values for the cells obtained for the indicated number of devices per type processed from CB. conv.: conventional, inv.: inverted, mn: mean. SD: standard deviation. Thickness is 100 nm.

Devices	Treatment	J_{sc} (A.m^{-2})	V_{oc} (V)	FF (%)	PCE (%) (PCE$_{mn}$±SD)
PBDB-T:ITIC[a]	conv. 100° C 10 min	142.0	0.887	65.9	8.1 (7.1±0.5)
PBDB-T:[70]PCBM[b]	conv.	118.1	0.870	69.9	7.1 (6.6±0.3)
PBDB-T:ITIC[c]	inv. 160° C 10 min	145.0	0.831	71.1	8.6 (8.1±0.4)
PBDB-T:[70]PCBM[d]	inv.	112.6	0.842	60.4	5.7 (5.0±0.5)

[a],[b]53 devices,[c]19 devices,[d]9 devices,

The better PCE performance of the ITIC-based cells is mainly due to increment in the short-circuit current density J_{sc}, resulting from the complementarity of the absorption of the donor and the acceptor materials. PBDB-T has an overlapping spectrum with [70]PCBM while it is complementary to the ITIC spectrum in the visible range (appendix **Figure A4.1a**). There is a 100 nm red-shift between the spectra of the two blends as seen in

Figure A4.1b. PBDB-T:ITIC film does not only absorb more in the visible range than PBDB-T:[70]PCBM but it also strongly absorbs at longer wavelengths, especially up to 800 nm in the IR region. Next, the better performance of the ITIC devices may also be explained by less trap-assisted recombination in their fresh devices compared to the [70]PCBM-based fresh devices (*n* values for the fresh devices in **Table 4.2**). The EQE spectra and the statistics of conventional devices are shown in **Figure A4.2.** On the other hand, when PBDB-T is replaced in the blends by PTB7-Th, the opposite trend is observed. That is more current from [70]PCBM-based devices as compared to ITIC ones. This observation is partly due to the complementarity of the absorption spectra of [70]PCBM and PTB7-Th.

4.2.2. Performance: Degradation and Stability

Figure 4.2 displays the degradation curves of the current-voltage parameters of conventional solar cells fabricated in an inert environment and measured in a glovebox with H_2O and O_2 levels below 0.1 ppm. **Figure 4.3** displays the degradation curves of the current-voltage parameters of inverted solar cells. The PCE degradation curves in **Figure 4.2a** reveal the same trend for all types of devices, thus, gradual decay of the efficiency which slows down over time with the ITIC-devices losing more in PCE. This is indicative of the role played by the donor and the acceptors, respectively, in the degradation process. It is observed that ITIC based devices are less stable than [70]PCBM based ones. Among the current-voltage

parameters in **Figure 4.2**, the FF in **Figure 4.2d** and **Figure 4.3b** accounts for the most loss in the PCE decay.

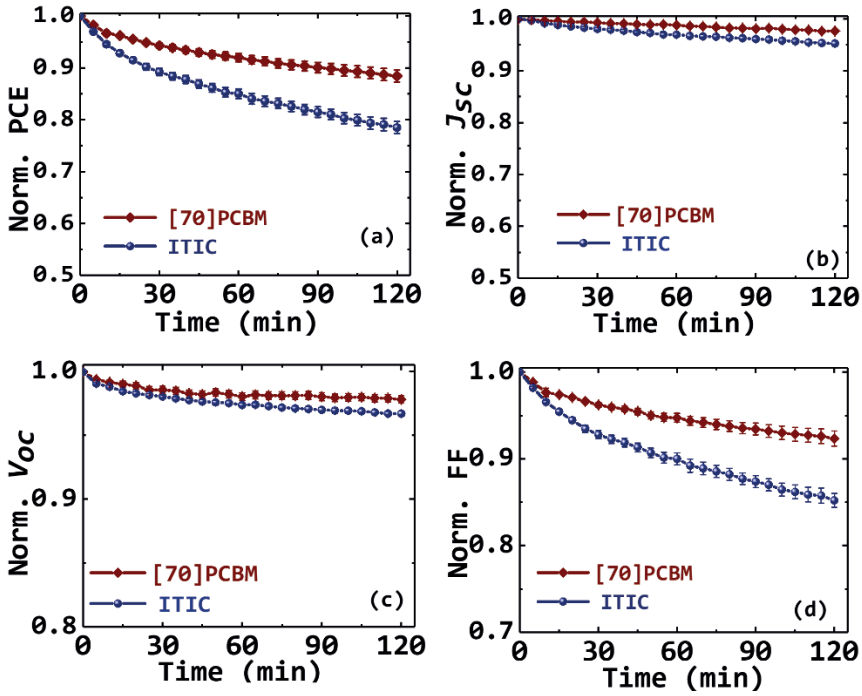

Figure 4.2: Time evolution of current-voltage parameters of conventional solar cells normalized to their initial values (at t=0 min) under continuous illumination (average of about 20 devices each): PCE **(a)**, J_{sc} **(b)**, V_{oc} **(c)**, and FF **(d)**. The main loss in PCE is due to a loss in FF.

The finding that ITIC-based devices are less stable than [70]PCBM-based ones is complementary to works by Cha et *al.* and by Baran et *al.* [37,38]. In their study, they found that the EH-IDTBR NFA-based devices are more stable than the [70]PCBM-based ones. Thus, different NFA acceptor molecules may show different behaviour. It is worth noting that Cha et *al.* used a lamp without UV during the exposure time and all considered devices in the two

studies were under their optimal conditions. Under such conditions, the [70]PCBM devices are processed with DIO while the NFA ones are not. In this case, two factors, in addition to the difference in molecules, would explain their observation, notably, the absence of UV-radiation and DIO in one type of device. The difference in decay curves is acceptor dependent and could be linked to D:A compatibility.

A closer look at the curves can only suggest the attenuation of the degradation either i) by the polymer structural modification (thus, changes in backbone structure) or ii) by the acceptors or iii) by the interaction/compatibility of both D and A and/or iv) by the reduction in mobility over time.

The first option cannot be the case as it would surely reflect in the same degradation pathway and strength since the same polymers are used with each of the acceptors. On the contrary, in **Figure 4.2a** PBDB-T:ITIC exhibited, on average, 22% PCE decay compared to PBDB-T:[70]PCBM which recorded 12%. Similar trends were observed in **Figure 4.3a** for inverted solar cells with an average of 19% decay for ITIC-based cells and 10% decay for [70]PCBM based cells. Also, for PTB7-Th based conventional cells, ITIC cells showed 38% decay in PCE compared to 9% decay for [70]PCBM cells.[36] This suggests that the acceptors play different roles in the acceleration or stabilisation of the photodegradation. Thus, perhaps the intricate compatibility of the acceptors with the donor material slows down or accelerates the photodegradation. To elucidate this point, absorption, AFM, charge transport, and TPV and extraction measurements are performed.

Absorption spectra of fresh and exposed blend films presented in appendix **Figure A4.1(c,d)** show no significant changes over the period of exposure (2 hours), explaining why we have observed almost no changes in J_{sc}. Also, there is no apparent change in the morphology of the blend films in **Figure 4.4**. The surface roughness before (**Figure 4.4a**) and after the exposure (**Figure 4.4b**) is about 1.3 nm for [70]PCBM-based films on 1 µm scale. The ITIC-based films under irradiation show no real changes in roughness on the same scale with roughness from 3.1 nm (**Figure 4.4c**) to 3.5 nm **Figure 4.4d**), however, the films seem to have become a bit more fibrillar.

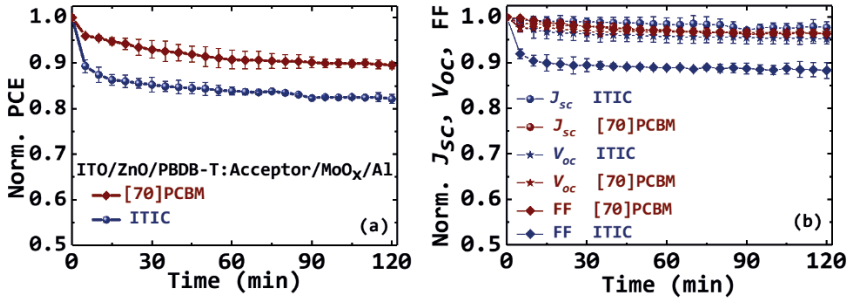

Figure 4.3: Performance under continuous illumination of PBDB-T-based inverted solar cells (average of more than 3 devices): PCE **(a)** and J_{sc}, V_{oc}, FF **(b)**. Also, here the main loss is due to FF, especially for the ITIC devices.

Single carrier devices of both pristine and blend materials are fabricated to check changes in electron and hole transport before and after light exposure. The degree of changes in mobility may be affected by the different interfaces used between the transport layer and/or the electrodes. To avoid this effect in the exposed devices, the active layers are exposed to light before the deposition of the top electrodes.

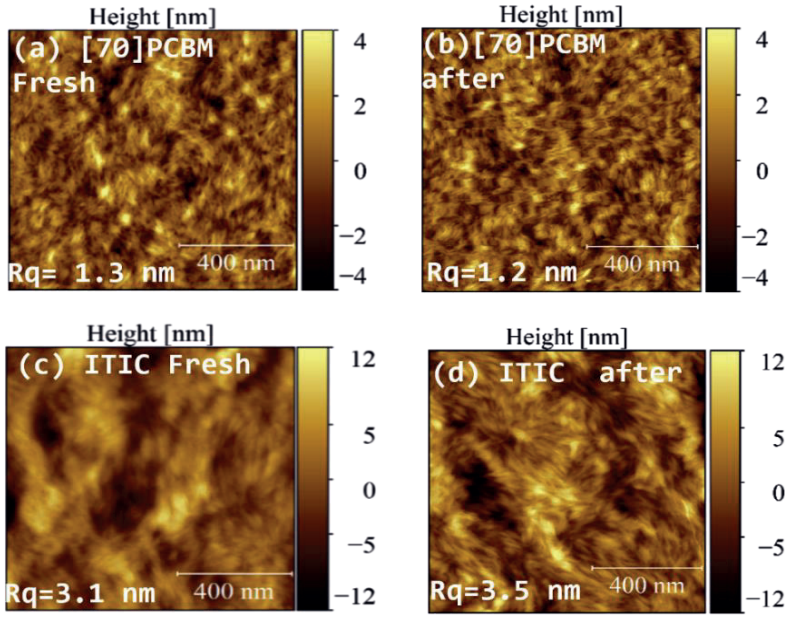

Figure 4.4: AFM images on 1 μm scale. PBDB-T:[70]PCBM film: fresh **(a)** and exposed **(b)**; PBDB-T:ITIC films fresh **(c)** and exposed **(d)**. Reproduced with permission from Ref. [36].

The resulting current-voltage curves are presented in appendix **Figure A4.3**. **Figure A4.3(a,b)** in the appendix presents the hole and electron current of pristine materials before and after exposure. The electron currents of pristine ITIC and [70]PCBM show no change before and after light exposure, suggesting no observable degradation of the acceptor materials. However, a tiny decrease in hole current is observed for PBDB-T, resulting in a decrease in hole mobility of the pristine PBDB-T from $1x10^{-4}$ $cm^2V^{-1}s^{-1}$ to $6x10^{-5}$ $cm^2V^{-1}s^{-1}$. These observations suggest that PBDB-T slightly degrades under light exposure, while [70]PCBM and ITIC do not. PBDB-T:[70]PCBM single carrier devices showed a decrease in electron and hole currents

respectively in appendix **Figure A4.3(e,f)**) reducing the electron mobility of the blend from $2.7x10^{-4}$ $cm^2V^{-1}s^{-1}$ to $6.3x10^{-5}$ $cm^2V^{-1}s^{-1}$ and the hole mobility from $1x10^{-4}$ $cm^2V^{-1}s^{-1}$ to $4.5x10^{-5}$ $cm^2V^{-1}s^{-1}$. As the decrease in electron mobility is more significant, it resulted in more balanced charge mobilities as depicted by the reduction in the ratio of mobilities (μ_{max}/μ_{min}) from 2.7, towards unity, 1.4. Thus, charge transport could become more balanced in [70]PCBM based devices after light exposure. On the contrary, while the hole current of ITIC based blend remains almost constant in appendix **Figure A4.3c**, resulting in hole mobilities from $1.5x10^{-4}$ $cm^2V^{-1}s^{-1}$ to $1.7x10^{-4}$ $cm^2V^{-1}s^{-1}$, the electron current shows a decrease (see appendix **Figure A4.3d**), leading to a reduction in electron mobility from $5.1x10^{-5}cm^2V^{-1}s^{-1}$ to $2.8x10^{-5}cm^2V^{-1}s^{-1}$. Such decrease increases μ_{max}/μ_{min} further away from unity from 2.9 to 6.1. As a result, there is an imbalance in charge mobilities. This could mean that some charges remain in the device, forming undesirable space charge that may oppose the flow of new charge carriers, leading to less charge extraction during the photodegradation, and influencing the FF. This may explain why [70]PCBM-based solar cells are more photostable over time than the ITIC-based ones.

One reason for the reduction in electron currents of the blends is attributed to the formation of radical species in the active layer upon light exposure that act as electron traps, increasing trap-assisted recombination.[45] For further investigation, V_{oc} light intensity dependent measurements were performed on fresh and exposed (for 1 or 2 hours) solar cells. Figure A4.4(a,b) in the appendix displays the plots while Figure

A4.4c and **Table 4.2** show the average of the data. The *n* of PBDB-T:ITIC solar cells remained largely constant around 1.2 over time, indicating there was no increase in trap-assisted recombination during light exposure. PBDB-T:[70]PCBM-based cells on average demonstrated an increase in *n* from 1.43 for fresh devices to about 1.51 after 2 hours of light exposure, indicating an increase in trap-assisted recombination. Thus, the results point to the fact that the observed degradation in the devices, especially in the FF, is not due to electron traps. If that were to be the case, then ITIC based devices should not have degraded at all. Thus, though traps may have contributed in the PCE decay of [70]PCBM devices, the main reason behind the differences in degradation pathways of the two types of devices could be related to how balanced the charge mobilities are during light exposure.

Table 4.2: Average mobilities in $10^{-5}cm^2V^{-1}s^{-1}$, the ratio of mobilities (unitless), and average ideality factor (*n*) of fresh and exposed (1 hour and 2 hours) solar cells.

Devices PBDB-T	μ_h Fresh	μ_e Fresh	μ_{max}/μ_{min} Fresh	μ_h 1hr	μ_e 1hr	μ_{max}/μ_{min} 1hr	*n* Fresh	*n* 1hr	*n* 2hrs
ITIC	15	5.1	***2.9***	17	2.8	***6.1***	1.19	1.19	1.19
[70]PCBM	10	27	***2.7***	4.5	6.3	***1.4***	1.43	1.49	1.51

h hole; *e* electron; max (maximum); min (minimum)

To further investigate the origin of reduction of FF under light exposure, we performed transient measurements of recombination as well as extraction rates (k_{rec}, k_{ex}) in both [70]PCBM and ITIC-based solar cells to measure the ratio of the rate of recombination to that of extraction (k_{rec}/k_{ex}). It has been shown in the literature that when k_{rec}/k_{ex} increases, then the FF decreases.[46] To measure the recombination rate, we performed TPV

measurements under open circuit, using a small perturbation LED light intensity with a step function, which causes exponential decay of V_{oc} due to recombination of excess charge carriers.[47] A high input impedance of the oscilloscope (1 MΩ) was used to keep the device at open circuit. The recombination rate of the fresh and the degraded devices at 1 sun, as shown in **Table 4.3** for PBDB-T:ITIC and PBDB-T:[70]PCBM, remained largely constant at the different LED light intensities, namely, 0.52 and 0.05 sun.

The extraction rates are measured following experiment described elsewhere.[48] First, the devices are kept under a steady-state condition at a higher light intensity. Then the light intensity is slightly reduced, while the bias voltage is kept constant, which results in the extraction of extra photo-generated charge carriers. The charge carrier extraction rate is calculated by fitting an exponential function to the decay of the current, carried out under different applied voltages. While the recombination rate stays almost the same, the light exposure (at 1 sun for 2h) causes a reduction in the extraction rates for both types of blends due to a lowering of the mobility of charge carriers (see **Table 4.3**). This increases the k_{rec}/k_{ex} ratio. For example, k_{rec}/k_{ex} (at 0.52 sun) of PBDB-T:ITIC solar cell increased from 0.114 for the fresh device to 0.15 for the degraded device while that of PBDB-T:[70]PCBM solar cell increased from 0.06 to 0.088. As a consequence of the increase in k_{rec}/k_{ex}, FF is reduced from fresh to degraded devices upon light exposure.

The reduction in FF is more pronounced in the case of ITIC-based devices, which originates from a larger ratio of $\mu_{\max}/\mu_{\min}$. The highly unbalanced

mobilities make the formation of the space charges dominant in ITIC devices, as mentioned earlier.

Table 4.3: Recombination rate (k_{rec}), extraction rate (k_{ex}), k_{rec}/k_{ex}, and FF of PBDBT:ITIC and PBDBT:[70]PCBM devices under 0.52 sun and 0.05 sun (italic) LED light intensities, before and after 1 sun illumination for 2 hours.

Devices	Condition	I [sun]	$k_{rec(oc)}$ [μs^{-1}]	k_{ex} [μs^{-1}]	k_{rec}/k_{ex}	FF (%)
PBDBT:ITIC	Fresh	0.52	0.310	2.7	0.114	63.4
	Exposed		0.290	2	0.150	53.1
	Fresh	*0.05*	*0.075*	*2.7*	*0.028*	*71.0*
	Exposed		*0.069*	*2*	*0.034*	*63.3*
PBDBT:[70]PCBM	Fresh	0.52	0.230	4	0.060	70.5
	Exposed		0.230	2.6	0.088	66.8
	Fresh	*0.05*	*0.050*	*4*	*0.014*	*71.4*
	Exposed		*0.047*	*2.6*	*0.018*	*68.0*

Finally, to validate the obtained results by the transient measurements, the current-voltage curves of the fresh and the degraded devices (1h) are fitted using a drift-diffusion simulation.[49] The fitting procedure consists of i) scanning of a combination of randomly picked parameters within a reasonable range and ii) a fitting procedure optimizing the root mean squared (rms) errors of the key performance parameters J_{sc}, V_{oc}, and FF. All the best fits are shown in Ref. [36] and had rms errors lower than 1%. Note that only the relevant recombination model parameters, namely, bimolecular recombination and trap-assisted Shockley-Read-Hall recombination, are set as fitting parameters. The other parameters such as thicknesses or mobilities are taken from the experiment.

The fitting in **Figure 4.5a** shows that the PBDB-T:ITIC cells are adequately reproduced by only considering bimolecular recombination. On the other hand, a small number of traps had to be included to simulate the PBDB-

T:[70]PCBM cells properly in **Figure 4.5b**. These results are consistent with the measured ideality factors close to 1 for ITIC, indicating that bimolecular recombination is dominant in the ITIC-based devices, and 1.4–1.5 for [70]PCBM which indicates the presence of both bimolecular and trap-assisted recombination in this case. From the V_{oc} light intensity dependence measurements shown in **Figure A4.4**, it is concluded that recombination is not the main factor behind the observed degradation. Similarly, all the recombination parameters do not change much upon exposure, which indicates that the decay of the FF is not due to an increasing amount of recombination. Rather, the extraction rates change with time, pointing to changes in mobilities of the charge carriers. This is also consistent with the almost constant recombination rate obtained by the transient measurements. Also, as concluded from the SCLC and transient measurements, the main parameter responsible for the degradation of the FF is the deterioration of the charge transport as both electron and hole mobilities decrease upon exposure.

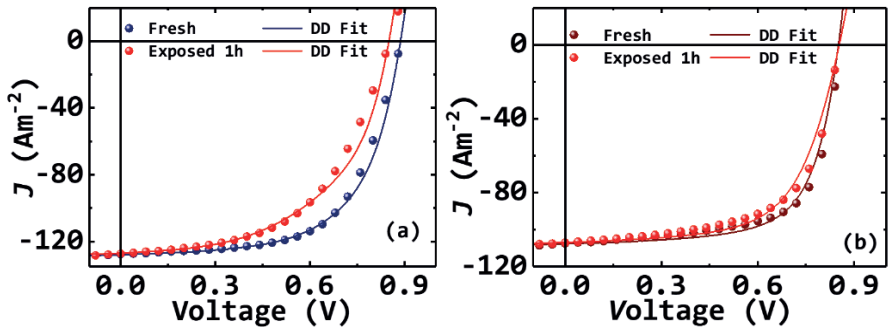

Figure 4.5: Current-voltage curves for fresh and exposed (1h) PBDB-T:ITIC **(a)** and PBDB-T:[70]PCBM **(b)** solar cells. Experimental (dot) and drift-diffusion (DD) fitted (line).

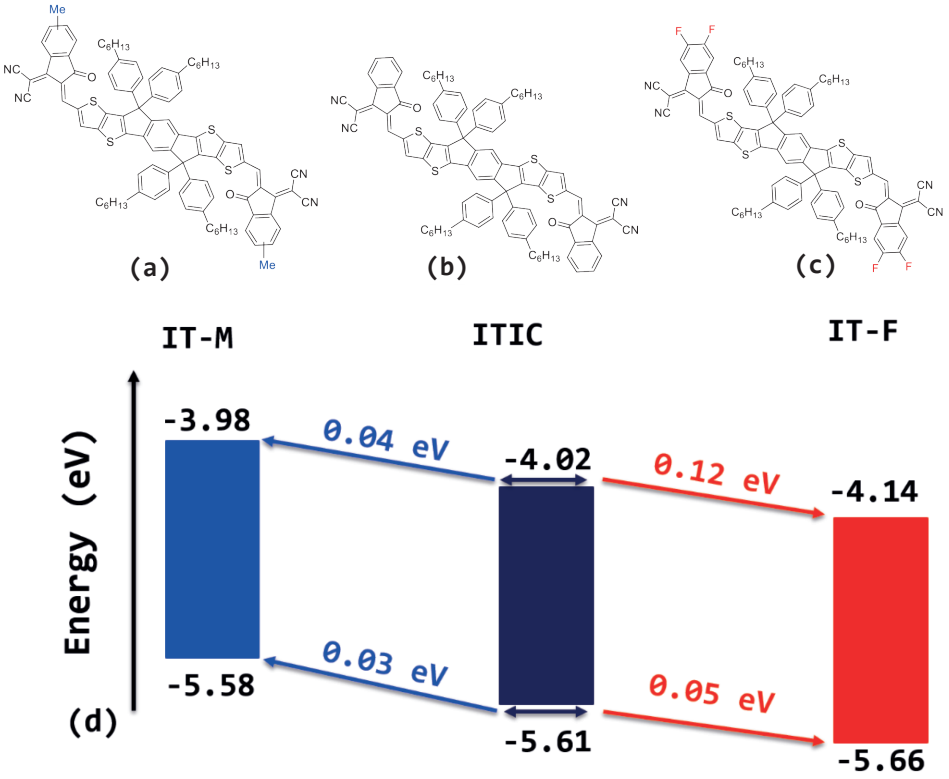

Figure 4.6: Chemical Structures of IT-M **(a)**, ITIC **(b)**, IT-F **(c)**, and their energy levels **(d)**.

4.3. Chemical Structure Changes in ITIC: Effect on Photostability

To enhance the PCE of ITIC-based non-fullerene OSCs, a number of ITIC derivatives were synthesised, namely, IT-M, IT-DM, IT-Th, IT-F, and IT-Cl.[26,35,42,43] Soon, the PCE of ITIC-based OSC soared from 11.5%[29] to about 14.2%[35] for IT-Cl-based single junction OSC. The addition of an electron-rich group like methyl to ITIC (making IT-M) increases the LUMO level and

thus, achieves a higher V_{oc} when matched with the same donor. Similarly, adding fluorine (F) or chlorine (Cl), strong electron-withdrawing halogen atoms, lowers the LUMO levels, redshifts absorption edges toward the near-infrared region, and improves intermolecular charge transport because of a better π-π stacking, thus improving the current J_{sc}.

Conventional and inverted PBDB-T:ITIC, PBDB-T:ITIC-M, and PBDB-T:IT-4F bulk heterojunction OSCs are fabricated. **Figure 4.6** shows the structures of the acceptor materials used together with their energy levels. The addition of the methyl group on the outer benzene rings of ITIC to form IT-M increases the LUMO and HOMO levels by 0.04 and 0.03 eV respectively, leading to a slightly higher optical band gap of 1.60 eV as against 1.59 eV for ITIC. A higher V_{oc} is obtained as a result of enhanced energy offset between the LUMO of the acceptor and the HOMO of the donor. In contrast, the LUMO and HOMO levels are respectively 0.12, and 0.05 eV lower for the fluorinated ITIC (IT-F) compared to ITIC, resulting in an optical band gap of 1.52 eV. A lower V_{oc} is observed, arising from a lower LUMO energy level. Finally, the LUMO or HOMO levels alignment between the donor and acceptors provide enough energy for an efficient charge dissociation and transfer, all of which are close to the estimated 0.3 eV[50] for the HOMO levels alignment and higher than that for the LUMO level alignments. **Table 4.4** highlights the *J-V* parameters of the best-performing devices, confirming the predicted trend of V_{oc} values from the energy level alignments shown in **Figure 4.6**.

The recorded PCEs are close to the literature values for the inverted devices.[29,52–55] Compared to the 0.831 mV for the inverted device of the

ITIC blend, the IT-M blend has an enhanced V_{oc} close to 900mV, while the IT-F based devices exhibit V_{oc} values much lower, around 700mV. The reduction in V_{oc} of the inverted devices compared to the conventional ones may be due to the inherent structural defects in the ZnO layer.[56] Overall, the efficiencies of the devices are lower than previously reported[29,52–54] due to differences in device fabrication processes and conditions.

Table 4.4: Photovoltaic parameters of the best performing conventional and inverted solar cells.

Devices	Structure	J_{sc} (mA.cm^{-2})	V_{oc} (V)	FF (%)	PCE (%)
PBDB-T:ITIC	Conventional	13.4	0.880	63.9	7.5
	Inverted	*14.5*	***0.831***	*71.1*	*8.6*
PBDB-T:IT-M	Conventional	12.9	0.917	60.2	7.8
	Inverted	*14.4*	***0.890***	*65.0*	*8.2*
PBDB-T:IT-F	Conventional	14.3	0.718	60.2	6.2
	Inverted	*14.5*	***0.684***	*57.5*	*5.7*

While these subtle changes in the ITIC structure seem to improve the efficiency of the solar cells, the effect of these molecular structure changes on stability remains unknown. Thus, we study the photodegradation behaviour in ITIC, IT-M, and IT-F based solar cells. **Figure 4.7** reveals the average photo-induced degradation behaviour of the conventional organic solar cells (six devices for each blend). **Figure 4.7a** shows in a burn-in behavior in the first 10-20 minutes of the illumination in all cells. A pronounced burn-in effect is recorded for the IT-F blends, lasting for 20 mins, compared to the ITIC and IT-M blends lasting only for 10 mins. The fast-initial (exponential) degradation process is followed by a stretched

exponential (a prolonged linear-like) regime which extends over the 2 hours. The PBDB-T:IT-M blends are the most photostable of the three with an average PCE loss of 12%, followed by 15% for the PBDB-T:ITIC blends, and finally 22% PCE loss for the PBDB-T:IT-F blends. While the J_{sc} remains practically constant for all three cells, the main loss in efficiency is due to the FF which recorded between 10-18% loss, with minor changes in V_{oc} (~ 6% decrease).

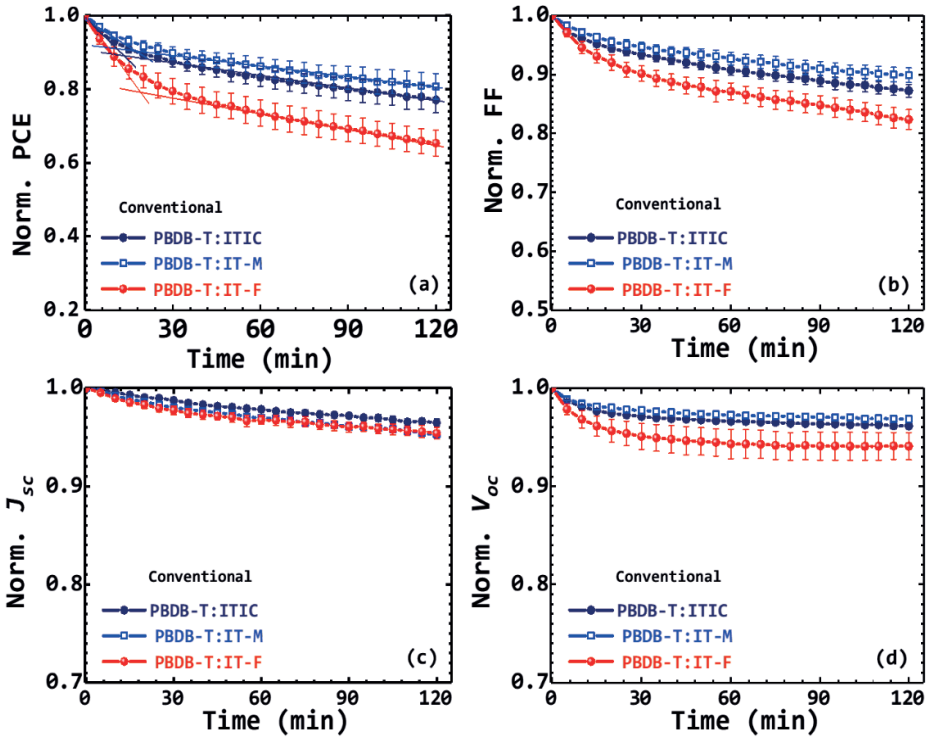

Figure 4.7: Evolution of average *J-V* parameters (minimum of 5 devices each with standard error in the mean) over time of the conventional cells: PCPE **(a)**, FF **(b)**, J_{sc} **(c)**, and V_{oc} **(d)**.

Since these parameters are related to the physical properties of the active layer materials and the devices, their evolution brings to light the degradation pathway within the devices. The minimal but similar decreasing trend in J_{sc} in all three devices means very little to no changes in both i) optical absorptions and ii) charge extraction at short circuit upon exposure. Whereas change in V_{oc} could indicate changes in recombination or that the energy levels of both the HOMO and the LUMO of the materials are experiencing some changes over the period of the experiment. We saw no changes in recombination as revealed by the almost constant value of the ideality factor of the three solar cells over time,[51] however, **Figure 4.7d** appears to reveal that the HOMO-LUMO levels of the IT-F blend have experienced pronounced change as compared to the other blends. However, these changes are not as significant as the changes in the FF.

As indicated in section 4.2, unbalanced mobilities induce different extraction rates at the electrodes and the build-up of space charge within the devices. The imbalance in mobility of the IT-F blend is more upset during the photodegradation process, due to a faster decrease in the electron mobility (-69%) compared to the hole mobility (-43%), resulting in even higher ratio compared to the rest of the blends.[51] The accumulation of charges obstructs the flow of currents, raises the charge carrier densities and thus explains the reason for the observed faster degradation for the IT-F blends.

However, inverted solar cells of the three blends show a dramatic change in the photodegradation behaviour of the IT-F blends, apparently becoming

as photostable as the other blends in all *J-V* parameters. Thus, the observed degradation is no more dominated by one *J-V* parameter. Even more surprising, the FF effect disappears, indicating that the degradation trend caused by the imbalance in charge transport may be due to the used interfacial layers.[51] These observations are further investigated and reported in details in ref. [51]. Very recently, it was also found by Du *et al.* that PBDB-T:IT-F inverted solar cells show prominent photostability with a filtered white LED light source (UV part removed) under an extended time of exposure.[55]

4.4. Conclusions

The study was designed to assess the role, if any, of the fullerene derivative ([70]PCBM) and non-fullerene (ITIC) acceptors in the photo-stability of their respective solar cells with PBDB-T (and PTB7-Th). It also envisaged to identify and explain the cause(s) of the degradation. The experiments confirmed on the one hand that, though ITIC based solar cells, when blended with PBDB-T, performed better in efficiency, it is poor for photo-stability in comparison to [70]PCBM. On the other hand, ITIC is less efficient and photo-stable than [70]PCBM when blended with PTB7-Th. These findings indicate that irrespective of the device structure, the polymer, or the initial efficiency, the [70]PCBM based devices are more photo-stable than the ITIC-ones. We identified the FF as the current-voltage parameter most responsible for the observed photodegradation. We

have also shown that trap-assisted recombination cannot be the reason behind the observed photo-degradation in the FF, though it could contribute to the degradation of the PCE of the [70]PCBM devices, since the ITIC devices exhibiting the most loss in FF have lower initial traps and do not show any increase in trap-assisted recombination over the time of exposure. Changes in mobilities upon light exposure are identified as the cause in the decay of the FF and as such, the main contributor to the observed difference in the photo-degradation of the solar cells.

We also determine the effect of the subtle changes such as methylation and fluorination of the ITIC acceptor on the efficiency and photostability of their organic conventional and inverted solar cells. Methylation of ITIC into IT-M improves the efficiency, mainly V_{oc}, but makes no significant difference to the performance of the organic solar cells in terms of stability. While IT-M seems to improve a bit the photostability of the devices in the conventional structure, it makes no difference under the inverted structure. However, fluorination of ITIC into IT-F decreases the efficiency of the cells irrespective of the device structure. In terms of photostability, IT-F is unstable compared to ITIC in conventional structure devices, while remaining as stable as ITIC and IT-M in inverted structure devices. Thus, the subtle changes in the ITIC play a role in the photodegradation of their non-fullerene solar cells.

Finally, these findings have important implications and contribute the first steps towards the understanding of the stability of fullerene and non-fullerene organic solar cells. They also contribute towards the

understanding of how the issues of stability are more complex than assumed initially: the apparent assumption that NFAs are more stable than FAs is not entirely correct. Also, the findings revealed that complementary absorption should not take precedence in the design rules for the synthesis of new molecules as it appears to be in the case for ITIC. Thus, there is still room for research into organic materials, be it acceptor or donor, that would be both efficient and stable.

Bibliography

[1] D. Abbaszadeh, N. Y. Doumon, G.-J. A. H. Wetzelaer, L. J. A. Koster, P. W. M. Blom, *Synth. Met.* **2016**, *215*, 64.

[2] C. Cui, W.-Y. Wong, Y. Li, *Energy Environ. Sci.* **2014**, *7*, 2276.

[3] G. Shi, J. Yuan, X. Huang, Y. Lu, Z. Liu, J. Peng, G. Ding, S. Shi, J. Sun, K. Lu, H. Q. Wang, W. Ma, *J. Phys. Chem. C* **2015**, *119*, 25298.

[4] C. Sun, Z. Wu, Z. Hu, J. Xiao, W. Zhao, H.-W. Li, Q.-Y. Li, S.-W. Tsang, Y.-X. Xu, K. Zhang, H.-L. Yip, J. Hou, F. Huang, Y. Cao, *Energy Environ. Sci.* **2017**, *10*, 1784.

[5] Y. Xie, X. Hu, J. Yin, L. Zhang, X. Meng, G. Xu, Q. Ai, W. Zhou, Y. Chen, *ACS Appl. Mater. Interfaces* **2017**, *9*, 9918.

[6] J. You, L. Dou, K. Yoshimura, T. Kato, K. Ohya, T. Moriarty, K. Emery, C.-C. Chen, J. Gao, G. Li, Y. Yang, *Nat. Commun.* **2013**, *4*, 1446.

[7] S. Zhang, L. Ye, J. Hou, *Adv. Energy Mater.* **2016**, *6*, DOI 10.1002/aenm.201502529.

[8] B. Fan, L. Ying, Z. Wang, B. He, X.-F. Jiang, F. Huang, Y. Cao, *Energy Environ. Sci.* **2017**, *10*, 1243.

[9] M. Graetzel, R. a J. Janssen, D. B. Mitzi, E. H. Sargent, *Nature* **2012**, *488*, 304.

[10] F. Guo, A. Karl, Q.-F. Xue, K. C. Tam, K. Forberich, C. J. Brabec, *Light Sci. Appl.* **2017**, *6*, e17094.

[11] X. Guo, C. Cui, M. Zhang, L. Huo, Y. Huang, J. Hou, Y. Li, *Energy Environ. Sci.* **2012**, *5*, 7943.

[12] J. Huang, C. Z. Li, C. C. Chueh, S. Q. Liu, J. S. Yu, A. K. Y. Jen, *Adv. Energy Mater.* **2015**, *5*, 4.

[13] B. Kan, Q. Zhang, M. Li, X. Wan, W. Ni, G. Long, Y. Wang, X. Yang, H. Feng, Y. Chen, *J. Am. Chem. Soc.* **2014**, *136*, 15529.

[14] A. R. Bin Mohd Yusoff, D. Kim, H. P. Kim, F. K. Shneider, W. J. da Silva, J. Jang, *Energy Environ. Sci.* **2015**, *8*, 303.

[15] Y. Qin, Y. Chen, Y. Cui, S. Zhang, H. Yao, J. Huang, W. Li, Z. Zheng, J. Hou, *Adv. Mater.* **2017**, *29*, 1.
[16] J.-D. Chen, C. Cui, Y.-Q. Li, L. Zhou, Q.-D. Ou, C. Li, Y. Li, J.-X. Tang, *Adv. Mater.* **2015**, *27*, 1035.
[17] S. H. Liao, H. J. Jhuo, P. N. Yeh, Y. S. Cheng, Y. L. Li, Y. H. Lee, S. Sharma, S. A. Chen, *Sci. Rep.* **2014**, *4*, 6813.
[18] C. Liu, C. Yi, K. Wang, Y. Yang, R. S. Bhatta, M. Tsige, S. Xiao, X. Gong, *ACS Appl. Mater. Interfaces* **2015**, *7*, 4928.
[19] Y. Xia, C. Musumeci, J. Bergqvist, W. Ma, F. Gao, Z. Tang, S. Bai, Y. Jin, C. Zhu, R. Kroon, C. Wang, M. R. Andersson, L. Hou, O. Inganäs, E. Wang, *J. Mater. Chem. A* **2016**, *4*, 3835.
[20] J. Yuan, W. Ma, *J. Mater. Chem. A* **2015**, *3*, 7077.
[21] Y. Xu, J. Yuan, J. Sun, Y. Zhang, X. Ling, H. Wu, G. Zhang, J. Chen, Y. Wang, W. Ma, *ACS Appl. Mater. Interfaces* **2018**, acsami.7b15000.
[22] B. Fan, L. Ying, P. Zhu, F. Pan, F. Liu, J. Chen, F. Huang, Y. Cao, *Adv. Mater.* **2017**, *1703906*, 1.
[23] M. An, F. Xie, X. Geng, J. Zhang, J. Jiang, Z. Lei, D. He, Z. Xiao, L. Ding, *Adv. Energy Mater.* **2017**, *7*, 2.
[24] Y. Firdaus, L. P. Maffei, F. Cruciani, M. A. Müller, S. Liu, S. Lopatin, N. Wehbe, G. O. N. Ndjawa, A. Amassian, F. Laquai, P. M. Beaujuge, *Adv. Energy Mater.* **2017**, *1700834*, 1.
[25] N. Gasparini, M. Salvador, S. Strohm, T. Heumueller, I. Levchuk, A. Wadsworth, J. H. Bannock, J. C. de Mello, H. J. Egelhaaf, D. Baran, I. Mcculloch, C. J. Brabec, *Adv. Energy Mater.* **2017**, *1700770*, 1.
[26] S. Li, L. Ye, W. Zhao, S. Zhang, S. Mukherjee, H. Ade, J. Hou, *Adv. Mater.* **2016**, *28*, 9423.
[27] X. Liu, B. Xie, C. Duan, Z. Wang, B. Fan, K. Zhang, B. Lin, F. J. M. Colberts, W. Ma, R. a. J. Janssen, F. Huang, Y. Cao, *J. Mater. Chem. A* **2018**, 395.
[28] T. Yu, X. Xu, G. Zhang, J. Wan, Y. Li, Q. Peng, *Adv. Funct. Mater.* **2017**, *27*, 1.
[29] W. Zhao, D. Qian, S. Zhang, S. Li, O. Inganäs, F. Gao, J. Hou, *Adv. Mater.* **2016**, 4734.
[30] J. Yuan, Y. Zhang, L. Zhou, G. Zhang, H.-L. Yip, T.-K. Lau, X. Lu, C. Zhu, H. Peng, P. A. Johnson, M. Leclerc, Y. Cao, J. Ulanski, Y. Li, Y. Zou, *Joule* **2019**, DOI 10.1016/J.JOULE.2019.01.004.
[31] Y. Cui, H. Yao, J. Zhang, T. Zhang, Y. Wang, L. Hong, K. Xian, B. Xu, S. Zhang, J. Peng, Z. Wei, F. Gao, J. Hou, *Nat. Commun.* **2019**, *10*, 2515.
[32] X. Xu, K. Feng, Z. Bi, W. Ma, G. Zhang, Q. Peng, *Adv. Mater.* **2019**, 1901872.
[33] L. Meng, Y. Zhang, X. Wan, C. Li, X. Zhang, Y. Wang, X. Ke, Z. Xiao, L. Ding, R. Xia, H. Yip, Y. Cao, Y. Chen, *Science (80-.).* **2018**, *2612*, 1.
[34] Y. Zhang, Y. Xu, M. J. Ford, F. Li, J. Sun, X. Ling, Y. Wang, J. Gu, J. Yuan, W. Ma, *Adv. Energy Mater.* **2018**, *8*, 1.
[35] S. Zhang, Y. Qin, J. Zhu, J. Hou, *Adv. Mater.* **2018**, *1800868*, 1.
[36] N. Y. Doumon, M. V Dryzhov, F. V Houard, V. M. Le Corre, A. Rahimi Chatri, P. Christodoulis, L. J. A. Koster, *ACS Appl. Mater. Interfaces* **2019**, *11*, 8310.
[37] H. Cha, J. Wu, A. Wadsworth, J. Nagitta, S. Limbu, S. Pont, Z. Li, J. Searle, M. F. Wyatt, D. Baran, J. S. Kim, I. McCulloch, J. R. Durrant, *Adv. Mater.* **2017**, *29*, 1.
[38] D. Baran, N. Gasparini, A. Wadsworth, C. H. Tan, N. Wehbe, X. Song, Z. Hamid, W. Zhang, M. Neophytou, T. Kirchartz, C. J. Brabec, J. R. Durrant, I. Mcculloch, *Nat. Commun.* **2018**, *9*, 2059.
[39] B. J. Tremolet De Villers, K. A. O'Hara, D. P. Ostrowski, P. H. Biddle, S. E. Shaheen, M. L. Chabinyc, D. C. Olson, N. Kopidakis, *Chem. Mater.* **2016**, *28*, 876.

[40] W. Kim, J. K. Kim, E. Kim, T. K. Ahn, D. H. Wang, J. H. Park, *J. Phys. Chem. C* **2015**, *119*, 5954.
[41] A. J. Pearson, P. E. Hopkinson, E. Couderc, K. Domanski, M. Abdi-Jalebi, N. C. Greenham, *Org. Electron. physics, Mater. Appl.* **2016**, *30*, 225.
[42] Y. Lin, J. Wang, Z.-G. Zhang, H. Bai, Y. Li, D. Zhu, X. Zhan, *Adv. Mater.* **2015**, *27*, 1170.
[43] W. Zhao, S. Li, H. Yao, S. Zhang, Y. Zhang, B. Yang, J. Hou, *J. Am. Chem. Soc.* **2017**, *139*, 7148.
[44] Z. Zheng, Q. Hu, S. Zhang, D. Zhang, J. Wang, S. Xie, R. Wang, Y. Qin, W. Li, L. Hong, N. Liang, F. Liu, Y. Zhang, Z. Wei, Z. Tang, T. P. Russell, J. Hou, H. Zhou, *Adv. Mater.* **2018**, *1801801*, 1801801.
[45] N. Y. Doumon, G. Wang, R. C. Chiechi, L. J. A. Koster, *J. Mater. Chem. C* **2017**, *5*, 6611.
[46] D. Bartesaghi, I. D. C. Pérez, J. Kniepert, S. Roland, M. Turbiez, D. Neher, L. J. A. Koster, *Nat. Commun.* **2015**, *6*, 7083.
[47] A. Rahimi Chatri, S. Torabi, V. M. Le Corre, L. J. A. Koster, *ACS Appl. Mater. Interfaces* **2018**, *2*, acsami.7b19234.
[48] V. M. Le Corre, A. R. Chatri, N. Y. Doumon, L. J. A. Koster, *Adv. Energy Mater.* **2017**, *7*, 1.
[49] L. J. A. Koster, E. C. P. Smits, V. D. Mihailetchi, P. W. M. Blom, *Phys. Rev. B* **2005**, *72*, 085205.
[50] D. C. Coffey, B. W. Larson, A. W. Hains, J. B. Whitaker, N. Kopidakis, O. V. Boltalina, S. H. Strauss, G. Rumbles, *J. Phys. Chem. C* **2012**, *116*, 8916.
[51] N. Y. Doumon, F. V. Houard, J. Dong, H. Yao, G. Portale, J. Hou, L. J. A. Koster, *Org. Electron.* **2019**, *69*, 255.
[52] X. Liu, L. Ye, W. Zhao, S. Zhang, S. Li, G. M. Su, C. Wang, H. Ade, J. Hou, *Mater. Chem. Front.* **2017**, DOI 10.1039/C7QM00182G.
[53] L. Ye, W. Zhao, S. Li, S. Mukherjee, J. H. Carpenter, O. Awartani, X. Jiao, J. Hou, H. Ade, *Adv. Energy Mater.* **2017**, *7*, 1.
[54] Z. Fei, F. D. Eisner, X. Jiao, M. Azzouzi, J. a. Röhr, Y. Han, M. Shahid, A. S. R. Chesman, C. D. Easton, C. R. McNeill, T. D. Anthopoulos, J. Nelson, M. Heeney, *Adv. Mater.* **2018**, *30*, 1.
[55] X. Du, T. Heumueller, W. Gruber, A. Classen, T. Unruh, N. Li, C. J. Brabec, *Joule* **2018**, 2, 1-12.
[56] D. Li, W. Qin, S. Zhang, D. Liu, Z. Yu, J. Mao, L. Wu, L. Yang, S. Yin, *RSC Adv.* **2017**, *7*, 6040.

Appendix 4 (A4)

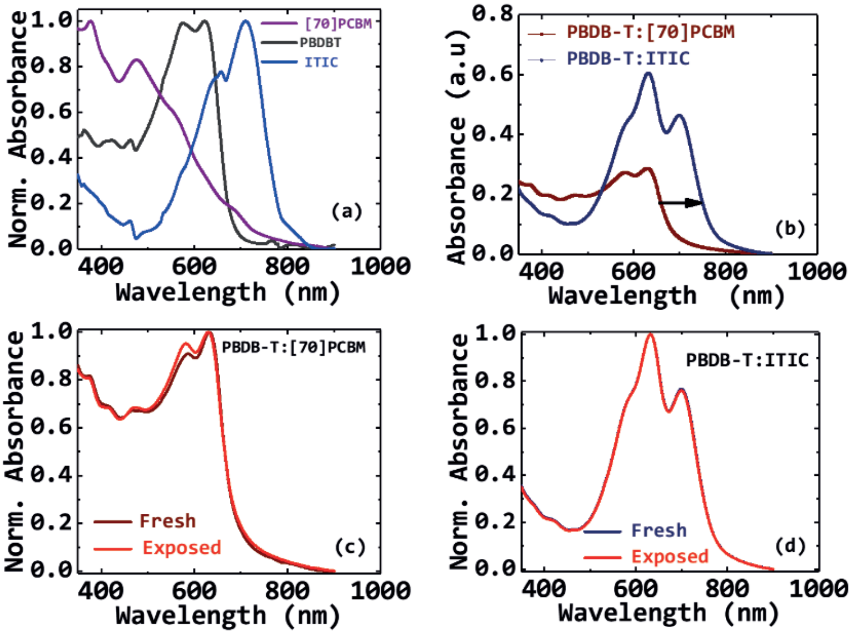

Figure A4.1: Normallised absorption spectrum of [70]PCBM, PBDB-T, and ITIC pristine fresh films **(a)**; raw (data) absorption spectrum PBDBT:[70]PCBM and PBDBT:ITIC fresh films **(b)**; Normalised absorbance of fresh and exposed (red) films of PBDBT: [70]PCBM **(c)**, and PBDBT:ITIC **(d)**.

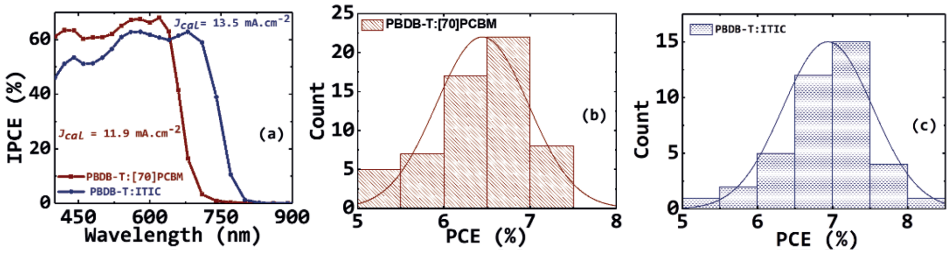

Figure A4.2: EQE spectra **(a)**; Device count of PBDB-T:[70]PCBM **(b)** and PBDB-T:ITIC **(c)** conventional devices.

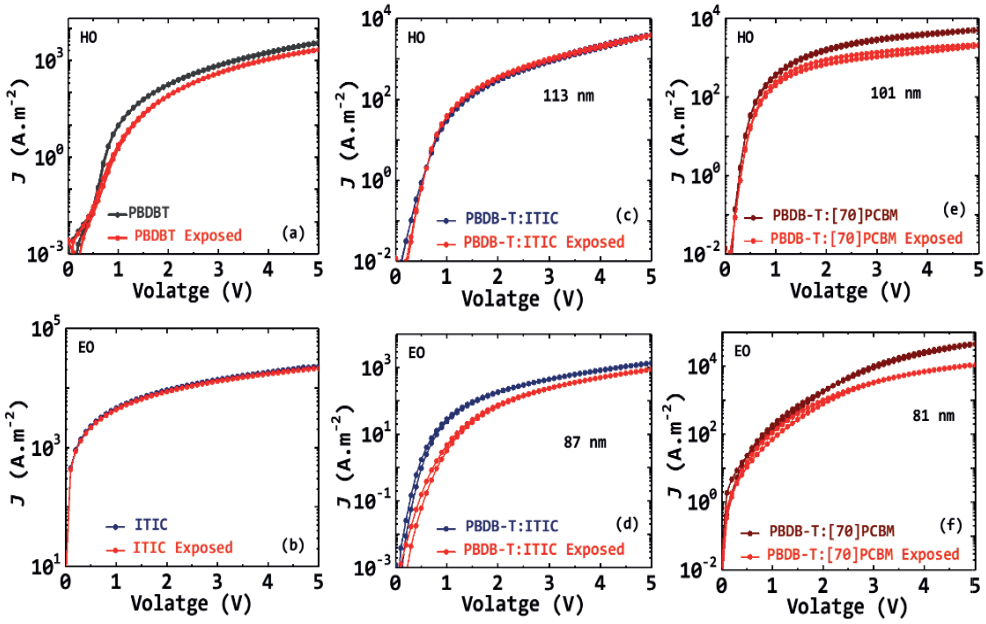

Figure A4.3: Current-voltage characteristics of fresh and exposed (1 hour - red). Top row: hole only (HO) devices of PBDB-T **(a)**, PBDB-T:ITIC **(c)**, and PBDB-T:[70]PCBM **(e)**. Bottom row: electron only (EO) devices of ITIC **(b)**, PBDB-T:ITIC **(d)**, and PBDB-T:[70]PCBM **(f)**.

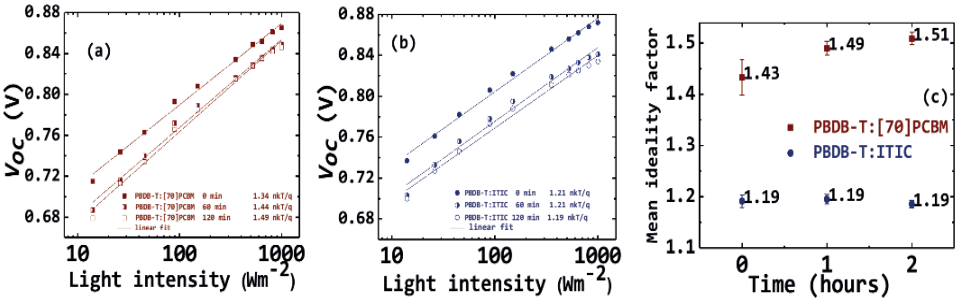

Figure A4.4: V_{oc} light intensity dependence of fresh and exposed (1 and 2hours) solar cells of PBDB-T:[70]PCBM **(a)** and PBDB-T:ITIC **(b)**. Average of the derived ideality factors **(c)**.

5

1,8-diiodooctane as a Photoacid

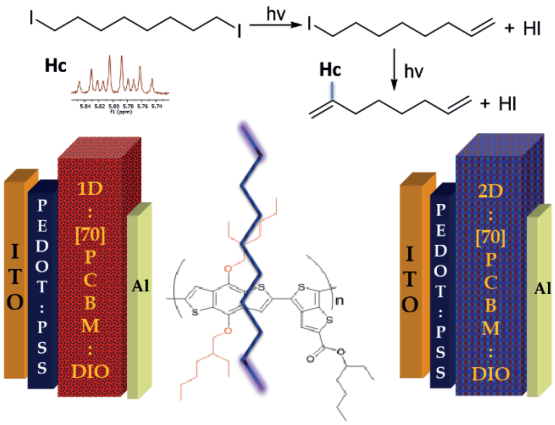

Chapter based on publications number 3, 5, 6, and 8

SUMMARY

1,8-diiodooctane (DIO) is one of the common additives used in organic photovoltaics for improved device efficiency. This chapter examines the effect of UV-light on the photostability of polymer solar cells processed with additives. In addition to the relationship between the polymer chemical structure and the photostability of the solar cells which is explored is explored in chapter 3, the effect of DIO on the polymer photostability studied: DIO as compared to i) 1-chloronaphthalene (CN) in the solar cells and ii) 1,8-octanedithiol (ODT) in solution. All 1D BDT-TT polymers are more photostable than their 2D counterpart over the period of exposure. While DIO acts as a photoacid and leads to accelerated degradation of the solar cells, CN does not. Acidity is known to be detrimental to the efficiency and photostability of organic solar cells. The degradation is initiated upon UV-irradiation by the cleavage of the side chains, resulting in more electron traps and by the formation of iodine, dissolved HI and carbon-centered radicals from DIO as revealed by 1H-NMR spectrum. The ODT spectra do not show such species; thus, the degradation mechanisms are not the same. Finally, the mechanisms behind the effect of DIO are explained, paving the way for the design of new, efficient as well as stable materials and additives.

5.1. Introduction

Additives play a central role in the advancement of the efficiency of organic solar cells. These additives, combined with the provision of novel materials, device architecture, and processing techniques, help yield power conversion efficiencies (PCEs) above 10% for single junction polymer-fullerene cells.[1–3] 1,8-diiodooctane is the widely used solvent additive in the field. A typical example is the combined use of these additives and the change in interfacial layers and electrodes in the use of inverted structure.[4–9] These strategies were combined recently to produce a power conversion efficiency (PCE) of 17.3% in all solution-processed multijunction solar cells.[10] The reported devices utilized DIO as an additive as well as PTB7-Th, a BDT-TT polymer.

It is shown that additives, such as DIO, have opposing effects on device performance, i.e., even though DIO aids in the improvement of device efficiency, it is an agent of accelerated degradation in the devices.[11–13] The reason behind this different effect is little understood, tricky to elucidate, and thus has been sporadically explained in the literature vis-a-vis different materials.[14–16]

This chapter aims to identify in general why DIO is bad for photodegradation of the solar cells using blends of BDT-TT polymers (or PBDB-T) with either [70]PCBM or ITIC as active layers (see **Figure 5.1**). In particular, taking a pair of BDT-TT polymers (PBDTTT-E and PBDTTT-ET, see **Figure 5.1(c,d)**), the relation between the photodegradation of polymer solar cells and DIO

is explored. The mechanism behind these effects is explained and thus, can be easily extrapolated to all BDT-TT polymer solar cells.

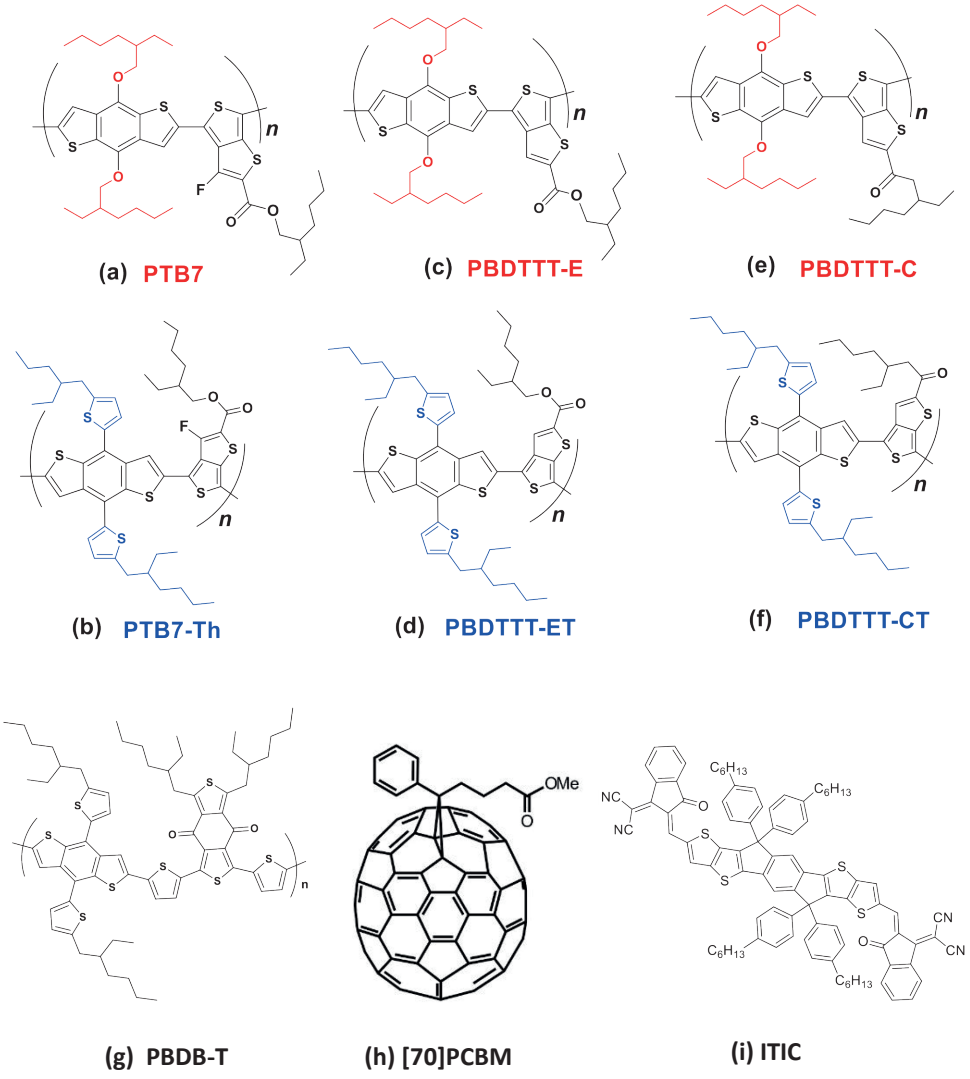

Figure 5.1: Chemical structures of the studied donor **(a-g)** and acceptor **(h,i)** materials in the active layer of the polymer solar cells processed with 1,8-diiodooctane (DIO).

We found that DIO acts as a photo-acid in the active layer of the solar cell, generating HI under illumination as compared to ODT. Acidity is known to be detrimental to the efficiency and stability of organic solar cells, and HI is a powerful acid (7 pKa units more acidic than HCl). And even the acidity of PEDOT:PSS[17–19] can have harmful effects on the active layer. In this case, the formation of HI inside the active layer upon UV-exposure is detrimental to the photostability of the devices.

5.2. Results and Discussions

5.2.1. Performance of Devices: Power Conversion Efficiency

Table 5.1 and **Figure 5.2** reveal the general performance of the polymer solar cells processed with and without DIO. **Figure 5.2** shows the difference in photodegradation curves for a couple of solar cells processed with and without DIO. The *J-V* parameters displayed in **Table 5.1**, show a better performance for 2D polymers (in blue) over the 1D as already observed in chapter 3 and for ITIC (in blue) over [70]PCBM as earlier noted in chapter 4. The improvement in performance can be explained by the combined effects of many factors. First, the red-shifted broader absorption band, which translates into an increase in J_{sc}. Improved charge carrier mobilities are observed. For example, μ_h is in the order of 1.9×10^{-3} $cm^2V^{-1}s^{-1}$ for PBDBTT-ET against 8.5×10^{-4} $cm^2V^{-1}s^{-1}$ for PBDBTT-E as obtained by the space-charge-current-limited measurements. Finally, there are fewer traps in the fresh state in some devices as compared to others, as suggested by the obtained

ideality factors (n). For example, in PBDBTT-ET blend solar cells have an ideality factor of 1.43 compared to that of PBDBTT-E solar cells with 1.67, as shown in **Table 5.1.**

Table 5.1: *J-V* parameters of the best-performing cells of all studied polymer solar cells processed with (bold) or without DIO (or CN). Blue: 2D BDT-TT or ITIC based solar cells.

Solar cell	Additive	J_{sc} ($A.m^{-2}$)	V_{oc} (V)	FF (%)	PCE (%)	n
PTB7:[70]PCBM[20]		115.2	0.773	58.4	5.2	1.50
PTB7:[70]PCBM	**DIO**	**140.0**	**0.740**	**68.3**	**7.1**	**-**
PTB7-Th:[70]PCBM[21]		156.0	0.804	68.7	8.6	1.09
PTB7-Th:[70]PCBM	**DIO**	**170.9**	**0.811**	**69.6**	**9.7**	**-**
PBDTTT-C:[70]PCBM[21]		123.3	0.743	45.5	4.2	1.07
PBDTTT-C:[70]PCBM	**DIO**	**140.6**	**0.696**	**58.4**	**5.7**	**-**
PBDTTT-CT:[70]PCBM[20]		126.0	0.839	64.9	5.8	1.00
PBDTTT-CT:[70]PCBM	**DIO**	**146.2**	**0.755**	**67.6**	**7.5**	**-**
PBDTTT-E:[70]PCBM[22]		102.3	0.686	55.4	3.9	1.67
PBDTTT-E:[70]PCBM	**DIO**	**131.0**	**0.646**	**68.0**	**5.8**	**1.43**
PBDTTT-E:[70]PCBM	**CN**	**87.0**	**0.660**	**56.4**	**3.2**	**-**
PBDTTT-ET:[70]PCBM[22]		127.3	0.727	55.3	5.1	1.43
PBDTTT-ET:[70]PCBM	**DIO**	**133.9**	**0.702**	**61.9**	**5.8**	**1.34**
PBDTTT-ET:[70]PCBM	**CN**	**103.0**	**0.740**	**56.3**	**4.3**	**-**
PBDB-T:[70]PCBM[23]		118.1	0.870	69.9	7.1	1.43
PBDB-T:[70]PCBM	**DIO**	**124.7**	**0.844**	**74.5**	**7.8**	**1.23**
PBDB-T:ITIC[23]		142.0	0.887	65.9	8.1	1.19
PBDB-T:ITIC	**DIO**	**135.7**	**0.898**	**62.0**	**7.6**	**1.09**

The addition of DIO during device processing notably increases J_{sc} and FF, and thus, generally improves the efficiencies of the device except for the ITIC-based device. This improvement in efficiency upon addition of DIO, as observed in a previous report[24], is attributed to several factors including better miscibility of the polymer:fullerene phases in the blend layer with a slight improvement of carrier mobilities. This improvement in efficiency is also reminiscent of the drop in the ideality factor. For example, the ideality factor of PBDTTT-E solar cells drops from 1.67 to 1.43 while that

of PBDBTT-ET cells drops from 1.43 to 1.34 in **Table 5.1**, suggesting a reduction in trap-assisted recombination in the devices processed with DIO.

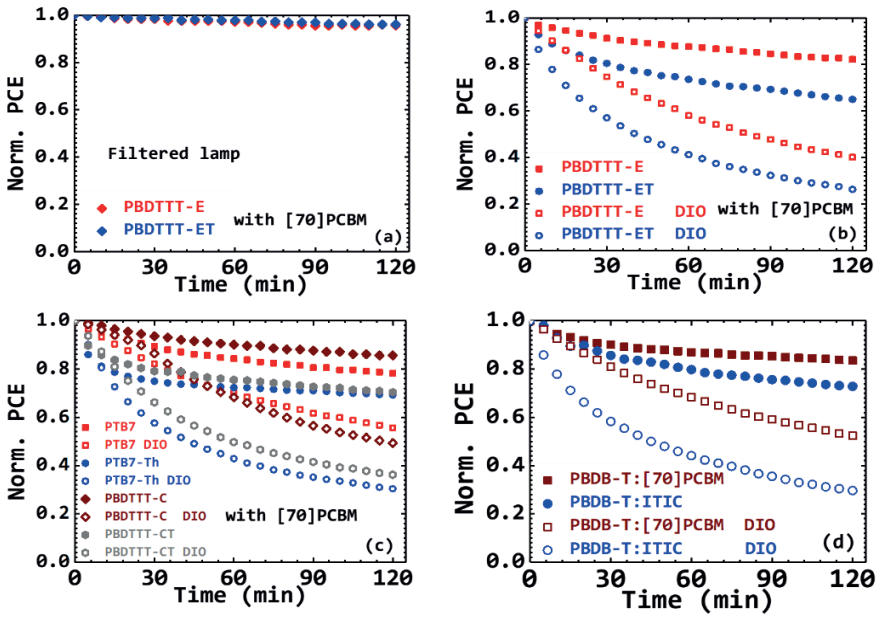

Figure 5.2: Time evolution of PCE of the solar cells processed with (open symbols) and without (full symbols) DIO, with UV-filtered **(a)** and unfiltered lamp **(b-d)**. The figure clearly shows that the photodegradation of the cells is due to the UV-part of the lamp and DIO exacerbates the photodegradation.

5.2.2. Effect of DIO on Photostability

DIO has a conflicting effect on the performance of the devices. First, a positive effect on morphology, that is homogeneous miscibility of the polymer:fullerene blend irrespective of the polymer, resulting in higher PCE as shown in **Table 5.1**. Next, a negative effect on device stability, that is an accelerated UV-degradation upon illumination as seen in **Figure 5.2b-d**. To have a better grasp of this negative effect, we conducted the

same experiments on devices with DIO as in the case of devices without DIO using a pair of BDT-TT polymers, PBDTTT-E, and PBDTTT-ET. It emerged that DIO has a pronounced destabilisation effect, coupled with the already discussed polymer chemical structure effect on the device photostability. For example, in **Figure 5.2b**, the PBDTTT-E polymer cell with DIO had a 60% decay in PCE (as opposed to 18% without DIO) while the PBDTTT-ET solar cells recorded 74% loss (as opposed to 36% without DIO). While PBDTTT-E remained more stable than PBDTTT-ET, both had experienced pronounced degradation compared to the devices without DIO. Consequently, the PBDTTT-E polymer cell with DIO had a T_{80} of 20 minutes while that of PBDTTT-ET had a T_{80} of < 10 minutes. To confirm the validity of the DIO effect on all PBDT-TT polymers, PTB7, PTB7-Th, PBDTTT-C, and PBDTTT-CT are also used and similar conflicting trends of improved efficiency but accelerated photodegradation in the presence of UV-light is observed with their PCE decays shown in **Figure 5.2c**.

The negative DIO effect is also observed for PBDB-T-based fullerene ([70]PCBM) and non-fullerene (ITIC) solar cells in **Figure 5.2d.** It must also be noted that DIO does not help in improving the PCE of the ITIC-based devices as DIO does not help in improving their morphology, which tends to show big islands. This may also explain their very rapid photodegradation as compared to the [70]PCBM-based devices, details of which are not discussed here. We now focus on fullerene solar cells using the BDT-TT pair of polymers PBDTTT-E and PBDTT-ET, as the basis for discussion in the rest of the chapter.

A look at the other *J-V* parameters in **Figure 5.3** reveals that for the devices without DIO, PBDTTT-ET suffered the most in J_{sc} loss while remaining almost stable in V_{oc} and FF as PBDTTT-E devices. However, devices with DIO recorded pronounced loss in all parameters with a similar degree of loss in V_{oc} and FF for both solar cells, while J_{sc}, recording the most loss, show different loss strength. PBDTTT-ET devices again suffered the most in J_{sc}.

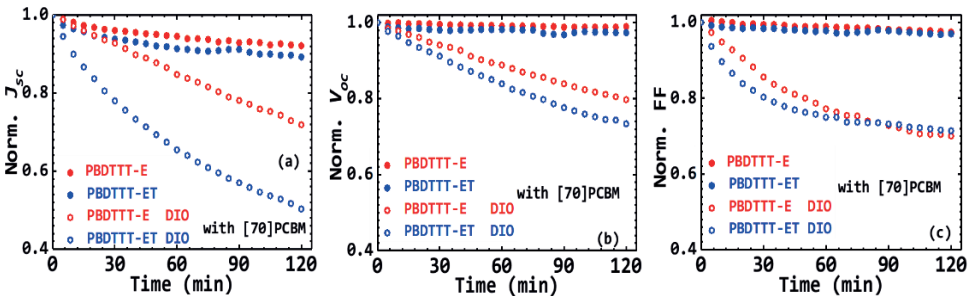

Figure 5.3: Time evolution of other *J-V* parameters of the solar cells processed with (open symbols) and without (full symbols) DIO: J_{sc} **(a)**, V_{oc} **(b)**, and FF **(c)**. The figure clearly shows that DIO exacerbates the photodegradation.

Charge transport studies are conducted with DIO embedded films to understand the phenomenon. From the results, it seems like DIO does not affect the hole and electron currents of the fresh devices if compared to fresh devices without DIO. Next, it is apparent from **Figure 5.4** that in general, DIO affects both polymers as well as [70]PCBM films under illumination. There is a pronounced reduction in hole currents of the pristine polymers (**Figure 5.4(a,b)**) and the electron currents of the blends (**Figure 5.4(e,f)**) in a similar order as observed for devices without DIO (**Figure 5.4 inset**), i.e., PBDTTT-ET > PBDTTT-E. It is very important to single out, for instance, the considerable reduction in the hole currents of the blends depicted in **Figure**

5.4c,d. This decrease, upon illumination, is two orders of magnitude compared to the zero reduction recorded for the blend hole currents of the devices without DIO in **Figure 5.4(c,d)** inset. This could be due to the coupled effects of DIO on both polymers and also [70]PCBM, as shown in **Figure A5.1a** in contrast to [70]PCBM without DIO in **Figure A5.1b**. In summary, it is clear from the charge transport that ET suffered more in current reduction under illumination, making PBDTTT-ET:[70]PCBM with DIO less stable than PBDTTT-E:[70]PCBM with DIO. This finding is entirely in agreement with the earlier observation among the PV parameters in **Figure 5.3a** that J_{sc} is the most responsible for the recorded PCE decay. Hence, DIO accelerates the degradation process but does not override the effect of the chemical structure.

To further visualize the effect of DIO in the films under UV, FTIR measurements are performed on drop cast films of polymers, fullerene, and blends from solution with and without DIO. For the DIO doped fullerene films, there was a continuous decrease in peaks at 1430 cm^{-1} and between 2800-3000 cm^{-1} with the disappearance of the shoulder peak at 1456 cm^{-1} and an initial increase with a subsequent decrease at the C=C stretching and at 1737 cm^{-1}.

Unlike the polymer films without DIO in **Figure 5.5(a,b)** where all peaks remained unchanged, in the case of the polymer films with DIO in **Figure 5.5c,d**, first, while the peaks at the C=C and C=O stretching (1500-1570 cm^{-1} and 1714 cm^{-1}) remained almost unchanged for PBDTTT-E, a rise in these peaks is observed for PBDTTT-ET films with DIO in contrast to PBDTTT-ET

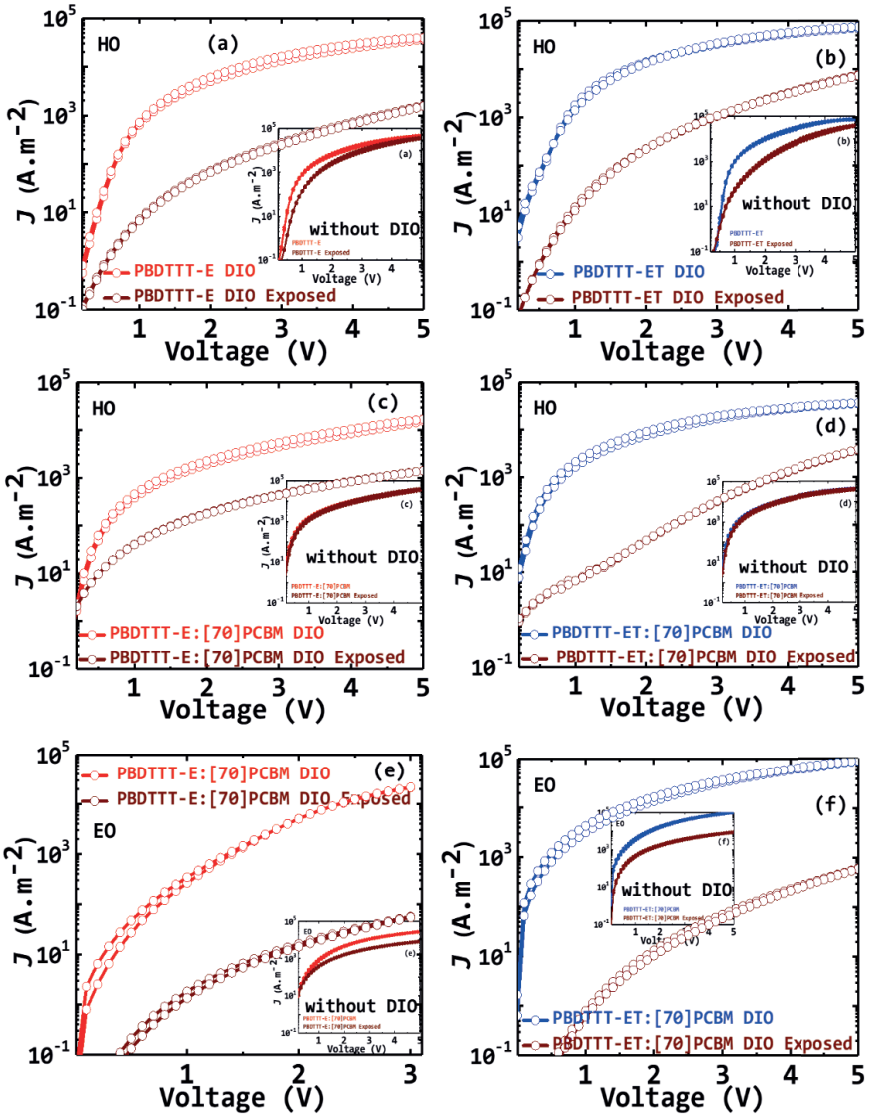

Figure 5.4: Current-Voltage characteristics of fresh and exposed (Brown) of PBDTTT-E and PBDTTT-ET based single carrier devices with and without (inset) DIO: pristine polymer hole-only **(a,b)**, blend hole-only **(c,d)**, and blend electron-only **(e,f)**.

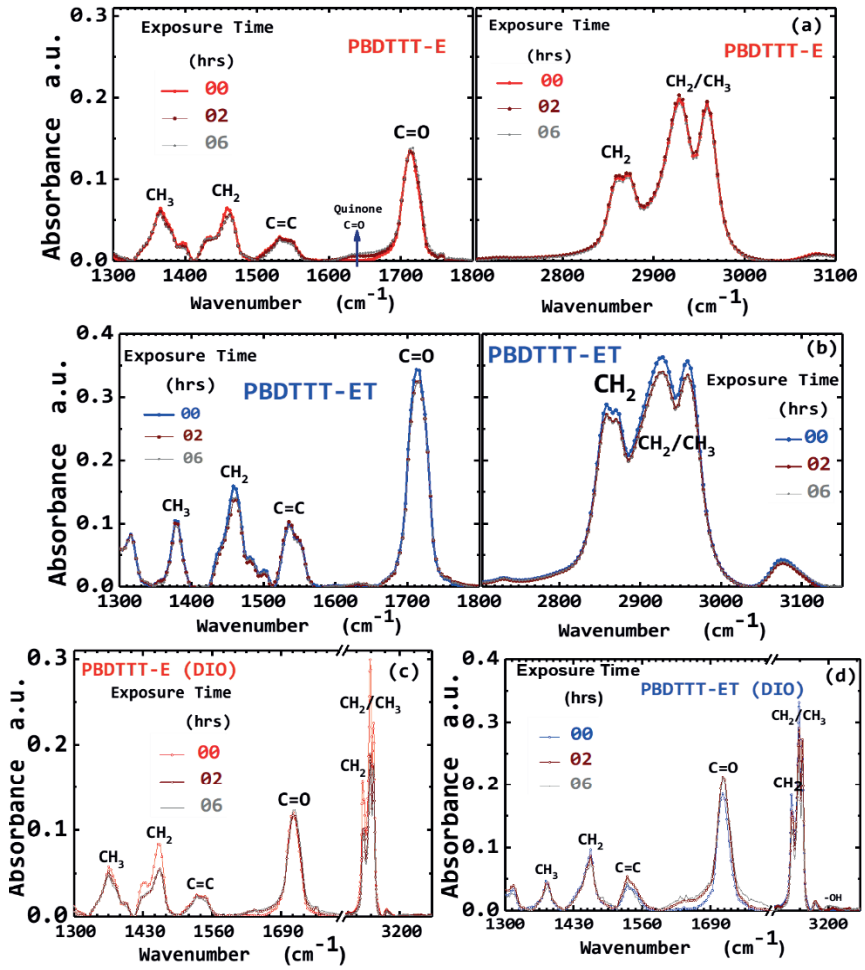

Figure 5.5: FTIR absorption spectra of fresh and exposed (2 and 6 hours) films of pristine polymers with (open symbols) and without (full symbols) DIO: PBDTTT-E **(a,c)** and PBDTTT-ET **(b,d)**.

films without DIO, leading to the appearance, at later stages of the illumination, of a carboxylic -OH peak at 3250 cm^{-1}. Next, there was a large decrease (compared to films without DIO) in the peaks at the CH_2 bending and at the aliphatic bands which was continuous for PBDTTT-ET films but got

stabilised and remained afterward constant for PBDTTT-E films. This is clear evidence that UV and DIO react more detrimentally with the PBDTTT-ET polymer than the PBDTTT-E polymer.

Finally, for the blend films with DIO in **Figure A5.2(a,b)**, there is a considerable increase in all peaks of the fresh films except at the C=C stretching which appeared almost to be quenched in the presence of DIO but reappeared under illumination. Upon illumination, there is a significant reduction in the intensity of all peaks due to the combined effects of UV and DIO reactions on polymer and fullerene except for the peaks at 1714 cm^{-1} and 1737 cm^{-1} of the PBDTTT-E blend which increased and stabilised at later stages. The substantial decrease, observed in the peaks, is continuous for PBDTTT-ET blends but stabilises for the PBDTTT-E blends at longer time of exposure.

Similar work using FTIR to explain the mechanism of the photoinduced oxidative radical reaction of PTB7-Th, PTB7-Th:[70]PCBM, and PTB7-Th:[70]PCBM with DIO has been conducted by Tremolet de Villers et *al.*[14], with similar conclusions. Based on their analysis, they proposed a radical initiated mechanism for the oxidation of PTB7-Th. They blamed the observed photoinduced oxidative reaction on the structure of PTB7-Th, pointing to the abstraction of the most acidic hydrogen, the one attached to the α carbon of the alkyl-side-chain-pendant on the BDT backbone unit[14] of PTB7-Th. In short, the FTIR data also point to the fact that upon illumination DIO is decomposed to fragments, possibly iodine radicals, that contribute to the accelerated photodegradation either passively or actively by

intrinsic interaction with (the fullerene, the polymers and) the blend materials without overriding the effect of the polymer chemical structure. Similar trends and varied degree of induced degradation effects are observed for most additives, whether halogenated[11,12,14,25] such as diiododecane, diiodohexane, diiodopentane, etc. or not[4,16,26–28] such as octanedithiol, butanedithiol, phenylnaphthalene, chloronaphtalene, etc.

5.2.3. The Role of DIO in the Degradation Process

Previously it was found that high boiling point additives, e.g., 1-chloronaphtalene (CN) precipitates the photo-oxidation of BDT-TT polymer:[70]PCBM blend films.[16] To check if CN also accelerates the photodegradation of the PBDTTT-E and PBDTTT-ET based solar cells are fabricated, and CN (≥ 85% technical grade with a boiling point of 260 °C) is used as an alternative to DIO. Solar cells are fabricated from blend solutions containing 0 and 3vol-% of DIO or CN and characterized under the same conditions. The *J-V* parameters of the cells processed with CN are also displayed in **Table 5.1**. **Figure A5.3** and **A5.4** reveal that the solar cells with CN and the solar cells without DIO show the same level of stability. Only the solar cells with DIO recorded accelerated PCE decay over time. All *J-V* parameters show the same stability trends as can be seen in the figures. The fact that CN does not further degrade the cells is offset by the observed decrease in the PCE of the cells with CN. It is also a testament to the unique role of DIO in the photodegradation.

To determine the exact role of DIO in the photodegradation process, we study the DIO effect in detail in PBDTTT-E and PBDTTT-ET based films and solar cells to understand the mechanism. There is a possibility that DIO might have significantly altered the nanostructure morphology of the blend films of PBDTTT-E:[70]PCBM and PBDTTT-ET:[70]PCBM active layers under the influence of the illumination, explaining the observed pronounced degradation as opposed to the postulated iodine radicals theory; changes that were not really observable under AFM. If that were to be the case, then any light source illumination of their solar cells should cause them to degrade differently. **Figure A5.5** shows the combined results of devices with DIO under continuous illumination with UV-filtered and unfiltered light, leading to the conclusion that all the devices do not degrade under the UV-filtered light.

First, these data reinforced the fact that the UV part of the light is responsible for the degradation. Next, not only does it reveal that UV affects the chemical structure of the polymers differently but also that it certainly reacts with the DIO molecules, through radical reaction by cleavage of carbon-iodine bonds. Thus, the formation of iodine radical species, a possible pathway of DIO reaction with UV, in its neutral state I_2 or ionized states (I^- and I_3^-), can intrinsically crosslink with the polymer chemical structure, dope the film[15], and cause pronounced detrimental reaction upon continuous UV-exposure.

As earlier indicated and in previous studies,[15,26,27] DIO could not completely be removed under high vacuum (10^{-8} Torr). This is consistent with

the huge losses recorded in the mobilities of the exposed DIO films and the loss recorded in the PV parameters. To explain this assertion, we first made a dilute solution of DIO-only and ODT-only (2.1 ml) with $CDCl_3$. Second, we also made dilute solutions (2 ml in volume) of the BDT monomers, with (0.1 ml DIO to the volume) or without DIO, at very low concentrations.

These solutions are prepared into sealed/air-tight NMR tubes in a glovebox under cleanroom environment and during measurement. Then, ^{1}H-NMR spectra are taken before and after UV exposure at intervals of 10 minutes for 2 hours and displayed in **Figure A5.6** showing the evolution of the backbone peaks of the monomers. Selected spectra of the evolution of all other peaks for the mixture of monomers and additives and the additives-only are shown in ref. [22].

The results from the NMR data as relative integrated peaks over time are consistent with the FTIR data. The analysis of the peaks of the backbone and the side chains revealed that the PBDTTT-E-monomer is more stable than PBDTTT-ET-monomer. Upon UV-exposure in the presence of DIO, there was an initial rise in peaks followed by a subsequent decrease with time. This decrease in peaks, however, starts to stabilise for the PBDTTT-E-monomer over time while it is almost continuous with a slow rate for the PBDTTT-ET-monomer. This observation, indeed, is clear evidence that DIO may have reacted with the polymers under UV. This reaction is undesirable for device stability in both polymer cells and even more, very detrimental to the alkylthienyl substituted polymers.

Upon selection of a specific area with chemical shifts between 4.8 and 6.0 ppm of the ^{1}H-NMR spectra of both monomer solutions in the presence of DIO, and UV-exposure, **Figure 5.6(a,b)** reveals the appearance of new peaks after 10 mins illumination that grew in intensity over time. These peaks are initially absent from the ^{1}H-NMR spectra of the monomer solutions without DIO. Vinyl protons are typically found in this ppm-range, suggesting the formation of alkenes during the degradation process in both monomer solutions. Peaks centered around 5.8 ppm belong to the vinylic proton at the 2 (or 7) position (H_c) of the alkene radical left after UV-radiation of DIO while peaks centered around 5.0 and 4.9 ppm belong respectively to the terminal vinylic protons (H_a and H_b).

In the aliphatic region, with chemical shifts between 0.8 and 1.1 ppm, we observed the formation of new peaks with a chemical shift around 0.87 ppm after UV-illumination, as shown in **Figure 5.6(c,d)**. These peaks only appeared when the solutions are exposed to UV light. From these data, we can formulate two hypotheses: either DIO reacts directly with the monomers/polymers upon UV-exposure or DIO decomposes into (radical species or other compounds which stay in) the film, in the case of the devices, altering the donor/acceptor domains and indirectly impacting the stability. These alterations could, in turn, be sources of additional electron and hole traps leading to the observed faster degradation.

To clarify this point of view, we conducted a ^{1}H-NMR study on DIO-only and ODT-only solutions which resulted in the observation of the same peaks for the DIO-only solution, again only following UV-exposure, pointing to our

second hypothesis. However, we did not see these peaks for the ODT-only solution. The fact that peaks only appear for the DIO-only solution in the olefinic and aliphatic regions of the spectra suggests that DIO undergoes homolytic C-I bond cleavage followed by hydrogen elimination to form HI and alkene and/or followed by hydrogen abstraction.

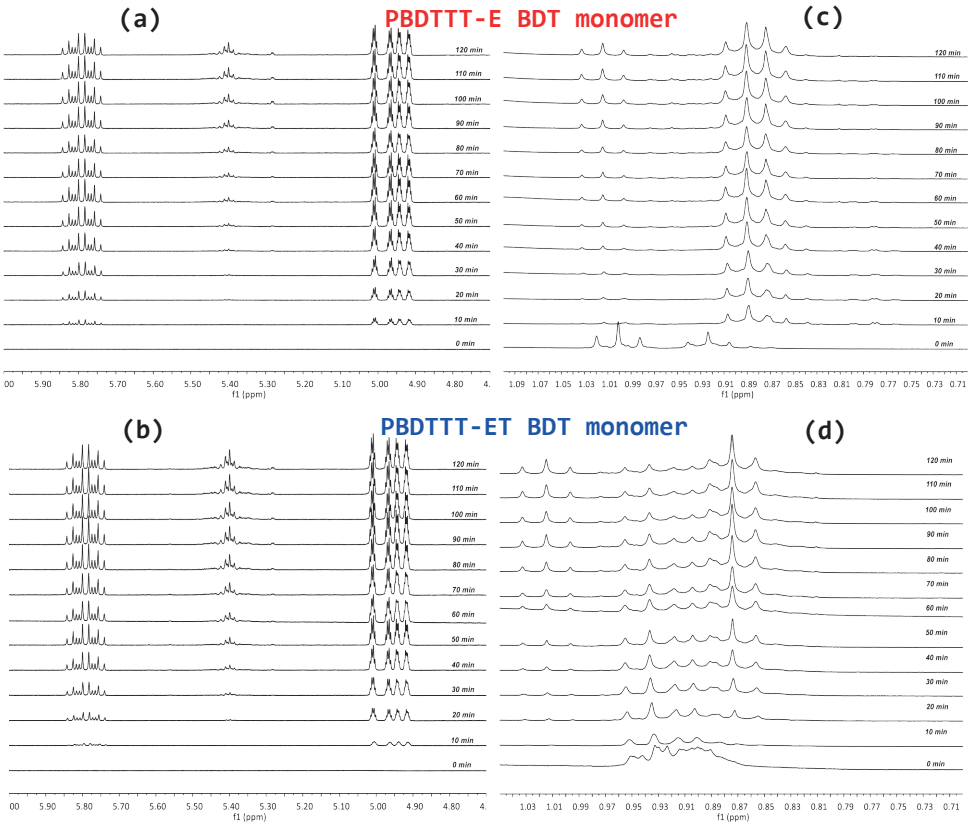

Figure 5.6: Selected peaks of ^{1}H-NMR spectra of monomer solutions with DIO recorded in an inert environment from sealed NMR tubes under irradiation with 315–400 nm light at intervals of 10 minutes from bottom-to-top starting from the initial spectrum showing signals (only under illumination). Peaks between 4.8 and 6.0 ppm in PBDTTT-E BDT monomer **(a)**, PBDTTT-ET BDT monomer **(b)**. Peaks between 0.8 and 1.1ppm in PBDTTT-E BDT monomer **(c)**, PBDTTT-ET BDT monomer **(d)**. Peaks centered around 5.8 ppm belong to the vinylic proton at the 2 (or 7) position (Hc) of the alkene radical left after UV-radiation of DIO while peaks centered around 5.0 and 4.9 ppm belong respectively to the terminal vinylic protons (H_a and H_b)- see Figure 5.7e. Reproduced with permission from Ref. [22].

The HI, iodine, and carbon-centered radicals are sufficiently reactive to react directly with the saturated carbon backbone of DIO. H· abstraction[14] has been previously speculated, though without experimental evidence, and thus being ascribed as the precursor to the phenomenon of photo-oxidative degradation of polymers in the presence of DIO when exposed to both air and light. We have shown that indeed this is partly the case isolating the molecules from oxygen in an inert atmosphere.

The key finding here is that when used in the active layer of the solar cell and under illumination, DIO is a photo-acid. And this is shown for the first time using a straightforward technique as ^{1}H-NMR. The HI formation under the sunlight kills the cells over time. The ODT-only solution spectra revealed no changes in spectra regarding the numbers, chemical shifts, and the ratio of peaks. Only the peak around 7.3 ppm disappeared after UV exposure, signaling an acceleration in the kinetics of deuterium exchange of the solvent with the thiol groups. These observations would explain why DIO solar cells degrade much faster in general than the ODT based and also suggest different degradation mechanisms for the additives.

Finally, based on the outcome from the NMR spectra leading to these observations, two pathways of degradation schemes were identified from DIO's reaction (shown in **Figure 5.7**) and could be used to explain the degradation reactions occurring in the active layers: H· abstraction induced degradation and H· elimination induced degradation. **Figure 5.7a** shows that upon UV illumination, DIO first goes through homolytic cleavage to produce a primary alkyl radical and iodine radical. Because of the high reactivity of the

primary alkyl radical, it readily abstracts hydrogen from the E-monomer, which gives iodooctane with a terminal methyl group (which appears around 0.87 ppm) and a relatively stable tertiary alkyl radical, followed by the homolytic cleavage of the C-O bond to form more stable oxygen radical and an alkene.

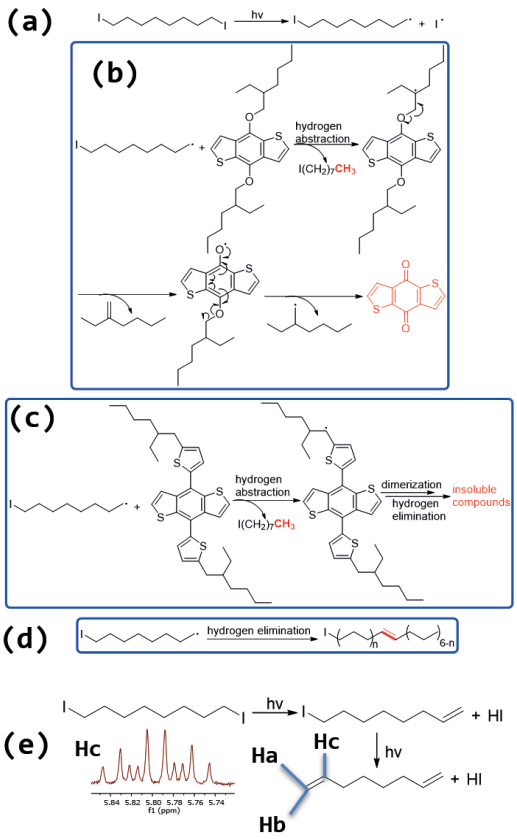

Figure 5.7: Possible degradation pathway after decomposition of DIO under UV light: Decomposition of DIO under UV light **(a)**; DIO decomposition induced degradation pathways: Hydrogen abstraction in PBDTTT-E BDT monomer **(b)**, PBDTTT-E ET BDT monomer **(c)**; and Hydrogen elimination in DIO with the formation of carbon-centered iodide radicals **(d)** and in DIO with the formation of HI **(e)**, an acid supported by the ^{1}H-NMR splitting pattern. Shown here, H_c is the vinylic proton at the 2 (or 7) position (H_c) of the alkene radical present in solution. Reproduced with permission from Ref. [22].

The occurrence of homolytic cleavage of the other C-O bond and rearrangement of the radical leads to the formation of a stable quinone moiety in **Figure 5.7b** along with a primary alkyl radical, propagating further decomposition. Thus, in the presence of DIO, there are two competing/cumulative routes to quinone formation: one due to DIO reaction with the polymer and the second due to a direct UV-reaction[21] with the polymer. This process explains why DIO accelerates the degradation process in PBDTTT-E-monomer and thus the PBDTTT-E-polymer solar cells.

In the case of the PBDTTT-ET-monomer, as shown in **Figure 5.7c**, a secondary alkyl radical which is stabilised by the thiophene instead of a third alkyl radical is produced by the hydrogen abstraction reaction. Although this radical is relatively stable, dimerisation and hydrogen elimination can still occur due to the reactivity of the radical, leading to the production of insoluble compounds not observable from the ^{1}H-NMR spectra. This reaction mechanism also strongly supports the fact that DIO indeed speeds up the degradation of ET-monomer and thus, PBDTTT-ET-polymer solar cells.

Finally, and as shown in **Figure 5.7d**, hydrogen elimination of DIO itself also occurs, forming HI, which is a strong acid, and competing simultaneously with the other pathways. HI is highly reactive and would kill the cells. The formation of HI generates alkenes in the system, which is evident from the ^{1}H-NMR spectra arising from the vinylic protons shown in **Figure 5.7e**. This observation is further supported by the predicted ^{1}H-NMR spectrum of the same alkene chain as depicted in ref. [22]. It should be noted that in general, the same photochemistry is probably active, over

a long period, in some other additives. Alkane dithiols,[28] for example, are contaminated with disulfides that are difficult to remove altogether, form readily upon exposure to ambient conditions and cleave homolytically in the presence of UV light.

5.3. Conclusions

We have confirmed that the addition of DIO precipitates the photodegradation and thus, negatively affects the photostability, reducing the lifetime of the cells: from more than 2 hours to 20 minutes for the PBDTTT-E polymer cells and from 30 minutes to less than 10 minutes for the PBDTTT-ET polymer cells. However, it does not alter the influence of the polymer chemical structure. We explain the mechanism behind the observed precipitation in photodegradation of the cells caused by the combined effect of the addition of the DIO and UV-exposure; and propose schemes for these mechanisms, supported by experimental evidence, for the differences observed for both types of polymers. All this information lead to a simple conclusion. DIO and other halogenated additives become photoacids and are inimical to the stability of the device as it is challenging to remove their residues from the film altogether. These findings inform us of ways to achieve efficient but stable materials and additives.

Bibliography

[1] A. Armin, Z. Chen, Y. Jin, K. Zhang, F. Huang, S. Shoaee, *Adv. Energy Mater.* **2017**, *1701450*, 1701450.

[2] X. Liu, H. Q. Wang, Y. Li, Z. Gui, S. Ming, K. Usman, W. Zhang, J. Fang, *Adv. Sci.* **2017**, *4*, 1.

[3] S. Nam, J. Seo, S. Woo, W. H. Kim, H. Kim, D. D. C. Bradley, Y. Kim, *Nat Commun* **2015**, *6*, 1.

[4] J. A. Bartelt, J. D. Douglas, W. R. Mateker, A. El Labban, C. J. Tassone, M. F. Toney, J. M. J. Fréchet, P. M. Beaujuge, M. D. McGehee, *Adv. Energy Mater.* **2014**, *4*, 1.

[5] Z. Liu, H. Ju, E. C. Lee, *Appl. Phys. Lett.* **2013**, *103*, 2.

[6] S. J. Lou, J. M. Szarko, T. Xu, L. Yu, T. J. Marks, L. X. Chen, *J. Am. Chem. Soc.* **2011**, *133*, 20661.

[7] L. A. Perez, J. T. Rogers, M. A. Brady, Y. Sun, G. C. Welch, K. Schmidt, M. F. Toney, H. Jinnai, A. J. Heeger, M. L. Chabinyc, G. C. Bazan, E. J. Kramer, *Chem. Mater.* **2014**, *26*, 6531.

[8] G. Shi, J. Yuan, X. Huang, Y. Lu, Z. Liu, J. Peng, G. Ding, S. Shi, J. Sun, K. Lu, H. Q. Wang, W. Ma, *J. Phys. Chem. C* **2015**, *119*, 25298.

[9] D. H. Wang, P. Morin, C. Lee, K. Ko, *J. Mater. Chem. A* **2014**, *2*, 1.

[10] L. Meng, Y. Zhang, X. Wan, C. Li, X. Zhang, Y. Wang, X. Ke, Z. Xiao, L. Ding, R. Xia, H. Yip, Y. Cao, Y. Chen, *Science* **2018**, *2612*, 1.

[11] Z. Wang, F. Zhang, L. Li, Q. An, J. Wang, J. Zhang, *Appl. Surf. Sci.* **2014**, *305*, 221.

[12] A. J. Pearson, P. E. Hopkinson, E. Couderc, K. Domanski, M. Abdi-Jalebi, N. C. Greenham, *Org. Electron. physics, Mater. Appl.* **2016**, *30*, 225.

[13] W. Kim, J. K. Kim, E. Kim, T. K. Ahn, D. H. Wang, J. H. Park, *J. Phys. Chem. C* **2015**, *119*, 5954.

[14] B. J. Tremolet De Villers, K. A. O'Hara, D. P. Ostrowski, P. H. Biddle, S. E. Shaheen, M. L. Chabinyc, D. C. Olson, N. Kopidakis, *Chem. Mater.* **2016**, *28*, 876.

[15] I. E. Jacobs, F. Wang, Z. I. Bedolla Valdez, A. N. Ayala Oviedo, D. J. Bilsky, A. J. Moulé, *J. Mater. Chem. C* **2018**, *6*, DOI 10.1039/C7TC04358A.

[16] S. Holliday, C. K. Luscombe, *Adv. Electron. Mater.* **2017**, *1700416*, 1700416.

[17] S. Lattante, *Electronics* **2014**, *3*, 132.

[18] Y. Sun, C. J. Takacs, S. R. Cowan, J. H. Seo, X. Gong, A. Roy, A. J. Heeger, *Adv. Mater.* **2011**, *23*, 2226.

[19] X. Li, F. Xie, S. Zhang, J. Hou, W. C. H. Choy, *Light Sci. Appl.* **2015**, *4*, 1.

[20] N. Y. Doumon, L. J. A. Koster, *Sol. RRL* **2019**, *3*, 1800301.

[21] N. Y. Doumon, G. Wang, R. C. Chiechi, L. J. A. Koster, *J. Mater. Chem. C* **2017**, *5*, 6611.

[22] N. Y. Doumon, G. Wang, X. Qiu, A. J. Minnaard, R. C. Chiechi, L. J. A. Koster, *Sci. Rep.* **2019**, *9*, 4350.

[23] N. Y. Doumon, M. Dryzhov, F. V Houard, V. M. Le Corre, A. Rahimi Chatri, P. Christodoulis, L. J. A. Koster, *ACS Appl. Mater. Interfaces* **2019**, *11*, 8310.

[24] L. J. Huo, *Angew. Chem. Int. Ed.* **2011**, *50*, 1.

[25] H. C. Liao, C. C. Ho, C. Y. Chang, M. H. Jao, S. B. Darling, W. F. Su, *Mater. Today* **2013**, *16*, 326.

[26] S. Cho, J. K. Lee, J. S. Moon, J. Yuen, K. Lee, A. J. Heeger, *Org. Electron. physics, Mater. Appl.* **2008**, *9*, 1107.

[27] H. Waters, N. Bristow, O. Moudam, S. W. Chang, C. J. Su, W. R. Wu, U. S. Jeng, M. Horie, J. Kettle, *Org. Electron. physics, Mater. Appl.* **2014**, *15*, 2433.

[28] Y. Xie, X. Hu, J. Yin, L. Zhang, X. Meng, G. Xu, Q. Ai, W. Zhou, Y. Chen, *ACS Appl. Mater. Interfaces* **2017**, *9*, 9918.

Appendix 5 (A5)

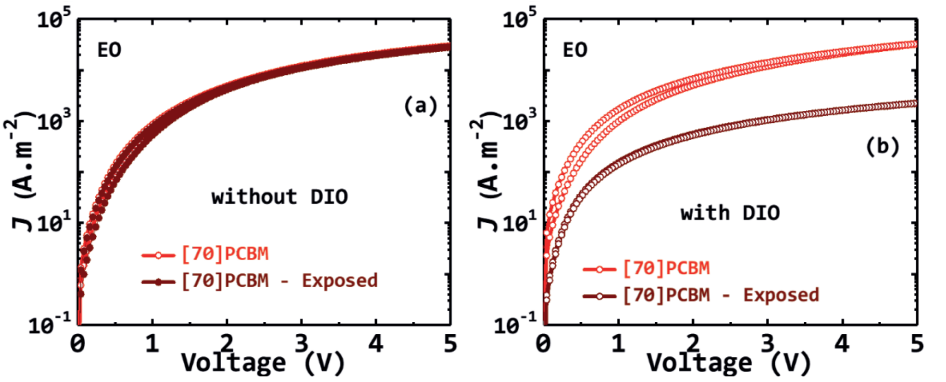

Figure A5.1: Current-Voltage characteristics of [70]PCBM electron-only devices, without **(a)** with **(b)** DIO.

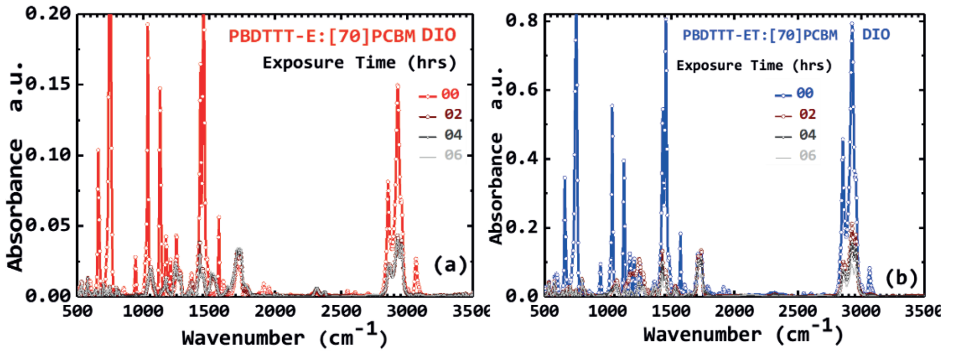

Figure A5.2: FTIR absorption spectra of fresh and exposed (2, 4, and 6 hours) films of blend films with DIO: PBDTT-E:[70]PCBM **(a)** and PBDTT-ET:[70]PCBM **(b)**.

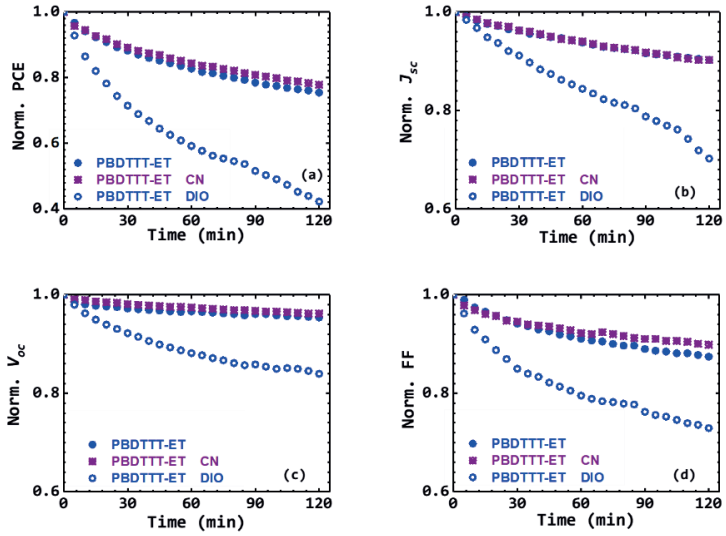

Figure A5.3: Performance of PBDTTT-ET:[70]PCBM solar cells under continuous illumination with no additive (blue, full symbol), with CN (purple) and with DIO (blue, empty symbol): PCE **(a)**, J_{sc} **(b)**, V_{oc} **(c)** and FF **(d)**.

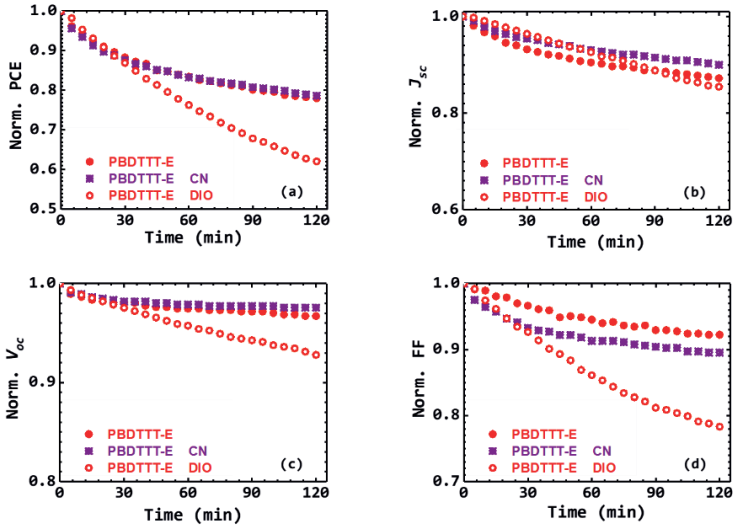

Figure A5.4: Performance of PBDTTT-E:[70]PCBM solar cells under continuous illumination with no additive (red, full symbol), with CN (purple) and with DIO (red, empty symbol): PCE **(a)**, J_{sc} **(b)**, V_{oc} **(c)** and FF **(d)**.

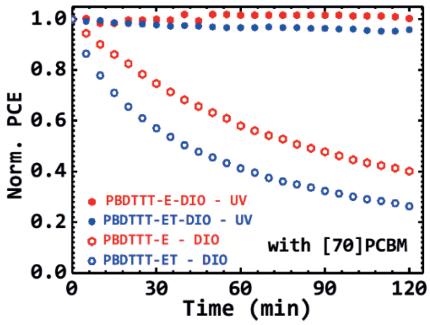

Figure A5.5: Evolution of PCE of PBDTTT-E:[70]PCBM and PBDTTT-ET:[70]PCBM cells with DIO. Filtered (full symbols) and unfiltered (open symbols) lamp.

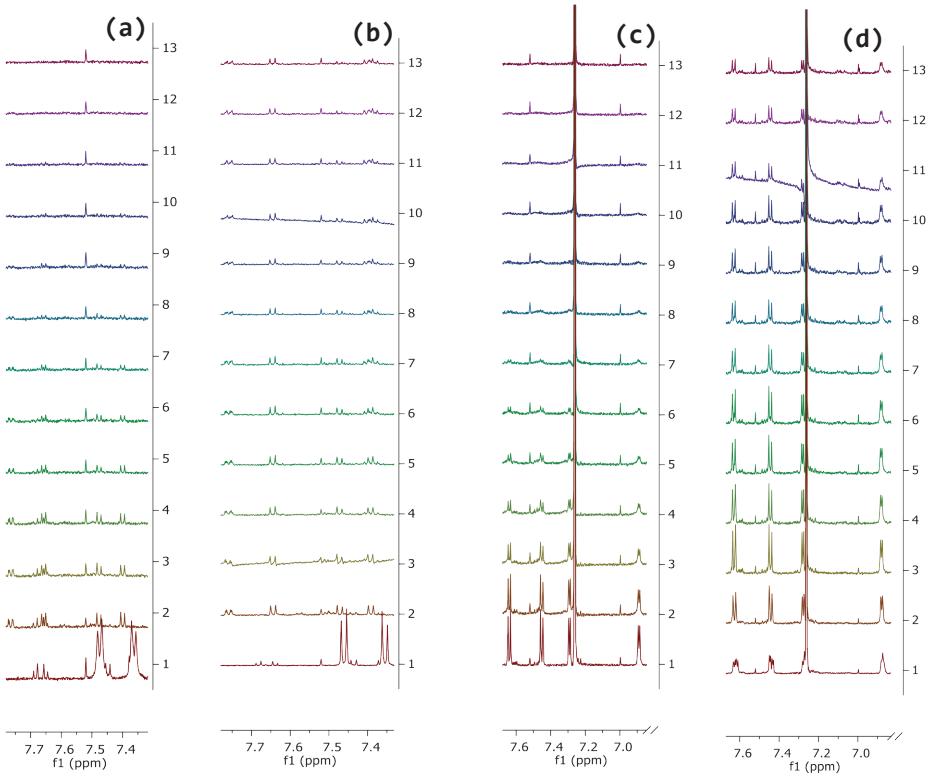

Figure A5.6: ^{1}H-NMR spectra of monomer solutions showing the backbone peaks under irradiation with 315-400 nm light at intervals of 10 minutes from bottom-to-top with the initial spectrum labelled as 1. PBDTTT-E BDT monomer **(a)** without DIO and **(b)** with DIO; PBDTTT-ET BDT monomer **(c)** without DIO and **(d)** with DIO. Reproduced with permission from Ref. [22]

6

Improved Photostability of Organic Solar Cells Using Ternary Blends

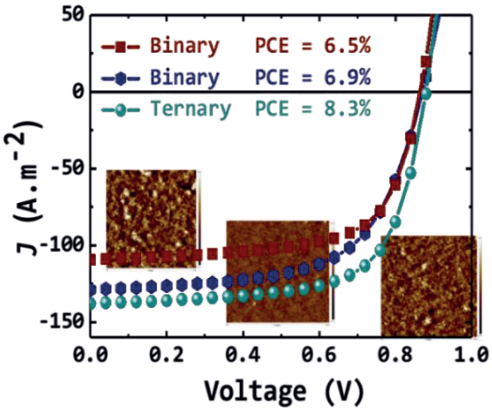

Chapter based on publications number 1 and 5

SUMMARY

Polymer solar cells are potentially key contributors to the next-generation organic photovoltaics for sustainable green sources of energy. However, the low stability of these solar cells is a hindrance to the commercialisation of this technology, and thus, needs more attention. Here, we show that with the right amount of [70]PCBM incorporated in polymer:ITIC binary cell in a ratio of D:A1:A2, ternary blend solar cells can be one way to photostabilise ITIC-based D:A binary blend solar cells.

We add [70]PCBM to PBDB-T:ITIC and PTB7-Th:ITIC binary blend solar cells in various ratios to fabricate ternary solar cells. The ternary solar cells outperform all binary cells in terms of efficiency and photostability with only a 10% average loss in efficiency under continuous illumination irrespective of the device structure. We identify changes in the molecular structure of the active layer blends as the main reason behind the observed photodegradation behaviour of the solar cells. The ternary blends are the most resilient to photo-induced molecular structural changes. This finding suggests that ternary organic solar cells could be a way to achieve photostable devices.

6.1. Introduction

Ternary blend organic solar cells (OSCs) differ from the well-known binary blend OSCs by one additional component in the mixture of their active layer organic materials. This means one can migrate from a donor:acceptor (D:A) binary system to either a D:A:A[1–4] or D:D:A[5–8] ternary system. The ternary blends achieved over the last few years a power conversion efficiency (PCE) of more than 16%[9–14] in single junction OSCs and lately a record 17.3%[15] in tandem structure serving as the rear sub-cell. This is because of the flexibility in choices of the additional D or A material such that a wider range of the solar spectrum is covered due to the complementarity of the additional material absorption profile to the parent cell's active layer absorption spectrum. The result could be an extension to the near infrared region or an improvement in the absorption strength for shorter wavelengths.[16,17]

The studies in the performance of the ternary blend solar cells have so far been only limited to the PCE. Then again, the same is true for the new class of binary OSCs, the non-fullerene acceptor (NFA) solar cells[7,18–20]. In chapter 4, we found that even though the NFA ITIC-based solar cells achieve better PCE than the fullerene [70]PCBM-based ones, they are less photostable. Only a few studies have tried to understand the stability issues related to these types of OSCs, and thus, study the degradation mechanisms in such cells.[1,21,22]

Here, we propose a systematic study of the incorporation of an appropriate amount of [70]PCBM into either PBDB-T:ITIC or PTB7-Th:ITIC binary blends to make photostable ternary blend solar cells.

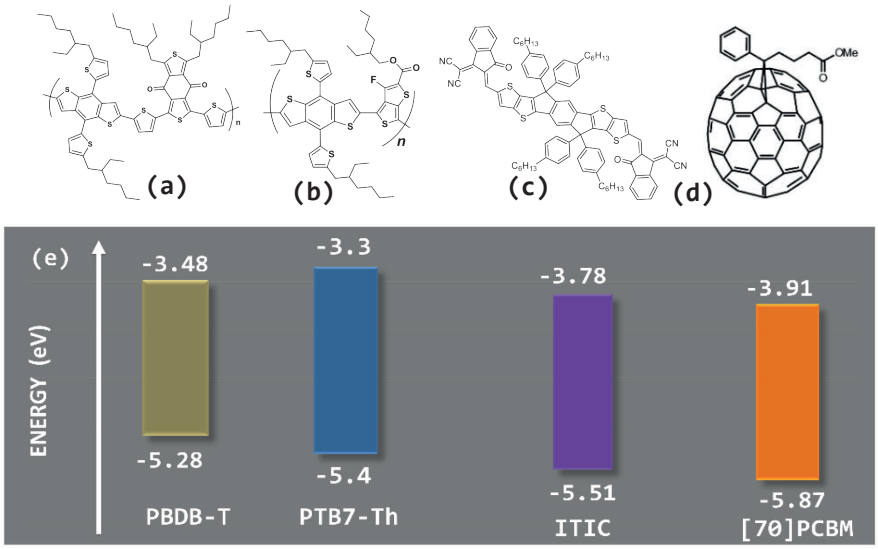

Figure 6.1: Chemical structures of the studied materials. Donor polymers: PBDB-T **(a)** and PTB7-Th **(b)**; acceptors: ITIC **(c)** and [70]PCBM **(d)**; with their energy level diagram **(e)**.

6.2. Results and Discussions: Performance of Devices

Binary blend conventional and inverted OSCs are fabricated on the one hand and ternary blends on the other hand by varying the acceptor ratio (A_1:A_2) from 0 to 1 for PBDB-T-based blends in a D:A_1+A_2 ratio of 1:1 dissolved in anhydrous chlorobenzene (CB) at a concentration of 20 mg.mL^{-1} (or 1:1.5 for PTB7-Th-based blends). The cells, kept at room temperature in an inert atmosphere, are exposed continuously to 1 sun illumination for 2 hours at open-circuit. **Figure 6.1** shows the molecular structures of the materials.

Figure 6.2(a,b) reveals the average photodegradation behaviour of the conventional (minimum of 10 devices) and inverted (minimum of 10 devices) cells. The PBDB-T:ITIC binary blend OSCs suffer the most in degradation with more than 20% efficiency loss after 2 hours of illumination, regardless of the configuration (-23% and -20% for conventional and inverted OSCs respectively). In contrast, as shown in **Figure A6.1**,[70]PCBM-based devices take advantage of the inverted configuration, with an enhancement in photostability from -16% to -12% efficiency loss. The most photostable blend is the ternary blend with a limited efficiency loss around -10% for both conventional and inverted configurations. Clearly, the ternary blend solar cells are more photostable than the binary blend solar cells.

Figure 6.2(c,d), and **Figure A6.2** display the corresponding degradation behaviour of the rest of the *J-V* parameters. Generally, as observed in **Figure A6.2,** the J_{sc} and V_{oc} remain relatively constant, excluding a potential photo-bleaching phenomenon (a loss in absorption) or changes in the HOMO and LUMO energy levels. However, as observed in chapter 4 and seen in **Figure 6.2(c,d)**, the FF shows the largest loss, and thus, remains the main contributor to the observed PCE loss in all three devices. The most significant finding is that the ternary blend solar cells are substantially more photostable than the ITIC based binary solar cells.

To ascertain this finding, PBDB-T is substituted with PTB7-Th, and the experiments are repeated for two best ratios of the ternary blends. **Figure A6.3** distinctively displays the PCE decay behaviour of the best devices. It shows that the observation is true for both polymers. It is important

to note that the degradation trends of the three solar cells are preserved irrespective of the device configuration, which allows excluding a possible impact of the different interfacial layers such as PEDOT:PSS, ZnO, MoO_3 or LiF on the evolution of the photovoltaic performances over time. These changes are hence inherent to the active layer. The single degradation plots of the devices reveal the real degradation behaviour of the three types of solar. The binary devices show a "burn-in" degradation behaviour known for solar cells under continuous illumination while the ternary ones only show a steady, gradual degradation behaviour. These findings do not imply that there is photostability beyond a couple of hours. Thus, more testing is needed to establish the long-term behaviour. However, there is a clear difference in the first two hours.

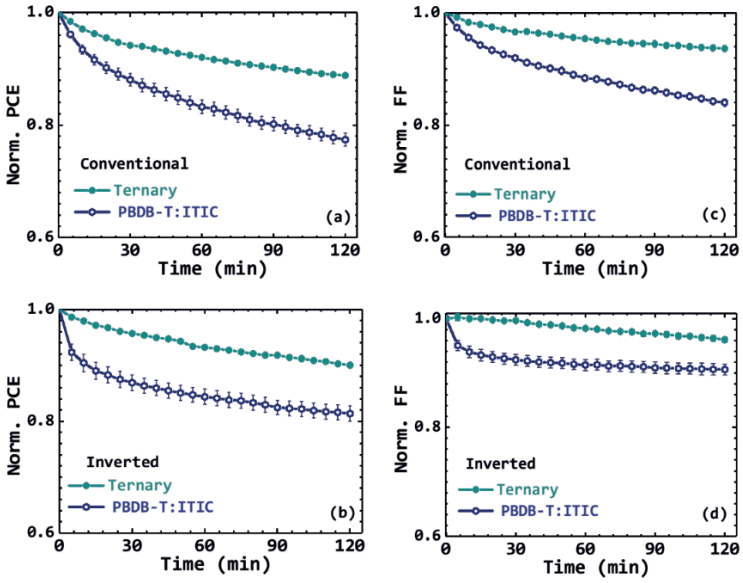

Figure 6.2: Photodegradation behaviour of PCE **(a,b)** and FF **(c,d)** of the conventional **(a,c)** and inverted **(b,d)** solar cells: ternary (sphere, cyan), and PBDB-T:ITIC (hexagon, blue).

Table 6.1: *J-V* parameters of a set of solar cells made under the same conditions for comparison: conventional (Conv.) and inverted (Inv., bold italic) where mn is the mean and SD is the standard deviation. Full ratio details of conventional solar cells can be seen in **Tables A6.1** and **A6.2**.

Devices	Structure	J_{sc} (mA.cm^{-2})	V_{oc} (V)	FF (%)	PCE (%) (PCE$_{mn} \pm$ SD)
Ternary	Conv.[a]	15.0	0.879	65.0	8.6 (7.6±0.5)
	Inv.[b]	***14.1***	***0.836***	***70.5***	***8.3*** **(8.0±0.3)**
PBDB-T:ITIC	Conv.[c]	13.6	0.895	64.1	7.8 (6.9±0.5)
	Inv.[d]	***14.1***	***0.842***	***68.2***	***8.1*** **(7.7±0.3)**
PBDB-T:[70]PCBM	Conv.[e]	10.9	0.864	66.1	6.4 (5.9±0.4)
	Inv.[f]	***12.8***	***0.766***	***65.9***	***6.5*** **(5.6±0.3)**

[a]27 devices; [b]11 devices; [c]13 devices; [d]18 devices; [e]10 devices; [f]19 devices

Additionally, the ternary blends outperform the binary blends in terms of PCE. **Table 6.1** shows the *J-V* parameters of the selected OSCs in each category, fabricated under the same conditions, while **Figure A6.4** displays the *J-V* curves of the best performing OSCs, their external quantum efficiency (EQE), the absorption spectra of their films, and the device statistics. Before conducting the photodegradation experiments on the studied OSCs, we first work out the ratio of the binary and ternary blends to have them practically under the same conditions. **Tables A6.1** and **A6.2** show the full range of the ratios covered for the conventional ternary blend OSCs as an example, while **Figure A6.5** shows the dependency of the *J-V* parameters on the blend ratios.

From this table, there are three ratios of PBDB-T:ITIC:[70]PCBM that recorded similar but highest PCEs, namely 1:0.9:0.1, 1:0.8:0.2, and 1:0.7:0.3. Thus, the photodegradation experiments are primarily conducted for these ratios together with the binary blends. Our study mainly

considered the 1:0.7:0.3 ratio for PBDB-T:ITIC:[70]PCBM as it yielded the best average PCE. Very recently, it was found by Wang *et al.* that the addition of [70]PCBM as a third component in PBDB-T:ITIC binary cells improves the efficiency, with 1:0.8:0.2 ratio yielding the best efficiency in their device structure[24], as is the case also in our study (see **Table A6.1**). Here, we show that [70]PCBM does not only improve the PCE of PBDB-T:ITIC binary cells, but also that of PTB7-Th:ITIC binary cells (with ratios of 1:0.5:0.5 and 1:0.75:0.75) as well as the photostability of the parent binary cells.

The absorption spectra of the fresh films are displayed in **Figure A6.4b.** Just as depicted in the EQE spectra in **Figure A6.4c,** the ternary film shows a slight improvement at lower wavelengths compared to the ITIC binary film while displaying similar contribution as ITIC binary at the longer wavelengths. Also, the AFM images show the ternary films as an intermediate morphology with the mean roughness of ~2.8 nm between the ITIC binary with the roughest morphology (~3.6 nm) and the [70]PCBM binary with the smoothest morphology (~1.2 nm). This may explain in part the better performance of the ternary cells as they benefit from enhanced nanomorphology[2,25] compared to the ITIC binary blends. The superior performance of the ternary blends in terms of PCE has been sparingly touted in the literature. However, the reason why they perform better in terms of photodegradation than the binary blends has not been thoroughly investigated and remained largely unclear.

To elucidate the photodegradation process, we resort to studying the differences in molecular packing that may occur in the films of the fresh

(0h) and the exposed (after 2h and 4h) states. The structure of the PBDB-T:ITIC, PBDB-T:PCBM and PBDB-T:ITIC:PCBM films and their time-dependence behaviour during exposure are studied by grazing incidence wide-angle X-ray scattering (GIWAXS). **Figure 6.3** shows the GIWAXS patterns and **Figure 6.4** their corresponding horizontal and vertical intensity cuts. As shown in **Figure 6.3**, the image of PBDB-T:ITIC fresh film shows an intense (010) peak located at q_z = 17.1 nm^{-1}, associated to a molecule π-π stacking distance of 0.38 nm and concentrated along the vertical direction (see **Figure 6.4d**), indicating a dominantly face-on orientation of the PBDB-T crystallites (see **Figure 6.3a**).

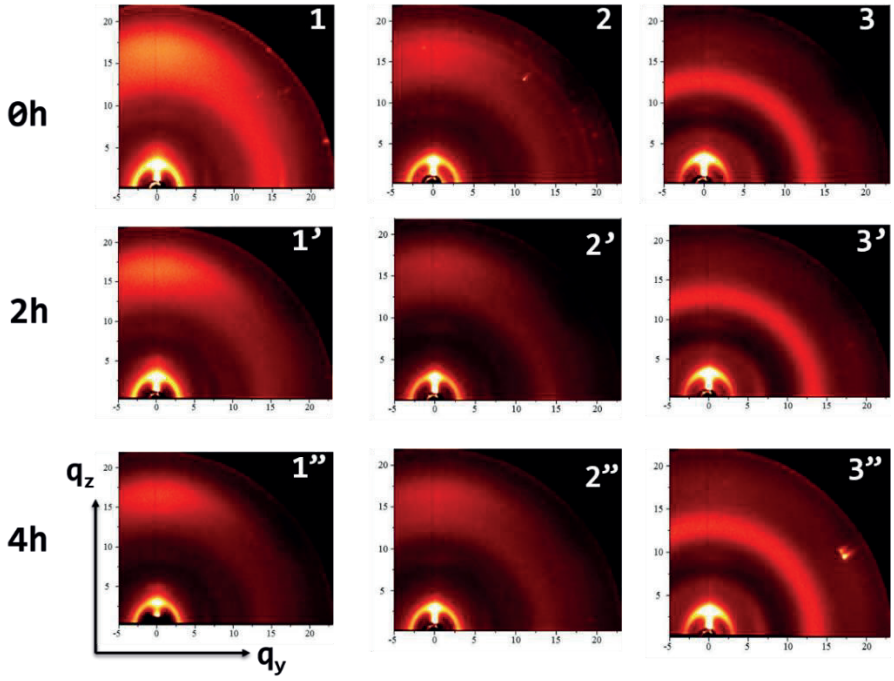

Figure 6.3: GIWAXS images of fresh (0h) and exposed (2h and 4h) films: PBDB-T:ITIC **(1, 1', 1")**, Ternary **(2, 2', 2")**, and PBDB-T:[70]PCBM **(3, 3', 3")**. Note that the intensity scale is the same for all the patterns.

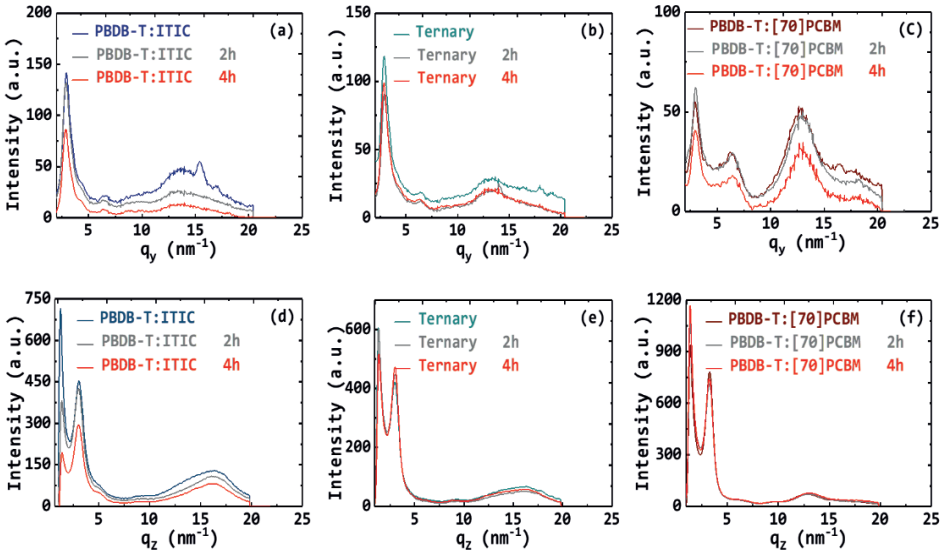

Figure 6.4: GIWAXS intensity plots of the fresh and exposed films (2h and 4h): in-plane intensities of PBDB-T:ITIC **(a)**, Ternary **(b)**, and PBDB-T:[70]PCBM **(c)** and out-of-plane intensities of PBDB-T:ITIC **(d)**, Ternary **(e)**, and PBDB-T:[70]PCBM **(f)**.

6

Conversely, the (010) peak of PBDB-T is not present in the GIWAXS pattern of the fresh PBDB-T:[70]PCBM film. Instead, the intensity of the (100) peak at q_z=2.9 nm^{-1} is much higher than the PBDB-T:ITIC fresh film, which means the PBDB-T:PCBM film is mainly packed as edge-on. The PBDB-T:ITIC:PCBM ternary blend fresh film shows a mixture of both binary structures; thus, a mixture of face-on and edge-on orientation.

The degradation upon light exposure was also assessed by GIWAXS. At different times during the exposure, the structural changes experienced for the three systems are quite different. Upon exposure, the (010) peak along the out-of-plane vertical direction of PBDB-T:ITIC film notably decreases over time together with a decrease of the (100) peak in the in-

plane horizontal direction. This intensity decrease reported in **Figure 6.4 (a,d)** suggests that the face-on packed crystallites significantly degrade and the molecular packing is negatively affected by light exposure. However, the edge-on packed crystallites also degraded dramatically as shown in the in-plane plots (see **Figure 6.4a**) of PBDB-T:ITIC films with the (010) peak at q_y=15.4 nm^{-1} disappearing after 2 hours and the out-of-plane (100) peak decreasing with time. The changes in the structure of the PBDB-T:ITIC films point clearly to a decrease in crystallinity and could impede charge mobility, creating unbalanced charges as already revealed in our previous study[22] explaining why the FF dropped the fastest. Thus, the PBDB-T:ITIC binary cells recorded the fastest PCE decay among the three cells.

In contrast, both the PBDB-T:PCBM and the PBDB-T:ITIC:PCBM ternary blend films are less affected by the exposure, with minimal structural changes upon exposure. This explains the relatively good stability of these two blends with respect to the PBDB-T:ITIC binary solar cells. As stated earlier, the structural changes experienced by the PBDB-T:ITIC cells, linked to the unbalanced charge carrier mobilities in their active layers, is the main reason behind the losses observed in the ITIC binary devices. We can thus conclude that the preserved crystallinity of the PBDB-T:ITIC:PCBM ternary blend films upon illumination is due to the incorporation of [70]PCBM into the PBDB-T:ITIC films. This is the reason why the ternary remains the most efficient. Key in this preservation of the crystallinity upon illumination over time is equally attributed to the

presence of [70]PCBM in the PBDB-T-based blends, helping to enhance the system's photostability.

6.3. Conclusions

The goal of this work is to find a way to make the non-fullerene acceptor ITIC based solar cells more photostable without compromising the power conversion efficiency. This study has shown that this is achievable using ternary blends by carefully tuning the ratio of the acceptors in the D:A_1:A_2 blends to maximise the output of the resulting ternary blend organic solar cells. In our case, the ratio of 1:0.7:0.3 in PBDB-T:ITIC:[70]PCBM blend helped in achieving this goal. Thus, the resulting ternary blend solar cells are more photostable than the two binary solar cells throughout the study, especially the PBDB-T:ITIC binary cells, while keeping higher efficiencies than both. The finding of the photostability of the ternary blend solar cells, in this particular case, is also not only valid for the ratios of 1:0.8:0.2 and 1:0.9:0.1 but also for a different donor polymer, PTB7-Th. The ternary blend resilience to photodegradation is explained by the fact that they retain more their crystallinity and molecular packing structure over time compared to the binary blends, especially the ITIC binary organic solar cells. These findings have significant implications for the understanding of the photodegradation mechanisms in [70]PCBM and ITIC based solar cells and suggest that a better understanding into the ternary blend solar cells could pave a way to more photostable devices.

Bibliography

[1] D. Baran, R. S. Ashraf, D. A. Hanifi, M. Abdelsamie, N. Gasparini, J. A. Röhr, S. Holliday, A. Wadsworth, S. Lockett, M. Neophytou, C. J. M. Emmott, J. Nelson, C. J. Brabec, A. Amassian, A. Salleo, T. Kirchartz, J. R. Durrant, I. McCulloch, *Nat. Mater.* **2017**, *16*, 363.

[2] R. Yu, S. Zhang, H. Yao, B. Guo, S. Li, H. Zhang, M. Zhang, J. Hou, *Adv. Mater.* **2017**, *29*, 1.

[3] W. Zhong, J. Cui, B. Fan, L. Ying, Y. Wang, X. Wang, G. Zhang, X. F. Jiang, F. Huang, Y. Cao, *Chem. Mater.* **2017**, *29*, 8177.

[4] H. Lu, J. Zhang, J. Chen, Q. Liu, X. Gong, S. Feng, X. Xu, W. Ma, Z. Bo, *Adv. Mater.* **2016**, *28*, 9559.

[5] Y. J. Hwang, H. Li, B. A. E. Courtright, S. Subramaniyan, S. A. Jenekhe, *Adv. Mater.* **2016**, *28*, 124.

[6] L. Zhong, L. Gao, H. Bin, Q. Hu, Z. G. Zhang, F. Liu, T. P. Russell, Z. Zhang, Y. Li, *Adv. Energy Mater.* **2017**, *7*, 1.

[7] J. W. Lee, Y. S. Choi, H. Ahn, W. H. Jo, *ACS Appl. Mater. Interfaces* **2016**, *8*, 10961.

[8] N. Gasparini, X. Jiao, T. Heumueller, D. Baran, G. J. Matt, S. Fladischer, E. Spiecker, H. Ade, C. J. Brabec, T. Ameri, *Nat. Energy* **2016**, *1*, 16118.

[9] N. Gasparini, L. Lucera, M. Salvador, M. Prosa, G. D. Spyropoulos, P. Kubis, H. J. Egelhaaf, C. J. Brabec, T. Ameri, *Energy Environ. Sci.* **2017**, *10*, 885.

[10] P. Cheng, J. Wang, Q. Zhang, W. Huang, J. Zhu, R. Wang, S. Y. Chang, P. Sun, L. Meng, H. Zhao, H. W. Cheng, T. Huang, Y. Liu, C. Wang, C. Zhu, W. You, X. Zhan, Y. Yang, *Adv. Mater.* **2018**, *30*, 1.

[11] Z. Xiao, X. Jia, L. Ding, *Sci. Bull.* **2017**, *62*, 1562.

[12] Y. Xie, F. Yang, Y. Li, M. A. Uddin, P. Bi, B. Fan, Y. Cai, X. Hao, H. Y. Woo, W. Li, F. Liu, Y. Sun, *Adv. Mater.* **2018**, *1803045*, 1803045.

[13] T. Kumari, S. M. Lee, S. H. Kang, S. Chen, C. Yang, *Energy Environ. Sci.* **2017**, *10*, 258.

[14] Q. An, X. Ma, J. Gao, F. Zhang, *Sci. Bull.* **2019**, *64*, 504.

[15] L. Meng, Y. Zhang, X. Wan, C. Li, X. Zhang, Y. Wang, X. Ke, Z. Xiao, L. Ding, R. Xia, H. Yip, Y. Cao, Y. Chen, *Science* **2018**, *2612*, 1.

[16] J. You, L. Dou, Z. Hong, G. Li, Y. Yang, *Prog. Polym. Sci.* **2013**, *38*, 1909.

[17] L. Lu, M. A. Kelly, W. You, L. Yu, *Nat. Photonics* **2015**, *9*, 491.

[18] H. Cha, S. Wheeler, S. Holliday, S. D. Dimitrov, A. Wadsworth, H. H. Lee, D. Baran, I. McCulloch, J. R. Durrant, *Adv. Funct. Mater.* **2018**, *28*, 1704389.

[19] H. Li, Y.-J. Hwang, B. A. E. Courtright, F. N. Eberle, S. Subramaniyan, S. A. Jenekhe, *Adv. Mater.* **2015**, *27*, 3266.

[20] N. Gasparini, M. Salvador, T. Heumueller, M. Richter, A. Classen, S. Shrestha, G. J. Matt, S. Holliday, S. Strohm, H.-J. Egelhaaf, A. Wadsworth, D. Baran, I. McCulloch, C. J. Brabec, *Adv. Energy Mater.* **2017**, *7*, 1701561.

[21] Y. Wang, M. J. Jafari, N. Wang, D. Qian, F. Zhang, T. Ederth, E. Moons, J. Wang, O. Inganäs, W. Huang, F. Gao, *J. Mater. Chem. A* **2018**, *6*, 11884.

[22] N. Y. Doumon, M. V. Dryzhov, F. V. Houard, V. M. Le Corre, A. Rahimi Chatri, P. Christodoulis, L. J. A. Koster, *ACS Appl. Mater. Interfaces* **2019**, *11*, 8310.

[23] N. Y. Doumon, F. V. Houard, J. Dong, P. Christodoulis, M. V Dryzhov, G. Portale, L. Jan, A. Koster, *J. Mater. Chem. C* **2019**, *5*, 5104.

[24] B. Wang, Y. Fu, C. Yan, R. Zhang, Q. Yang, Y. Han, Z. Xie, *Front. Chem.* **2018**, *6*, 1.

[25] M. Campoy-Quiles, Y. Kanai, A. El-Basaty, H. Sakai, H. Murata, *Org. Electron.* **2009**, *10*, 1120.

Appendix 6 (A6)

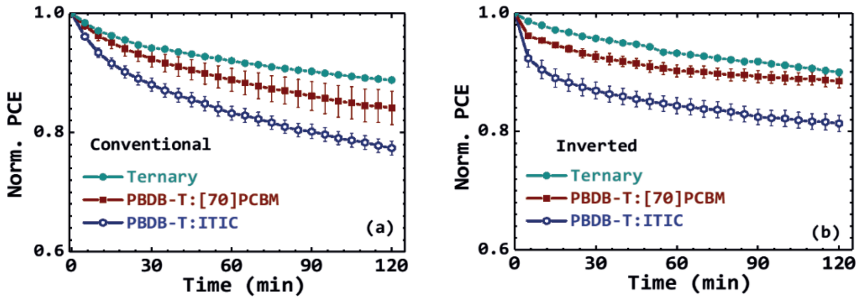

Figure A6.1: Photodegradation behaviour of PCE of the conventional **(a)** and the inverted **(b)** solar cells: Ternary (sphere, cyan), PBDB-T:[70]PCBM (square, brown) and PBDB-T:ITIC (circle, blue).

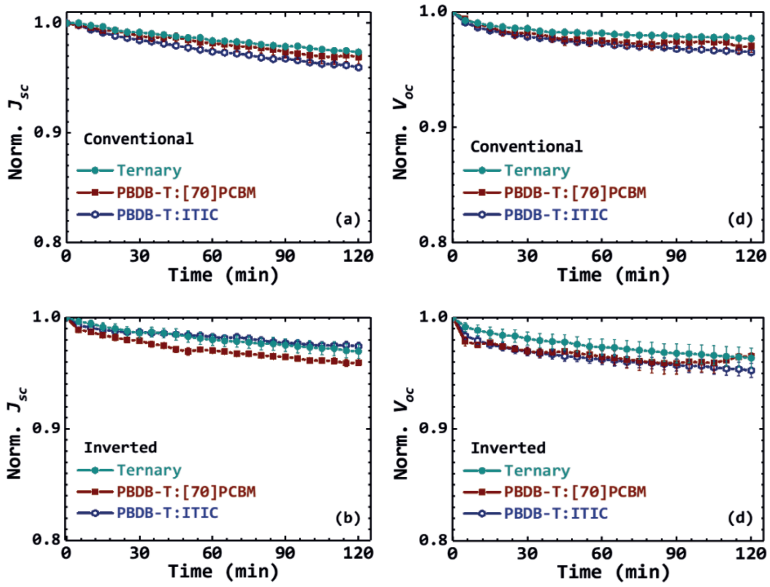

Figure A6.2: Photodegradation behaviour of J_{sc} **(a,b)** and V_{oc} **(c,d)** of the conventional **(a,c)** and the inverted **(b,d)** solar cells.

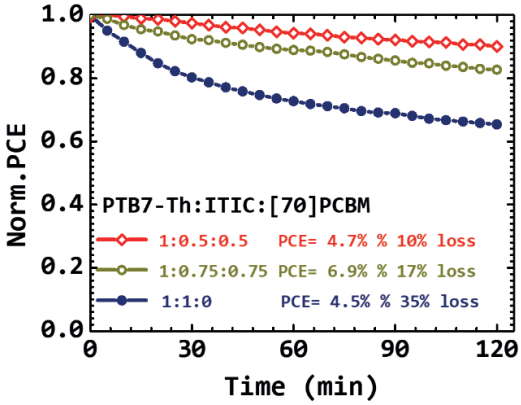

Figure A6.3: Photodegradation behaviour of the PCE: single plot of different ratio ternary vs. PTB7-Th:ITIC binary conventional solar cells.

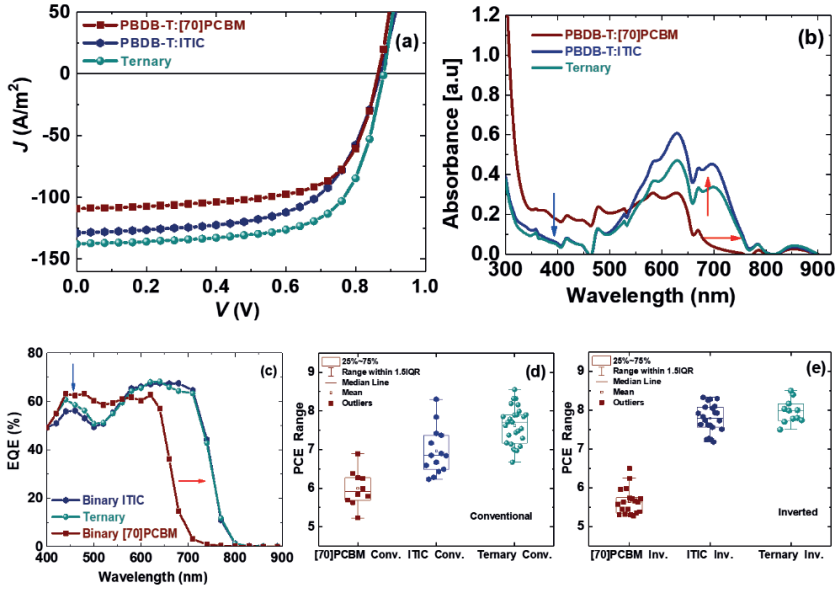

Figure A6.4: *J-V* curves and EQE of best performing conventional solar cells **(a,c)**, absorption spectra of their corresponding films **(b)**, and devices PCE statistics **(d,e)**. Ternary (27 conventional and 11 inverted devices), PBDB-T:[70]PCBM (10 conventional and 19 inverted devices) and PBDB-T:ITIC (14 conventional and 22 inverted devices). Reproduced with permission from Ref. [23].

Table A6.1: Ratio dependent evolution of the photovoltaic parameters of PBDB-T:ITIC:[70]PCBM conventional solar cells. Reproduced with permission from Ref. [23].

Number to ratio	Ratio (1:i:j with j=1-i)	J_{sc} ($A.m^{-2}$)	V_{oc} (V)	FF (%)	Best PCE (%)	Avg. PCE (%)	Avg. Degradation (%)
1	1:1:0	142	0.887	65.9	8.3	7.0	23.4
2	1:0.9:0.1	140	0.885	66.2	8.2	7.8	20.5
3	1:0.8:0.2	150	0.879	65.0	8.6	7.7	16.8
4	1:0.7:0.3	145	0.876	65.6	8.3	8.0	11.0
5	1:0.5:0.5	124	0.882	64.1	7.0	6.5	13.9
6	1:0.3:0.7	122	0.872	64.2	6.8	6.4	13.6
7	1:0.2:0.8	124	0.880	64.3	7.0	6.1	13.5
8	1:0.9:0.1	113	0.875	65.8	6.5	6.1	13.1
9	1:0:1	121	0.839	71.9	7.3	6.1	16

Table A6.2: Ratio dependent evolution of the photovoltaic parameters of PTB7-Th:ITIC:[70]PCBM conventional solar cells. Reproduced with permission from Ref. [23].

Number to ratio	Ratio (1:i:j with j=1-i)	J_{sc} ($A.m^{-2}$)	V_{oc} (V)	FF (%)	Best PCE (%)	Avg. PCE (%)	Avg. Degradation (%)
1	1:1:0	112.6	0.810	49.5	4.5	4.2	34.6
2	1:0.9:0.1	116.9	0.812	49.7	4.7	4.6	27.6
3	1:0.8:0.2	114.7	0.799	53	4.9	4.8	20.3
4	1:0.7:0.3	87.6	0.804	55.8	3.9	3.9	23.3
5	1:0.5:0.5	110.7	0.803	51.7	4.7	4.6	9.4
6	1:0.75:0.75	147.3	0.817	57.7	6.9	6.7	17.3
7	1:0.5:1	145.7	0.822	59.9	7.2	7.1	18.6
8	1:0.25:1.25	147.3	0.825	61.2	7.4	7.2	18.9
9	1:0:1.5	147	0.804	65.3	7.7	7.4	18.7

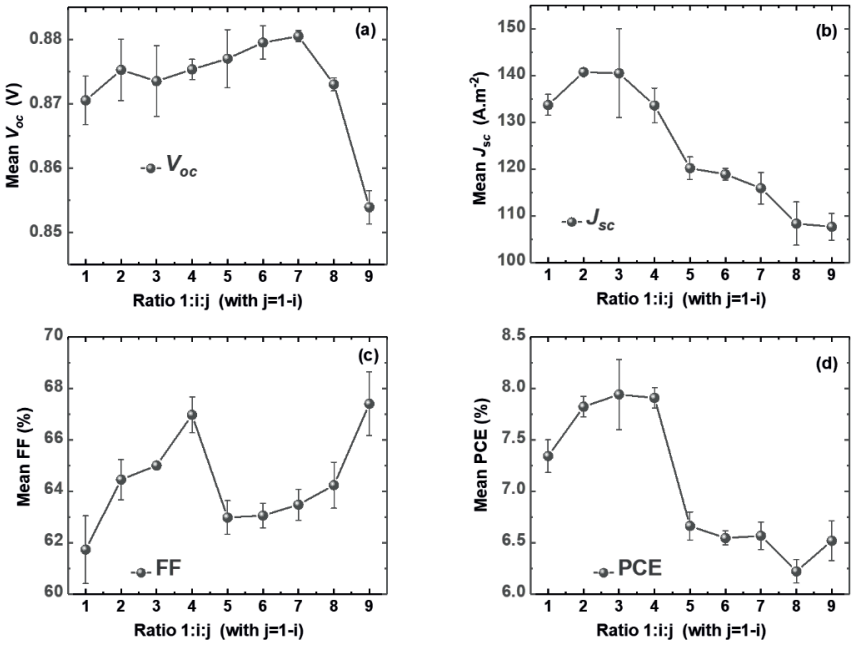

Figure A6.5: Ratio dependent average photovoltaic performance of conventional PBDB-T-based solar cells: V_{oc} **(a)**, J_{sc} **(b)**, FF **(c)**, and PCE **(d)**. The correct ratio for the numbers 1,2,3 … and 9 can be seen in Table A6.1. Reproduced with permission from Ref. [23].

7

Critical Issues, Current State of Solar Cell Technologies, and Impacts of our Contributions

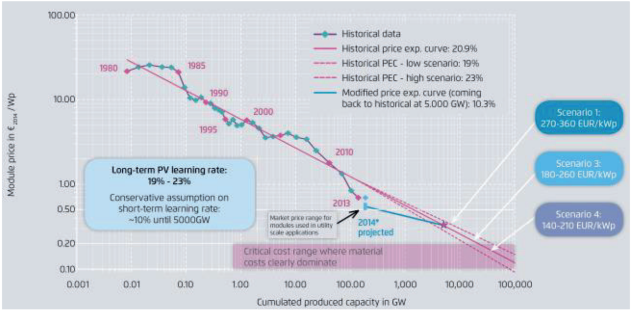

Source: Fraunhofer Institute for Solar Energy Systems ISE

"Patience can cook stone." – African Proverb

7.1. Introduction

On stage, the Duke of Cambridge Prince Williams was interviewing the renowned natural historian, Sir David F. Attenborough. This was at the 2019 World Economic Forum (WEF) in Davos, Switzerland. Suddenly, a billboard appeared which read: “In 2050 there would be more plastics in our oceans than fishes.” That sounds scary. Indeed, it is a cry again about human behaviour and attitude towards nature, contributing to the degrading environment. What is equally alarming is the earth rising temperature. We need to take drastic actions to remedy and avert the foretold catastrophe.

High-stakes decisions to slow down global warming attributed heavily to the usage of fossil fuels and coal as our primary source of energy are hardly forthcoming. While some countries including Costa Rica, Norway, and South Korea have announced earlier bans, the governments of The Netherlands, Denmark, Ireland, India, Israel, and recently Sweden promised to ban the sale of cars with internal combustion engines by 2030.[1] Other countries are expected to follow suit but not until 2040 (or 2050) in the case of France and the United Kingdom (or Germany). However, Germany announced the end of coal power generation by 2038.[2]

The focal point in all of this brouhaha is energy, its sources, production, and consumption. We need to rethink energy holistically, and its usage to the very base of the design of gadgets to be energy self-efficient. There is a need for a global, holistic, and greener energy transition.

7.2. Progress in Solar Technology

7.2.1. Requirements for the establishment of any technology

For any technology to be commercially viable, it must address three major areas, namely, efficiency, reliability, and cost. Thus, when translating photovoltaic technology from laboratory to commercial market, low cost, high power conversion efficiency, and high-level of reliability/stability (or long lifetime) are the three key parameters to consider in addition to other factors, such as low toxicity, low energy payback time, etc.[3] In this thesis, we focus on the third parameter: reliability, thus, we study the instability aspect of the polymer solar cell technology.

7.2.2. Current State of Solar Technologies on the Market

In their study "Current and Future Cost of Photovoltaics"[4], researchers from the Fraunhofer Institute for Solar Energy go further than a previous 20-year projection since 2015 of solar electricity price, predicting solar as cheap as 2 euro cents per kilowatt-hour in the sunniest parts of Europe by 2050. In general, PV appears to do well on the market. This is demonstrated by commercial-operational efficiency and lifetime of respectively 22% and more than 20 years for silicon technology. The 20-year projection from 2015[5] on how cheap electricity from solar can get is mostly driven by this technology. Organic PV technology, however, is faced with challenges. The advent of novel materials such as non-fullerene

acceptors has propelled the OPV technology to new heights in terms of power conversion efficiency[6], viable applications as in flexible surfaces, and the emergence of many companies including NanoFlex[7], Infinity PV[8], to mention a few. These companies are as a result of the hard work of the PV scientific community in advancing the technology at the laboratory level with first commercial evidence.[3,9–15] Some of these efforts from the community are captured on the newly established national renewable energy laboratory (NREL) champion module efficiency chart.[16]

The companies mentioned above are yet to capture the market as they have not fully satisfied the efficiency-reliability-cost rule. They have made great strides in terms of efficiency, hoping to cut down on cost, but their greatest predicament is the issue of stability/lifetime: the very theme of this thesis. Why is this so important? Because according to estimates, with a 15% operational-efficiency and a 20 year lifetime, (hybrid) organic solar cells could produce electricity at a cost of less than 7 cents per kilowatt-hour.[17] This, however, remains a matter of debate.

7.3. Impacts of Our Contributions

Despite the recent increase in efficiency as depicted in chapter 1, OPVs lag behind other technologies such as silicon and perovskites. The last 3-5 years alone saw a steep rise in efficiency with power conversion efficiencies over 16% for single junction devices and over 17% for tandem devices. Finally, OPVs are on the road to commercial reality.[18] The reason

is not only that the operational efficiency is not yet at the level of other established solar technologies, but also especially because of stability and lifetime issues which are less addressed compared to efficiency. Our contribution to this area of the puzzle for commercial viability is in threefold. First, to understand the mechanisms behind the degradation behaviour of these solar cells, thus their short lifetime. Second, to identify the differences in the contribution of the existing state-of-the-art materials on the market to this phenomenon. Finally, to propose a way to more stable solar cells. In chapters 3, 4, and 5, we look at some of the state-of-the-art workhorse donor materials, while in chapters 4 and 6, we study some of the state-of-the-art workhorse acceptors. In chapter 5 we pay particular attention to the role of additives, especially 1,8-diiodooctane, used in the active layer of the state-of-the-art organic solar cells on the photodegradation; and finally, in chapter 6 we propose a way to make ITIC non-fullerene organic solar cells more stable.

7.3.1. Impacts within the Scientific Community

Chapter 3: The findings in this chapter enhance our knowledge on the role played by the chemical structure of the state-of-the-art polymer donor materials, such as the benzodithiophene (BDT) unit-polymers, in the photostability of polymer:fullerene solar cells. First, we highlight the role played in the photodegradation by the two types of side chains attached to the BDT-units in the benzodithiophene-co-thienothiophene (BDT-TT)

polymers, namely alkoxy and alkylthienyl side chains. We were the first to explicitly point out that despite the positive effect known for the alkylthienyl side-chains on efficiency, they are bad for photostability[19]. Other studies follow suit in that direction, also pointing out they are simply bad for photooxidative stability of films and devices.[20,21] We proceed to explain how the photodegradation occurs in both class of polymers, the route, and the similarities and differences in the observed degradation trends.

> *"Compared to molecular engineering of BDT-TT polymers to boost device efficiency, studies on their chemical stability as well as device degradation mechanism are indeed relatively lack. In this perspective, ..., this work deserves acceptance." - Anonymous (with permission from RSC JMC C)*

Similarly, we moved to the TT-units of the BDT-TT polymers and addressed the effect of the energy level modulation of the TT-units on photodegradation. Through reduction and/or fluorination of the TT-unit, energy level modulation is achieved, enabling an increase in the V_{oc} of the component solar cells, thus an increase in PCE. However, how these changes affect photostability is unknown. We reveal that the fluorination of the TT-units or having alkyl-ester groups as substituents on the TT-units is bad for photostability. However, when these alkyl-ester groups are reduced into ketone substituents, the photostability greatly improves.

Chapter 4: We take our understanding a step further about the role played by the chemical structure of the acceptor materials in the photostability of polymer solar cells. We look at the state-of-the-art workhorse acceptors such as the fullerene acceptor (FA) derivative (e.g. [70]PCBM) and the non-

fullerene acceptor (NFA) derivatives (e.g., ITIC, IT-M, and IT-F). First, in a battle of FA versus NFA, we demonstrated that irrespective of the polymer, the cell structure, or the initial efficiency, the [70]PCBM-based devices are more photostable than the ITIC ones.[22] The finding that ITIC-based devices are less stable than [70]PCBM-based ones is complementary to other works[23,24] that found that NFA-based devices are more stable than the [70]PCBM-based ones. With our finding, one cannot fully claim that NFAs are better than FAs in terms of stability. Thus, it is now an accepted fact in the field that different (NFA acceptor) molecules may show different photostability behaviours.[25]

Next, we focused on the ITIC derivative acceptors and addressed the effect of the structural changes in the ITIC molecule on the photodegradation of their organic solar cells. By the usual modification to this small molecule acceptor – either by methylation (addition of $-CH_3$ groups) or by halogenation (addition of fluorine atom, F) of the outer benzene ring to make either IT-M or IT-F – energy level modulation is achieved, increasing PCE. We revealed that the methylation of ITIC (IT-M) improves the device efficiency but has no noticeable effect on the device photostability. While the fluorination decreases the device efficiency, the stability of the IT-F based solar cells depends on the device structure. Again, what these results point to is that improvement in PCE is material dependent, and there is no direct

"The authors present an interesting study that compares the photostability of organic solar cells based on the typical small molecule acceptor ITIC and its two derivatives (IT-M and IT-F). Overall, this work addresses the important topic of photostability for organic solar cells, ..." – Anonymous (with permission from Org. Elec.)

correlation between improvement in efficiency and that of stability. Similar findings have been obtained by Du et *al*.[25]

Chapter 5: In this chapter, we discuss one of the key elements that have helped in pushing the efficiency of OPVs higher before the advent of non-fullerenes, solvent additives. The typically used solvent additive in OPVs is 1,8-diiodooctane (DIO). Even in today's start-of-the-art highest performing OPV that recorded 17.3%[26], DIO was used. It is known that DIO has conflicting effects on the performance of OPVs: an increase in efficiency but a decrease in stability.[27] Different groups tried to explain how DIO affects the stability of different polymer solar cells. Our contribution is two-fold. First, we emphasise that DIO is generally beneficial to OPVs in terms of efficiency except for the ITIC-based solar cells. Second, using the BDT-TT polymers as a case study, we arrived at a more accurate explanation of how DIO under the effect of UV-radiation is detrimental to photostability and showed the process through which it happens. The degradation is initiated upon UV-irradiation by the cleavage of the side chains, resulting in more electron traps and by the formation of iodine, dissolved HI and carbon-centred radicals from DIO. Thus, DIO acts as a photo-acid in OPVs.

Chapter 6: Here, we set out to identify ways we can use to improve the stability of organic solar cells. We had two ideas: (i) exploring ternary blends as a potential way to pave the way for photostable organic solar cells and (ii) using radical scavengers as anti-oxidants to improve the ambient stability of organic solar cells. While the other idea is still

under investigation, the first has been explored enough in its early stage. We propose three components (ternary) active layer blend for more photostable organic solar cells at the expense of two components (binary) active layer blends. Our study is based on PBDB-T or PTB7-Th as donor material with [70]PCBM and ITIC as acceptor materials in a D:A_1:A_2 configuration as opposed to D:A configuration. We observe a faster photo-induced degradation in the binary solar cells, whereas the ternary solar cells present a slow, steady decay. Though we could not extensively explain the results, this finding suggests that ternary organic solar cells could be a way to achieve photostable devices. And we hope that these new results and findings would help move the field forward in that direction as anticipated by one of the reviewers.

"The manuscript proposed by Doumon et al. on "Improved photostability in ternary blend organic solar cells: the role of [70]PCBM" is interesting because they propose a ternary blend to improve the stability of organic solar cells. The research on ternary solar cells are still very interesting and insights about stability would help the field move forward." – Anonymous (with permission from RSC JMC C)

7.3.2. Impacts: Potential for Society

The ultimate aim of our work is to alter the way the world now uses solar energy. This alteration can only happen when the third area (for commercial viability), reliability, is equally satisfied. The future should focus not only on efficiency but also on durability and flexibility. So, what once was static, heavy, rigid, and costly, will become mobile, lightweight, flexible, and (maybe) inexpensive.[7] How can this be achieved? Through the

understanding of the phenomena that hinder this possible future. By understanding the fundamental mechanisms involved, for example, issues of degradation, stability, and lifetime: the key to unlock a host of new applications in the solar world. Where does this start? In the research laboratories with potentially transferable skills to industry. A problem can only be solved when the roots/causes are well understood. Our contributions certainly aided in that direction and showed a potential way of achieving that.

Bibliography

[1] Steve Hanley, "Sweden Will Ban Sale Of Gasoline & Diesel Cars After 2030. Germany Lags Behind | CleanTechnica," https://cleantechnica.com/2019/01/23/sweden-will-ban-sale-of-gasoline-diesel-cars-after-2030-germany-lags behind/?fbclid=IwAR1JDhZUHKh_VxWk78WTLg7mpnPXzq8Elyrm9b2_24oH3oh4OKeU1bI2yb g, **2019 (accessed on Jan. 27, 2019).**

[2] Markus Wacket, "Germany to phase out coal by 2038 in move away from fossil fuels | Reuters," https://www.reuters.com/article/us-germany-energy-coal/germany-should-fully-phase-out-coal-by-2038-commission-idUSKCN1PK04L, **2019 (accessed on Jan. 27, 2019).**

[3] L. Meng, J. You, Y. Yang, *Nat. Commun.* **2018**, *9*, 5265.

[4] J. N. Mayer, S. Philipps, N. S. Hussein, T. Schlegl, C. Senkpiel, *Current and Future Cost of Photovoltaics Long-Term Scenarios for Market Development.*, **2015**, pp. 82.

[5] Energiewende Team, "How cheap can solar get? Very cheap indeed – Energy Transition," https://energytransition.org/2015/09/how-cheap-can-solar-get/, **2015 (accessed on Feb. 4, 2019).**

[6] L. Meng, Y. Zhang, X. Wan, C. Li, X. Zhang, Y. Wang, X. Ke, Z. Xiao, L. Ding, R. Xia, H. Yip, Y. Cao, Y. Chen, *Science* **2018**, *2612*, 1.

[7] "NanoFlex Overview | NanoFlex Solar Photovoltaic Technologies | NanoFlex Power Corporation," http://www.nanoflexpower.com/compoverview, **(accessed on Feb. 10, 2019).**

[8] "infinityPV," https://infinitypv.com/, **(accessed on Feb. 6, 2019).**

[9] Y. Lin, S. Dong, Z. Li, W. Zheng, J. Yang, A. Liu, W. Cai, F. Liu, Y. Jiang, T. P. Russell, F. Huang, E. Wang, L. Hou, *Nano Energy* **2018**, *46*, 428.

[10] G. Sun, M. Shahid, Z. Fei, S. Xu, F. D. Eisner, T. D. Anthopolous, M. A. McLachlan, M. Heeney, *Mater. Chem. Front.* **2019**, DOI 10.1039/C8QM00610E.

[11] S. Xiong, L. Hu, L. Hu, L. Sun, F. Qin, X. Liu, M. Fahlman, Y. Zhou, *Adv. Mater.* **2019**, 1806616.

[12] M. Manceau, D. Angmo, M. Jørgensen, F. C. Krebs, *Org. Electron. physics,*

Mater. Appl. **2011**, *12*, 566.
[13] Y. Lin, Y. Jin, S. Dong, W. Zheng, J. Yang, A. Liu, F. Liu, Y. Jiang, T. P. Russell, F. Zhang, F. Huang, L. Hou, *Adv. Energy Mater.* **2018**, *8*, 1.
[14] Y. Galagan, J.-E. J. M. Rubingh, R. Andriessen, C. C. Fan, P. W. M. Blom, S. C. Veenstra, J. M. Kroon, *Sol. Energy Mater. Sol. Cells* **2011**, *95*, 1339.
[15] S. Bae, H. Kim, Y. Lee, X. Xu, J.-S. Park, Y. Zheng, J. Balakrishnan, T. Lei, H. R. Kim, Y. Il Song, Y.-J. Kim, K. S. Kim, B. Ozyilmaz, J.-H. Ahn, B. H. Hong, S. Iijima, *Nat. Nanotechnol.* **2010**, *5*, 574.
[16] NREL, *Natl. Renew. Energy Lab.* **2019 (accessed on Mar. 6, 2019)**.
[17] M. McGrath, "Organic solar cells set 'remarkable' energy record," https://www.bbc.com/news/science-environment-45132427, **2018 (accessed on Feb. 6, 2019)**.
[18] F. Gao, L. J. A. Koster, T.-Q. Nguyen, N. Stingelin, *Adv. Energy Mater.* **2018**, *8*, 1802706.
[19] N. Y. Doumon, G. Wang, R. C. Chiechi, L. J. A. Koster, *J. Mater. Chem. C* **2017**, *5*, 6611.
[20] A. Giovannitti, K. J. Thorley, C. B. Nielsen, J. Li, M. J. Donahue, G. G. Malliaras, J. Rivnay, I. McCulloch, *Adv. Funct. Mater.* **n.d.**, DOI 10.1002/ADFM.201706325.
[21] S. Holliday, C. K. Luscombe, *Adv. Electron. Mater.* **2017**, *1700416*, 1700416.
[22] N. Y. Doumon, M. V. Dryzhov, F. V. Houard, V. M. Le Corre, A. Rahimi Chatri, P. Christodoulis, L. J. A. Koster, *ACS Appl. Mater. Interfaces* **2019**, acsami.8b20493.
[23] D. Baran, N. Gasparini, A. Wadsworth, C. H. Tan, N. Wehbe, X. Song, Z. Hamid, W. Zhang, M. Neophytou, T. Kirchartz, C. J. Brabec, J. R. Durrant, I. McCulloch, *Nat. Commun.* **2018**, *9*, 2059.
[24] H. Cha, J. Wu, A. Wadsworth, J. Nagitta, S. Limbu, S. Pont, Z. Li, J. Searle, M. F. Wyatt, D. Baran, J. S. Kim, I. McCulloch, J. R. Durrant, *Adv. Mater.* **2017**, *29*, 1.
[25] X. Du, T. Heumueller, W. Gruber, A. Classen, T. Unruh, N. Li, C. J. Brabec, *Joule* **2018**, 2, 1-12.
[26] L. Meng, Y. Zhang, X. Wan, C. Li, X. Zhang, Y. Wang, X. Ke, Z. Xiao, L. Ding, R. Xia, H.-L. Yip, Y. Cao, Y. Chen, *Science* **2018**, *361*, 1094.
[27] W. Kim, J. K. Kim, E. Kim, T. K. Ahn, D. H. Wang, J. H. Park, *J. Phys. Chem. C* **2015**, *119*, 5954.

Summary

Despite the recent increase in efficiency as depicted in chapter 1, OPVs lag behind other technologies such as silicon and perovskites. The last 3-5 years alone saw a steep rise in efficiency with power conversion efficiencies over 16% for single junction devices and over 17% for tandem devices. Finally, OPVs are on the road to commercial reality. The reason is not only that the operational efficiency is not yet at the level of other established solar technologies, but also especially because of stability and lifetime issues which are less addressed compared to efficiency. Our contribution to this area of the puzzle for commercial viability is in three folds. First, it is to understand the mechanisms behind the degradation behaviour of these solar cells, thus their short lifetime. Second, to identify the differences in the contribution of the existing state-of-the-art materials on the market to this phenomenon. Finally, to propose a way to more stable solar cells. In chapters 3, 4, and 5, we look at some of the state-of-the-art workhorse donor materials, while in chapters 4 and 6, we studied some of the state-of-the-art workhorse acceptor materials. In chapter 5 we pay particular attention to the role of additives, especially 1,8-diiodooctane, used in the active layer of the state-of-the-art organic solar cells on the photodegradation; and finally, in chapter 6 we propose a way to make ITIC non-fullerene organic solar cells more stable.

Chapter 3: The findings in this chapter enhance our knowledge on the role played by the chemical structure of the state-of-the-art polymer donor materials, such as the benzodithiophene (BDT) unit-polymers, in the photostability of polymer:fullerene solar cells. First, we highlight the role played in the photodegradation by the two types of side chains attached to the BDT-units in the benzodithiophene-co-thienothiophene (BDT-TT) polymers, namely alkoxy and alkylthienyl side chains. We were the first to explicitly point out that despite the positive effect known for the alkylthienyl side-chains on efficiency, they are bad for photostability. Other studies follow suit in that direction, also pointing out they are simply bad for photooxidative stability of films and devices. We proceed to explain how the photodegradation occurs in both class of polymers, the route, and the similarities and differences in the observed degradation trends.

Similarly, we moved to the TT-units of the BDT-TT polymers and addressed the effect of the energy level modulation of the TT-units on photodegradation. Through reduction and/or fluorination of the TT-unit, energy level modulation is achieved, enabling an increase in the V_{oc} of the component solar cells, thus an increase in PCE. However, how these changes affect photostability is unknown. We reveal that the fluorination of the TT-units or having alkyl-ester groups as substituents on the TT-units is bad for photostability. However, when these alkyl-ester groups are reduced into ketone substituents, the photostability greatly improves.

Chapter 4: We take our understanding a step further about the role played by the chemical structure of the acceptor materials in the photostability of polymer solar cells. We look at the state-of-the-art workhorse acceptors such as the fullerene acceptor (FA) derivative (e.g. [70]PCBM) and the non-fullerene acceptor (NFA) derivatives (e.g., ITIC, IT-M, and IT-F). First, in a battle of FA versus NFA, we demonstrated that irrespective of the polymer, the cell structure, or the initial efficiency, the [70]PCBM-based devices are more photostable than the ITIC ones. The finding that ITIC-based devices are less stable than [70]PCBM-based ones is complementary to other works that found that NFA-based devices are more stable than the [70]PCBM-based ones. With our finding, one cannot fully claim that NFAs are better than FAs in terms of stability. Thus, it is now an accepted fact in the field that different (NFA acceptor) molecules may show different photostability behaviours.

Next, we focused on the ITIC derivative acceptors and addressed the effect of the structural changes in the ITIC molecule on the photodegradation of their organic solar cells. By the usual modification to this small molecule acceptor – either by methylation (addition of $-CH_3$ groups) or by halogenation (addition of fluorine atom, F) of the outer benzene ring to make either IT-M or IT-F – energy level modulation is achieved, increasing PCE. We revealed that the methylation of ITIC (IT-M) improves the device efficiency but has no obvious effect on the device photostability. While the fluorination decreases the device efficiency, the stability of the IT-F based solar cells depends on the device structure. Again, what these results point to is that improvement in PCE is material dependent, and there is no direct correlation between improvement in efficiency and that of stability.

Chapter 5: In this chapter, we discuss one of the key elements that have helped in pushing the efficiency of OPVs higher before the advent of non-fullerenes, solvent additives. The typically used solvent additive in OPVs is 1,8-diiodooctane (DIO). Even in today's start-of-the-art highest performing OPV that recorded 17.3%, DIO was used. It is known that DIO has

conflicting effects on the performance of OPVs: an increase in efficiency but a decrease in stability. Different groups tried to explain how DIO affects the stability of different polymer solar cells. Our contribution is two-fold. First, we emphasise that DIO is generally beneficial to OPVs in terms of efficiency except for the ITIC-based solar cells. Second, using the BDT-TT polymers as a case study, we arrived at a more accurate explanation of how DIO under the effect of UV-radiation is detrimental to photostability and showed the process through which it happens. The degradation is initiated upon UV-irradiation by the cleavage of the side chains, resulting in more electron traps and by the formation of iodine, dissolved HI and carbon-centred radicals from DIO. Thus, DIO acts as a photo-acid in OPVs.

Chapter 6: Here, we set out to identify ways we can use to improve the stability of organic solar cells. We had two ideas: (i) exploring ternary blends as a potential way to pave the way for photostable organic solar cells and (ii) using radical scavengers as anti-oxidants to improve the ambient stability of organic solar cells. While the other idea is still under investigation, the first has been explored enough in its early stage. We propose three components (ternary) active layer blend for more photostable organic solar cells at the expense of two components (binary) active layer blends. Our study is based on PBDB-T or PTB7-Th as donor material with [70]PCBM and ITIC as acceptor materials in a D:A_1:A_2 configuration as opposed to D:A configuration. We observe a faster photo-induced degradation in the binary solar cells, whereas the ternary solar cells present a slow, steady decay. Though we could not extensively explain the results, this finding suggests that ternary organic solar cells could be a way to achieve photostable devices. And we hope that these new results and findings would help move the field forward in that direction as anticipated by one of the reviewers.

Samenvatting

Ondanks de recente verbetering van de efficiëntie van organische zonnecellen zoals beschreven in hoofdstuk 1, lopen organische zonnecellen nog steeds achter op zonnecellen op basis van silicium of perovskiet. De laatste 3-5 jaar is de efficiëntie gestegen tot 16% voor conventionele en 17% voor tandem cellen. Eindelijk zijn organische zonnecellen op weg naar commerciële toepassingen. De reden dat commerciële toepassingen nog schaars zijn is niet alleen dat de efficiëntie achter loopt, maar ook de levensduur, waar nog veel minder onderzoek naar gedaan is. Onze bijdrage aan de commercialisering bestaat uit drie delen. Allereerst, worden de degradatiemechanismen in organische zonnecellen en daarmee de redenen voor hun korte levensduur besproken. Ten tweede worden de verschillen tussen nieuwe materialen en de resulterende effecten op de levensduur behandeld. Tot slot wordt een route naar efficiëntere zonnecellen voorgesteld. In de hoofdstukken 3, 4, en 5, worden de meest gebruikte recente donor-materialen besproken, waar in de hoofdstukken 4 en 6 een aantal van de meest gebruikte recente acceptor-materialen besproken worden. In hoofdstuk 5 wordt de rol van additieven in de actieve laag, in het bijzonder 1,8-diiodooctaan, besproken en de invloed die deze hebben op de licht-geïnduceerde degradatie. Tot slot wordt in hoofdstuk 6 een manier voorgesteld om ITIC fullereen-vrije zonnecellen stabieler te maken.

Hoofdstuk 3: Onze bevindingen in dit hoofdstuk leren ons wat voor rol de chemische structuur van recente donor materialen, zoals benzodithiofeen (BDT) gebaseerde polymeren, speelt in de fotostabiliteit van polymeer:fullereen zonnecellen. Als eerste werpen we licht op de rol van alkoxy en alkylthienyl zijketens van de BDT-monomeren in benzodithiofeen-co-thienothiofeen (BDT-TT) polymeren. Wij hebben als eerste aangetoond dat ondanks het positieve effect van alkylthienyl zijketens op efficiëntie, de fotostabiliteit achteruitgaat. Ander onderzoek volgde in dezelfde richting, waar gewezen werd op het negatieve effect op fotostabiliteit van lagen en zonnecellen. Daarna leggen we uit hoe fotodegradatie plaatsvindt in beide polymeren, langs welke route dat gebeurt, en de overeenkomsten en verschillen in de geobserveerde degradatie trends.

Op vergelijkbare wijze hebben we in TT-monomeren in de BDT-TT-polymeren gekeken naar het effect van energieniveau modulatie van de TT-monomeren op fotodegradatie. Door reductie en/of fluorinatie van het TT-monomeer wordt

het energieniveau gemoduleerd, waardoor een hogere open klemspanning, resulterend in een hogere conversie efficiëntie mogelijk wordt. Wat voor effect deze veranderingen hebben op de fotostabiliteit is onbekend. Wij tonen aan dat fluorinatie van de TT-monomeren, of het hebben van alkyl-ester groepen als substituenten op de TT-monomeren, slecht is voor de fotostabiliteit. Echter, wanneer deze alkyl-ester groepen gereduceerd worden tot keton-substituenten, wordt de fotostabiliteit veel beter.

Hoofdstuk 4: wij proberen nog een stap verder te gaan in ons begrip van het effect op de fotostabiliteit van de chemische structuur van acceptor-materialen. We nemen de nieuwste veelgebruikte acceptoren zoals het veelgebruikte fullereen-acceptor (FA) derivaat [70]PCBM en de niet-fulerene-acceptor (NFA) derivaten, zoals ITIC, IT-M, en IT-F, onder de loep. Ten eerste hebben we in een vergelijking tussen FA en NFA materialen laten zien dat onafhankelijk van het polymeer, de cel structuur, of initiële efficiëntie, de [70]PCBM-gebaseerde zonnecellen stabieler zijn dan de ITIC-gebaseerde cellen. De vondst dat ITIC-gebaseerde cellen minder stabiel zijn dan [70]-PCBM-gebaseerde cellen is in tegenstelling tot ander werk in het veld, waar gevonden werd dat NFA-gebaseerde zonnecellen stabieler zijn dan [70]PCBM varianten. Onze bevindingen in acht nemende, kan er niet zomaar gezegd worden dat NFA-gebaseerde zonnecellen stabieler zijn dan [70]PCBM varianten. Het is nu een algemeen geaccepteerd feit dat verschillende NFA-moleculen verschillende fotostabiliteit kunnen vertonen.

Vervolgens hebben we ons gefocust op ITIC-derivaten en het effect van structurele veranderingen in het ITIC-molecuul op de fotostabiliteit van de resulterende zonnecellen. Door gebruikelijke aanpassingen aan het molecuul, dan wel methylering door de additie van een -CH3 groep dan wel halogenering door de toevoeging van een F atoom, wordt het energie niveau van het molecuul gemoduleerd, waardoor de efficiëntie van de zonnecel toeneemt. Wij hebben laten zijn dat methylering van ITIC, resulterend in IT-M, de efficiëntie van zonnecel doet toenemen, maar geen duidelijk effect heeft op de fotostabiliteit. Halogenering, resulterend in IT-F, reduceert de efficiëntie, maar de stabiliteit hangt af van de gekozen zonnecelarchitectuur. Wederom wijzen de resultaten uit dat de efficiëntieverbetering afhangt van het materiaal en dat er geen directe correlatie is tussen verbeteringen in efficiëntie en stabiliteit.

Hoofdstuk 5: In dit hoofdstuk wordt een van de belangrijkste oorzaken van de efficiëntieverbeteringen sinds het gebruik van NFA-materialen besproken, namelijk toevoegingen aan de oplosmiddelen. De meest gebruikte toevoeging in organische zonnecellen is 1,8-diiodooctaan (DIO). Zelfs in de meest efficiënte zonnecel tot nu toe, van 17,3%, is DIO gebruikt. Het is bekend dat het gebruik van DIO zowel voor als nadelen heeft: de efficiëntie gaat

vooruit, maar de levensduur gaat achteruit. Verschillende groepen hebben geprobeerd te verklaren hoe DIO de stabiliteit van verscheidene zonnecellen aantast. Onze bijdrage bestaat uit twee delen. Ten eerste constateren wij het feit dat DIO over het algemeen een positieve invloed heeft op de efficiëntie, maar niet in het geval van ITIC-gebaseerde zonnecellen. Ten tweede hebben wij door BDT-TT-polymeren in groter detail te analyseren, een verklaring gevonden voor het degradatiemechanisme. De degradatie komt door het verbreken van de verbinding met de zijketen door uv-straling, waardoor er meer elektronenvallen gegenereerd worden, er iodine ontstaat, opgelost HI vormt, en radicalen van DIO ontstaan. DIO functioneert dus als foto geactiveerd zuur in organische zonnecellen.

Hoofdstuk 6: In dit hoofdstuk zoeken we manieren om de stabiliteit van organische zonnecellen te verbeteren. Er zijn twee verschillende methoden onderzocht: (i) gebruik maken van een extra actief molecuul bovenop het gebruikelijke donor-acceptor paar en (ii) het gebruik van afvangers van vrije radicalen als antioxidanten. De laatstgenoemde methode is nog in ontwikkeling, over het gebruik van de eerste methode zijn er al voorlopige conclusies. Wij stellen voor om drie actieve componenten de voorkeur te geven over de gebruikelijke configuratie met twee actieve componenten. Onze studie is gebaseerd op PBDB-T of PTB7-Th als donor materiaal en [70]PCBM en ITIC als acceptor materialen in een D:A1:A2 configuratie, in tegenstelling tot de gangbare D:A configuratie. We nemen een snellere degradatie waar in de binaire configuratie, waar de degradatie in de ternaire configuratie langzamer verloopt. Een mechanisme dat dit verschil verklaart is niet gevonden. We hopen dat deze nieuwe resultaten het veld voorwaarts kunnen helpen zoals gesuggereerd door één van de externe beoordelaars van het bijbehorende artikel.

List of Acronyms

n	ideality factor
ε_o	permittivity of free space
ε_r	static relative permittivity
α	incident angle
μ_e	electron mobility
μ_h	hole mobility
μ_{on}	charge carrier mobility
μ_{min}	minimum mobility
μ_{max}	maximum mobility
γ	recombination coefficient
γ_n	electric field-activation factor
K_{ex}	extraction rate
K_{rec}	recombination rate
D	diffusion coefficient
τ	exciton lifetime
$\pi-$	pi–
$\sigma-$	sigma–
Đ	polydispersity
1D	One-dimensional
2D	Two-dimensional
[60]PCBM	[6,6]-Phenyl C_{61} butyric acid methyl ester
[70]PCBM	[6,6]-Phenyl C_{71} butyric acid methyl ester
A	acceptor
AE-	alkyl-ester-
AFM	atomic force microscopy
AK-	alkyl-ketone-
Al	aluminium
AL	active layer
AM 1.5G	air mass 1.5 global

A_p	alkoxy-polymer
AT_p	alkylthienyl-polymer
Au	gold
BDT	benzodithiophene
BDT-TT	benzodithiophene-thienothiophene
BHJ	bulk heterojunction
Ca	calcium
CB	conduction band, chlorobenzene
$CDCl_3$	deuterochloroform
CF	chloroform
CH_3	methyl
CH_4	methane
C_2H_6	ethane
Cl	chlorine
CN	1-chloronaphthalene
Cr	chromium
D	donor
D/A	donor/acceptor
D:A	donor:acceptor
D:A:A	donor:acceptor:acceptor
D:D:A	donor:donor:acceptor
DIO	1,8-diiodooctane
E_g	bandgap
EO	electron-only
EQE	external quantum efficiency
ETL	electron transporting layer
F	fluorine
FA	fullerene acceptor
FF	fill factor
FTIR	Fourier transform infrared
G	generation rate of free charges
GIWAXS	grazing incidence wide-angle X-ray scattering
^{1}H-(NMR)	proton or hydrogen-1 (nuclear magnetic resonance)

HI	hydrogen iodide
HO	hole-only
HOMO	highest occupied molecular orbital
H_2O	water
HTL	hole transporting layer
IDT	indacenodithiophene
IR	infrared
ITIC	3,9-bis(2-methylene-(3-(1,1-dicyanomethylene)-indanone))-5,5,11,11-tetrakis(4-hexylphenyl)-dithieno[2,3-d:2',3'-d']-s-indaceno[1,2-b:5,6-b']dithiophene
IT-Cl	3,9-bis(2-methylene-((3-(1,1-dicyanomethylene)-6,7-dichloro)-indanone))-5,5,11,11-tetrakis(4-hexylphenyl)-dithieno[2,3-d:2',3'-d']-s-indaceno[1,2-b:5,6-b']dithiophene
IT-F	3,9-bis(2-methylene-((3-(1,1-dicyanomethylene)-6,7-difluoro)-indanone))-5,5,11,11-tetrakis(4-hexylphenyl)-dithieno[2,3-d:2',3'-d']-s-indaceno[1,2-b:5,6-b']dithiophene
IT-M	3,9-bis(2-methylene-((3-(1,1-dicyanomethylene)-6/7-methyl)-indanone))-5,5,11,11-tetrakis(4-hexylphenyl)-dithieno[2,3-d:2',3'-d']-s-indaceno[1,2-b:5,6-b']dithiophene
ITO	indium tin oxide
J	current density
J_{SC}	Short-circuit current density
J-V	current density-voltage
K_B	Boltzmann constant
KBr	potassium bromide
L	thickness
LED	light emitting diode
L_D	exciton diffusion length
LiF	lithium fluoride

LUMO	lowest occupied molecular orbital
M_{BDT}	BDT monomer
mn	mean
M_w	molecular weight
M_A	alkoxy-BDT monomer
M_{AT}	alkylthienyl-BDT monomer
MDMO-PPV	poly[2-methoxy-5-(3’,7’-dimethyloctyloxy)-1,4-phenylenevinylene]
MEH-PPV	poly[2-methoxy-5-(2-ethylhexyloxy)-1,4-phenylenevinylene]
MoO_X	molybdenum oxide
N_2	nitrogen
NFA	non-fullerene acceptor
NIR	near infrared
O_2	oxygen
OC	Open-circuit
o-DCB	ortho-dichlorobenzene
ODT	octanedithiol
OLED	organic light emitting diode
OPV	organic photovoltaic
OSC	organic solar cell
P3HT	poly(3-hexylthiophene)
PBDB-T	poly[(2,6-(4,8-bis(5-(2-ethylhexyl)thiophen-2-yl)-benzo[1,2-b:4,5-b’]dithiophene))-alt-(5,5-(1’,3’-di-2-thienyl-5’,7’-bis(2-ethylhexyl)benzo[1’,2’-c:4’,5’-c’]dithiophene-4,8-dione)]
PBDT-TT	polybenzodithiophene-thienothiophene
PBDTTT-C	poly[(4,8-bis-(2-ethylhexyloxy)-benzo(1,2-b:4,5-b’)dithiophene)-2,6-diyl-alt-(4-(2-ethylhexanoyl)-thieno[3,4-b]thiophene-)-2-6-diyl)]
PBDTTT-CF	poly[(4,8-bis-(2-ethylhexyloxy)-benzo(1,2-b:4,5-b’)dithiophene)-2,6-diyl-alt-(4-(2-ethylhexanoyl)-thieno[3,4-b]thiophene-)-2-6-diyl)]

PBDTTT-CT	2,6-Bis(trimethyltin)-4,8-bis(5-(2-ethylhexyl)thiophen-2-yl)benzo[1,2-b :4,5-b']dithiophene
PBDTTT-E	poly[(4,8-bis-(2-ethylhexyloxy)-benzo(1,2-b:4,5-b')dithiophene)-2,6-diyl-alt-((2-ethylhexyl)-thieno(3,4-b)thiophene-4-carboxylate))-2,6-diyl)]
PBDTTT-ET	poly[(4,8-bis(5-(2-ethylhexyl)thiophen-2-yl)-benzo[1,2-b;4,5-b]dithiophene)-2,6-diyl-alt-(4-(2-ethylhexyl)-thieno[3,4-b]thiophene-4-carboxylate))-2,6-diyl)]
PCE	power conversion efficiency
PEDOT:PSS	poly(3,4-ethylenedioxythiophene)-poly(styrenesulfonate)
Pd	palladium
ppm	parts per million
PPV	phenylenevinylene
PSC	polymer solar cell
PTB7	poly[(4,8-bis-(2-ethylhexyloxy)-benzo(1,2-b:4,5-b')dithiophene)-2,6-diyl-alt-(4-(2-ethylhexyl)-3-fluorothieno[3,4-b]thiophene-)-2-carboxylate-2-6-diyl)]
PTB7-Th	poly[4,8-bis(5-(2-ethylhexyl)thiophen-2-yl)benzo[1,2-b;4,5-b']dithiophene-2,6-diyl-alt-(4-(2-ethylhexyl)-3-fluorothieno[3,4-b]thiophene-)-2-carboxylate-2-6-diyl)]
q_e, e	electric charge
q_y	in-plane modulus of scattering vector
q_z	out-of-plane modulus of scattering vector
SC	short circuit
SCLC	space charge limited current
SD	standard deviation
T	temperature
T_{80}	lifetime (solar cell)
TPV	transient photovoltage
TT-	thienothiophene-
UV	ultraviolet
UV-Vis	ultraviolet-visible
UV-Vis-NIR	ultraviolet-visible-near infrared

V	voltage
VB	valence band
V_{bi}	built-in voltage
V_{int}	internal voltage
V_{oc}	Open-circuit voltage
V_{rs}	voltage drop due to series resistance
v/v	volume/volume
v%	volume percent
WI	tungsten iodide
ZnO	zinc oxide

List of Publications

"Wisdom or knowledge is not like money to be tied up and hidden." – Ghana (~Akan) Proverb

List of Publications

(1) **Doumon, N. Y.**; Houard, V.; Dong, J.; Christodoulis, P.; Dryzhov, M. V; Portale, G.; Jan, L.; Koster, A. Improved Photostability in Ternary Blend Organic Solar Cells: The Role of [70]PCBM. *J. Mater. Chem. C* **2019**, *5*, 5104–5111. https://doi.org/10.1039/c8tc06621c.

(2) **Doumon, N. Y.**; Houard, F. V.; Dong, J.; Yao, H.; Portale, G.; Hou, J.; Koster, L. J. A. Energy Level Modulation of ITIC Derivatives: Effects on the Photodegradation of Conventional and Inverted Organic Solar Cells. *Org. Electron.* **2019**, *69*, 255–262. https://doi.org/10.1016/j.orgel.2019.03.037.

(3) **Doumon, N. Y.**; Wang, G.; Qiu, X.; Minnaard, A. J.; Chiechi, R. C.; Koster, L. J. A. 1,8-Diiodooctane Acts As a Photo-Acid in Organic Solar Cells. *Sci. Rep.* **2019**, *9*, 4350. https://doi.org/10.1038/s41598-019-40948-1.

(4) Ye, G.; **Doumon, N. Y.**; Rousseva, S.; Liu, Y.; Abdu-Aguye, M.; Loi, M. A.; Hummelen, J. C.; Koster, L. J. A.; Chiechi, R. C. Conjugated Polyions Enable Organic Photovoltaics Processed from Green Solvents. *ACS Appl. Energy Mater.* **2019**, *2*, 2197–2204. https://doi.org/10.1021/acsaem.8b02226.

(5) **Doumon, N. Y.**; Dryzhov, M. V; Houard, F. V; Le Corre, V. M.; Rahimi Chatri, A.; Christodoulis, P.; Koster, L. J. A. Photostability of Fullerene and Non-Fullerene Polymer Solar Cells: The Role of the Acceptor. *ACS Appl. Mater. Interfaces* **2019**, *11* (8), 8310–8318. https://doi.org/10.1021/acsami.8b20493.

(6) **Doumon, N. Y.**; Koster, L. J. A. Effects of the Reduction and/or Fluorination of the TT-Units in BDT-TT Polymers on the Photostability of Polymer:Fullerene Solar Cells. *Sol. RRL* **2019**, *3* (3), 1800301. https://doi.org/10.1002/solr.201800301.

(7) Le Corre, V. M.; Chatri, A. R.; **Doumon, N. Y.**; Koster, L. J. A. Response to Comments on Charge Carrier Extraction in Organic Solar Cells Governed by Steady-State Mobilities. *Adv. Energy Mater.* **2018**, *7* (22), 1803125. https://doi.org/10.1002/aenm.201701138.

(8) **Doumon, N. Y.**; Wang, G.; Chiechi, R. C.; Koster, L. J. A. Relating Polymer Chemical Structure to the Stability of Polymer:Fullerene Solar Cells. *J. Mater. Chem. C* **2017**, *5* (26), 6611–6619. https://doi.org/10.1039/C7TC01455D.

(9) Agyei-Tuffour, B.; **Doumon, N. Y.**; Rwenyagila, E. R.; Asare, J.; Oyewole, O. K.; Shen, Z.; Petoukhoff, C. E.; Zebaze Kana, M. G.; Ocarroll, D. M.; Soboyejo, W. O. Pressure Effects on Interfacial Surface Contacts and Performance of Organic Solar Cells. *J. Appl. Phys.* **2017**, *122* (20), 205501. https://doi.org/10.1063/1.5001765.

(10) Le Corre, V. M.; Chatri, A. R.; **Doumon, N. Y.**; Koster, L. J. A. Charge Carrier Extraction in Organic Solar Cells Governed by Steady-State Mobilities. *Adv. Energy Mater.* **2017**, *7* (22), 1701138. https://doi.org/10.1002/aenm.201701138.

(11) Zhou, D.; **Doumon, N. Y.**; Abdu-Aguye, M.; Bartesaghi, D.; Loi, M. A.; Anton Koster, L. J.; Chiechi, R. C.; Hummelen, J. C. High-Quality Conjugated Polymers via One-Pot Suzuki-Miyaura Homopolymerization. *RSC Adv.* **2017**, *7* (44), 27762–27769. https://doi.org/10.1039/c7ra03539j.

(12) Abbaszadeh, D.; Wetzelaer, G.-J. A. H.; **Doumon, N. Y.**; Blom, P. W. M. Efficient Polymer Light-Emitting Diode with Air-Stable Aluminum Cathode. *J. Appl. Phys.* **2016**, *119* (9), 1–7. https://doi.org/10.1063/1.4943190.

(13) Abbaszadeh, D.; **Doumon, N. Y.**; Wetzelaer, G.-J. A. H.; Koster, L. J. A.; Blom, P. W. M. Effect of the Layer Thickness on the Efficiency Enhancement in Bilayer Polymer Light-Emitting Diodes. *Synth. Met.* **2016**, *215*, 64–67. https://doi.org/10.1016/J.SYNTHMET.2016.02.003.

(14) Asuo, I. M.; Gedamu, D.; Ka, I.; **Doumon, N. Y.**; Basu, S.; Pignolet, A.; Cloutier, S. G.; and Nechache, R. Stable and Efficient Solar Cells from Ambient-Processed Mixed Cation Perovskites. (Submitted)

(15) Abdu-Aguye M.;* **Doumon N. Y.**;* Terzic I.; Dong J.; Portale G.; Loos K.; Koster L. J. A.; Loi M. A. Can ferroelectricity improve organic solar cells? (* Equal contribution, submitted)

(16) Rousseva S.; den Besten H.; Doting E. L.; **Doumon N. Y.**; Douvogianni E.; Koster L. J. A.; and Hummelen J. C. Approaching double-digit dielectric constant values with fullerene derivatives. (Submitted)

Curriculum Vitae

P Participation/Attendance
PP Poster Presentation
T Talk
IT Invited Talk

Education

2015–2019: Early stage researcher (PhD employee), Photophysics and Optoelectronics, Zernike Institute for Advanced Materials, University of Groningen, Groningen – The Netherlands
2012–2013: Master of Arts (MA, Honours College) in Leadership, University of Groningen, Groningen – The Netherlands
2011–2013: Master of Science (MSc, Topmaster) in nanoscience, Zernike Institute for Advanced Materials (ZIAM), University of Groningen, Groningen – The Netherlands
2010–2011: Master of Science in theoretical physics, African University of Science and Technology (AUST), Abuja – Nigeria
2006–2009: Bachelor of Science in physics, University of Ghana, Legon, Accra – Ghana

Conferences, Seminars, Workshops, & Summer Schools

2019 Institut national de recherche supérieure, Varennes, Canada (IT)
2019 Ecole de technologies supérieures, Montréal, QC – Canada (IT)
2019 Next-Gen IV: PV materials, Groningen, The Netherlands (P, Volunteer)
2019 MRS Spring Meeting, Phoenix, Arizona – USA (T)
2018 Pratt School of Engineering, Duke University, Durham, NC – USA (IT)
2018 E-MRS 2018 Spring Meeting, Strasbourg - France (PP)
2018 LMPV 2018 conference, Amsterdam -The Netherlands (PP)
2018 Physics@Veldhoven 2018, Veldhoven – The Netherlands (PP)
2017 9th International 2017 A-MRS conference, Gaborone – Botswana (T)
2017 Dutch 2017 perovskite workshop, Groningen – The Netherlands (P)
2017 Next generation PV materials III, Groningen – The Netherlands (PP)
2017 E-MRS 2017 Spring Meeting, Strasbourg - France (Talk)
2017 Vlieland 2017 Meeting, Groningen – The Netherlands (PP)
2016 E-MRS 2016 Fall Meeting, Warsaw - Poland (T)
2016 Quantsol 2016 summer school (P)
2016 LMPV 2016 conference, Amsterdam -The Netherlands (P)
2016 FOM Veldhoven 2016 conference, Veldhoven – The Netherlands (P)
2015 Next-generation OPV II, Groningen – The Netherlands (P)

Awards, Positions, & Functions

2019 People's Choice Award RuG 2019 3-minutes thesis Competition
2011 Zernike institute scholarship
2010 Dr. Ngozi Okonjo-Iweala/African Development Bank scholarship
2008 Most dedicated member of the physics students' association of Ghana (PHYSAG), Legon Branch, University of Ghana

2016 E-MRS Fall 2016 conference: symposium (Acting) session chair
2015–2018 Teaching Assistant for various courses, University of Groningen
2011–2013 President African students' community (ASC) – Groningen
Member of Groningen international students' platform (GISP)
2011–2012 Student member, curriculum committee for topmaster programme
2010–2011 Student welfare committee, AUST, Abuja

Acknowledgements

"Wisdom is like a baobab tree; no one individual can embrace it." – Ghana (~Ewe) Proverb

Akpe!!! Merci!!! Thank you!!! Bedankt!!! ¡¡¡Gracias

The journey to the PhD thesis began a while ago with a trip from Abuja for the topmaster interview in March 2011. Since then, numerous individuals have been part of the different instances leading to this day.

"*There are more colourful flowers on the path of life, but the prettiest ones have the sharpest thorns*" – African proverb. I have decided to pluck a prettier colourful flower, a PhD. Again many of you got involved in the pains inflicted by the thorns. In the end, it is all colourful, joyful, and rewarding. Therefore, it is only proper to say a big "AKPE!!! MERCI!!! THANK YOU!!! BEDANKT!!! ¡¡¡GRACIAS!!!" to the almighty **God** for his providence, protection, inspiration, and most importantly, for the gift of life, and to any person that enriched my experience here.

To my wife, Ivy: Your unconditional love has brought us through thick and thin. This day, I say "Thank you" for always being there. Even when you did not understand me, you supported me. I know the distance weighed a lot on our efforts, but you stood firmly by my side: Thank you for being such a beautiful, lovely, caring, and understanding soul next to my craziness and stubbornness amid our ambitions. The journey was long, but I sailed through. There is a very crucial one left, and you know it, and as usual, I expect us to be there for each other: keeping the dream alive.

To my scientific family, in Ewe, we usually say: *"Wisdom is like a baobab tree; no one individual can embrace it."* I have the privilege to work among some of the best minds around on Zernike campus whom I shared a lot over the six years at the institute and especially, these last four years in the Photophysics and OptoElectronics (POE) group. First to the academics who guided me through this period of my life.

- **Jan Anton Koster**: The four-year journey began with you. Your e-mail on the 12-01-2015 came as a surprise: "I've been providing references for you, but now I'm writing about an open PhD position in my group… An advertisement is on the university website…… Would you be interested?" I decided to pursue your proposed project amid alternatives. I must say I have never regretted that choice. Since then, it has been an enjoyable experience. As the Ugandan proverb goes "*Without a leader, black ants are confused*", you have been a phenomenal leader, supervisor, and counsellor. This has been epitomised by the 1st ever best PhD supervisor awarded to you on the 07-06-2018. We had our share of challenges. I feel like I have shared not only in your wisdom and knowledge but also in some of your personal and professional achievements. I am proud of you as my promotor and daily supervisor through working together and collaborating with other scientists. You have always encouraged us to attend conferences. One such occasion is the time spent together in Strasbourg during the E-MRS 2018: Thank you for the precious time spent together mainly with my friends and me as well. In their words: "You are a cool guy" ☺ Finally the Akan proverb says: "*When the king has good counsellors, his reign is peaceful*." I do feel like a good counsellor now, and so I would like to share my thoughts which are in line with the African Proverb: "*Milk and honey have different colours, but they share the same house peacefully*." I urge you to always keep this harmonious but very international aspect of the group. It is beautiful!!!
- **Ryan Chiehci**: Your name appeared in the e-mail sent by Jan Anton together with that of Adrii Minnaard. Then again for a meeting concerning the first project that led to our first publication together. I realised then that my life would somehow be stuck to yours as a crucial player in our research. I am always amazed at the many ideas you bring forth anytime we meet to discuss project-related issues in your office. Honestly, I do usually only keep the first three ideas. Of course, you are a chemist by training, and I am a physicist. Nevertheless, those were very useful, much appreciated, and fruitful ideas. Thanks for your time, your pivotal role in the project, our other collaborations, and your supervision.
- **Maria Antonietta Loi**: Thank you for your support and advice on and off the periodical evaluations. I will always remember two things: first, your spirited lifestyle and energy and next, "Guys, connect your brains ☺." Thank you for the memorable times at the group meetings and outings. You wanted and urged that I finish the PhD in three years, but research, as you know, decided otherwise. Now that it is done you can be proud and happy for me. Thank you for being our teacher and a second mother to us all.
- **To the assessment committee:** I sincerely thank you, **René A. J. Janssen, Thomas Kirchartz, and Maxim S. Pchenitchnikov** for your time and effort towards assessing and providing feedback on the thesis, and its final approval. I appreciate your valuable inputs.

Moving on to the scientists I have actively and passively shared the labs with; I must say there is no better time than now to be once more grateful

to you all. As I reflect and pen down a few words in recognition of the part you played in this journey, let it also serve as an everlasting "THANK YOU." As such, it is only reasonable to start with you:

- **Gongbao Wang**: as my primary collaborator, we were supposed to work hand in hand on our common interdisciplinary project which alas could not be achieved. However, we found our way to still collaborate on projects that developed over the years through the assistance of Jan Anton and Ryan, especially the ones I developed on the BDT-TT polymers and DIO. Even though sometimes we worked on different diapasons, we always finally get the results. Thank you for your time, ideas, and the collaborations over the years on the three projects.
- **Vincent M. Le Corre**: We have shared a lot over the years, conferences, summer school, workshops, meetings, and lunches. Our first conference was in Warsaw Poland: memories not to forget, especially the plate of food we could not finish in the Polish restaurant which forced us to eat Thai for the rest of the stay ☺. We did almost everything together and of course, partly the research too, which led to our three publications. Thank you for being my paranymph, seldom French-speaking practice partner in crime, a friend, an office mate, and most importantly for your time and useful discussions.
- **Azadeh Rahimi Chatri**: Thank you for the collaboration leading to the fourth paper. I cherish the moments we shared at the summer school, the dance floors in Solmaz's home and PhD defence party. These memories, I will treasure.
- **Gang Ye**: When Ryan initiated the collaboration between you and me, little, did we know that it was going to be very involving and time-consuming? However, it was a pleasure to be involved and making it together with success. Everything went on just smoothly, of course, not the entire research but our work relation. We shared quite some moments with discussions, ideas, work, and sometimes plans together with Sylvia. Thank you for your kindness, openness, and fruitful discussion and collaboration.
- **Mustapha Tisan Abdu-Aguye**: July 2010 was the beginning of our collaborations. I still remember that white paper we wrote together in AUST. This time around, it is about ferroelectric block copolymers in OPVs. I would say this happened because of your persistence and the environment provided by the POE group. You kept bugging me with your ideas on collaborative projects. We could not undertake all, but we can at least be grateful for having each other, sharing ideas, and working together. Finally, you and I can only appreciate our efforts as scientists. Thank you for being still a part of this journey.
- **Sylvia Rousseva**: We met about 1.5 years ago. Kees and Jan Anton directed you to me. Since then, we became lab partners, and later got involved in different projects. It was a real pleasure working with you and having an in-dept discussion with you on various topics. Thank you for being part of this journey, and I wish you success for the rest of your PhD research and career.

- **Xinkai Qiu**: Your skills on the AFM set-up was evident during the training sessions, and right after we began to do some measurements together. Thank you for your willingness and readiness to engage in discussions and for your time. I will not forget the jokes about me and the coffee machine ☺.
- **Jingjin Dong**: GIWAXS measurements became very crucial to my last few projects. The ternary and the ITIC derivatives projects made the inputs from GIWAXS unavoidable. You became the automatic point of contact or the easier target ☺. You were very kind and willing to help, and so we began to work together and had fruitful discussions. Thank you for the help, your smiles, and your flexibility.
- **Maria A. Izquierdo Morelos**: You are such a spirited lady and scientist. Usually, people appreciate successful collaborations. However, I would like to state that even though our collaboration did not bear the desired fruit for both parties, I am grateful for sharing ideas, time, and work duties with you. Thank you for your friendship. Funny memory and anecdote to remember "Mustifafa" ☺. Wishing you the best in your future career.

The achievements recounted in the thesis would not have been possible without you **Martijn**, **Misha**, **Panos**, and **Felix**. In Ghana, we say: *"An army of sheep led by a lion can defeat an army of lion led by a sheep."* I am proud of the progress and the achievements we made together, and it is only right to highlight some of the moments:

- **Martijn Oudshoorn** (Dutch): My first bachelor student full of energy. Your enthusiasm and spirit contaminated the group by the time you left, and I could hear people say: "He is good." Though your project on thermally stimulated current is a tough one to handle, you managed to finish it on a good note. Thank you for allowing me to guide you through your thesis.
- **Mikhail V. Dryzhov** (Russian): My second bachelor student who wanted to do all. You did two (2) projects with me: the bachelor of science thesis and the honours college bachelor thesis. This shows how dedicated and hardworking you are, eager to do more and sometimes overzealous. Our project on FA and NFA solar cells ended up into a publication, and together we have opened other ramifications to the subject. Thank you also for becoming my friend, for the good moment we shared. I wish you well with your new endeavours.
- **Panagiotis Christodoulis** (Greek): My first master student coming in through the topmaster programme in nanoscience. You took on one of the ramifications from the above-described project. Your stay was very short as it was for the short project, but we were able to make some progress in the ternary blends project (which ended up in a publication with some future works from Felix and me). Results you successfully presented at the 2018 nanosymposium. I wish you all the best and success in the next chapter.
- **Felix V. Houard** (French): My second master student, coming in to do an external internship in our group. Working with you was a

pleasure. First, we continue and finish the establishment of a protocol for making reproducible inverted structure solar cells – something we successfully established for the first time in the Koster group. Next, we implemented the inverted structure in the ternary blend degradation project. Finally, we embarked on the ITIC derivatives solar cells degradation project. You grew in confidence and understanding of the topics. I knew it would be so, that is why it was not difficult to provide you with a reference letter for your PhD applications just a few weeks into your stay in the group. I am happy and proud you got one of these PhD positions. I wish you the best in your new adventure in Florence and Rennes, hoping that I have equipped you well for this journey.

I want to thank all other members of POE, both current and past, especially **Marten, Jian, Shuyan, Wytse, Simon, Herman, Natasha, Dima, Bart, Mustapha, Sampson, Artem,Tejas, Solmaz, Niels, Davide, Daniel, Mark, Vlad, Hong-Hua,** and **Jorge,** for your company, useful discussion, time shared in the lab, at various meetings, group outings, and Christmas dinners. In particular, **Sampson,** we shared the cleanroom the most and had discussions within and outside the confines of those walls. **Marten** for discussions in particular on teachings and grading assignments and for your time and help on the various translations. **Bart** for our time together at the 2019 MRS spring meeting, in the EQE lab fixing and calibrating both EQE set-ups and also for our seldom but interactive discussions.

Many thanks go to all members of the FOM focus group, especially **Difei, Riccardo, Viktor, Saurabh, Jane, Sri, Remco,** and **Kees,** for our precious time and discussions. Thank you, **Remco** and **Kees** for the coordination of the meetings. Those were good times with presentations and the exclusive treatment with drinks and snacks. A special thanks to **Kees** for our seldom discussions and fruitful encounters.

The scientific family would not have been complete without acknowledging the Zernike 2011-2013 topmaster cohort members. Thanks also to my then mentor, **Paul van Loosdrecht,** and the then coordinator of this prestigious programme, **Caspar van der Wal**. With this thesis, I think we can all agree that the circle is almost complete.

A huge “Thank You” to the technicians I worked with especially **Arjen Kamp** and **Teodor Zaharia** for keeping the labs and the equipment running. For a timely response to our needs, problems, and training even in those tight periods. A big “Thank You” to you, **Rick van der Reijd,** for the help during the collaborative work with Gongbao.

It would not be fully smooth in the institute and the POE group without you **Renate Hekkema-Nieborg**. Thank you for your time, the lovely exchanges between us from time to time and for the hardest job of keeping tabs on our administrative matters; organising promptly our meetings, paper works and reconciling our timetables when it became difficult. You are such a wonderful secretary.

Now to my family of friends. Staying in Groningen would have been a very hard experience if not for you all. I cannot but start with the African students' community (ASC). I must say it was an honour serving this association and the Groningen international students' platform (GISP). Thank you for the atmosphere you provided and the great works done over the years. I would like to thank some good friends with whom I have worked on the ASC board, and without whom the ASC would not have been alive today in RuG: **Sarah T. van Erwin, Jenneke Steggeman, Jolvie K. Mahoungo, Amisah Z. Bakuri Antwi-Berko, James Barimah, Sampson Adjokatse**, and **Mustapha T. Abdu Aguye**.

On a personal note, you have allowed me to grow more as a leader and to meet and share ideas with some of the RuG leaders in the person of the then rector magnificus **Elmer Sterken**, the then president of the RuG **Sibriand Poppema,** to name just a few. Thank you for the opportunities and for the unforgettable moment: the invitation to the honorary doctorate of the African icon, one of the voices against the apartheid regime in South Africa, **Desmond Tutu** (special thanks for your gesture), to behold, to chat, to share pleasantries and gifts, and to capture that memorable occasion into unforgettable pictures. I am grateful for all of that.

On the fun side, I think **Alpha, Sarah, Jolvie, Marlene, Jenneke, Anani, Andrew, Gerber, Ketty, Rita, La Verne, Playtorn, Vamba** and many more contributed in keeping us sane while studying, working, serving the ASC and keeping it real and fun. I missed those times and treasured those memories. The revival of the ASC symposium which has become an enormous success and a yearly event is one of such examples, fulfilling our dreams. I want to thank you all and all future boards that made it possible. It is worth noting that among the lot some of you have deeply impacted me or shared deeper connections with me, and it is only right to acknowledge you though not exhaustively:

- **Andrew Banda**: You were the very first friend I made in Groningen in 2011 while we were all looking for a bike to buy. One can never skip the bikes while a story is narrated in The Netherlands, right! Since then we got stuck to each other. It became more than friendship when we realised we shared in the same dreams for ourselves and Africa, the same convictions, and the same faith. We became brothers from different wombs. Thank you for the support, the advice, and the times spent together. Thank you also for making my first time in Southern Africa a memorable one in December 2017 during my visit from the AMRS meeting in Gaborone-Botswana. It was an enjoyable time both on and off the road from Botswana to Zambia. You also shared in my union with Ivy with your presence here in Groningen in December 2018. We are truly grateful. All the best!!!
- **Sampson Adjokatse**: my Ghanaian brother, and housemate during the PhD journey. Thank you for linking me to AUST and for your support as a brother, friend throughout the years. I remembered the troubles we went through looking for accommodation to the extent that we were asked "to be couples" as that would be the key to get an apartment easily. But anyway, with the grace of God, we made it. I

am proud of your achievements. Stay connected, blessed, and surge ahead.

- **Kwaku A. Sarpong & Paul O. Omane**: My PhD would not be enjoyable nor complete without both of you. Thanks for being such wonderful housemates. Your human nature, humility, and friendliness are what made our lives and stay entertaining.
- **Ceciel Nieuwenhout**: We first met in Ghana in 2014 when you visited Manfred for the holidays. We quickly became friends and discovered our passion for "energy", though from different angles. We do have, however, fruitful discussions. Thank you for being a true Dutch friend. I wish you well for the continuation of both your PhD and political lives ☺.
- **Mustapha Tisan Abdu-Aguye**: You are one of the first people I connected with in AUST in 2010, and since then we remain excellent friends. We experienced a lot together. In brief, we are inseparable. My office and desk practically served as a second office for you. We have been there for each other in moments of joy, good fortunes, sorrows, troubles, and pains. It is for no reason why you are one of my paranymphs and my best man. Thank you for your warm friendship and brotherhood, for your time and advice and also for all our fun times together. It was nice times spent together in and outside our homes, at some of the coffee breaks with **Linda**, and in the kitchen in early days in Groningen learning how to cook. As we remain connected forever, I wish to say that distance and tribulations can never affect this bond. Stay focused and blessed.
- **Sarah Bomkapre & Mo Kor**: You are my brethren from another country. It is a real pleasure knowing you both. Thank you for the sporadic fun times in Munich-Germany. You were always ready to host me/us. I will always cherish the 2015-2016 Christmas season spent together with our other fellow brothers as "one lost but found family." Thank you for sharing in the life journey of Ivy and myself, for the critical role you played during our union in Groningen. Hopefully, we will see you in Ghana soon.
- **Cor & Elsa Snijder**: Our acquaintance began through HOST. Immediately you became my Dutch family. We quickly realised how connected we are in ideologies, life, beliefs, and moral values. You hosted me several times in your home for dinner. We shared meals, pleasantries, thoughts, and more importantly, words of encouragement and prayers. Thank you for hosting some of my guests during our wedding last December and also for being part of that memorable day in our life. You will forever be in our hearts. And please, you are always welcome to Ghana.
- **Josef K. A. Amuzu**: Thank you for your support over the years.

To **Linda, Osman, Benedito, Nong, Spyros, Inoussa, Toto, Francisco, Lami, Franck, Pierre, Mohamed, Zainab, Nathaniel, Joram, Nathaniel, Niya, Alexandra, Nikki, Robyn, Mehdi, Coralie, Sokona, Désiré, Elizabeth, Emmanuel**, and the many more who have one way or the other made my experience here an enjoyable one. You guys have impacted my life with invasive intelligence, humour, teachings, and friendliness. Thank you all, beautiful

people, for your time, resources, and friendship. My heart is forever engraved with your faces and names. To the **St. Augustinus student parish lectors' ministry, Ghana Connect community, and the ASC football team**, thank you for your wonderful spirit of friendship and athletics. For fun times on the pitch. It was fun over the years.

Finally, to **my parents and siblings**: As the African proverb has it: *"There is no fool who is disowned by his family."*

- First to my mum, **Essie Awunyo**, for your selfless dedication towards keeping this family together, for providing for us even in the most challenging times. Without you, I could not have plucked these flowers. Your call on 3rd July 2010 is the catalyst for my recent successes. Your constant calls and prayers have led me through times. Thank you, "mama".
- Next, to my father, **Frederick Doumon**, for being the stronghold, planting the seeds. Words cannot describe your support and constant dedication. Your advice always resounded in my mind and kept me going. Thank you for everything.
- And finally, to my siblings **Marius**, **Modester,** and **Biova Doumon** for your supports, the moments we shared, the kind words of encouragements and the tough times we went through together. They have made me stronger, responsible, and a better version of myself. Especially, **Biova** to whom my getting a PhD is like a battle that must be won as soon as possible. Thank you all for your constant reminder that "I need to do this" not only for my scientific curiosity but also for your pride and possible challenge: "Nothing should stand in your way." Thank you **Biova** for that faithful call to mum. Congratulations!!! **Modester** for also starting a new chapter.

As I close with this African proverb: *"The beauty of a woman becomes useless if there is no one to admire it."*, I hope you had a lovely and admirable read of this thesis.

Akpe!!! Merci!!! Thank you!!! Bedankt!!! ¡¡¡Gracias

Nutifafa